

Ionomer Compatibilized
Low Density Polyethylene - Tapioca Starch Blends
Biodegradability and Photodegradability

Thesis submitted to
Cochin University of Science and Technology
in partial fulfillment of the requirements
for the award of the degree of
Doctor of Philosophy
under the
Faculty of Technology

by
Zeena. P. Hamza



Department of Polymer Science and Rubber Technology
Cochin University of Science and Technology
Kochi- 682 022, Kerala, India
<http://psrt.cusat.ac.in>

October 2012



Department of Polymer Science and Rubber Technology
Cochin University of Science and Technology

Kochi - 682 022, Kerala, India
<http://psrt.cusat.ac.in>

Dr. Thomas Kurian
Professor

Tel: 0484-2575723 (Off)
0484-2575144 (Res)
E-mail: drtkurian@gmail.com

Date:.....

Certificate

This is to certify that the thesis entitled **“Ionomer Compatibilized Low Density Polyethylene – Tapioca Starch Blends *Biodegradability and Photodegradability*”**, which is being submitted by Ms. Zeena. P. Hamza, in partial fulfilment of the requirements of the degree of Doctor of Philosophy, to Cochin University of Science and Technology (CUSAT), Kochi, Kerala, India, is a record of the bonafide research work carried out by her under my guidance and supervision.

Ms. Zeena has worked on the research problem for about six years (2006-2012) in the Department of Polymer Science and Rubber Technology of CUSAT. In my opinion, the thesis has fulfilled all the requirements as per the regulations. The results embodied in this thesis have not been submitted for any other degree or diploma.

Thomas Kurian
(Supervising Teacher)

Declaration

I hereby declare that the thesis entitled “**Ionomer Compatibilized Low Density Polyethylene – Tapioca Starch Blends *Biodegradability and Photodegradability***” is a record of the original research work carried out by me under the supervision of Dr. Thomas Kurian, Professor, Department of Polymer Science and Rubber Technology, Cochin University of Science and Technology, Kochi, Kerala, India. No part of this thesis has been presented for any other degree from any other institution.

Kochi
Date:

Zeena. P. Hamza

Acknowledgement

I humbly bow before the Almighty God who enlightens me with wisdom and grace for success in my life.

I express my profound sense of gratitude to my supervisor Dr. Thomas Kurian, Professor, Department of Polymer Science and Rubber Technology, Cochin University of Science and Technology (CUSAT) for his efficient guidance and unfailing inspiration, throughout the tenure of my research work,

I am extremely thankful to Prof. Sunil K. Narayanankutty, Head, Department of Polymer Science and Rubber Technology, CUSAT for providing me with the laboratory facilities to carry out my research work in the Department.

I am grateful to Prof. K. E. George, Prof. Rani Joseph, Prof. Philip Kurian, Prof. Eby Thomas Thachil, Ms. Jayalatha Gopalakrishnan, Technical Staff and Administrative Staff of the Department of Polymer Science and Rubber Technology, CUSAT for their personal interest, support and valuable advice.

The co-operation, help and lively environment extended to me by the fellow researchers of the Department of Polymer Science and Rubber Technology, CUSAT are sincerely appreciated.

I would like to thank Dr. Sarita G. Bhat, Head, Department of Biotechnology, CUSAT and Mr. Raghul Subin (Research Scholar) for providing me the facilities at the Microbial Genetic Laboratory, and their continuous help during the biodegradation studies.

I am thankful to Mr. S.P. John, Managing Director, Jemsons Starch & Derivatives, Aroor, Alapuzha, for providing the samples of biopolymers.

I owe immensely to all my teachers right from my school days to the post graduate level for their blessings.

I am indebted to Mr. Govindhankutty and Mr. Sathyanathan (former Heads), Mrs. M. M. V. Premila (Head) and Faculty Members of the Department of Chemistry, Govt. Brennen College, Thalassery, for their support and cooperation.

I wish to thank the University Grants Commission, New Delhi for the award of Teacher Fellowship under FIP for the completion of the research work,

The encouragement, affection, and prayers of my family members especially my parents, parents in-law, sisters, brothers in-law, sisters in-law, my husband Mr. Aneez, and our children Fiza, Fahad and Farzeen throughout the course of this work are gratefully acknowledged.

Zeena. P. Hamza

Preface

Plastics play an important role in our daily lives as it offers a growing range of applications in many fields. Many of the physical and chemical properties of plastics make them ideal materials for a variety of products. However most of the plastics have poor biodegradability and may have lifetime of over hundred years. Biodegradable plastics are of great importance due to the nonavailability of land for solid waste disposal, reduction of fertility of land by accumulation of plastic based surface litter and public perception of hazards to human and animal health. However, the practical uses of some of the popular biodegradable plastics are limited because of their poor mechanical properties and high cost that rarely meet the industrial and public requirements. Thus, a unique combination of degradative and mechanical properties of blends of biopolymers with conventional polymers seems to have great applications. In these blends properties of the components may be synergistically combined so that certain homopolymer drawbacks as well as the cost/property ratio are minimized. However, most of the polymer blends are found to be immiscible and incompatible which results in blends with poor mechanical properties. Addition of a compatibilizer to immiscible blends modifies its compatibility and brings about an enhancement in the mechanical properties.

Polyethylenes, especially low density polyethylene (LDPE) is one of the most widely used polyolefin polymers by virtue of their relatively low cost, light weight, low temperature toughness, low moisture absorption, good optical properties, good flexibility, ease of processing and recycling. LDPE (density range of 0.915–0.940 g/cm³) has a high degree of short and long chain branching.

Starch has been considered as a useful material in certain thermoplastic applications because of its biodegradability, easy availability, non-toxicity, low permeability, high degree of purity and low cost.

Ionomers are ionic polymers having a hydrocarbon backbone containing pendant acid groups which are partially neutralized to form salt groups. These salt groups are typically carboxylate (COO^-) or sulphonate (SO_3^-) type, while the monomers used to create the polymer backbone are mostly olefinic in nature. Ionomers have the unique ability to compatibilize certain incompatible blends. When ionomers are added to the binary blends, they form ionic cross links at the interface of the blends and improve the mechanical properties of the blends.

Biodegradation is the chemical degradation of materials brought about by the action of naturally occurring microorganisms. Biodegradation is a relatively rapid process under suitable conditions of moisture, temperature and oxygen availability. The logic behind blending biopolymers such as starch with inert polymers like polyethylene is that if the biopolymer component is present in sufficient amount, and if it is removed by microorganisms in the waste disposal environment, then the base inert plastic should slowly degrade and disappear.

The present work focuses on the preparation of biodegradable and photodegradable blends based on low density polyethylene incorporating small quantities of ionomers as compatibilizers.

The thesis consists of eight chapters. The first chapter presents an introduction to the present research work and literature survey. The details of the materials used and the experimental procedures undertaken for the study are described in the second chapter. Preparation and characterization of low

density polyethylene (LDPE)-biopolymer (starch/dextrin) blends are described in the third chapter. The result of investigations on the effect of polyethylene-co-methacrylic acid ionomers on the compatibility of LDPE and starch are reported in chapter 4. Chapter 5 has been divided into two parts. The first part deals with the effect of metal oxides on the photodegradation of LDPE. The second part describes the function of metal stearates on the photodegradation of LDPE. The results of the investigations on the role of various metal oxides as pro-oxidants on the degradation of ionomer compatibilized LDPE-starch blends are reported in chapter 6. Chapter 7 deals with the results of investigations on the role of various metal stearates as pro-oxidants on the degradation of ionomer compatibilized LDPE-starch blends. The conclusion of the investigations is presented in the last chapter of the thesis.

Abstract

The current research has been undertaken to explore the biodegradability and photodegradability of low density polyethylene (LDPE). Various amounts of biopolymers (either starch or dextrin) of various particle sizes were blended with low density polyethylene. The properties of the blends were evaluated by measuring mechanical properties, melt flow indices (MFI), biodegradability, photodegradability, photobiodegradability, water absorption, infrared spectroscopy (FTIR), dynamic mechanical analysis (DMA), thermogravimetry (TGA), differential scanning calorimetry (DSC) and scanning electron microscopy (SEM). Biodegradability of the compositions prepared from the blends of low density polyethylene and biopolymers has been verified using a culture medium containing *Vibrios* - an amylase producing bacteria, and by soil burial. The photodegradability of low density polyethylene and its blends with biopolymers has been improved by the addition of small quantities of pro-oxidants (metal oxides/metal stearates). The potential of zinc and sodium salts of polyethylene-co-methacrylic acid ionomers as compatibilizer for low density polyethylene-starch blends too has been evaluated. The properties of the ionomer compatibilized blends were compared with the properties of the maleic anhydride (MA) compatibilized blends. The results of the degradation studies show that the blends of low density polyethylene and biopolymers are partially biodegradable and addition of pro-oxidants enhances the degradability of low density polyethylene-starch blends. The improvement in mechanical properties of the blends after the addition of ionomers indicates that the ionomers are effective compatibilizers` for low density polyethylene-starch blends and

the presence of ionomers does not adversely affect the biodegradation of the blends.

Key words: Low density polyethylene, Starch, Dextrin, Biodegradability, Photodegradability, Biopolymers, Melt flow index, Dynamic mechanical analysis, Thermogravimetry, Differential scanning calorimetry, Scanning electron microscopy, *Vibrios*, Soil burial test, Pro-oxidant, Metal oxide, Metal stearate, Ionomer, Polyethylene-co-methacrylic acid ionomer, Compatibilizer

Contents

Chapter 1

GENERAL INTRODUCTION 01 - 52

1.1	Polyethylene -----	04
1.1.1	Low density polyethylene -----	06
1.1.2	Structure and properties of LDPE -----	07
1.1.3	Applications -----	08
1.2	Degradation of plastics -----	08
1.2.1	Biodegradation -----	11
1.2.1.1	Mechanism of biodegradation -----	11
1.2.1.2	Factors affecting the biodegradation -----	12
1.2.1.3	Biodegradable polymers -----	14
1.2.1.4	Starch -----	15
1.2.1.5	Dextrin -----	16
1.2.2	Photodegradation -----	17
1.2.2.1	Pro-oxidants -----	18
1.2.3	Thermal degradation -----	20
1.3	Degradation of polyolefins -----	20
1.3.1	Mechanism of polyolefin degradation -----	21
1.3.2	Enhancement of degradation of polyolefins -----	23
1.3.2.1	Polyolefin-biodegradable polymer blends -----	24
1.3.2.2	Pretreatment of polymers -----	25
1.3.2.2.1	Physical methods -----	25
1.3.2.2.2	Chemical methods -----	26
1.4	Polymer blends -----	26
1.4.1	Factors affecting miscibility and immiscibility of polymer blends -----	30
1.5	Compatibilization -----	31
1.5.1	Methods of compatibilization -----	32
1.5.2	Applications of compatibilization -----	33
1.6	Ionomers -----	34
1.6.1	Types of ionomers -----	35
1.6.2	Polyethylene based ionomers -----	36
1.6.3	Ionomer as compatibilizer -----	37
1.7	Scope and objectives of the work -----	39
	References -----	41

Chapter 2

MATERIALS AND EXPERIMENTAL

TECHNIQUES 53 - 67

2.1	Materials -----	53
2.1.1	Low density polyethylene (LDPE)-----	53
2.1.2	Starch and dextrin-----	53
2.1.3	Ionomers -----	53
2.1.4	Pro-oxidants -----	54
2.1.4.1	Metal oxides -----	54
2.1.4.2	Metal stearates -----	54
2.1.5	Other chemicals -----	54
2.2	Preparation of blends -----	55
2.2.1	Melt mixing-----	55
2.2.2	Preparation of test specimens -----	56
2.3	Characterization -----	57
2.3.1	Mechanical properties-----	57
2.3.2	Melt Flow Index (MFI) -----	57
2.3.3	Biodegradation studies -----	57
2.3.3.1	Bacterial strains -----	57
2.3.3.2	Purification of Vibrios -----	58
2.3.3.3	Screening for amylase producers -----	58
2.3.3.4	Medium for Biodegradation studies. -----	59
2.3.3.5	Preparation of consortia of amylase producers for biodegradation studies-----	59
2.3.3.6	Biodegradation studies on blends using the consortium --	59
2.3.3.6.1	Preparation of blends-----	59
2.3.3.6.2	Preparation of inoculum & shake flask culture --	60
2.3.4	Soil burial test -----	60
2.3.5	Photodegradation by UV rays-----	61
2.3.6	Water absorption characteristics-----	61
2.3.7	Fourier transform infrared spectroscopy (FTIR)-----	61
2.3.8	Dynamic Mechanical Analysis (DMA) -----	62
2.3.9	Thermogravimetric analysis (TGA) -----	63
2.3.10	Differential scanning calorimetry (DSC) -----	64
2.3.11	Morphological studies-----	65
	References-----	66

Chapter 3

BIOPOLYMER FILLED LOW DESNSITY

POLYETHYLENE 69 - 97

3.1	Introduction-----	70
3.2	Results and discussion -----	71

3.2.1	Mechanical properties-----	71
3.2.2	Melt flow measurements-----	74
3.2.3	Biodegradation studies-----	76
3.2.3.1	In culture medium-----	76
3.2.3.2	Soil burial test-----	79
3.2.4	Water absorption studies-----	82
3.2.5	Fourier transform infrared spectroscopic analysis-----	83
3.2.6	Dynamic mechanical analysis-----	87
3.2.7	Thermogravimetric analysis-----	89
3.2.8	Differential scanning calorimetry-----	91
3.2.9	Morphological studies-----	92
3.3	Conclusions-----	94
	References-----	95

Chapter 4

COMPATIBILIZED LOW DENSITY POLYETHYLENE- STARCH BLENDS99 - 130

4.1	Introduction-----	100
4.2	Results and discussion-----	102
4.2.1	Mechanical properties-----	102
4.2.2	Melt flow measurements-----	110
4.2.3	Biodegradation studies-----	111
4.2.4	Water absorption studies-----	115
4.2.5	Fourier transform infrared spectroscopic analysis-----	116
4.2.6	Dynamic mechanical analysis-----	120
4.2.7	Thermogravimetric analysis-----	121
4.2.8	Differential scanning calorimetry-----	123
4.2.9	Morphological studies-----	125
4.3	Conclusions-----	127
	References-----	128

Chapter 5

PRO-OXIDANT FILLED LOW DENSITY POLYETHYLENE131 - 153

5.1	Introduction-----	132
5.2	Results and discussion-----	133
5.2.1	Metal oxides as pro-oxidants-----	133
5.2.1.1	Mechanical properties-----	133
5.2.1.2	Melt flow measurements-----	135
5.2.1.3	Photodegradability studies-----	135
5.2.1.4	Water absorption studies-----	138
5.2.1.5	FTIR spectroscopy-----	138

5.2.1.6 Dynamic mechanical analysis-----	140
5.2.1.7 Differential scanning calorimetry (DSC)-----	141
5.2.1.8 Morphological studies -----	142
5.2.2 Metal stearates as pro-oxidants -----	142
5.2.2.1 Mechanical properties-----	142
5.2.2.2 Melt flow measurements -----	144
5.2.2.3 Photodegradation studies -----	144
5.2.2.4 Water absorption studies -----	146
5.2.2.5 FTIR spectroscopy -----	147
5.2.2.6 Dynamic mechanical analysis-----	149
5.2.2.7 Differential scanning calorimetry (DSC) -----	149
5.2.2.8 Morphological studies -----	150
5.3 Conclusions -----	151
References -----	152

Chapter 6

EFFECT OF METAL OXIDES AS PRO- OXIDANTS ON IONOMER COMPATIBILIZED LOW DENSITY POLYETHYLENE-STARCH BLENDS.....155 -183

6.1 Introduction-----	156
6.2 Results and discussion -----	157
6.2.1 Mechanical properties -----	157
6.2.2 Melt flow measurements-----	160
6.2.3 Biodegradation studies -----	161
6.2.4 Photodegradation studies -----	165
6.2.5 Photobiodegradation studies -----	168
6.2.6 Water absorption studies-----	171
6.2.7 FTIR spectroscopy -----	173
6.2.8 Dynamic mechanical analysis -----	175
6.2.9 Thermogravimetric analysis (TGA) -----	176
6.2.10Differential scanning calorimetry (DSC) -----	178
6.2.11Morphological studies -----	180
6.3 Conclusions -----	181
References -----	182

Chapter 7

EFFECT OF METAL STEARATES AS PRO- OXIDANTS ON IONOMER COMPATIBILIZED LOW DENSITY POLYETHYLENE-STARCH

BLENDs185 - 214

7.1	Introduction-----	186
7.2	Results and discussion-----	187
7.2.1	Mechanical properties-----	187
7.2.2	Melt flow measurements-----	190
7.2.3	Biodegradation studies -----	191
7.2.4	Photodegradation studies -----	195
7.2.5	Photobiodegradation studies -----	198
7.2.6	Water absorption studies-----	201
7.2.7	FTIR spectroscopy-----	203
7.2.8	Dynamic mechanical analysis -----	205
7.2.9	Thermogravimetric analysis (TGA) -----	206
7.2.10	Differential scanning calorimetry -----	209
7.2.11	Morphological studies -----	211
7.3	Conclusions-----	212
	References -----	213

Chapter 8

SUMMARY AND CONCLUSIONS215 - 218

LIST OF SYMBOLS AND ABBREVIATIONS219 - 220

PUBLICATIONS221- 224

RESUME225 - 226

....❧....

GENERAL INTRODUCTION

C o n t e n t s	1.1	<i>Polyethylene</i>
	1.2	<i>Degradation of plastics</i>
	1.3	<i>Degradation of polyolefins</i>
	1.4	<i>Polymer blends</i>
	1.5	<i>Compatibilization</i>
	1.6	<i>Ionomers</i>
	1.7	<i>Scope and objectives of the work</i>

During the past few decades, synthetic plastics have replaced traditional materials such as paper, glass, steel and aluminium in many applications. Significant aspect of plastics material growth globally has been the innovation of newer application areas of plastics such as automotive field, rail, defence, aerospace, medical and healthcare, electrical and electronics, telecommunication, building and infrastructure, furniture, etc. World-wide, the plastics consumption has an average growth rate of 5% and it will touch a figure of 227 million tons by 2015 [1]. One of the key growth segments in the case of plastics is “packaging” which accounts for over 35% of the global consumption. Global per capita consumption [2] of plastics is given in Table 1.1.

Table 1.1 Global per capita consumption of plastics (in kg)

World average	26
North America	90
West Europe	65
East Europe	10
China	12
India	5
South East Asia	10
L. America	18

Polyolefins accounts for 53% of the total consumption of plastics materials (PE - 33.5% and PP - 19.5%), followed by PVC – 16.5%, PS - 8.5%, PET and PU - 5.5%, styrene copolymers (ABS, SAN, etc.) – 3.5%, others (engineering plastics, high performance plastics, speciality plastics, blends, alloys, and thermosetting plastics) – 13%.

The nonbiodegradable plastic waste discarded from the packaging sector has considerable environmental impact. However, the removal of plastics from packaging applications is not a viable option, as the use of non-plastic packagings would result in a dramatic increase in weight and volume of packaging materials besides prohibitive quantities of additional energy consumption [3].

Synthetic plastics have been developed for durability and resistance to various forms of degradation. The environmental degradation of used plastics is not a simple process. Degradation of plastics under extreme conditions such as incineration is not a simple physical process, and thus it is not considered when referring to environmental degradation [4]. Despite the continuing growth of recycling processes, source reduction and energy

recovery, some proportion of the plastic waste will always require disposal. Figure 1.1 depicts the pie chart showing various types of plastics waste. The most common method for disposing of municipal solid waste is landfilling [5]. Several hundred thousand tons of waste plastics are discarded into the environment every year and most of it ends up in landfills. In recent years, concern about the garbage disposal crisis has grown as landfill capacity diminishes and sites for new landfills become increasingly difficult to find [6].

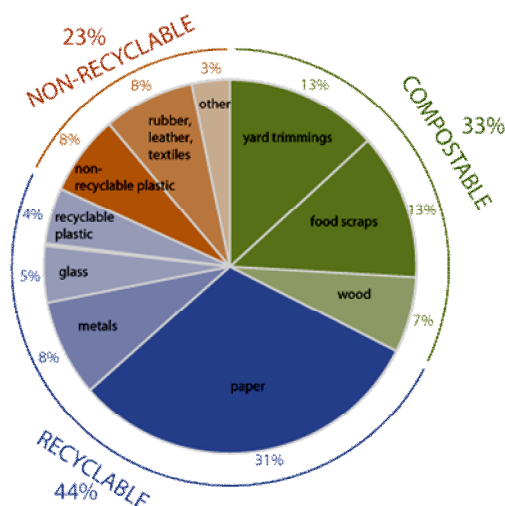


Figure 1.1 Pie chart showing various types of plastic waste

The growing issues on plastic waste management and environmental concerns have led to active research on biodegradable plastics. Polyolefins are the major components of plastic waste from domestic garbage. Among various polyolefins, polyethylenes have the largest tonnage of consumption in the world and are the major constituent in the plastic litter [7]. In the past decades, many scientists have worked on modification of polyethylenes to increase its biodegradability. The sensitivity of polyethylenes to biodegradation can be

enhanced by blending them with polymers from natural resources such as starch and dextrin [8-9]. Polyethylenes form immiscible blends with biopolymers and this incompatibility results in poor mechanical properties [10-11]. The use of ionomers as compatibilizers, in polymer blends has been the subject of many patents [12].

1.1 Polyethylene

Polyethylene (PE) is the simplest thermoplastic hydrocarbon polymer consisting of long chains formed by the combination of ethylene (Figure 1.2).

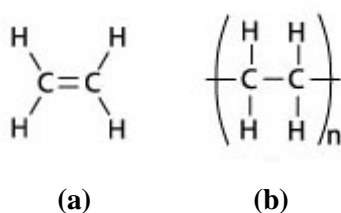


Figure 1.2 Chemical structure of: (a) ethylene and (b) polyethylene

Polyethylene can be produced through radical polymerization, anionic addition polymerization, ion coordination polymerization or cationic addition polymerization. This is because ethylene does not have substituent groups that influence the stability of the propagation head of the polymer. Each of these methods results in a different type of polyethylene [13].

Polyethylene is classified into several different categories based mostly on its density and branching. The mechanical properties of PE depend significantly on variables such as the extent and type of branching, the crystal structure and the molecular weight. The important grades of polyethylenes are:

- Low density polyethylene (LDPE)

- High density polyethylene (HDPE)
- Linear low density polyethylene (LLDPE)
- Ultra high molecular weight polyethylene (UHMWPE)
- Ultra low molecular weight polyethylene (ULMWPE or PE-WAX)
- High molecular weight polyethylene (HMWPE)
- High density cross-linked polyethylene (HDXLPE)
- Cross-linked polyethylene (PEX or XLPE)
- Medium density polyethylene (MDPE)
- Very low density polyethylene (VLDPE)

LDPE is defined by a density range of 0.915–0.940 g/cm³. LDPE is created by free radical polymerization. The high degree of branching with long chains gives molten LDPE unique and desirable flow properties.

HDPE is defined by a density greater or equal to 0.941 g/cm³. HDPE has a low degree of branching and thus stronger intermolecular forces and tensile strength.

LLDPE is defined by a density range of 0.915–0.925 g/cm³. LLDPE is a substantially linear polymer with significant numbers of short branches, commonly made by copolymerization of ethylene with short-chain alpha-olefins (for example, 1-butene, 1-hexene and 1-octene). LLDPE has higher tensile strength than LDPE, it exhibits higher impact and puncture resistance than LDPE. Lower thickness (gauge) films made from LLDPE have better environmental stress cracking resistance.

UHMWPE is the polyethylene with a molecular weight in millions, usually between 3.1 and 5.67 million. The high molecular weight makes it a very tough material, but results in less efficient packing of the chains into the crystal structure as evidenced by densities less than high density polyethylene (for example, 0.930–0.935 g/cm³).

PEX is a medium- to high-density polyethylene containing cross-links introduced into the polymer structure, changing the thermoplastic into an elastomer. The high-temperature properties of the polymer are improved, its flow is reduced and its chemical resistance is enhanced.

MDPE is defined by a density range of 0.926–0.940 g/cm³. It is less notch sensitive than HDPE and its stress cracking resistance is better than that of HDPE.

VLDPE is defined by a density range of 0.880–0.915 g/cm³. VLDPE is a substantially linear polymer with high levels of short-chain branches, commonly made by copolymerization of ethylene with short-chain alpha-olefins (for example, 1-butene, 1-hexene and 1-octene). VLDPE is most commonly produced using metallocene catalysts due to the greater comonomer incorporation exhibited by these catalysts.

1.1.1 Low density polyethylene

Among the various polyethylenes, low density polyethylene is the most widely used polymer with desirable properties, well known technology of production, and low cost [14]. The excellent mechanical and dielectric properties of low density polyethylene make it indispensable for cable manufacturing and packaging applications. The widespread applications of low density polyethylene in the areas like food packaging,

agriculture, retail industry etc. lead to the accumulation of polymeric wastes in the environment. Low density polyethylene is not biodegradable because of its high molecular weight, hydrophobic nature and lack of functional groups recognizable by microbial enzymatic systems [15]. LDPE is commonly recycled and has the number "4" as its recycling symbol (figure 1.3) [16].



Figure 1.3 Recycling symbol of LDPE

1.1.2 Structure and properties of LDPE

LDPE (figure 1.4) has more branching than HDPE, so its intermolecular forces (instantaneous dipole-induced dipole attraction) are weaker, its tensile strength is lower, and its resilience is higher. Also, since its molecules are less tightly packed and less crystalline because of the side branches, its density is lower. LDPE contains the chemical elements carbon and hydrogen.

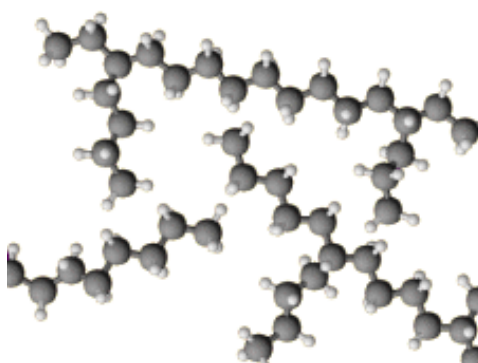


Figure 1.4 Structure of low density polyethylene

1.1.3 Applications

LDPE is widely used for manufacturing various containers, dispensing bottles, wash bottles, tubing, plastic bags for computer components, and various moulded laboratory equipment. Its most common use is in plastic bags [17]. Other products made from it include:

- Trays and general purpose containers
- Corrosion-resistant work surfaces
- Parts that need to be weldable and machinable
- Parts that require flexibility, for which it serves very well
- Very soft and pliable parts
- Packaging for juice and milk (cartons made from liquid packaging board - a laminate of paperboard and LDPE (as the water-proof inner and outer layer), and often with a layer of aluminium foil for aseptic packaging).
- Playground slides, and
- Plastic wraps

1.2 Degradation of plastics

Materials undergo degradation by natural processes. Heat, light, short wavelength electromagnetic radiation, radioactive emissions, chemicals and interaction with microorganisms can degrade materials. Degradation is defined as a process that results in change in the properties of materials, which reduces the ability of the material to perform its intended function [18]. Degradation is usually reflected in changes in mechanical, optical or electrical characteristics of materials. The changes include bond scission,

chemical transformation and formation of new functional groups [19]. The plastics may be categorized according to the nature of degradation to which they are subjected to, into the following categories:

- **Non-degradable plastics**

Commodity plastics are stable for a specific useful life-time, depending on the application and the environment. In some environments, objects made from them remain intact over many years. Their persistence originates from their high mechanical strength, hydrophobicity and resistance to microbial attack.

- **Readily degradable plastics**

Readily degradable plastics undergo self destruction after the end of its service life. The degradation of these plastics is gradual and cannot be predefined to some extent based on the selection of the type and amount of stabilizing additives. Such a material, after its lifespan, either returns to the ecosystem in an environmentally harmless manner or becomes very brittle and its fragments may pollute the environment.

- **Plastics of controlled degradation**

The goal of controlled degradation or programmed degradation is to program plastics to degrade in a predetermined time under specific conditions according to the needs of particular applications. Addition of photosensitizing group to the polymer chains facilitate programmed degradation through photodegradation [20-23]. Some polyolefin additives allow oxidative programmed degradation that results from oxidation which is to be initiated at a pre-defined time, either by natural daylight, or by heat or both or even by mechanical stress [24].

A programmed degradable plastic has adequate performance properties initially and shows no significant change in properties during the desired lifetime. After a pre-determined period of use, degradation is to begin upon disposal, starting with fragmentation or surface erosion.

▪ **Environmentally degradable plastics**

Environmentally degradable plastics (EDP) include a wide group of natural and synthetic polymeric materials that undergo chemical change under the influence of environmental factors. The chemical change must be followed by complete microbial assimilation of degradation products resulting in the formation of carbon dioxide and water. According to literature [25] the process of degradation of EDP comprises two phases: disintegration and mineralization. During the initial phase, disintegration is associated with the deterioration in physical properties, such as discoloration, embrittlement and fragmentation. The second phase is assumed to be the ultimate conversion of plastic fragments to CO₂, CH₄, and water [26].

EDP can be synthesized on renewable or non-renewable feedstocks. Examples of EDP from renewable feedstocks include cellulose, starch, starch esters, collagen, polyhydroxy alkanoates, polylactic acid, etc. and that from non-renewable feedstocks are polyvinyl alcohol, polycaprolactone and aliphatic-aromatic copolyesters. EDP are often used as blends or composites in which two or more biodegradable materials are combined to provide optimal performance while maintaining or enhancing complete biodegradability [27].

The degradation of polymers may proceed by one or more mechanisms, including biodegradation, photodegradation or thermal degradation,

depending on the polymer environment and applications. The combination of different factors from the environment such as sunlight, heat and humidity also has synergistic effects on the degradation [28].

1.2.1 Biodegradation

Biodegradation or biotic degradation is the chemical degradation of materials brought about by the action of naturally occurring microorganisms such as bacteria, fungi and algae [29].

Aerobic biotic degradation results in the formation of carbon dioxide and water, whereas in anaerobic biotic degradation, methane and carbon dioxide are the final products [30]. Plastics are biodegraded aerobically in wild nature, anaerobically in sediments and landfills and partly aerobically and partly anaerobically in composts [31].

1.2.1.1 Mechanism of biodegradation

Biodegradation is fundamentally an electron transfer process catalyzed by microbial enzymes. Electrons are removed from organic substrates to capture the biological energy that is available through the oxidation of reduced materials and moved through electron transfer chains composed of a series of compounds to terminal electron acceptors. In aerobic biodegradation oxygen is the terminal electron acceptor. When oxygen is absent anaerobic degradation become dominant and nitrate (NO_3^-), sulphate (SO_4^-), ferric (Fe^{3+}), manganese (Mn^{3+} , Mn^{4+}), and bicarbonate (HCO_3^-) ions can serve as terminal electron acceptors [32].

There are two steps involved in the biodegradation process [33]. The first one is the depolymerisation or chain cleavage of the polymer to

oligomers (biofragmentation) which leads to the increase of surface of the material [34]. The depolymerisation step normally occurs outside the microorganism and involves both exo and endo -enzymes. Exo-enzymes cause sequential cleavage of the terminal monomer in the polymer chain, while endo-enzymes cause random scission on the main chain. In the former case a water soluble oligomer is liberated into the reaction media and the rate of the molecular weight reduction of the residual polymer is small. In the latter case the molecular weight and the mechanical properties of the remaining polymer are quickly reduced. Molecular weight reduction is mainly caused by hydrolysis or oxidative chain scission [35]. Polyesters, polyanhydrides, polycarbonates and polyamides are mainly degraded by hydrolysis whereas non-hydrolyzable polymers such as polyolefins, natural rubber, lignins and polyurethanes undergo oxidative degradation. For many polymers, hydrolysis and oxidation occur simultaneously in the environment.

In the second step microbodies attack and digest the product, this is transformed to by-products which are assimilated by the microbodies, and mineralized. Mineralization is defined as the conversion of the polymers into biomass, minerals, CO₂, CH₄ and nitrogen compounds.

1.2.1.2 Factors affecting the biodegradation

The rate of biodegradation was found to be affected by several factors. Nature of the polymeric materials such as their structure and morphology, environmental conditions, organisms used for degradation are the main factors affecting biodegradation.

Synthetic biodegradable polymers contain hydrolysable linkages such as amide, ester, urea, and urethane along the polymer chain that are

susceptible to biodegradation by microorganisms and hydrolytic enzymes. When the monomeric and polymeric ester ureas synthesized from D-, L-, and DL-phenyl alanines are subjected to enzyme-catalyzed degradation, the pure L-isomer was degraded much faster than the DL-isomers [36]. A polymer containing both hydrophobic and hydrophilic segments seems to have a higher biodegradability than those polymers containing either hydrophobic or hydrophilic structures only. The polymer chain of the synthetic polymer must be flexible enough to fit into the active site of the enzyme to undergo biodegradation. Flexible aliphatic polyesters are readily degraded by biological systems, but the more rigid aromatic poly(ethylene terephthalate) is considered to be bioinert [37-39]. Increased branching in polymeric materials will reduce the rate of degradation. Maximizing the linearity of the molecule reduces steric hindrance and facilitates the maximum susceptibility of the molecule to enzymatic attack and promotes assimilation by microorganism.

Synthetic polymers with short repeating units are more crystalline, making the hydrolysable groups inaccessible to enzymes, whereas synthetic polymers with long repeating units would be less likely to crystallize and might be biodegradable [40]. In the in-vitro chemical and enzymatic degradations of polymers, it was found that the composition of the copolymer giving the lowest melting point is most susceptible to degradation [41]. The lowest packing order corresponds with the fastest degradation rate.

Environmental conditions such as soil temperature, soil moisture content, degree of aeration (a measure of the concentration of oxygen), soil pH, presence of suitable microbes, presence of contaminants and their concentration, availability of nutrients, presence of electron acceptors,

redox potential, etc. affect the naturally occurring biodegradation at a given site [42]. Low temperature strongly inhibits degradation in soil. Water content of the soil supports hydrolytic degradation. Aeration supports oxidative degradation and the degree of aeration determines whether aerobic or anaerobic biotic degradation or both takes place. Biotic degradation also requires that the soil may be microbially active [43].

1.2.1.3 Biodegradable polymers

Acceptable standards define a fully biodegradable polymer as a polymer that is completely converted by microorganisms to carbon dioxide, water, minerals and biomass without leaving any potentially harmful substances.

- **Natural biodegradable polymers**

Natural polymers or biopolymers are polymers formed in nature during the growth cycles of all organisms. Polysaccharides such as starch and cellulose, chitin, polypeptides like gelatin, and bacterial polyesters such as poly- β -hydroxy butyrate (PHB) are examples of natural polymers.

- **Polymers with hydrolysable backbones**

Polymers with hydrolysable backbones have been found to be susceptible to biodegradation. Polyesters such as poly(glycolic acid) (PGA), poly(glycolic acid-co-lactic acid) (PGA/LA), poly(ϵ -caprolactone) (PCL), polyamide, polyurethane, polyanhydride, poly(amide-enamine), etc. are incorporated in this category.

- **Polymers with carbon backbones**

Vinyl polymers are generally not susceptible to hydrolysis. Their biodegradation requires an oxidation process and most of the biodegradable vinyl polymers contain an easily oxidisable functional group. Poly(vinyl alcohol) (PVA), poly(vinyl acetate) (PVAc) and polyacrylates are coming under this category [44-46].

1.2.1.4 Starch

Starch is a polymer which occurs widely in plants. The principal crops used for its production include potatoes, corn, rice and tapioca. Starch is a physical combination of linear amylose (figure 1.5) and branched amylopectin (figure 1.6) polymers, but it contains a single type of carbohydrate (glucose). Both cellulose and starch are composed of hundreds or thousands of D-glucopyranoside repeating units. In starch the glucopyranoside ring is present in the α -form while in cellulose it exists in β -form. These units are linked together by acetal bonds formed between the hemiacetal carbon atoms, C₁ of the cyclic glucose structure in one unit and a hydroxyl group at either the C₄ (for cellulose and amylose) or the C₆ (for the branch units in amylopectin) atoms in the adjacent unit. Amylose is crystalline but soluble in boiling water whereas amylopectin is insoluble in boiling water. The α -1,4-link in both components of starch is attacked by amylases and the α -1,6-link in amylopectin is attacked by glucosidases.

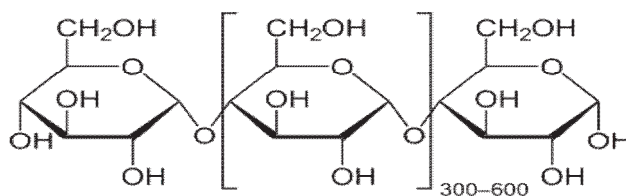


Figure 1.5 Structure of amylose

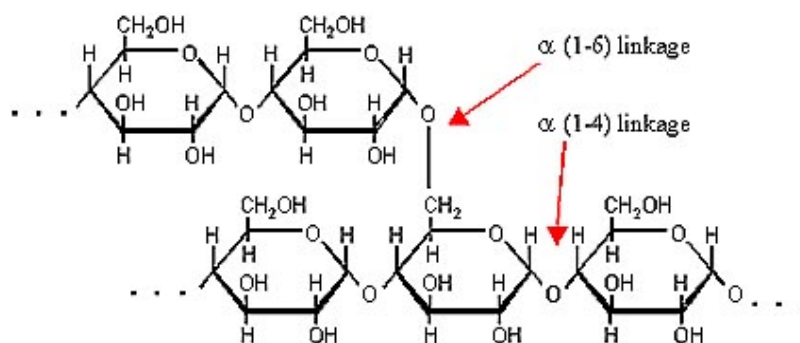


Figure 1.6 Structure of amylopectin

Starch films possess low permeability and are attractive materials for food packaging [47]. Starch is also useful for making agricultural mulch films because it degrades into harmless products when placed in contact with soil microorganisms. Although starch is a polymer, its stability under stress is not high. At temperatures higher than 150 °C, the glycosidic linkages start to break, and above 250 °C the starch grain endothermally collapses. At low temperatures, retrogradation, a phenomenon of reorganization of the hydrogen bonds and aligning of the molecular chain during cooling is observed.

The starch molecule has two important functional groups, the –OH group with nucleophilic character that is susceptible to substitution reactions and the C-O-C bond that is susceptible to chain breakage. Crosslinking or bridging of the –OH groups changes the structure into a network while increasing the viscosity, reducing water retention and increasing its resistance to thermomechanical shear [48].

1.2.1.5 Dextrin

Dextrins are a group of low-molecular-weight carbohydrates produced by the hydrolysis of starch or glycogen. Dextrins are mixtures of polymers of D-glucose units linked by α -(1,4) or α -(1,6) glycosidic bonds (figure 1.7).

Dextrins can be produced from starch using enzymes like amylases, as during digestion in the human body and during malting and mashing, or by applying dry heat under acidic conditions (pyrolysis or roasting). The latter process is used industrially, and also occurs on the surface of bread during the baking process, contributing to flavour, colour and crispness. Dextrins produced by heat are also known as pyrodextrins. During roasting under acidic conditions the starch hydrolyses and short chain starch parts partially re-branches with α -(1,6) bonds to the degraded starch molecule [49]

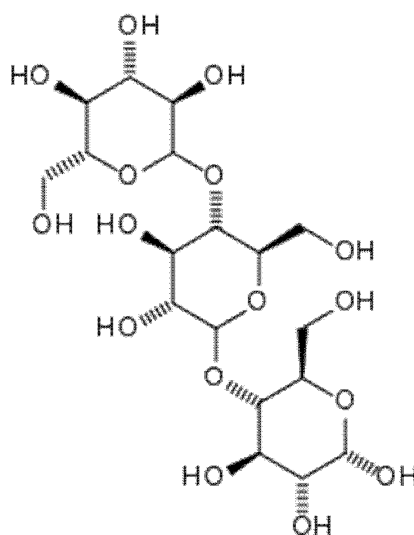


Figure 1.7 Structure of dextrin

Dextrins are white, yellow or brown powders that are partially or fully water-soluble, yielding optically active solutions of low viscosity. White and yellow dextrins from starch roasted with little or no acid is called British gum.

1.2.2 Photodegradation

The photodegradation of polymers is related to their ability to absorb tropospheric solar radiation. This includes the UV-B terrestrial radiation

(~295-315 nm) and UV-A radiation (~315-400 nm) responsible for the direct photodegradation (photolysis, initiated photo-oxidation). Visible part of sunlight (400-760 nm) accelerates polymeric degradation by heating. Infrared radiation (760-2500 nm) accelerates thermal oxidation [50]. Most plastics tend to absorb high-energy radiation in the ultraviolet portion of the spectrum, which activates their electrons to higher reactivity and causes oxidation, cleavage, and other degradation [51].

Oxo-biodegradation process uses two methods to start the biodegradation which are photodegradation (UV) and oxidation. The UV degradation uses UV light to degrade the end product. The oxidation process uses heat to break down the plastic. Both methods reduce molecular weight of the plastic and allow it to biodegrade [52].

There are two principal strategies to render polyethylene oxo-biodegradable [53]. The first is based on the introduction of a certain content of carbonyl groups directly into the polyethylene chain, or on the α -position of short branches during copolymerization processes, and the second is incorporation of pro-oxidants. Definitely, the latter is economically practical, as it respects current production and processing technologies.

1.2.2.1 Pro-oxidants

Pro-oxidants are chemicals that induce oxidative stress by creating reactive oxygen species [54]. The pro-oxidant and molecular oxygen are present mostly in the amorphous region of the polymer and hence the oxidation predominantly takes place there and leaves the crystalline region intact [55]. Materials with time programmed mechanical properties can be prepared by using a balanced mixture of antioxidant and pro-oxidant

additives. During exposure to the weather when the capacity of the antioxidant is used up, there will be a relatively faster loss of mechanical properties of the polymer due to the presence of pro-oxidant leading to its fragmentation.

Transition metal ions are the most widely reported pro-oxidant additives currently in use. The attractiveness of these additives lies in their ability to catalyse the decomposition of hydroperoxides into free radicals. The most commonly used transition metals include iron, cobalt and manganese. Iron is highly effective in accelerating photodegradation while manganese and cobalt are sensitive to thermal degradation [56].

Metal oxide polymer additives such as TiO_2 and ZnO are known UV absorbers and are often added to impart a white colour. The photostability of the metal oxides is very dependent on surface treatment, particle size and crystalline form. The UV stabilising effect of ZnO in polyolefins is well recognised [57-58]. The control of photoactivity via introduction of metal ions into the lattice has also been reported [59-60]. Similarly the effect of transition metal doped TiO_2 on the photodegradation of polyethylene has recently been reported [61]. European patent EP1696004 describes the use of transition metal coated pigments and fillers as pro-degradants [62]. The use of a transition metal coating on fillers such as the anatase or rutile form of titanium dioxide offers improved performance. The addition of TiO_2 with other metal stearate pro-oxidants has also been reported [63-64]. Preferred examples of prodegradants include manganese stearate, manganese oleate, manganese acetate, cobalt acetate, cobalt stearate, cupric oleate and ferric acetate [65-67].

1.2.3 Thermal degradation

Thermal degradation of polymers has great interest as it contributes to the solution of environmental problems [68]. Thermal degradation of polymers is the molecular deterioration as a result of overheating. Pyrolysis of plastics at different temperatures allows simultaneous decomposition and separation [69-70]. These processes result in the production of combustible gases and energy, with the reduction of landfilling as an added advantage [71-72]. The rate of thermal degradation directly depends upon the temperature, with higher values at higher temperatures. At high temperatures the components of the long chain backbone of the polymers begin to separate (molecular scission) and react with one another to change the properties of the polymer. The chemical reactions involved in thermal degradation lead to physical and optical property changes relative to the initially specified properties. Thermal degradation generally involves changes to the molecular weight of the polymer and the typical property changes include, reduced ductility, embrittlement, chalking, colour changes, cracking and general reduction in other desirable properties [73].

1.3 Degradation of polyolefins

In natural conditions, the degradation of plastics is a very slow process and it is a function of environmental factors such as temperature, humidity of air, moisture in the polymer, pH, absorption of solar energy, polymer properties and biochemical factors. Polyolefins are the most problematic plastics due to their hydrophobicity, high molecular weight, and lack of functional group recognizable by microorganisms [74]. The lack of water solubility of the additives used for the stabilization of the polymer further slow down the rate of degradation.

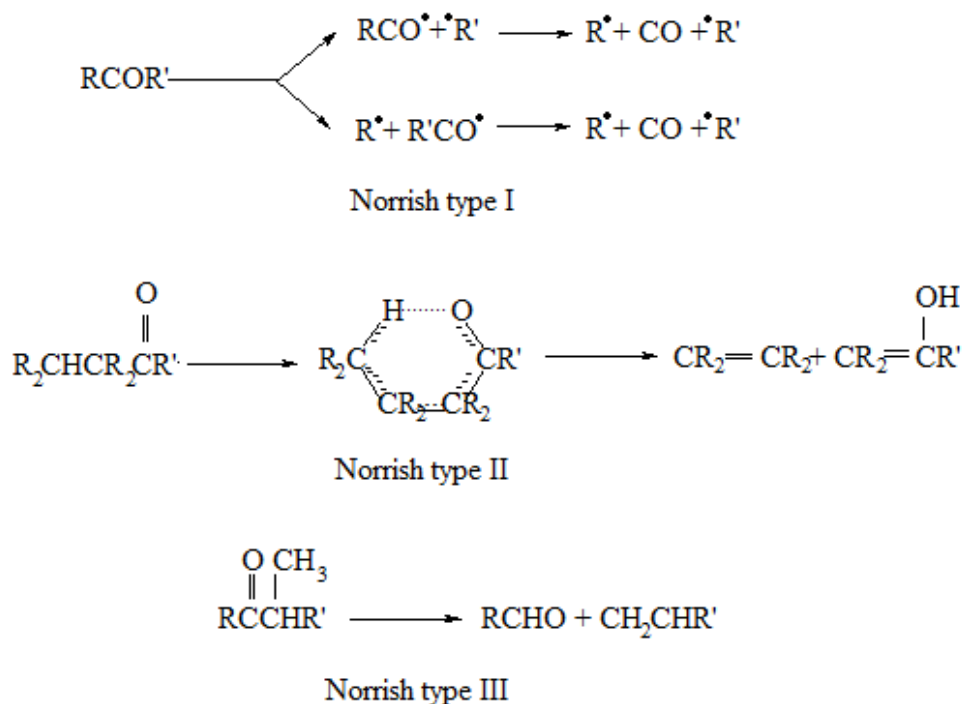
In both photo and thermal degradation of polyolefins, the resistance to degradation increases with increasing density of the polymer. This is because of the presence of lesser number of branches in the backbone of polyolefins that results in very low permeability to gases and a smaller number of tertiary carbon atoms that result in very few sensitive points of attack [75-77]. In addition to chain branching, chain defects, such as unsaturation, can also influence the rate of degradation. The oxidation susceptibility of polyolefins can be listed as follows: iPP (isotactic polypropylene) > LDPE > LLDPE > HDPE. Oxidative degradation in polypropylene leads primarily to chain scission, whereas in polyethylene cross linking occurs during the initial stages [78].

1.3.1 Mechanism of polyolefin degradation

Few reports have been published that elucidate the mechanism of degradation of polyolefins. Polyolefins are high molecular weight polymers, hydrophobic and thus not easily degraded by abiotic or biotic factors [79]. Due to their massive size, these molecules are unable to enter microbial cells to get digested by intracellular enzymes and they are inaccessible to the action of extracellular enzymes produced by microorganisms due to their excellent barrier properties. Exposure to UV radiation and heat is known to promote degradation of most polymers but polyolefins degrade very slowly under environmental conditions [61].

During photo-oxidation, cleavage occurs predominantly at the weak points which have lower bond energies and leads to the formation of free radicals [80]. The radicals can react with atmospheric oxygen and activate the oxidation of the polymer. This stepwise reaction produces carbonyls, aldehydes and acids [81-83]. The carbonyl group, if exposed again to UV,

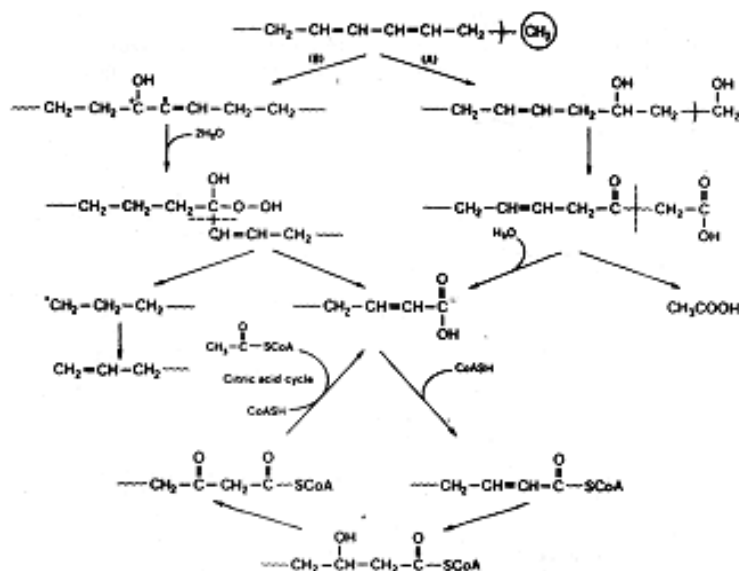
can follow Norrish type I and/or Norrish type II reaction to generate terminal double bond or ester group (scheme 1.1) [84-85].



Scheme 1.1 Norrish type reactions

During microbial assimilation, a decrease in carbonyl groups is noted. The carboxylic acids formed react with coenzyme A (CoA) to remove two carbon fragments, acetyl-CoA. The latter is metabolized in the citric acid cycle to produce carbon dioxide and water as the final degradation products. Photo-oxidation enhances the rate of biodegradation of the polymer which leads to the scission of the main chain in the polymer thereby leading to the formation of low molecular weight products. This results in the generation of large surface area due to its embrittlement and also a greater degree of hydrophilicity due to the introduction of carbonyl groups. All these factors further promote the biodegradation of the polymer

[86]. Tentative model for the biodegradation mechanism of LDPE is given in scheme 1.2.



Scheme 1.2 Tentative model for the biodegradation mechanism of LDPE:
(A) through oxidation of both main chains and end groups and
(B) through oxidation of exclusively main chain ends [81]

1.3.2 Enhancement of degradation of polyolefins

Efforts have been made to enhance the rate of biodegradation of polyolefins. The rate of biodegradation of polyolefins can be enhanced by:

- blending them with biodegradable natural polymer or with biodegradable synthetic polymer
- mixing with pro-oxidants
- carrying out pretreatment which includes exposure to thermal, UV, microwave or high energy radiation or chemicals
- isolating and growing microorganisms that can efficiently degrade these polymers

- improving the attachment of the organisms on the polymer surface by using surface active agents or including the microorganism to produce surfactant, and
- through genetic modification of the microorganism

1.3.2.1 Polyolefin-biodegradable polymer blends

Blending of natural polymers such as starch, chitin, cellulose, etc. with synthetic polymers is a strategy to enhance biodegradation. The percentage of natural polymer added in the blends affects the physical and mechanical properties of the synthetic polymers. The final properties of the blends depend on its morphology, crystalline nature of the polymer, interaction between the natural and synthetic polymer and processing conditions of the blends [87]. Starch provides higher oxygen permeability which helps in the release of degradation products from the sample, thus making the matrix hollow, increasing the surface to volume ratio [88-92].

The rate of biodegradation of polyolefins can also be enhanced by blending them with biodegradable synthetic polymer [93]. Copolymers of ethylene and styrene with vinyl ketone (methyl vinyl ketone) are being promoted as photodegradable plastics [15]. 80:20 blend of polycaprolactone (PCL) and polyethylene show enhanced fungal growth. The amorphous region of the blend which is contributed by PCL is degraded in 16 weeks [94]. Blends of LDPE-PCL and PP-PCL when reacted with partially purified lipase enzyme from *Rhizopus arrhizus* show a high level of biodegradability. The PCL content in the blend is degraded whereas LDPE and PP polymers in the blend remained unchanged [95].

1.3.2.2 Pretreatment of polymers

Pretreatment of polymers by physical or chemical methods prior to biodegradation have been reported to enhance the degradation process considerably.

1.3.2.2.1 Physical methods

Polymer waste dumped in the open undergoes photo initiation process by UV radiation in the sunlight and leads to the formation of free radicals. These radicals propagate forming further radicals in the polymer thereby increasing its reactivity. This pretreatment leads to a decrease in the weight average molecular weight of the polymer [96-97]. LDPE subjected to UV irradiation for 60 hours (pretreatment) showed a weight loss of 6.2% after keeping for 30 days in a culture medium containing *Brevibacillus borstelensis* [98]. Enhancement of degradation of UV irradiated polyethylene has been well understood [99].

Thermal pretreatment makes the polymer more potent to microbial attack. Thermal treatment oxidizes the chain thereby introducing hydroxyl, carboxyl and hydroperoxyl groups and makes the polymer more hydrophilic which is more conducive for the attachment of the organism. Thermally treated LDPE showed increase in carbonyl index by 23% and when treated with *Phanerochaete chrysosporium* (a fungus) showed increase in double bond index in three months indicating chain size reduction [100]. Thermally pretreated LDPE films containing pro-oxidants show 60% mineralization in six months during composting leading to a drop in molecular weight [24]. 48% degraded fragments were extracted in boiling acetone from thermally pretreated LDPE films containing pro-oxidant after 100 days immersion in river water [77].

High-energy radiations such as electron beam and gamma radiation can facilitate the biodegradation of polymer. Electron beam radiation is a form of ionising energy with low penetration and high dosage rates. Gamma rays are energetic form of electromagnetic radiation produced by radioactive decay of nuclei. The energy of radiation impinging on the polymer is absorbed by it; bringing required changes to it by way of producing radicals which can initiate several reactions in the polymer. Electron beam irradiated polymeric materials become brittle due to reduction in its molecular weight due to degradation [101]. Gamma irradiation leads to change in mechanical and electrical properties of PP [102].

1.3.2.2.2 Chemical methods

Chemicals attack the polymer chains resulting in the reduction in physical properties. It reacts or oxidise the functional groups in the chain and also can lead to depolymerisation. Chemicals form radicals and also allow solvent to permeate through the plastic leading to its dissolution. The FTIR data of LDPE, HDPE and PP after treatment with sulphuric acid show negative peak at 1740cm^{-1} indicating that the acid attacks and destroys carbonyl impurities [103]. PP treated with nitric acid at various concentrations and temperature showed that at 100°C its strength decreased considerably, while the weight loss remains unchanged [104].

1.4 Polymer blends

A polymer blend or polymer mixture is a member of a class of materials analogous to metal alloys, in which at least two polymers are blended together to create a new material with different physical properties [105]. It is well known that polymer/polymer blending is an effective method for improving the original physical properties of one or both of the

components, or for preparing new polymeric materials that exhibit widely variable properties without parallel in homopolymers [106]. Usually, there are two means to produce polymer composites: mixing them in the solutions, and blending the components in the molten state. The latter one is much more favourable in industry, since the production process can take place in conventional processing equipment with high yield. The market for polymer composites has increased dramatically during the last decades, mainly in the packaging, automotive and building area. However, most polymer composites are not immiscible. Polymer composites will be miscible only if free energy of mixing is negative:

$$\Delta G_{mix} = \Delta H_{mix} - T\Delta S_{mix}$$

The gain in entropy ΔS_{mix} is negligible, and the free energy of mixing can only be negative if the heat of mixing, ΔH_{mix} is negative, which requires specific interaction between the blend components. Their interactions may range from strong ionic bonding to weak and nonbonding interactions, such as hydrogen bonding. Usually, only van der Waals interaction occurs, which explains why polymer miscibility is the exception rather than the rule [107].

Contrary to the mixing of low molecular weight species, the mixing of two dissimilar polymers usually leads to a mixture with a phase-separated structure. The enthalpy of mixing is mainly responsible for the miscibility of polymer mixtures. The miscibility behaviour of different polymers is subsequently related to interactions between the components, which could be of different nature, for example dipole-dipole interactions, ionic interactions, or hydrogen bonding. Therefore, polymer blends can be distinguished by their phase behaviour. The most important methods for

judging the phase behaviour of polymer mixtures are thermal analysis by differential scanning calorimetry (DSC), or microscopic methods.

Polymer blending technology holds bright promise because of the following factors [108-111].

- 1) Blends are more economical to produce and generally have a lower technical risk than developing a new polymer or polymeric grade. They offer a cost-effective means to fill the gap in performance of existing materials.
- 2) Blends usually improve the critical properties required for end use. New materials, with properties either unique or intermediate between those of the blend components, are produced.
- 3) Blends often increase revenue/sales without major expenditure of capital investment.
- 4) Blends offer commodity plastics producers an easy way to enter the lucrative specialty segment of the business.
- 5) Waste plastics materials may be turned into useful products by blending them with similar or different plastics [112-113].
- 6) Polymer blending technology has the potential to produce plastics with various degrees of stability [114-115].

Polymer blends can be broadly divided into three categories:

- **Immiscible polymer blends** (heterogeneous polymer blends): This is by far the most populous group, having a completely phase-separated structure. If the blend is made of two polymers, two glass transition temperatures will be observed; the glass transition temperatures of

the components in the blends are exactly the same as for the pure components. Immiscible polymer blends form the same kind of structures as discussed for the compatible blends, but the size of the domains is usually larger. The interfacial strength in the immiscible blends is quite low, leading to adhesive failure and poor mechanical properties [116-117]. The morphology of immiscible blends can be modified by the addition of compatibilizers, which act like emulsifiers in oil/water mixtures. In order to overcome the subject of immiscibility in polymer blends, and to develop blends with satisfactory overall physicomachanical properties, compatibilization is practiced to optimize interfacial tension, to generate a dispersed phase of limited size and strong interfacial adhesion, and to improve the stress transfer between the component phases [118].

- **Compatible polymer blends:** Systems that are either partially miscible or completely immiscible but offer attractive mechanical performance are often designated as compatible polymer blends. The macroscopically uniform properties are usually caused by sufficiently strong interactions between the component polymers [119]. These blends usually have two glass transition temperatures, which may slightly deviate from the T_g of the blend components. The deviation of the glass transition temperatures from the T_g of the blend components might be different, and depends on the partial miscibility of each component in the other. On a microscopic scale, these polymer blends have a phase-separated structure (morphology) which could be of different nature, depending on the composition of the blends. Usually the major component forms the matrix phase, wherein particles of the minor phase are dispersed. In

the area of a 1:1 mixture, bicontinuous morphology can also be observed. The size of the dispersed particles is related to the interfacial tension and the viscosity ratio between the matrix and the dispersed phase. Another important feature of compatible blends is the high interfacial strength in these systems, which is mainly responsible for the attractive properties of these products. The most popular system belonging to this group is polycarbonate/acrylonitrile butadiene styrene polymer (PC/ABS) blends.

- **Miscible polymer blends** (homogeneous polymer blend): In miscible blends, the chain segments of the different polymers are miscible on a molecular level with a single-phase structure. These blends show only a single glass transition temperature (T_g), which mainly depends on the composition of the blend. Polyphenylene-ether/polystyrene blends are considered to be the most important example for miscible blends.

1.4.1 Factors affecting miscibility and immiscibility of polymer blends

A number of factors play role in the miscibility and immiscibility of polymer blends and alloys [120]. These are listed as:

- **Polarity**
Polymers with similar structure and with similar polarity are likely to form miscible polymer blends [121-122]. Difference in polarity leads to immiscibility.
- **Ratio of polymers**
For immiscible polymers, it is quite possible that a small amount of one polymer may be soluble in large amount of other polymer, thus

ratio of polymers play an important role in deciding the miscibility of polymer blends and alloys [123].

- **Specific group attraction**

Polymers that are attached to each other by hydrogen bonds, ion-dipole, donor-acceptor adduct, transition metal complexes, etc. are likely to impart miscibility [124-127].

1.5 Compatibilization

The formation of multi-phase systems is not necessarily an unfavourable event since many useful properties, characteristic of a single phase, may be preserved in the blend while other properties may be averaged according to the blend composition. Proper control of overall blend morphology and good adhesion between the phases are required in order to achieve good mechanical properties. Any modification of a blend which increases its compatibility can be termed compatibilization. In polymer blends, the compatibilizers are usually copolymers (block or graft copolymers) consisting of different segments which are miscible with the respective components of the blend. The influence of these copolymers has been related to their tendency to be preferentially located at the interface between phases and to the capability of their individual chain segments to penetrate into the phase to which they are chemically identical or similar [128]. During the melt mixing procedure the compatibilizer acts as polymeric surfactant, therefore the interfacial tension between the immiscible polymers is reduced, which leads to a significant particle size reduction of the dispersed phase. During the melt mixing process of immiscible polymers, the particle size of the dispersed phase first decreases as a consequence of the applied shear forces. At a certain particle size the tendency for coalescence of the

particles increases as a consequence of the increasing number of particles, therefore the average particle size grows again with mixing time.

In a multiphase blend, the interactions between the phases occur across the interface, and so the driving force for phase separation is located at the interfacial region. One of the main mechanisms of compatibilization is to reduce the interfacial tension between the phases. The mechanical behaviour of the multiphase system will depend on the nature of the interface and its ability to transmit stresses from one phase to the other. Thus, the adhesion between the phases is an important determinant of how the blend will respond to stress, that is, of mechanical properties such as tensile strength and toughness. One of the advantages of the use of compatibilizers is to decrease the interfacial tension as well as to increase the adhesion between the phases, by having chains present at the interface which are entangled with both the phases [129].

1.5.1 Methods of compatibilization

Generally, compatibilization is accomplished either by addition of a compatibilizer or introduction of reactive compatibilization. The former usually has a block structure, with one constitutive block miscible with one blend component and a second block miscible with the other blend component [107]. However, due to the lack of economically viable and industrially practical routes for synthesizing such additives, preformed block or graft copolymers have not been used extensively for compatibilization [130]. For physical modification the commercial polymer can be modified according to the requirement for miscibility in immiscible blends. Modification of polymer has become a major route to obtain structural and functional polymers with the desired physical and

chemical properties at lower cost [131]. Blending, cross linking, surface modification and graft copolymerization with pendent groups are effective methods [132-137].

An attractive alternative route, reactive compatibilization, is to form the block or graft copolymer *in situ* during blend preparation via interfacial reaction of added functionalized polymeric components. For the added polymers, functional groups can be placed along the chain by copolymerization or by grafting or at the chain end by special techniques [129]. The formation of copolymers at the interface will significantly reduce the dimensions of the phase domains and interfacial tension, stabilize the phase morphology, and strengthen the interface.

1.5.2 Applications of compatibilization

The compatibilizer is very effective in reducing the interfacial tension and improving interfacial adhesion by chain entanglement or bridging at the interphase. In a wider sense, the compatibilization is any chemical or physical action that results in stabilization of polymer blend morphology. Compatibilization promotes the formation of an interlocking structure that allows equal sharing of imposed stresses and might therefore improve the properties of the blends [138].

The application of compatibilizer is not only limited to the immiscible blends, but they can be used for refrigerant composition, compatibilizing the inorganic fillers such as calcium carbonate, glass fibers, talc or clay[139-141]. As a result the filler will adhere better to the polymer matrix and the properties of the final composite will be enhanced.

1.6 Ionomers

Ionomers constitute a class of synthetic polymers, which contain up to 15 mol% of ionic groups along a non-ionic polymer backbone. The pendant salt (e.g. carboxylic acid) groups present in the polymer are neutralized either partially or completely with metal ions [142]. The difference in polarity between the polar ionic groups and nonpolar polymer backbone results in the aggregation of the ionic groups in the polymer matrix. Thus, ionic groups tend to microphase separate and form ion-rich domains or ionic aggregates referred to as multiplets with sizes in the range of few nanometers. These ionic aggregates act as ionic cross-links which are responsible for the unique properties of ionomers [143-144]. The physical structure of ionomer is distinguished by interchain ionic bonding [145]. Due to the dissociation of the interchain ionic bonding at high temperatures, ionomers can be processed using standard thermoplastic processing methods. The ionic interactions and subsequent polymer properties are dependent on the type of polymer chain, ionic content, type of ionic moiety, degree of neutralization and type of cation. This combination of excellent properties and processing ease has led to the use of ionomers in much high performance material applications [146-148].

Most of the ionomers synthesized have carboxylate, sulfonate and to much lesser extent phosphate and phosphonates as pendant anions. It is well known that sulfonated ionomers associate much stronger than the carboxylated analogues [149]. This makes it very difficult to process sulfonated ionomers. An additional disadvantage is that they have to be fully neutralized in order to avoid thermal degradation at elevated temperatures. Carboxylated ionomers can be processed at elevated temperatures and partial neutralization of carboxylated groups results in stable ionomers.

1.6.1 Types of ionomers

The physical, mechanical and viscoelastic properties of ionomers are strongly dependent on the morphology of the ionomers. Several parameters such as the architecture of ionomers, flexibility of the backbone, dielectric constant of the polymer matrix, ionic content, degree of neutralization, chemical nature of the ionic groups and the presence of plasticizers determine the morphology in ionomers [150]. The architecture of the ionomer is one of the most important parameters that determine the morphology. By controlling the location of the ionic functionality on the polymer chain, a range of ionomers with large variation in architectures, such as random ionomers, telechelic ionomers, segmented ionomers and block ionomers can be synthesized [151].

- Most commercial ionomers, such as poly(ethylene-co-methacrylic acid) copolymers, which are partially neutralized with sodium or zinc hydroxides and sulfonated poly(tetrafluoroethylene) are **random ionomers** in which the ionic functionalities are randomly distributed along the polymer backbone.
- **Monochelic** is the ionomer with a single ion placed at the end of polymer chain and can be prepared by anionic polymerization [152]. Polystyrene (PS) containing terminal carboxylate anion is an example this type of ionomer.
- In **telechelics**, ion or ion pair is placed at each end of the polymer chain [153]. This type of ionomer can be synthesized by anionic or melt polymerization. Telechelic star is formed when three or multiple arm stars are tipped at each arm end by an ionic group. Polyisobutylene (PIB) with sulphonic acid at the terminal positions are example of telechelic stars [154].

- **Block ionomers** have a regular architecture. Diblock (AB-type) [155], triblock (ABA-type) [156], star block [157] and dendrimer [158] are the major types.

1.6.2 Polyethylene based ionomers

Ionomers based on polyethylene are copolymers with pendant carboxylate groups in which the polyethylene backbone is the major component. The most widely used ionomers of this class have been based on poly(ethylene-co-methacrylic acid) (EMAA) (figure 1.8). Poly(ethylene-co-acrylic acid) (EAA) series ionomers too belongs to this class. The methacrylic acid and acrylic acid content of these ionomers is in the range 3-10 weight %. The metal cation used for neutralization may be monovalent (Na^+ or Li^+), divalent (Ba^{2+} , Mg^{2+} or Zn^{2+}), or trivalent (Al^{3+}). The characteristic properties of these materials include excellent tensile properties, good clarity, high melt viscosities [159] and marked reduction in haze after neutralization. The degree of crystallinity of ionomers is comparable to that of conventional polyethylene. However, ionic interactions are invoked to effect two changes: nucleation of crystallites, and increase in viscosity that slows down the growth of crystallites into spherulites [160].

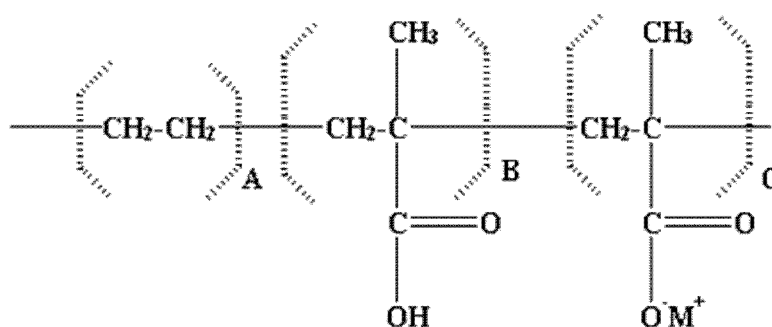


Figure 1.8 Metal salts of poly(ethylene-co-methacrylic acid)

The inclusion of a few mole % ionic groups along the backbone has a tremendous effect upon the morphology and properties of the polymer. Poly(ethylene-co-methacrylic acid) ionomers typically show an increased melt viscosity, toughness, clarity, and adhesion. The increased clarity, a desirable property in packaging applications, is due to the reduction of crystallinity in the copolymer. The presence of the methacrylic acid units and the neutralized carboxylate anion/cation pairs provides sites for ionic interaction. Hydrogen bonding between carboxylic acid moieties will form dimers. Interactions between ion pairs, and the non-polar nature of the backbone, will cause the ions to aggregate together. At low mole % incorporation of methacrylic acid, or low % neutralization, the ion pairs will exist as isolated polar groups in the bulk polymer. However, above a certain critical ionic concentration, the ion pairs will assemble into larger groups. The end result is the formation of an ion rich phase within the bulk of the polymer. The assembled ionic aggregates act as thermally reversible cross-links, greatly modifying the viscoelastic properties of the resulting polymer. These aggregations of ions have been termed "multiplets".

1.6.3 Ionomer as compatibilizer

Ionomers have attracted interest for many years because of their unique properties as homopolymers and their ability to compatibilize certain incompatible blends [161-163]. In the case of polypropylene (PP)-based blends, different kinds of ionomers have been used to compatibilize them. Thus, ionomers based on poly(ethylene-co-methacrylic acid) (PEMA) have been used in PP-based nanocomposites [164] and in blends of PP with liquid crystalline polymers (LCP) [165] and poly(ethylene-co-vinyl alcohol) (EVOH) [166-169]. Ionomers of poly(ethylene-co-acrylic acid) have been used in PP/LCP blends [170], ionomers of poly(ethylene-

methacrylic acid-isobutylacrylate) in PP/polyamide-6 (PP/PA6) blends [171-172], and liquid-crystalline ionomers in blends of PP with both polyamide and poly(butylene terephthalate) [173-175]. The use of ionomers containing ionic sulfonate groups, as compatibilizers in polymer blends has been the subject of many patents [176-178]. The utilization of a polyester ionomer as a minor component compatibilizer have a significant effect on the phase morphology and mechanical properties of polyester/polyamide blends through the presence of specific interactions between the ionomer sulfonate group/counterion and the amide linkage of the polymer [179]. An increase in the ion content and ionomer incorporation resulted in reduced phase separated domain sizes as well as increased interphase mixing. The ionomer enhances the ultimate mechanical properties of the blends as a result of increased interfacial adhesion [180].

While polar and nonpolar polymers are immiscible due to the very low entropy of mixing, miscibility enhancement can be achieved when an ionomer is used as a compatibilizer. The intermolecular polar-polar interactions of ionomer with polar polymer lower the heat of mixing so that the thermodynamics of blending can lead to miscibility improvement of the blend components. The use of ionomer is particularly attractive in this respect since the ionic groups introduce the possibility of strong ion-ion, ion pair- ion pair or ion-dipole interactions with polar polymer. The incorporation of ionomer modifies the blend properties profoundly. The presence of ionomer at the interface between immiscible polymer blend reduces the interfacial tension, leading to the stabilization which retards dispersed phase coalescence, and strengthens the interface between the phases. A significant achievement in the physical properties of the blend may

be considered as an evidence for the significant reduction in the dimensions of the phase domains [181].

Samios et al [182] have reported that the melt-mixed blends of poly(ethylene-co-cyclohexane 1,4-dimethanol)/poly(ethylene-co-vinyl alcohol) (PETG/EVOH) may be compatibilized using the sodium or zinc salt of poly(ethylene-co-acrylic acid). Zinc-neutralized and sodium-neutralized ionomers have been extensively studied as blend compatibilizers for the polyamide-polyethylene system [183-188]. The addition of compatibilizer has shown repeatedly an increase in compatibility between the two components, including improvements in mechanical properties, barrier properties and smaller dispersed domain sizes [189-191].

1.7 Scope and objectives of the work

Low density polyethylene (LDPE), the most common polymer used in the world, is the major polymer present in the municipal solid waste, since they are completely resistant to microbial or enzymatic attack. A more economical way to improve the biodegradability of low density polyethylene is the blending of LDPE with renewable polymers from natural sources. Among the commercially available natural polymers, starch has received much attention due to its availability, inexpensiveness, renewability and biodegradability. Since the rate of degradation of starch is higher than that of the polyethylene, the presence of starch in the polyethylene packaging enhances the biodegradation process. The logic behind the incorporation of biopolymer in LDPE is that if the biodegradable component is present in the sufficient amount, and if it is removed by microorganism in the waste disposal environment, then the base inert plastic should slowly disintegrate and disappear.

However, nonpolar polyethylene is thermodynamically incompatible with polar starch. An increase in the starch content in the blend deteriorates the physico-mechanical characteristics of the products owing to incompatibility of the blend components. The starch concentration in a blend with polyethylene should be fairly high to make the composite biodegradable. The development of biodegradable polymeric materials combining high biodegradability with good mechanical properties still remains as a cherished desire of researchers in material science and polymer composite technology.

Compatibilization of the blend components is one of the ways to enhance the miscibility of polymers in a blend. By the introduction of a compatibilizer, an increase in stress transfer between the continuous and dispersed phases in blend is facilitated, improving the mechanical properties of the blend. Ionomers have the unique ability to compatibilize certain incompatible blends. When ionomers are added to the binary blends, they form ionic cross links at the interface of the blends and improve the mechanical properties of the blends.

It is known that the photo-oxidation is an important first degradation step for non-hydrolysable materials such as polyethylene. Photo-oxidation increases the amount of low molecular weight material by breaking bonds and increasing the surface area. In the second degradation step microorganisms may utilize the degradation products. Among many approaches used to induce degradation in polyethylene, use of pro-oxidants which induce abiotic oxidation, leading to the reduction of molecular mass to levels where the material becomes susceptible to microbial attack has been gaining popularity recently. Pro-oxidants help in the insertion of oxygen

atom into the polymer chain. Increased surface area as well as increased oxygen permeability can enhance degradation.

The present work is an attempt to improve the biodegradability and photodegradability of low density polyethylene. The specific objectives of the present work are:

- Preparation of biodegradable blends based on low density polyethylene
- Evaluation of effectiveness of polyethylene-co-methacrylic acid ionomers as compatibilizer for the blends of low density polyethylene and starch
- Investigation of mechanical, thermal, spectroscopic, morphological and flow characteristics of the blends.
- Exploration of biodegradability and photodegradability of ionomer compatibilized low density polyethylene-starch blends
- Investigation of the effect of metal oxides and metal stearates as pro-oxidants on ionomer compatibilized low density polyethylene-starch blends

References

- [1] Thompson, R. C.; OIsen, Y.; Mitchell, R. P.; Davis, A.; Rowland, S. J.; John, A. W. G.; McGonigle, D.; Russell, A. E.; *Science* 2004, 304, 838.
- [2] http://cipet.gov.in/plastics_statics.html
- [3] Amass, W.; Amass, A.; Tighe, B.; *Polym Int* 1998, 47, 89.
- [4] Vert, M.; Dos Santos, I.; Ponsart, St.; Alauzet, N.; Morgat, J. L.; Coudane, J.; Garreau, H.; *Polym Int* 2002, 51, 840.

- [5] Bohlmann, G.; Toki, G.; Chemical economics handbook, SRI International ed., 2004.
- [6] Orhan, Y.; Buyukgungor, H.; Inter Biodeter Biodegr 2000, 45, 49.
- [7] Sailaja, R. R. N.; Seetharamu, S.; React Funct Polym 2008, 68,831.
- [8] Clarinval, A.; Halleux, J.; Classification of biodegradable polymers, in: Smith R (Ed.); Biodegradable Polymers for Industrial Applications, Woodhead, London, 2005.
- [9] Griffin, G. J. L.; Adv Chem Ser 1974, 134, 114.
- [10] Paul, D. R.; Vincen, C. E.; Locke, C. E.; Polym Eng Sci 1972, 12, 157.
- [11] Hallden, A.; Ohisson, B.; Wesslen, B.; J Appl Polym Sci 2000, 78, 2416.
- [12] Weaver, E. P.; Eur Pat EP86069 A2 (1983).
- [13] Baker, M. A. M.; Mead, J.; Thermoplastics, in: Harper, C. A (Ed); Handbook of plastics, elastomers and composites, 4th edn, McGraw-Hill, New York, 2002.
- [14] Pedroso, A. G.; Rosa, D. S.; Polym Adv Technol 2005, 16, 310.
- [15] Chiellini, E.; Corti, A.; Sift, G.; Polym Degrad Stab 2003, 81,341.
- [16] Kresser, T. O. J.; Polyolefin Plastics, Van Nostrand Reinhold Company, New York, 1969.
- [17] Brydson, J. A.; Plastics Materials, 7th edn, Butterworth-Heinemann, Jordan Hill, Oxford, 1999.
- [18] Charlesby, A.; Radiation Chemistry of Polymers, in: Farhataziz; Rodgers, M. A. J.(Eds.); Irradiation of Polymers, USA: VCH Publishers, Inc. 1987.
- [19] Pospisil, J.; Nespurek, S.; Macromol Symp 1997, 115, 63.
- [20] Agamuthu, P.; Faizura, P. N.; Waste Manage Res 2005, 23, 95.
- [21] Albertsson, A. C.; Eur Polym J 1980, 16, 623.
- [22] Narayan, R.; ACS Symp Ser 1992, 476.

- [23] Rabek, J.; Photodegradation of polymers-physical characteristics and application, Springer, Germany, 1996.
- [24] Jakubowicz, I.; Polym Degrad Stabil 2003, 80, 39.
- [25] Krzan, A.; Hemjinda, S.; Miertus, S.; Corti, A.; Chiellini, E.; Polym Degrad Stab 2006, 91, 2819.
- [26] www.ics.trieste.it
- [27] Baciú, R.; Swift, G.; Synthetic polymers that environmentally degrade by a combination of abiotic and biotic processes, BEPS/SPI, Chicago, June 2006.
- [28] Shah, P. B.; Bandopadhyay, S.; Bellare, J. R.; Polym Degrad Stab 1995, 47, 165.
- [29] Weiland, M.; Daro, A.; David, C.; Polym Degrad Stab 1995, 48, 275.
- [30] Kyrikou, I.; Briassoulis, D.; J Polym Environ 2007, 15, 125.
- [31] Gu, J. D.; Ford, T. E.; Mitton, D. B.; Mitchell, R.; Microbial corrosion of metals, in: Revie, W. (Ed.); The Uhlig Corrosion Handbook, 2nd edn, New York, Wiley, 2000, pp. 27-915.
- [32] Stevens, E. S.; Green plastics: an introduction to the new science of biodegradable plastics, Princeton University Press, 2002.
- [33] Bonhomme, S.; Cuer, A.; Delort, A. M.; Lemaire, J.; Sancelme, M.; Scott, G.; Polym Degrad Stab 2003, 81, 441.
- [34] Bhattacharya, M.; Reis, R. L.; Correlo, V.; Boesel, L.; In: Smith, R. (Ed.); Biodegradable Polymers for Industrial Applications, Woodhead Publishing Limited, Cambridge, London, 2005.
- [35] Matsumura, S.; Mechanism of Biodegradation, In: Smith, R. (Ed.); Biodegradable Polymers for Industrial Applications, Woodhead Publishing Limited, Cambridge, London, 2005.
- [36] Huang, S. J.; Bansleben, D. A.; Knox, J. R.; J Appl Polym Sci 1979, 23, 429.
- [37] Bailey, W. J.; Okamoto, Y.; Kuo, W. C.; Narita, T.; in: Sharpley, J. M.; Kaplan, A. M. (Eds); Proc 3rd Int Biodegradation Symp, Applied Science Publishers, New York, 1976, 765.

- [38] Potts, J. E.; in: Grayson, M.(Ed.); Kirk- Othmer Encyclopedia of Chemical Technology, Suppl. Vol., Wiley-Interscience, New York, 1984, 626.
- [39] Tokiwa, Y.; Suzuki, T.; Agric Biol Chem, 1977, 41, 265.
- [40] Huang, S. J.; Bitritto, M.; Leong, K. W.; Paulisko, J.; Roby, M.; Knox, J. R.; Adv Chem Ser 1978, 169, 205.
- [41] Zeikov, G. E.; Livshitzm, U. S.; Polym Degrad Stab 1987, 17, 65.
- [42] Matsunaga, M.; Whitney, P. J.; Polym Degrad Stab 2000, 70, 325.
- [43] Calmon-Decriaud, A.; Bellon-Maurel, V.; Silvestre, F.; Adv Polym Sci 1998, 135,207.
- [44] Casey, J. P.; Manly, D. C.; in: Proc 3rd Int Biodegradation Symp, Applied Science Publishers, New York, 1976, 819.
- [45] Rosato, D. V.; in: Rosato, D. V.; Schwartz, R. T.(Eds); Environmental Effects on Polymeric Materials, Wiley-Interscience, New York, 1968, pp. 991.
- [46] Brown, A. E.; Mod Plast, 1946, 23, 189.
- [47] Otey, F. H.; Westhoff, R. P.; Russell, C. R.; Ind Eng Chem Prod Res Dev 1977, 16, 305.
- [48] Huang, J. C.; Shetty, A. S.; Wang, M. S.; Adv Polym Technol 1990, 10, 23.
- [49] Finar, I. L.; Organic Chemistry Vol 2: Stereochemistry and the Chemistry of Natural Products, 5th edn, Pearson Education (Singapore) Pte. Ltd., 1973, pp. 339-341.
- [50] Gugumus, F.; in: Pospisil, J.; Klemchuk, P. P. (Eds.); Photo-oxidation of polymers and its inhibition, Oxidation inhibition in organic materials, CRC press, 1990, pp. 29-162.
- [51] Shah, A. A.; Hasan, F.; Hameed, A.; Ahmed, S.; Biotech Advances 2008, 26, 246.
- [52] <http://www.willowridgeplastics.com/faqs.html>, 2005.

- [53] Arnaud, R.; Dabin, P.; Lemaire, J.; Al-Malaika, S.; Chohan, S.; Coker, M.; *Polym Degrad Stab* 1994, 46, 211.
- [54] Puglia, C. D.; Powell, S. R.; *Environ Health Perspect* 1984, 57, 11.
- [55] Albertson, A. C.; Karlsson, S.; *Prog in Polym Sci* 1990, 15, 177.
- [56] Ammala, A.; Bateman, S.; Dean, K.; Petinakis, S.; Sangwan, P.; Wong, S.; Yuan, Q.; Yu, L.; *Prog Polym Sci* 2010, doi:10.1016/j.progpolymsci.2010.12.002.
- [57] Ammala, A.; Hill, A. J.; Meakin, P.; Pas, S. J.; Turney, T. W.; *J Nanopart Res* 2002, 4, 167.
- [58] Hill, A. J.; Turney, T.; Ammala, A.; *PMSE*, 2003, 89, 719.
- [59] Casey, P. S.; Boskovic, S.; Lawrence, K.; Turney, T.; in: *NSTI Nanotech 2004, Vol 3, Technical Proceedings*, Boston, 2004.
- [60] Casey, P. S.; Rossouw, C. J.; Boskovic, S.; Lawrence, K. A.; Turney, T. W.; *Superlattices Microstruct* 2006, 39, 97.
- [61] Kemp, T. J.; McIntyre, R. A.; *Polym Degrad Stab* 2006, 91, 3020.
- [62] Janssens, M.; Daponte, T.; Pat EPI 1696004, assigned to Schulman Plastics, 2006.
- [63] Li, J.; Ren, J.; Pat CN 101260195, assigned to Li, J., 2008.
- [64] Ren, J.; Li, J.; Pat CN 101311206, assigned to Ren, J., 2008.
- [65] Roy, P. K.; Surekha, P.; Rajagopal, C.; Choudhary, V.; *Polym Degrad Stab* 2006, 91, 8.
- [66] Roy, P. K.; Titus, S.; Surekha, P.; Tulsi, E.; Deshmukh, C.; Rajagopal, C.; *Polym Degrad Stab* 2008, 93, 22.
- [67] Roy, P. K.; Surekha, P.; Raman, R.; Rajagopal, C.; *Polym Degrad Stab* 2009, 94, 1033.
- [68] Martin-Gullon, I.; Esperanza, M.; Font, R.; *J Anal Appl Pyrolysis* 2001, 58, 635.

- [69] Marongiu, A.; Faravelli, T.; Bozzano, G.; Dente, M.; Ranzi, E.; J Anal Appl Pyrolysis 2003, 70, 519.
- [70] Kiran, N.; Ekinci, E.; Snape, C. E.; Resour Conserv Recycl 2000, 29, 273.
- [71] Ceamanos, J.; Mastral, J. F.; Millera, A.; Aldea, M. E.; J Anal Appl Pyrolysis 2002, 63, 93.
- [72] Bockhorn, H.; Hornung, A.; Hornung U.; Schawaller, D.; J Anal Appl Pyrolysis 1999, 48, 93.
- [73] Olayan, H. B.; Hamid, H. S.; Owen, E. D.; J Macromol Sci Rev Macromol Chem Phys 1996, 36, 671.
- [74] Arutchelvi, J.; Sudhakar, M.; Arkatkar, A.; Doble, M.; Bhaduri, S.; Uppara, P. V.; Indian J Biotech 2008, 7, 9.
- [75] Wiles, D. M.; Scott, G.; Polym Degrad Stab 2006, 91, 1581.
- [76] Feldman, D.; J Polym Environ 2002, 10, 163.
- [77] Chiellini, E.; Corti, A.; D'Antone, S.; Baci, R.; Polym Degrad Stab 2006, 91, 2739.
- [78] Eyenga, I. I.; Focke, W. W.; Prinsloo, L. C.; Tolmay, A. T.; Macromol Symp 2002, 178, 139.
- [79] Haines, J. R.; Alexander, M.; Appl Microbiol 1974, 28, 1084.
- [80] Davis, A.; Sims, D.; Photooxidation and stabilization, in Weathering of polymers, UK, Springer, 1983, pp.112-120.
- [81] Albertson, A. C.; Barenstedt, C.; Karlsson, S.; Lindberg, T.; Polymer 1995, 36, 3075.
- [82] Albertson, A. C.; J Appl Polym Sci 2003, 22, 3419.
- [83] Khabbaz, F.; Albertson, A. C.; Karlsson, S.; Polym Degrad Stab 1999, 63, 127.
- [84] Albertson, A. C.; Andersson, S. O.; Karlsson, S.; Polym Degrad Stab 1987, 18, 73.

- [85] Vasile, C.; Degradation and decomposition, in: Vasile, C.; Seymour, R. B. (Eds.) *Handbook of Polyolefins Synthesis and Properties*, New York, Marcel Dekker Inc, 1993, pp. 479-506.
- [86] Arkatkar, A.; Arutchelvi, J.; Sudhakar, M.; Bhaduri, S.; Uppara, P. V.; Doble, M.; *The Open Environ Eng J* 2009, 2, 68.
- [87] Oldak, D.; Kaczmarek, H.; *J Mater Sci* 2005, 40, 4189.
- [88] Rutkowska, M.; Heimowska, A.; Krasowska, K.; Janik, H.; *Polish J Environ Sci* 2002, 11, 267.
- [89] Johnson, K. E.; Pometto III, A. L.; Nikolo, Z. L.; *Appl Environ Microb* 1993, 59, 1155.
- [90] El-Shafei, H. A.; El-Nasser, N. H. A.; Kanosh, A. L.; Ali, M.; *Polym Degrad Stab* 1998, 62, 361.
- [91] Zeena, P. H.; Dilfi, A. K. F.; Kurian, T.; Bhat, S. G.; *Int J Polym Mater* 2009, 58(5), 257.
- [92] Dilfi, A. K. F.; Zeena, P. H.; Kurian, T.; Bhat, S. G.; *Polym-Plast Technol* 2009, 48(6), 602.
- [93] Ioannis, S.; Annis, A.; *J M S- Rev Macromol Chem Phys* 1999, 39(2), 205.
- [94] Tilstra, L.; Johnsonbaugh, D.; *J Environ Polym Degrad* 1993, 1, 257.
- [95] Lwamoto, A.; Tokiwa, Y.; *Polym Degrad Stabil* 1994, 45, 205.
- [96] Koutny, M.; Sancelme, M.; Dabin, C.; Pichon, N.; Delort, A. M.; Lemaire, J.; *Polym Degrad Stabil* 2006, 91, 1495.
- [97] Albertson, A. C.; Sares, C.; Karlsson, S.; *Acta Polymerica*, 1993, 44, 243.
- [98] Hadad, D.; Geresh, S.; Sivan, A.; *J Appl Microbiol*, 2005, 98, 1093.
- [99] Onodera, K. Y.; Mukumoto, H.; Katsuyaya, Y.; Saiganji, A.; Tani, Y.; *Polym Degrad Stabil* 2001, 72, 323.
- [100] Sepulveda, T. V.; Torres, E. F.; Guzman, A. M.; Gonzalez, M. L.; Quintero, G. T.; *J Appl Polym Sci* 1999, 73, 1435.

- [101] Yoshii, F.; Meligiz, G.; Sasaki, T.; Makuuchi, K.; Rabie, A. M.; Nishimoto, S.; Polym Degrad Stab 1995, 49, 315.
- [102] Demertzis, P. G.; Franz, R.; Welle, F.; Packag Technol Sci 1991, 12, 119.
- [103] Cameron, G. G.; Main, B. R.; Polym Degrad Stabil 1983, 5, 215.
- [104] Volcheck, M.; Goryainova, A. V.; Klinov, I. Y.; Chem Petrol Eng 1968, 4, 911.
- [105] Strobl, G. R.; The Physics of Polymers Concepts for Understanding Their Structures and Behavior, Springer-Verla, 1996, ISBN 3-540-60768-4.
- [106] Nishio, Y.; Polysaccharides II 2006, 97, 151.
- [107] Koning, C.; Duin, V. M.; Pagnouille, C.; Jerome, R.; Prog Polym Sci 1998, 23, 4.
- [108] Utracki, L. A.; Polym Eng Sci 1982, 22, 1166.
- [109] Utracki, L. A.; Polym Plast Technol Eng 1984, 22, 27.
- [110] Hamielec, L. A.; Polym Eng Sci 1986, 26, 111.
- [111] Hamid, S. H.; Atiqullah, M.; JMS-Rev Macromol Chem Phys 1995, 35, 495.
- [112] Milgrom, J.; Polym Plast Technol Eng 1982, 18, 167.
- [113] Sadrmoahagheh, C.; Scott, G.; Setudeh, E.; Polym Plast Technol Eng 1985, 24, 149.
- [114] Bremer, W. P.; Polym Plast Technol Eng 1982, 18, 137.
- [115] Kolawole, E. G.; Agboola, M. O.; J Appl Polym Sci 1982, 27, 2317.
- [116] Campoy, I.; Aribas, J. M.; Zaporta, M. A. M.; Marco, C.; Gomez, M. A.; Fatou, J. G.; Eur Polym J 1994, 31(5), 475.
- [117] Favis, B. D.; Hhalifoux, J. P.; Polymer 1988, 29, 1761.
- [118] Barlow, J.; Paul, D.; Polym Eng Sci 1984, 24, 525.
- [119] <http://goldbook.iupac.org/CT07581.html>
- [120] Vyas, H. A.; PhD Thesis 2009, The Maharaja Sayajirao University of Baroda, Vadodara, India.

- [121] Gaylord, N. G.; Chemtech, 1976, 392.
- [122] Paul, D. R.; Newmann, S.; Polymer Blends, 2, Academic press, New York, 1978.
- [123] Markham, R. L.; Adv Polymerization Tech 1991, 10, 231.
- [124] Utracki, L. A.; Polymer Alloys and Blends, Hanser, New York, 1990.
- [125] Barlow, J. W.; Shaver, G.; Paul, D. R.; Compalloy 1989, 89, 221.
- [126] Gaylord, N. G.; J Macromol Sci Chem 1989, A26(8), 1211.
- [127] Xanthos, M.; Dagli, S. S.; Polym Eng Sci 1991, 31(13), 929.
- [128] Rudin, A; J Macromol Sci Rev Macromol Chem 1980, 19, 267.
- [129] Datta, S.; Lohse, D. J.; Poymeric Compatibilizers Use and Benefits in Polymer Blends, Hanser Publishers, Munich Vienna New York, 1996.
- [130] Paul, D. R.; Bucknall, C.; Polymer Blends, Wiley, 2000.
- [131] Meister, J. J.; Polymer Modification: Principle, Techniques and Applications, 1 edn, Marcel Dekker, New York, 2000.
- [132] Song, Y.; Liu, F.; Sun, B.; J Appl Polym Sci 2005, 95, 1251.
- [133] Song, Y.; Sun, P.; Henry, L. L.; Sun, B.; J Membr Sci 2005, 67, 251.
- [134] Rengarajan, R.; Vicic, M.; Lee, S.; J Appl Polym Sci 1991, 39, 1783.
- [135] Qian, Y.; Wei, Y.; Tu, J.; Guan, R.; Song, Y.; Polym Eng Soc 1995, 1, 200.
- [136] Zhou, J.; Yan, F.; J Appl Polym Sci 2004, 93, 948.
- [137] Jung, W. C.; Park, K. Y.; Kim, J. Y.; Suh, K. D.; J Appl Polym Sci 2003, 88, 2622.
- [138] Ajji, A.; Utracki, L. A.; Polym Eng Sci 1996, 36, 1574.
- [139] Patent No: 485/MUMNP/2003 assigned to E.I.Du Pont De Nemours and Company, 2003.
- [140] Patent No: 3553/DELNP/2006 assigned to Eastman Chemical Company, 2006.

- [141] Hindryckx, F.; Dubois, P.; Patin, M.; Jerome, R.; Teyssie, P.; Marti, G. M.; J Appl Polym Sci 1995, 56, 1093.
- [142] Eisenberg, A.; Kim, J. S.; Introduction to ionomers, John Wiley & Sons, Inc, 1998.
- [143] Tant, M. R.; Mauritz, K. A.; Wilkes, G. L. (Eds.); Ionomers: Synthesis, Structure, Properties and Applications, Blackie Academic and Professional, London, 1997.
- [144] Schlick, S. Ionomers: Characterization, Theory, and Applications, CRC Press, Boca Raton, FL, 1996.
- [145] Eisenberg, A.; Rinaudo, M.; Polym Bull 1990, 24,671.
- [146] Bazuin, C. G.; In: Polymeric Materials Encyclopedia, Salamone, J. C., (Ed.); CRC, Boca Raton, FL, 3454, 1996.
- [147] Hara, M.; In: Polymeric Materials Encyclopedia, Salamone, J. C., (Ed.); CRC, Boca Raton, FL, 3473, 1996.
- [148] Longworth, R.; In: Ionic Polymers, Holliday, (Ed.); Applied Science Publishers, London, Ch 2, 1973.
- [149] Venkateshwaran, L. N.; York, G. A.; Deporter, C. D.; McGrath, J. E.; Wilkes, G. L.; Polymer 1992, 33, 2277.
- [150] Eisenberg, A.; Hird, B.; Moore, R. B.; Macromolecules 1990, 23, 4098.
- [151] Karanam, S.; Nano-scale Ionic Cross-links in Polymers Controlled synthesis, Morphology and Mechanical properties, Eindhoven University Press, Eindhoven, The Netherlands, 2003.
- [152] Eisenberg, A.; Adv Polym Sci, 1967.
- [153] Jerome, R.; In: Telechelic Polymers: Synthesis and Applications, Geothals, E. J., (Ed.); CRC, Boca Raton, FL, Ch 11, 1989.
- [154] Bagrodia, S.; Mohajer, Y.; Wilkes, G. L.; Storey, R. F.; Kennedy, J. P.; Polym Bull 1983, 9, 174.
- [155] Selb, J.; Gallot, Y.; J Polym Sci Polym Lett Ed 1975,13, 615.

- [156] Weiss, R. A.; Sen, A.; Willis, C. L.; Pottick, L. A.; *Polymer* 1991, 32, 1867.
- [157] Storey, R. F.; George, S. E.; Nelson, M. E.; *Macromolecules* 1991, 24, 2920.
- [158] Vanhest, J. C. M.; Baars, M. W. P. L.; Elissan-Roman, C.; Van Genderen, M. H. P.; Meijer, E. W.; *Macromolecules* 1995, 28, 6689.
- [159] Rees, R. W.; (to E.I.DuPont de Nemours and Co.), U.S.Patent 3264272, 1966.
- [160] Rees, R. W.; (to E.I.DuPont de Nemours and Co.), U.S.Patent 3404134, 1968.
- [161] Gimenez, E.; Lagaron, J. M.; Saura, J. J.; Gavara, R.; *Rev Plast Mod* 2001, 82, 568.
- [162] Samios, C. K.; Kalfoglou, N. K.; *Polymer* 1998, 39, 3863.
- [163] Kalfoglou, N. K.; Samios, C. K.; Papadopolulou, C. P.; *J Appl Polym Sci* 1998, 68, 589.
- [164] Liu, H.; Lim, H. T.; Ahn, K. H.; Lee, S. J.; *J Appl Polym Sci* 2007, 104, 4024.
- [165] Vallejo, F. J.; Eguiazabal, J. I.; Nazabal, J.; *Polymer* 2000, 41, 6311.
- [166] Abad, M. J.; Ares, A.; Barral, L.; Canao, J.; Diez, F. J.; Garcia-Garabal, S.; Lopez, J.; Ramirez, C.; *J Appl Polym Sci* 2004, 94, 1763.
- [167] Abad, M. J.; Ares, A.; Barral, L.; Eguiazabal, J. I.; *Polym Int* 2005, 54, 673.
- [168] Montoya, M.; Abad, M. J.; Barral, L.; Bernal, C.; *Eur Polym J* 2006, 42, 265.
- [169] Montoya, M.; Abad, M. J.; Barral Losada, L.; Bernal, C.; *J Appl Polym Sci* 2005, 98, 1271.
- [170] Son, Y.; Weiss, R. A.; *Polym Eng Sci* 2001, 41, 329.
- [171] Willis, J. M.; Favis, B. D.; *Polym Eng Sci* 1988, 28, 1416.
- [172] Willis, J. M.; Favis, B. D.; Lavallee, C.; *J Mater Sci* 1993, 28, 1749.
- [173] Li, Y.; Zhang, B. Y.; Feng, Z.; Zhang, A.; *J Appl Polym Sci* 2002, 83, 2749.
- [174] Zhang, A.; Zhang, B.; Feng, Z.; *J Appl Polym Sci* 2002, 85, 1110.

- [175] Zhang, B. Y.; Sun, Q. J.; Li, Q. Y.; Wang, Y.; J Appl Polym Sci 2006, 102, 4712.
- [176] Roura, M. J.; Eur Pat 1981, EP34704.
- [177] Inoue, K. K.; Jpn Pat 1982, JP57102948.
- [178] Weaver, E. P.; Eur Pat 1983, EP86069.
- [179] Gemeinhardt, G. C.; Moore, A. A.; Moore, R. B.; Polym Eng Sci 2004, 44, 1721.
- [180] Gemeinhardt, G. C.; Moore, R. B.; Macromolecules 2005, 38, 2813.
- [181] Xavier, T.; PhD Thesis 2002, Cochin University of Science and Technology, Kochi, Kerala, India.
- [182] Samios, C. K.; Kalfoglou, N. K.; Polymer 2001, 42, 3687.
- [183] Castagna, A.M.; Wang, W; Winey, K.I; Runt, J; Macromol 2010, 43(24), 10498.
- [184] Castagna, A.M.; Wang, W; Winey, K.I; Runt, J; Macromol 2011, 44(8), 2791.
- [185] Hall, L. M; Stevens, M. J; Frischknecht, A. L; Macromol 2012, 45(19), 8097.
- [186] Yeh, J. T.; Fanchiang, C. C.; Cho, M. F.; Polym Bull 1995, 35, 371.
- [187] Leewajankul, P.; Pattanaolarn, R.; Ellis, J. W.; Nithitanakul, M.; Grady, B. P.; J Appl Polym Sci 2003, 89, 620.
- [188] Lahor, A.; Nithitanakul, M.; Grady, B. P.; Eur Polym J 2004, 40, 2409.
- [189] Fairley, G.; Prud'homme, R. E.; Polym Eng Sci 1987, 27, 1495.
- [190] Sinthavathavorn, W.; Nithitanakul, M.; Magaraphan, R.; Grady, B. P.; J Appl Polym Sci 2008, 107, 3090.
- [191] Sinthavathavorn, W.; Nithitanakul, M.; Grady, B. P.; Magaraphan, R.; Polym Bull 2009, 63, 23.

.....OR.....

MATERIALS AND EXPERIMENTAL TECHNIQUES

Contents	2.1 <i>Materials</i>
	2.2 <i>Preparation of blends</i>
	2.3 <i>Characterization</i>

This chapter gives a brief description of the materials used for the study and experimental procedures adopted.

2.1 Materials

2.1.1 Low density polyethylene (LDPE)

The film grade low density polyethylene (LDPE 24FS040) from Reliance Industries Limited, Mumbai, India, with melt flow index (190 °C/2.16 kg) of 4 g/10 min and density (23 °C) of 0.922 g/cm³ was supplied by Periyar Polyfilms, Edayar, Kerala, India.

2.1.2 Starch and dextrin

The tapioca starch (100 and 300 mesh) and dextrin (100, 200 and 300 mesh) were obtained from Jemsons Starch & Derivatives, Aroor, Alappuzha, Kerala. As these fillers were hygroscopic in nature they were oven dried at 120 °C for 1h prior to mixing.

2.1.3 Ionomers

Ionomers used in this study were

- a) Zinc salt of poly(ethylene-co-methacrylic acid) (HIMILAN 1702 EMAAZn) with melt flow index (190 °C/2.16 kg) of 16 g/10 min, and

- b) Sodium salt of poly(ethylene-co-methacrylic acid) (HIMILAN 1555 EMAANa) with melt flow index (190°C/2.16 kg) of 10 g/10 min.

These ionomers were supplied by Mitsubishi Plastics, Inc., Japan.

2.1.4 Pro-oxidants

The pro-oxidants used in this study include metal oxides and metal stearates.

2.1.4.1 Metal oxides

The metal oxides used in this study were iron oxide, manganese dioxide and titanium dioxide (anatase and rutile grades). The iron oxide was supplied by Merck Specialities Pvt. Ltd., Mumbai, India. Manganese dioxide was supplied by Qualigens Fine Chemicals, Mumbai, India. Titanium dioxide (anatase and rutile grades) were supplied by Associated Chemicals, Edappally, Kerala, India.

2.1.4.2 Metal stearates

The metal stearates used in this study were ferric stearate, manganese stearate, copper stearate, magnesium stearate and zinc stearate. Ferric stearate, manganese stearate and copper stearate were supplied by Jingjiang Concord Plastics Technology Co. Ltd. China. Magnesium stearate and zinc stearate were supplied by Alfa Chemicals, Ernakulam, Kerala, India.

2.1.5 Other chemicals

The maleic anhydride was supplied by Loba Chemie Pvt. Ltd., Mumbai and the dicumyl peroxide was supplied by Associated Chemicals, Edappally, Kochi, Kerala.

2.2 Preparation of blends

Blends were prepared by melt mixing [1] method because it is:

- environmentally benign
- suitable for most of the polymers
- compatible with practicing polymer processing operations
- the most popular method for industrial applications

2.2.1 Melt mixing

A Thermo Haake Polylab system (Rheocord 600p, figure 2.1) equipped with roller-type rotors was used for melt mixing. The mixing chamber has a volumetric capacity of 69 cm³.

A mixing time of 8 minutes was given for all the compounds at a rotor speed of 30 rpm at 150 °C. LDPE was first melted for 2 minutes followed by the addition of filler. Mixing was continued for another 6 minutes.

In the case of maleated blends initially the LDPE was melted for 2 minutes and then grafted with maleic anhydride (1%) using dicumyl peroxide as the initiator. The biofiller was then added and the mixing was continued for a total duration of 8 minutes. Different compositions for each filler were prepared. The neat LDPE was also masticated under the same conditions.

In the case of ionomer compatibilized blends, LDPE together with ionomer was melted for 2 minutes followed by the addition of fillers. Mixing was continued for another 6 minutes.



Figure 2.1 Thermo HAAKE polylab system. (Mixing chamber and the rotors are also shown)

2.2.2 Preparation of test specimens

The test specimens were prepared from neat LDPE and the compounds by moulding in an electrically heated hydraulic press for 5 minutes at 150 °C under a pressure of 20MPa. After moulding, the samples were cooled down to room temperature under pressure.

2.3 Characterization

2.3.1 Mechanical properties

The mechanical properties were evaluated using Shimadzu Autograph AG-I series universal testing machine at a crosshead speed of 50 mm/min. Tensile strength, elongation at break and elastic modulus were measured according to ASTM D-882 (2002)[2]. Averages of at least five sample measurements were taken to represent each data point.

2.3.2 Melt Flow Index (MFI)

An extrusion plastometer was used for measuring the melt flow index of polymer melts according to ASTM D-1238 [3]. The rate of extrusion through a die of specified length and diameter was measured under prescribed conditions of temperature and load as a function of time. Melt flow index is calculated and reported as g/10min. This index is inversely related to molecular weight [4].

The melt flow index (MFI) of each blend of LDPE with filler was measured using a CEAST Modular Line Melt Flow Indexer in accordance with ASTM method D-1238 using a 2.16 kg load at a melt temperature of 190 °C.

2.3.3 Biodegradation studies

The biodegradation studies on the blends were carried out according to ASTM D-6691 [5].

2.3.3.1 Bacterial strains

Bacterial cultures were obtained from culture collections of *Microbial Genetic Lab, Department of Biotechnology, Cochin University of Science and Technology*. These cultures were isolated from sediment samples

collected from different locations of Cochin backwaters and Mangalavanam mangroves. These cultures were previously identified as genus *Vibrionacea* based on their morphological and biochemical characteristics outlined in Bergey's Manual of Systematic Bacteriology [6]. They were preserved in 10 mL glass bottles employing paraffin oil overlay method.

2.3.3.2 Purification of *vibrios*

A loopful of the preserved cultures were transferred by spread plated onto Thiosulphate Citrate Bile salt Sucrose (TCBS) agar plates (Himedia) and was incubated at 37 °C for 24 hours. Isolated yellow and green colored single colonies were picked, purified on nutrient agar plates (quadrant streaking), sub cultured on nutrient agar slants with 1% NaCl and was kept at 4 °C for further studies.

The isolates were identified as *Vibrios* based on their morphological and biochemical characteristics outlined in Bergey's Manual of Systematic Bacteriology [6] which include Gram staining, oxidation/fermentation reaction with glucose (MOF test) and oxidase test. The isolates that are gram negative rods, fermentative in MOF test and behaved positive in oxidase test were streaked onto nutrient agar slants containing 1% NaCl. They were stocked at 4 °C for further studies.

2.3.3.3 Screening for amylase producers

Plate assay method was employed for the screening of amylase producers. Nutrient agar medium supplemented with 1% starch and 1% NaCl was used for the plate preparation [7]. All the isolates were spot inoculated onto the nutrient plates and incubated at 37 °C for 2 days. After incubation, the plates were flooded with Grams iodine for visualizing the zone of clearance around the colony. The clearing zones indicate the production of

amylase enzyme by the isolates. From the results, potential amylase producers were selected based on the diameter of zone of clearance around colonies.

2.3.3.4 Medium for biodegradation studies.

Minimal medium was used for testing the degradation of the blends. The composition and pH of 1L of amylase minimal medium [8] is given in Table 2.1.

Table 2.1 Composition and pH of amylase minimal medium

Peptone	6.0 g
MgSO ₄	0.5 g
KCl	0.5 g
Starch	1 g
NaCl	1 g
pH	7 ± 0.3

2.3.3.5 Preparation of consortia of amylase producers for biodegradation studies

The isolates with largest zones of clearance in the primary screening for starch degradation were selected to make up the consortium to study the degradation of starch/dextrin plastic blended films. 15 isolates of *Vibrios* which were optimum producers based on the plate assay were selected and were grown to OD₆₀₀=1.00. The culture suspension was centrifuged to harvest the cells and the cells were resuspended in physiological saline for use as inoculums. 1 ml of each culture was aseptically transferred to the minimal media.

2.3.3.6 Biodegradation studies on blends using the consortium

2.3.3.6.1 Preparation of blends

The blends were prepared by melt mixing in a Thermo HAAKE PolyLab system. The moulding was done using an electrically heated

hydraulic press. The test specimens for checking the biodegradation were cut from the samples according to ASTM D-882 [2].

2.3.3.6.2 Preparation of inoculum & shake flask culture

To prepare the inoculum the individual isolates of the consortium were grown overnight at 37 °C at 120 rpm on an Orbitek shaker (Scigenics Pvt. Ltd, Chennai, India) in nutrient broth (Himedia, Mumbai) pH 7.0 ±0.3 with 1% NaCl. The cells were harvested by centrifugation at 5000 rpm (2292g) for 20 minutes, washed with physiological saline and then pooled. 5 ml of this pooled culture ($OD_{660} = 1$) was used to inoculate 50 mL amylase minimal medium [8] lacking starch. The samples prepared from the blends previously wiped with 70% alcohol were added to this medium and these strips acted as the sole source of carbon. Incubation was in the Orbitek environmental shaker at 37 °C and 120 rpm for a total period of 3 months with regular sampling. The medium without the inoculum with corresponding starch-plastic blends and subjected to the same treatment as above were used as controls.

2.3.4 Soil burial test

The soil burial test was also carried out for evaluating the biodegradability of the blends. The soil was taken in pots and the plastic strips were placed in it. The bacterial culture was supplied to the soil. Care was taken to ensure that the samples were completely covered with soil. The pot was then kept at room temperature. The loss in weight and tensile strength was measured after thorough washing with water and drying in oven until constant weight to determine the extent of biodegradability.

2.3.5 Photodegradation by UV rays

Disinfection lamps (TUV lamps) are low pressure mercury-vapour discharge lamps consisting of a tubular glass envelope, emitting shortwave ultraviolet radiation with a radiation peak at 253.7nm (UV-C) for germicidal action. The glass filters out the 185nm ozone-forming line. A protective coating on the inside limits the depreciation of the useful UV-C radiation output (longlife lamps). They are applied in a variety of photochemical processes.

In the present study, the plastic film samples were cut to 8x1 cm size and exposed under a 30-watt shortwave UV lamp at a distance of 30 cm. The plastic films were then taken out after one month to determine tensile strength using a universal testing machine. Average weight of the test specimens, before and after the degradation studies were carried out using a Sartorius-0.1 mg electronic balance. The FTIR and DSC were used for the characterization and monitoring for the functional group changes in the samples during irradiation.

2.3.6 Water absorption characteristics

Water absorption was measured using 3 x 1 inch film strips of <1mm thickness according to ASTM D-570-81 [9] method. Water absorption measurements were performed by soaking the samples in distilled water. The water absorption was calculated as the weight difference and is reported as percentage increase of the initial weight. The results reported are average of three measurements.

2.3.7 Fourier transform infrared spectroscopy (FTIR)

Fourier transform infrared spectra (FTIR) are generated by the absorption of electromagnetic radiation in the frequency range 400 to 4000

cm^{-1} by organic molecules. Different functional groups and structural features in the molecules absorb energy at characteristic frequencies. The frequency and intensity of absorption are the indication of the bond strength and structural geometry in the molecule. The FTIR spectra of the samples were recorded in the transmittance mode using a Thermo Nicolet, Avatar 370 FTIR spectrophotometer in the spectral range of $4000\text{--}400\text{ cm}^{-1}$ [10].

2.3.8 Dynamic mechanical analysis (DMA)

Dynamic mechanical analysis is a technique used to study the various molecular transitions of materials. It is most useful for studying the viscoelastic behaviour of polymers [11]. A sinusoidal stress is applied and the strain in the material is measured, allowing the determination of the complex modulus. The temperature of the sample or the frequency of the stress are often varied, leading to variations in the complex modulus; this approach can be used to locate the glass transition temperature of the material, as well as to identify transitions corresponding to other molecular motions.

Dynamic Mechanical Analyzer (DMA Q-800, TA instruments) was used to study the viscoelastic properties of the samples. DMA analysis was conducted at a constant frequency of 1 Hz. A temperature ramp was run from $40\text{ }^{\circ}\text{C}$ to $100\text{ }^{\circ}\text{C}$ to get an overview of the thermomechanical behaviour of the samples. The dynamic storage modulus, loss modulus and $\tan \delta$ were measured.

The storage modulus measures the stored energy, representing the elastic portion, and the loss modulus measures the energy dissipated as heat, representing the viscous portion [12].

The tensile storage and loss moduli are defined as follows:

Storage modulus:

$$E' = \frac{\sigma_0}{\varepsilon_0} \cos \delta$$

Loss modulus:

$$E'' = \frac{\sigma_0}{\varepsilon_0} \sin \delta$$

Phase angle, Tan (δ):

$$\tan \delta = \frac{E''}{E'}$$

2.3.9 Thermogravimetric analysis (TGA)

Thermogravimetric analysis is a type of testing performed on samples that determines changes in weight in relation to change in temperature, while the substance is subjected to a controlled temperature programme [13]. Thermograms provide information about the decomposition temperatures of various polymeric preparations, and their thermal stability.

Thermogravimetric analysis was carried out in a TGA Q-50 thermal analyzer (TA Instruments) under a nitrogen atmosphere. The samples were heated from room temperature to 600 °C at a heating rate of 20 °C/min and a nitrogen gas flow rate of 40-50 cm³/min. The sample weights varied from 10-15 mg. The weight changes were noted with the help of an ultra sensitive microbalance.

The data of weight loss versus temperature and time was recorded online using the TA Instrument's Q Series Explorer software. The analysis of the thermogravimetric (TG) and derivative thermogravimetric (DTG) curves were done using TA Instrument's Universal Analysis 2000 software

version 3.3 B. The temperature at which weight loss is maximum (T_{\max}) was evaluated.

2.3.10 Differential scanning calorimetry (DSC)

Differential scanning calorimetry is a thermoanalytical technique in which the difference in the amount of heat required to increase the temperature of a sample and reference is measured as a function of temperature. Both the sample and reference are maintained at nearly the same temperature throughout the experiment. It is one of the most widely accepted techniques for studying the crystallization characteristics of polymers and their blends [14-15].

Using this technique it is possible to observe fusion and crystallization events as well as glass transition temperatures (T_g). As the temperature increases, an amorphous solid will become less viscous. At some point the molecules may obtain enough freedom of motion to spontaneously arrange themselves into a crystalline form. This is known as the crystallization temperature (T_c). This transition from amorphous solid to crystalline solid is an exothermic process, and results in a peak in the DSC signal. As the temperature increases the sample eventually reaches its melting temperature (T_m). The melting process results in an endothermic peak in the DSC curve. The ability to determine transition temperatures and enthalpies makes DSC a valuable tool in producing phase diagrams for various chemical systems [16].

Crystallinity of the samples was studied using a TA Q-100 thermal analyzer (TA Instruments) under nitrogen atmosphere with a heating rate of $10\text{ }^{\circ}\text{C}/\text{min}$. Samples of 5-10 mg were heated in a nitrogen atmosphere from $-50\text{ }^{\circ}\text{C}$ to $150\text{ }^{\circ}\text{C}$ and kept at $150\text{ }^{\circ}\text{C}$ for 3 min to erase the thermal history.

Then a cooling was performed from 150 °C to -50 °C, followed by a second heating from -50 °C to 150 °C at the same rate. The percentage of crystallinity was calculated from the DSC traces as follows.

$$\% \text{ Crystallinity} = (\Delta H_{f(\text{obs})} / \Delta H_{f(100\% \text{ crystalline})}) \times 100$$

where $\Delta H_{f(\text{obs})}$ is the enthalpy associated with melting of the material and $\Delta H_{f(100\% \text{ crystalline})}$ is the enthalpy of 100% crystalline polyethylene reported in the literature to be 286.7J/g [17].

2.3.11 Morphological studies

Morphology of the polymer blends depends on a range of parameters: the polymer molecules, interfacial tension, shear mixing, mechanical and physical properties of the blends [18-19]. Scanning electron microscopy (SEM) is a powerful technique used to evaluate the morphology of blends. In this technique, an electron beam is scanned across the specimen resulting in back scattering of electrons of high energy, secondary electrons of low energy and X-rays. These signals are monitored by detectors (photo multiplier tube) and magnified. An image of the investigated microscopic region of the specimen is thus observed in a cathode ray tube and photographed.

In the present study the tensile fractured surfaces were mounted on a metallic stub with the help of a silver tape and conducting paint in the upright position and were sputter coated with platinum within 24 hours of fractures in a JFC 1600 Autofine coater and then examined under JEOL model JSM-6390LV scanning electron microscope (SEM).

References

- [1] Wei, S.; Changshui, F.; Dong, X.; Quan, R.; J Mater Sci 1999, 34, 5995.
- [2] Annual Book of ASTM Standards, D-882, 08.01, 2004.
- [3] Annual Book of ASTM Standards, D-1238, 08.01, 2004.
- [4] Strong, A. B.; Plastics Materials and Processing, 2nd edn. Prentice Hall, New Jersey, USA, 1996.
- [5] Annual Book of ASTM Standards, D-6691, Vol.08.03, 2004.
- [6] Buchanan, R. E.; Gibbons, N. E.; Bergey's manual of systematic bacteriology, 8th edn, The Williams and Wilkins Co., Baltimore, 1974, 747.
- [7] Furniss, B. S.; Hannaford, A. J.; Rogersm, V.; Smith, P. W. G.; Tatchell, A. R. (Eds); Vogel's textbook of practical organic chemistry, 4th edn, Longman Publications, England, 1978.
- [8] Bernfed, P. C.; Adv Enzymol 1951, 12, 379.
- [9] Annual Book of ASTM Standards, D-570, Vol.08.01, 2004.
- [10] Griffiths, P.; de Hasseth, J.A.; Fourier Transform Infrared Spectrometry, 2nd edn, Wiley-Blackwell, 2007, ISBN 0471194042.
- [11] Murayama, T.; Dynamic Mechanical Analysis of Polymeric Materials, Elsevier Publishing Company, Amsterdam, 1978.
- [12] Meyers.; Chawla.; Mechanical Behavior of Materials, 1999, 98-103.
- [13] McNeil, C; In: Allen, G, editor, Comprehensive polymer science 1989, vol 5, ch 15, Pergamon Press, New York.
- [14] Busigin, C.; Lahtinern, R.; Thomas, G.; Woodharms, R. T.; Polym Eng Sci 1984, 24, 169.
- [15] Zhu, W. P.; Zhang, G. P.; Yu, J. Y.; Dai, G. J.; J Appl Polym Sci 2004, 91, 431.
- [16] Dean, J. A.; The Analytical Chemistry Handbook, McGraw Hill Inc, New York, 1995, 15.1–15.5.

- [17] Gugumus, F.; Polym Degrad Stab 1996, 52,131.
- [18] Sawyer, L.C.; Grubb, D.T.; Polymer Microscopy, 2nd edn, Chapman and Hall, 2-6 Boundary Row, London, 1996.
- [19] Woodward, A. E.; Atlas of polymer morphology, Hanser, New York, 1989.



BIOPOLYMER FILLED LOW DENSITY POLYETHYLENE

Contents	3.1	<i>Introduction</i>
	3.2	<i>Results and discussion</i>
	3.3	<i>Conclusions</i>

Low density polyethylene (LDPE) was blended with various dosages of starch (100 and 300 mesh size) and dextrin (100, 200 and 300 mesh size). Mechanical, thermal, FTIR, and morphological (SEM) studies on the blends have been carried out. The melt flow indices (MFI) of the blends were measured. The percentage water absorption of each composition was calculated. Biodegradability of the samples prepared from the blends has been verified using culture medium containing *Vibrios* - an amylase producing bacteria, which were isolated from sediment samples collected from different locations of Cochin backwaters and Mangalavanam mangroves. Soil burial test too of the samples was conducted. The biodegradability tests on the blends indicate that the blends are partially biodegradable. Scanning electron micrographs validate the bio-degradability in LDPE-starch and LDPE-dextrin blends.

3.1 Introduction

Low density polyethylene is one of the most widely used polyolefin polymer for packaging applications with well known technology of production and low cost and exhibits desirable properties, such as light weight, good tensile and tear strength, good barrier properties to oxygen, heat sealability and resistance to biodegradation [1]. The resistance of low density polyethylene to biodegradation is attributed to its hydrophobicity, high molecular weight and lack of functional groups recognizable by microbial enzymatic system. These properties restrict the use of these materials in applications where biodegradability is a desirable quality [2]. Biodegradable polymers can be broken into small segments by enzyme-catalyzed reactions induced by the microorganisms. Thus a viable solution is to combine the different features and benefits of materials from both petroleum and natural resources, to produce useful blends that may satisfy both economical and environmental requirements [3]. The incorporation of biopolymers to plastic matrix in films leads to physical embrittlement of polymer, leaving a porous plastic film, which enhances the accessibility of the plastic molecules to oxygen and microorganisms [4-5]. Because of its low cost, renewability and biodegradability, starch has been considered as a polymer with a high potential for packaging applications [6]. Starch and its derivatives have been extensively used with other polymers to improve the biodegradability of resulting blends [7-8]. Plastics made of a mixture of biopolymer and low density polyethylene constitutes an alternative solution for the plastic waste accumulation problem [9-10].

This chapter presents the preparation of LDPE-biopolymer [starch (100 and 300 mesh) and dextrin (100, 200 and 300 mesh)] blends and

evaluation of various properties. Three compositions (5,10 and 15 weight %) with each filler grade were prepared and characterized by assessing their mechanical properties, MFI, biodegradability, water absorption, FTIR spectra, thermal properties and SEM. Designations of the samples used in this chapter and their descriptions are given in Table 3.1.

Table 3.1 Description of sample designations

Sample designation	Description
LDS100	LDPE-starch 100 mesh
LDS300	LDPE-starch 300 mesh
LDD100	LDPE-dextrin 100 mesh
LDD200	LDPE-dextrin 200 mesh
LDD300	LDPE-dextrin 300 mesh

3.2 Results and discussion

3.2.1 Mechanical properties

Figure 3.A shows typical stress-strain curve for LDPE, LDS300 and LDD300. Figures 3.1 and 3.2 show the variation of tensile strength and elastic modulus of LDPE-starch blends. The tensile strength and elastic modulus were found to decrease both in the case of LDS100 and LDS300 blends indicating that starch behaves as non-reinforcing filler. The tensile strength of LDS100 blends is lower compared to LDS300 blends. The elastic modulus of LDS300 blends decreases up to a starch concentration of 10 weight%, and then shows a marginally increasing tendency.

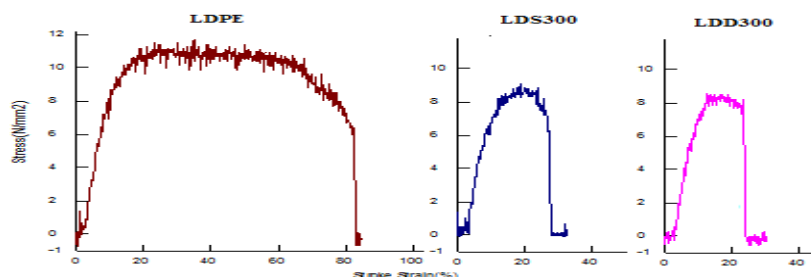


Figure 3.A Typical stress-strain curves of LDPE, LDS300 and LDD300

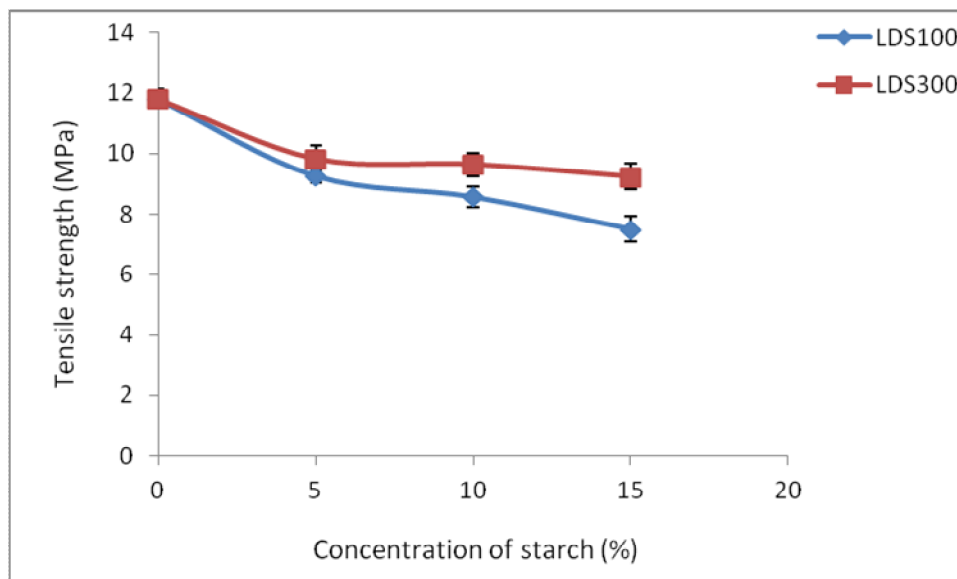


Figure 3.1 Variation of tensile strength with concentration of starch in LDPE-starch blends

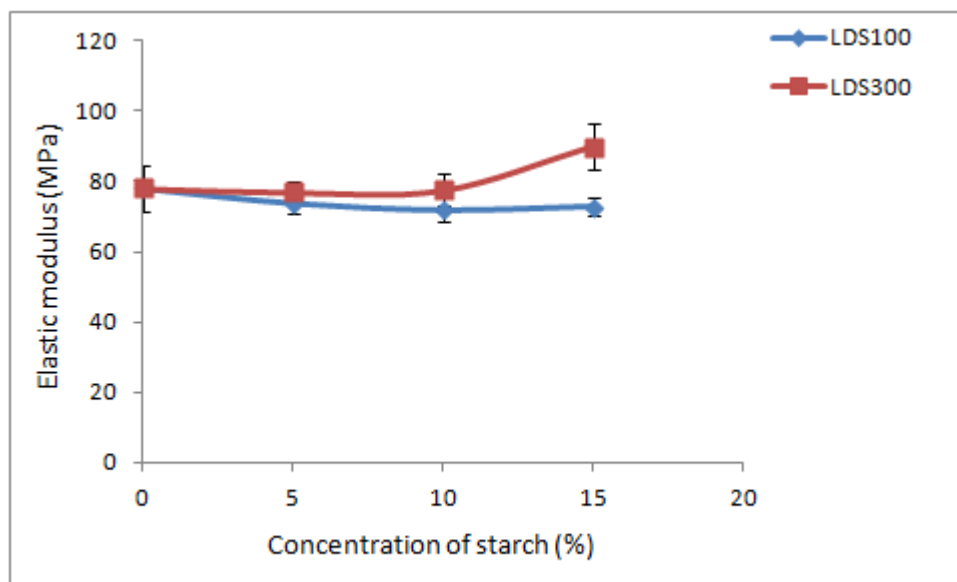


Figure 3.2 Variation of elastic modulus with concentration of starch in LDPE-starch blends

Figures 3.3 and 3.4 show the variation of tensile strength and elastic modulus of LDPE-dextrin blends. The tensile strength and elastic modulus were found to decrease marginally on incorporating dextrin. The tensile strength of LDD100 and LDD200 blends are almost same. The blend containing LDD300 shows marginally lower tensile strength as compared to the other blends. The elastic modulus of all the blends decreases as the loading of filler increased.

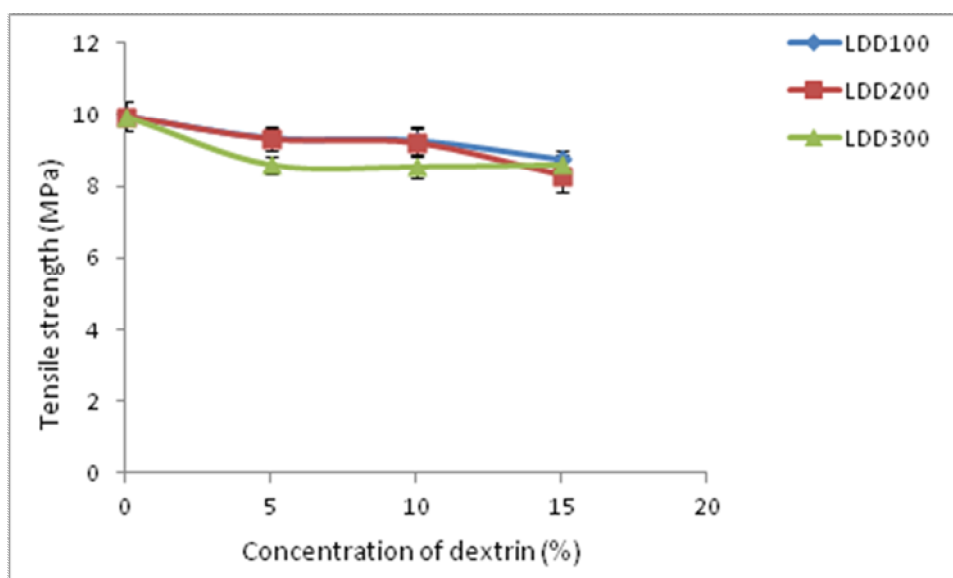


Figure 3.3 Variation of tensile strength with concentration of dextrin in LDPE-dextrin blends

The decrease in tensile strength and elastic modulus may be due to weakness of interfacial adhesion of hydrophilic starch and dextrin with hydrophobic matrix of LDPE. As the starch concentration increases, there is less effective cross-sectional area of LDPE towards the spherical starch and dextrin. Starch and dextrin exhibit hydrophilic properties and strong intermolecular association via hydrogen bonding due to hydroxyl groups on the surface. This hydrophilic nature and strong intermolecular hydrogen

bonding make these fillers less compatible with hydrophobic LDPE [11-12]. The reduction in the mechanical properties of LDPE on incorporation of starch and dextrin suggests that the fillers have no reinforcing effect on LDPE.

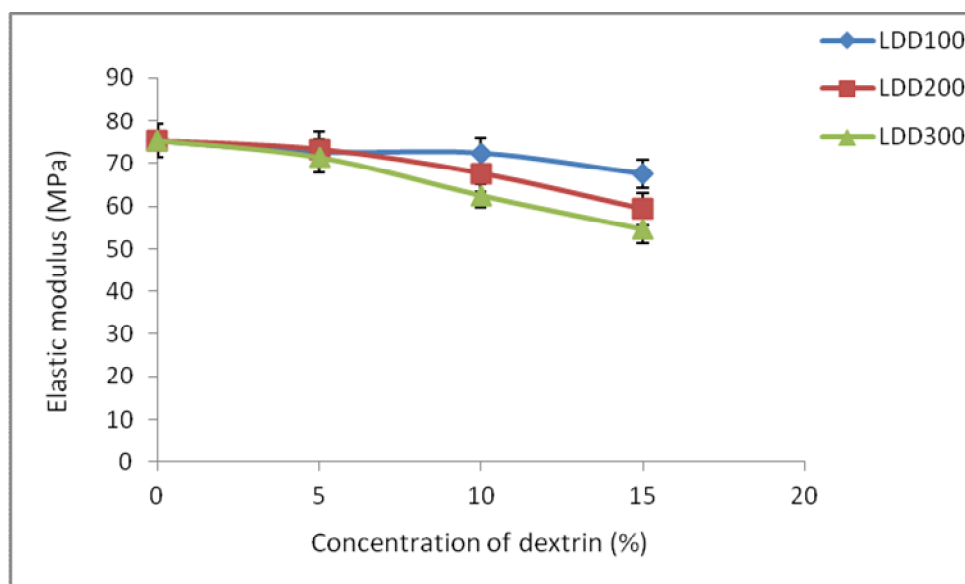


Figure 3.4 Variation of elastic modulus with concentration of dextrin in LDPE-dextrin blends

3.2.2 Melt flow measurements

The melt flow index is one of the most common parameters specified when describing a polymer. Figures 3.5 and 3.6 show the variation of the melt flow indices of LDPE-starch and LDPE-dextrin blends. In all cases the melt flow indices remain almost unchanged up to a concentration of 5 weight % of the biopolymer, and then show a decreasing tendency at higher loading of the filler. Low melt flow index indicates a higher melt viscosity [13]. Thus the addition of starch and dextrin resulted in the increase in melt viscosity as a result of the poor miscibility of LDPE and the biopolymer.

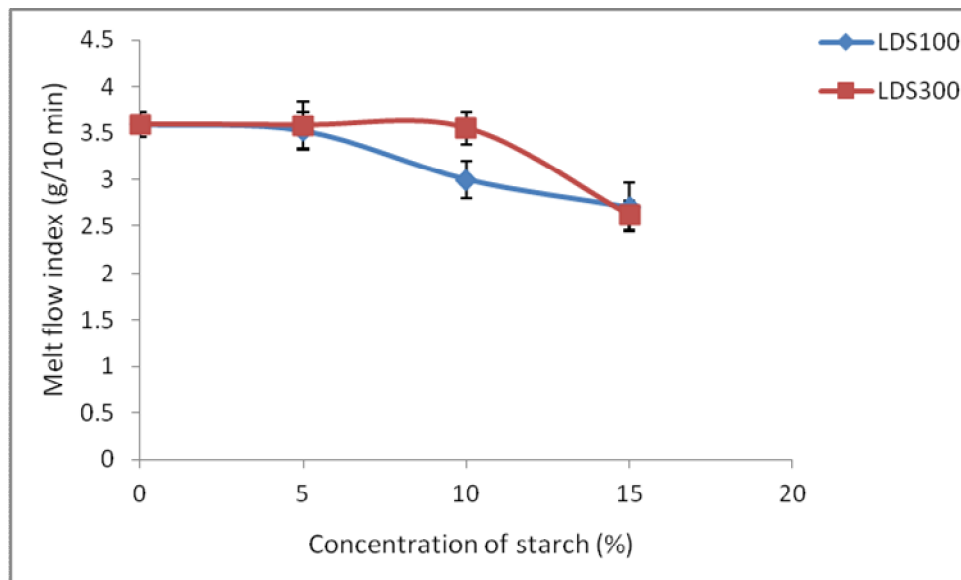


Figure 3.5 Variation of melt flow index with concentration of starch in LDPE-starch blends

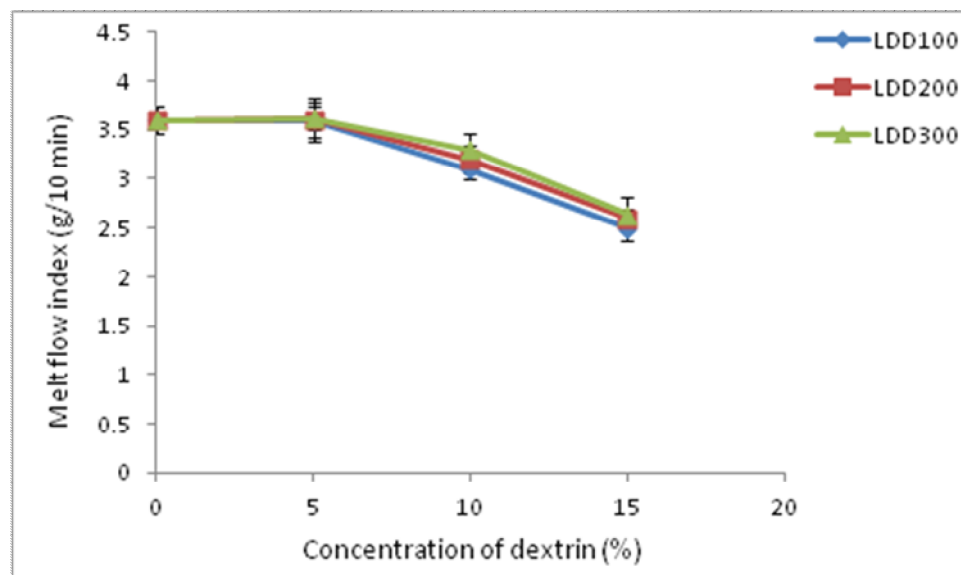


Figure 3.6 Variation of melt flow index with concentration of dextrin in LDPE-dextrin blends

The melt flow index gives information about the degree of entanglements of polymer chains by chemical or physical cross links [14]. The low melt flow indices at higher concentration of the biopolymers are apparently due to increased entanglement of the polymer chains of LDPE and biopolymers.

3.2.3 Biodegradation studies

3.2.3.1 In culture medium

Figures 3.7 and 3.8 show the decrease in tensile strength of LDPE-starch and LDPE-dextrin blends after immersing the strips in culture medium in shake culture flask for 8 weeks. There is significant variation in tensile strength of the samples indicating higher degree of biodegradation.

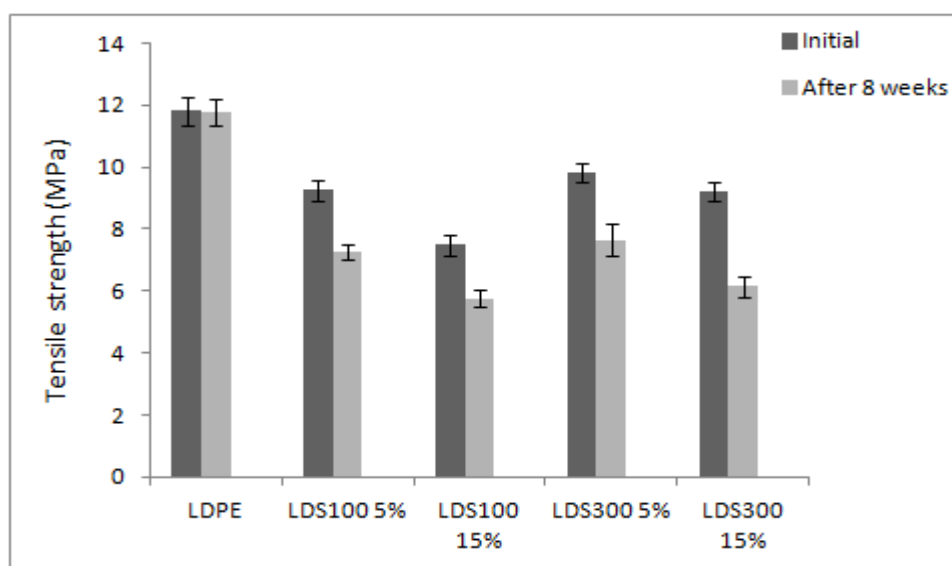


Figure 3.7 Biodegradation of LDPE-starch blends after immersion in culture medium in shake culture flask for 8 weeks (As evident from tensile strength)

Tables 3.2 and 3.3 show the percentage decrease in tensile strength of LDPE-starch and LDPE-dextrin blends after biodegradability test in culture

medium for 8 weeks. The tensile strength of the blends decreased after biodegradability studies in culture medium. For blends containing higher concentrations of starch, the % loss in tensile strength is higher suggesting a higher degree of biodegradation in the case of these blends.

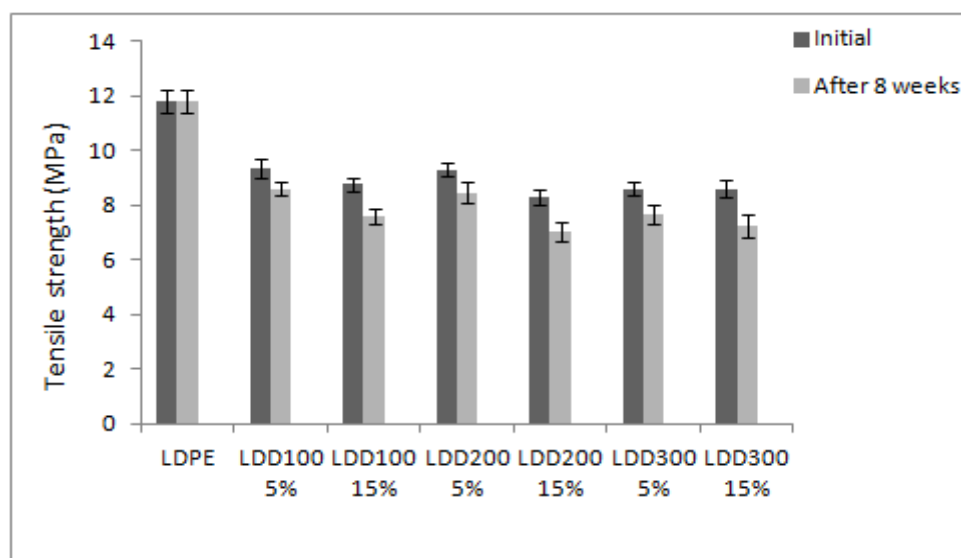


Figure 3.8 Biodegradation of LDPE-dextrin blends after immersion in culture medium in shake culture flask for 8 weeks (As evident from tensile strength)

Table 3.2 Percentage decrease in tensile strength of LDPE-starch blends after biodegradation in culture medium for 8 weeks

Sample	Initial tensile strength(MPa)	Tensile strength after 8 weeks (MPa)	% decrease in tensile strength
LDPE	11.805	11.8	0.04
LDS100 5%	9.26	7.25	21.71
LDS100 15%	7.5	5.76	23.2
LDS300 5%	9.821	7.65	22.11
LDS300 15%	9.233	6.14	33.50

Table 3.3 Percentage decrease in tensile strength of LDPE-dextrin blends after biodegradation in culture medium for 8 weeks

Sample	Initial tensile strength(MPa)	Tensile strength after 8 weeks (MPa)	% decrease in tensile strength
LDD100 5%	9.36	8.60	8.12
LDD100 15%	8.77	7.60	13.34
LDD200 5%	9.32	8.45	9.34
LDD200 15%	8.29	7.05	14.96
LDD300 5%	8.61	7.68	10.80
LDD300 15%	8.61	7.23	16.03

Table 3.4 Weight loss of LDPE-starch blends after biodegradation in culture medium in shake culture flask for eight weeks

Sample	Initial weight (g)	Weight after 8 weeks (g)	% weight loss
LDPE	0.2137	0.2137	0.00
LDS100 5%	0.1291	0.1206	6.58
LDS100 15%	0.1648	0.1494	9.35
LDS300 5%	0.1866	0.1704	8.68
LDS300 15%	0.2143	0.1784	16.75

Table 3.5 Weight loss of LDPE-dextrin blends after biodegradation in culture medium in shake culture flask for eight weeks

Sample	Initial weight (g)	Weight after 8 weeks (g)	% weight loss
LDPE	0.2137	0.2137	0.00
LDD100 5%	0.1774	0.1753	1.18
LDD100 15%	0.1638	0.1614	1.47
LDD200 5%	0.1705	0.1677	1.64
LDD200 15%	0.2067	0.2020	2.27
LDD300 5%	0.2009	0.1974	1.74
LDD300 15%	0.1773	0.1699	4.17

Tables 3.4 and 3.5 show the weight loss of LDPE-biopolymer blends after biodegradation in culture medium. It can be seen that after

eight weeks there is significant weight loss in all the blends and this weight loss is higher for blends having high biopolymer content. For blends containing low amounts of starch or dextrin, the filler is apparently almost covered by LDPE and thus is not accessible to microorganisms. On the contrary, in blends with higher biopolymer content, the biopolymer is more exposed and consequently a greater portion of it is consumed by microbes [15-16].

3.2.3.2 Soil burial test

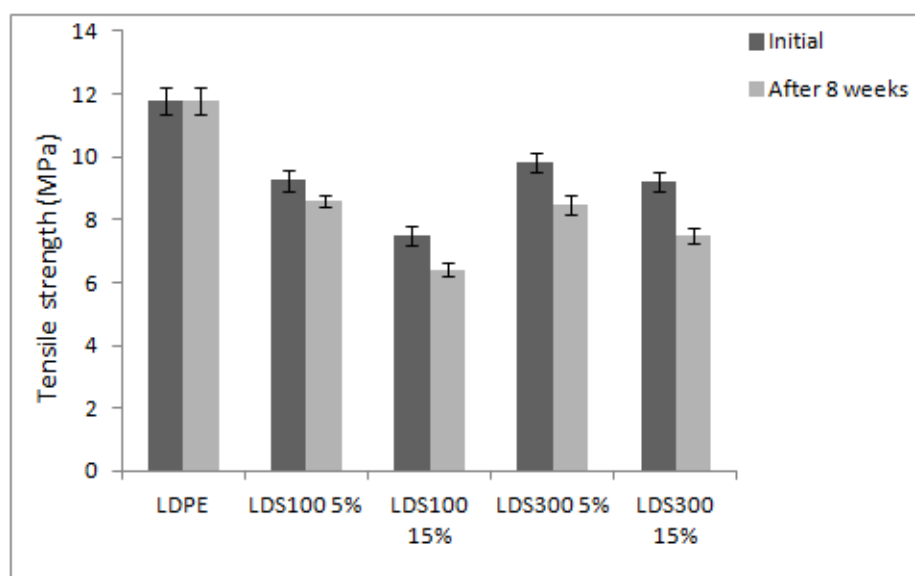


Figure 3.9 Biodegradation of LDPE-starch blends after soil burial test for 8 weeks (Evident from tensile strength)

Figures 3.9 and 3.10 show the variation in tensile strength of LDPE-starch and LDPE-dextrin blends after the soil burial test. Tables 3.6 and 3.7 show the percentage loss in tensile strength of LDPE-starch and LDPE-dextrin blends after biodegradation by soil burial. Tensile strength decreases considerably on increasing the filler content indicating an increase in rate of biodegradation.

Tables 3.8 and 3.9 show the percentage weight loss of LDPE-starch and LDPE-dextrin blends after burial in soil for 8 weeks. Both LDPE-starch and LDPE-dextrin blends show weight loss indicating that these blends are partially biodegradable. Soil environment contains different kinds of microorganisms. Weight losses of polymer in the soil burial test could be assumed as an indicator of biodegradation in the landfills or natural environment.

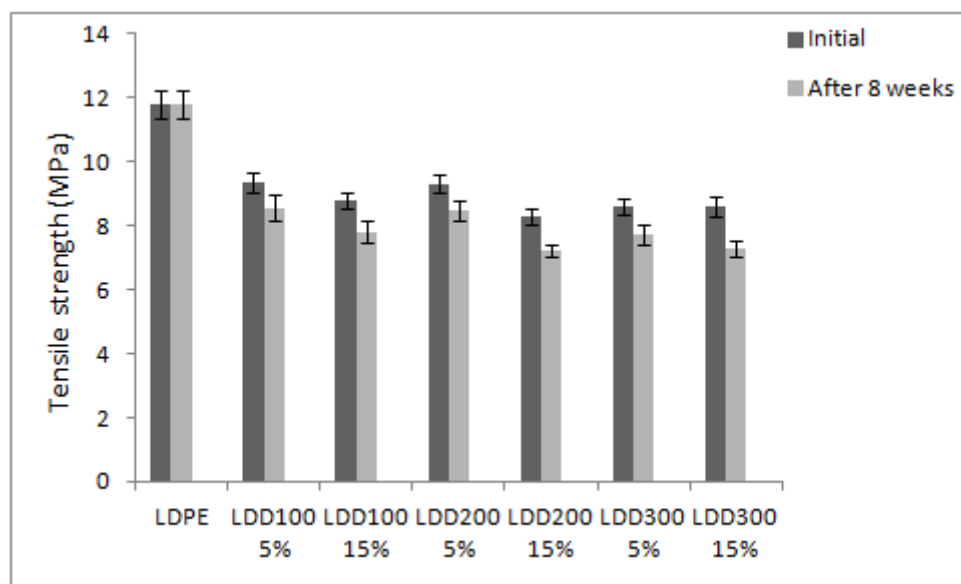


Figure 3.10 Biodegradation of LDPE-dextrin blends after soil burial test for 8 weeks (Evident from tensile strength)

Table 3.6 Percentage decrease in tensile strength of LDPE-starch blends after soil burial test for 8 weeks

Sample	Initial tensile strength(MPa)	Tensile strength after 8 weeks (MPa)	% decrease in tensile strength
LDPE	11.805	11.8	0.04
LDS100 5%	9.26	8.59	7.24
LDS100 15%	7.5	6.42	14.4
LDS300 5%	9.821	8.47	13.76
LDS300 15%	9.233	7.5	18.77

Table 3.7 Percentage decrease in tensile strength of LDPE-dextrin blends after soil burial test for 8 weeks

Sample	Initial tensile strength(MPa)	Tensile strength after 8 weeks (MPa)	% decrease in tensile strength
LDD100 5%	9.36	8.56	8.55
LDD100 15%	8.77	7.80	11.06
LDD200 5%	9.32	8.50	8.79
LDD200 15%	8.29	7.23	12.79
LDD300 5%	8.61	7.72	10.34
LDD300 15%	8.61	7.28	15.45

Table 3.8 Weight loss of LDPE and LDPE-starch blends after biodegradation by soil burial for eight weeks

Sample	Initial weight (g)	Weight after 8 weeks (g)	% weight loss
LDPE	0.1321	0.1321	0.00
LDS100 5%	0.1705	0.1677	1.64
LDS100 15%	0.2221	0.2135	3.87
LDS300 5%	0.1873	0.1831	2.24
LDS300 15%	0.1773	0.1699	4.17

Table 3.9 Weight loss of LDPE and LDPE-dextrin blends after biodegradation by soil burial for eight weeks

Sample	Initial weight (g)	Weight after 8 weeks (g)	% weight loss
LDPE	0.1321	0.1321	0.00
LDD100 5%	1.0663	1.0654	0.08
LDD100 15%	0.4113	0.4072	1.00
LDD200 5%	1.6112	1.6093	0.11
LDD200 15%	0.1928	0.1904	1.25
LDD300 5%	0.5421	0.5362	1.08
LDD300 15%	0.1886	0.1861	1.33

3.2.4 Water absorption studies

Tables 3.10 and 3.11 show the percentage water absorption values of the LDPE-starch and LDPE-dextrin blends respectively. It was found that, the water uptake depends on the starch or dextrin content of the blend and the duration of exposure. The highest rate for water absorption was observed in both the cases during the first 2-9 days for all the blends.

Table 3.10 Water absorption of LDPE and LDPE-starch blends

Sample	Percentage weight increase of the samples in:						
	1 (day)	2 (days)	6 (days)	9 (days)	16 (days)	23 (days)	36 (days)
LDPE	0.03	0.03	0.03	0.03	0.03	0.03	0.03
LDS100 5%	0.32	0.47	0.69	0.74	0.87	0.91	0.97
LDS100 10%	0.90	1.15	1.60	1.68	1.87	1.94	1.97
LDS100 15%	1.06	1.41	2.07	2.30	2.63	2.79	2.90
LDS300 5%	0.45	0.62	0.84	0.94	0.97	0.99	1.00
LDS300 10%	0.67	0.89	1.33	1.45	1.71	1.85	1.97
LDS300 15%	1.70	2.14	2.75	2.84	3.06	3.15	3.15

Table 3.11 Water absorption of LDPE and LDPE-dextrin Blends

Sample	Percentage weight increase of the samples in:						
	1 (day)	2 (days)	6 (days)	9 (days)	16 (days)	23 (days)	36 (days)
LDPE	0.03	0.03	0.03	0.03	0.03	0.03	0.03
LDD100 5%	0.16	0.34	0.68	0.76	0.96	1.06	1.13
LDD100 10%	0.20	0.37	0.83	1.00	1.35	1.55	1.90
LDD100 15%	0.30	0.48	1.14	1.43	1.99	2.38	2.88
LDD200 5%	0.06	0.5	0.37	0.44	0.63	0.80	0.93
LDD200 10%	0.19	0.40	0.79	1.03	1.27	1.55	1.85
LDD200 15%	0.46	0.60	1.59	1.91	2.35	2.73	2.85
LDD300 5%	0.06	0.15	0.38	0.51	0.65	0.78	0.91
LDD300 10%	0.09	0.34	0.91	1.13	1.60	1.76	1.90
LDD300 15%	0.41	0.57	1.00	1.14	1.61	1.93	2.35

Since starch and dextrin are hydrophilic in nature, blends with high starch or dextrin percentage show high water uptake. Starch based synthetic materials tend to absorb water because the hydroxyl groups in starch can form hydrogen bonds with water. Since starch is hydrophilic, it has a high tendency to attract water molecules. This may be the reason for improved susceptibility of the LDPE-biopolymer blends to microbial attack and more degradation observed after immersing the blends in culture medium and also after soil burial. It has been reported that the water molecules added to starch particles are strongly bonded as in a hydrate [17]. The absorption of water is related to its rate of diffusion into the blends. Probably, water penetrated into the films and bonded to the hydroxyl group of starch forcing the starch granules to swell. This might have reduced the gap between the molecules.

3.2.5 Fourier transform infrared spectroscopic analysis

Fourier transform infrared spectroscopy is very useful to study the miscibility of the polymer blends [18-19]. Figures 3.11, 3.12 and 3.13 show the FTIR spectra of neat LDPE, starch (300 mesh) and dextrin (300 mesh) respectively. The spectra show characteristic absorption bands of LDPE, starch and dextrin, the vibrational assignments of which are reported in Table 3.12. Two peaks at 3317 cm^{-1} and 1000 cm^{-1} were observed which correspond to the O-H stretching vibrations of starch and dextrin. A typical IR spectrum of the dextrin presents bands at 3365 cm^{-1} (O-H), $2851\text{--}2940\text{ cm}^{-1}$ (CH), $1040\text{--}1110\text{ cm}^{-1}$ (C-O) [20]. Figure 3.14 and 3.15 show the FTIR spectra LDPE-starch and LDPE-dextrin blends respectively. All the characteristic peaks of pure LDPE and pure starch and dextrin can be seen in the spectra of blends which show that the whole spectrum is the superposition of the spectra of pure polymers. This reveals that IR spectral bands are not affected by the compositions of blends, which

indicates that there is no specific interaction between biopolymers and LDPE. Information about different stages of degradation can be obtained by subtracting the spectrum of the pure polymer from the spectrum of the degraded sample [21-23].

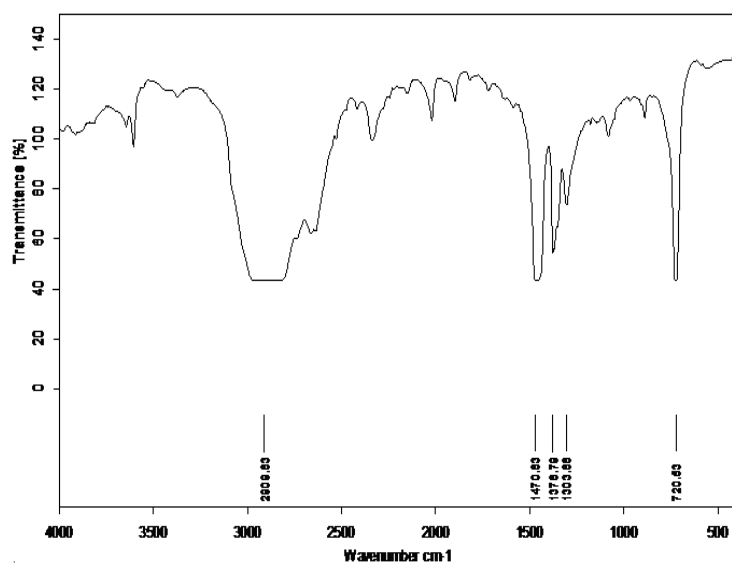


Figure 3.11 FTIR spectra of neat LDPE

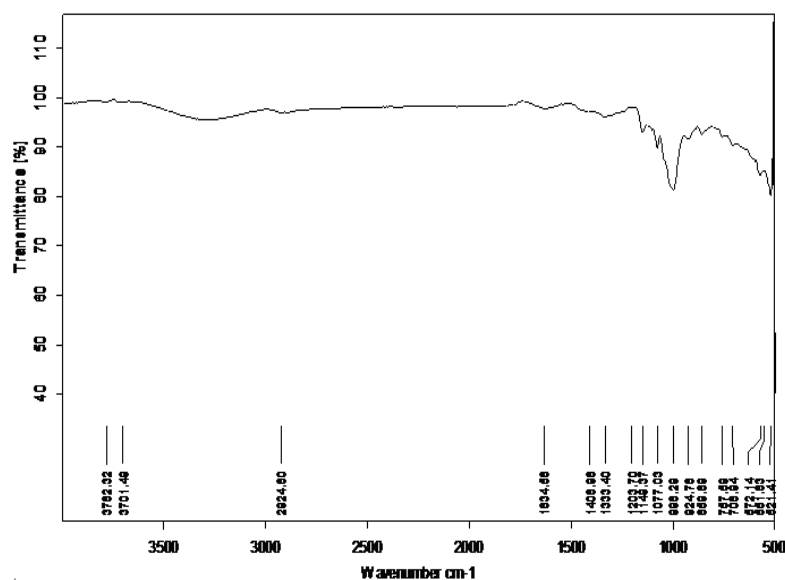


Figure 3.12 FTIR spectra of starch (300 mesh)

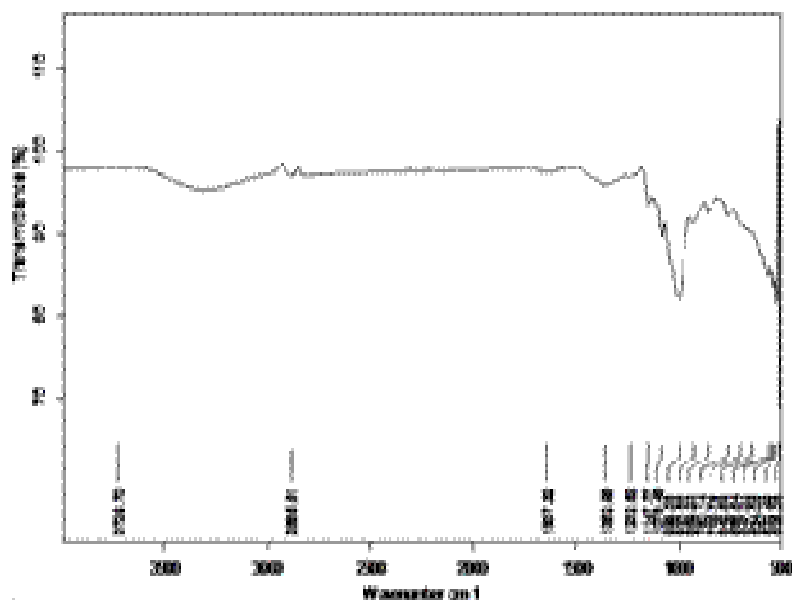


Figure 3.13 FTIR spectra of dextrin (300 mesh)

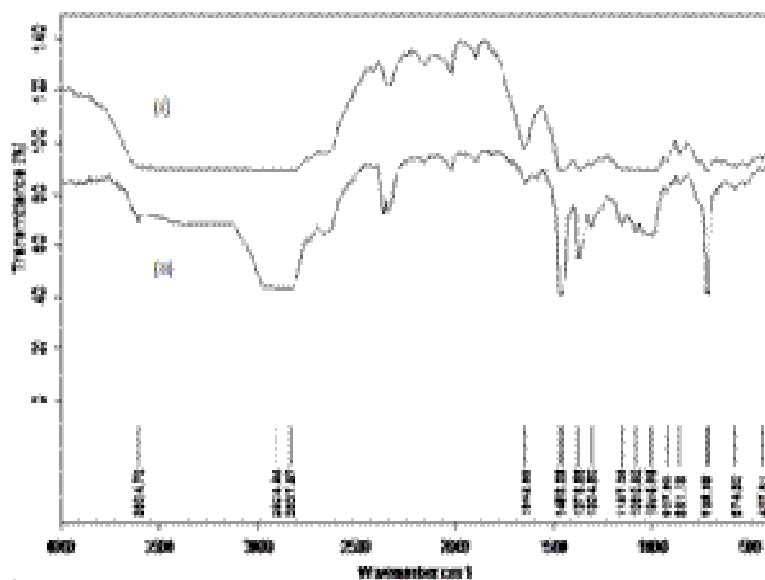


Figure 3.14 FTIR spectra of LDPE-starch (LDS300 15 weight%): (i) before biodegradation and (ii) after biodegradation in culture medium for eight weeks

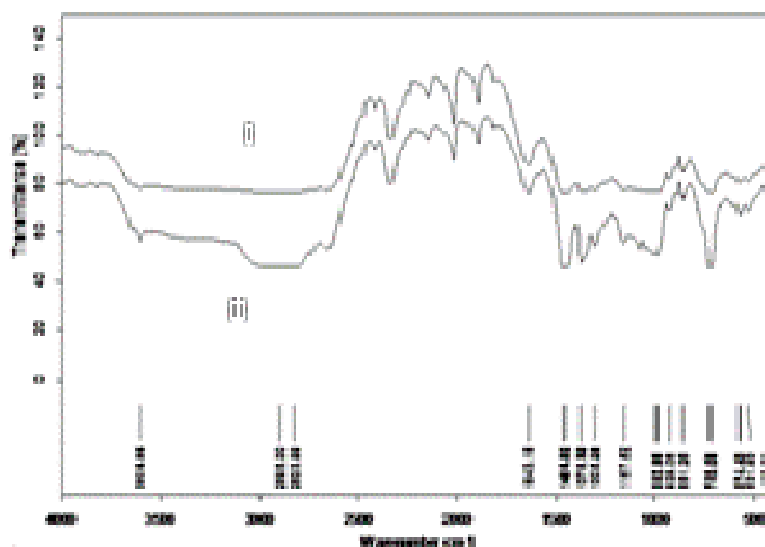


Figure 3.15 FTIR spectra of LDPE-dextrin (LDD300 15 weight%): (i) before biodegradation and (ii) after biodegradation in culture medium for eight weeks

Table 3.12 Characteristic FTIR spectral peaks in LDPE, starch and dextrin

Sample	Peak position (cm ⁻¹)	Characteristic group
LDPE	2909	C-H stretching
	1470	CH ₂ scissor and asymmetric bending
	1376, 1303	C-H bending
	720	CH ₂ rocking
Starch	3729	O-H stretching with absorbed water
	2885	C-H stretching
	1637	O-H bending with absorbed water
	1362	C-H bending and wagging
	1260-1000	C-O stretching (C-O-C and C-O-H)
	998	O-H deformation
Dextrin	3317	O-H stretching
	1352	C-H bending
	1150-1000	C-O stretching
	999	O-H deformation

Comparison of the spectra of LDPE-biopolymer blends before and after biodegradation shows notable differences in the C-O stretching absorbance at 1260-1000 cm^{-1} region, indicating the removal of biopolymer from the plastic film. After biodegradation, slight decrease in intensities of broad O-H stretching peak at 3700-3000 cm^{-1} region and O-H bending peak at 1640 cm^{-1} confirmed the loss of absorbed water as starch is removed by microorganisms.

3.2.6 Dynamic mechanical analysis

Dynamic mechanical analysis (DMA) was carried out to get information about molecular motion, with a focus on miscibility and interactions between the components. The molecular origins of the mechanical relaxations in polyethylene have been explained by Frubing et al. [24]. A complex α process comprises of relaxation in the crystallites and another one in the amorphous regions. This is primarily caused by the longitudinal chain transport through the crystallites of the semi crystalline polymer which, at their turn, facilitates the reorganization in the adjacent amorphous regions. The β process is attributed to the glass rubber transitions in the amorphous phase, which takes place around -30°C . The γ process also has its origin in the amorphous phase, but involves more localized motion than the β process [25].

Table 3.13 Dynamic Mechanical Analysis of LDPE and LDPE-starch blend

Sample	T ($^{\circ}\text{C}$)	Tan δ at T
LDPE	73.85	0.2525
LDS300 15%	69.66	0.2279

(T = Temperature at which tan δ is maximum)

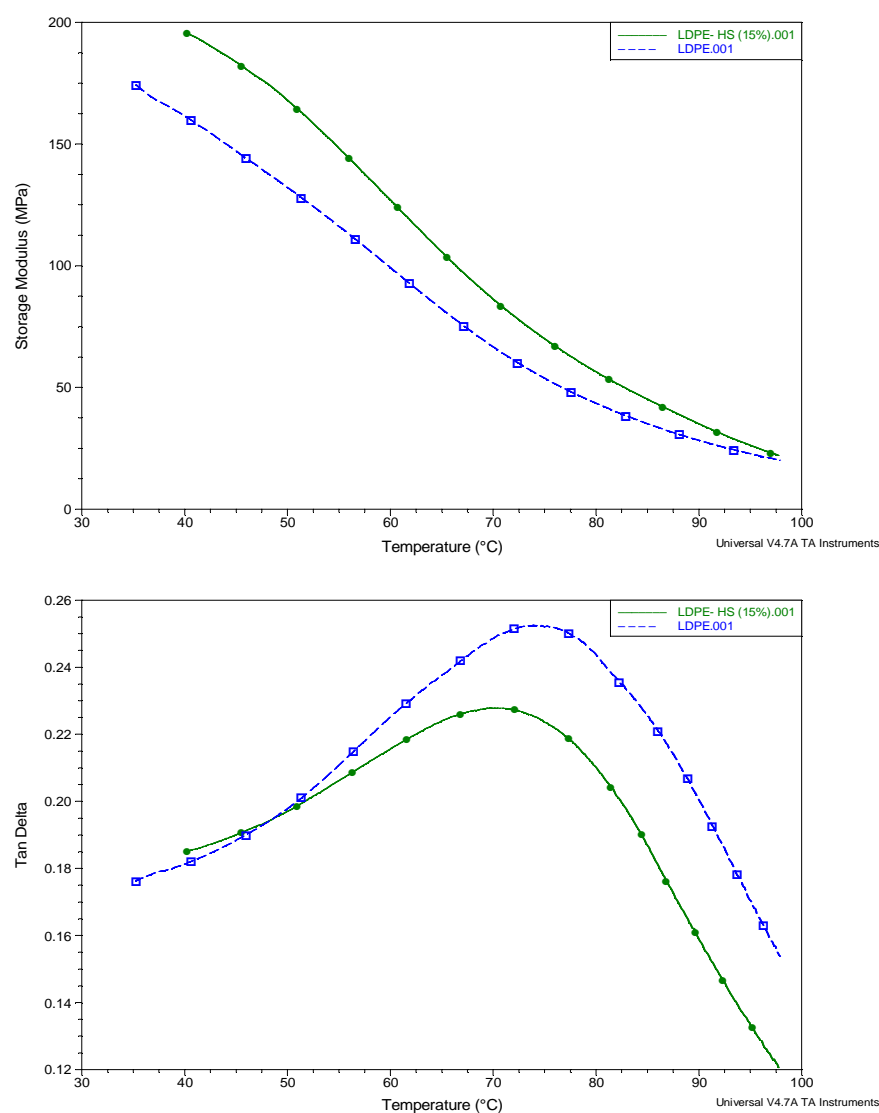


Figure 3.16 Results of dynamic mechanical analysis of LDPE and LDPE-starch blend

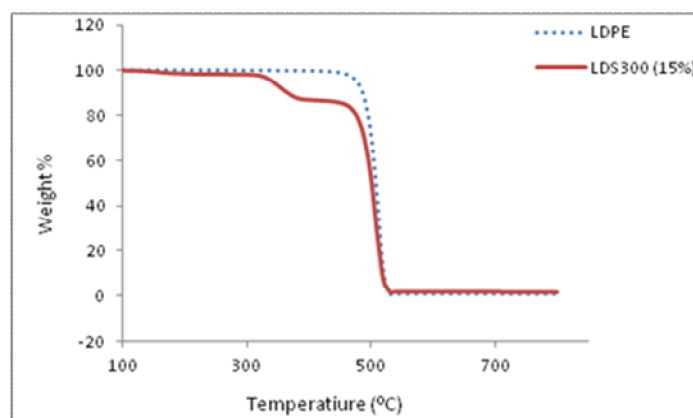
Figure 3.16 shows the variation in storage modulus and loss factor ($\tan \delta$) of LDPE and LDPE-starch blends measured over the temperature range from 40 °C to 100 °C. The glass transition of LDPE is not visible in this region. The temperature at which $\tan \delta$ was maximum was 73.85 °C for LDPE. This temperature is related to α relaxation, which has been interpreted as relaxation of the constrained molecules with reduced

mobility located near crystallites [26]. LDPE-starch blend shows higher storage modulus as compared to pure LDPE due to the stiffening imparted by the starch molecules. Pure LDPE shows a high damping ($\tan \delta$) as compared to the blend. The lower $\tan \delta$ value shown by the blend (Table 3.13) is attributed to the stiffening of the LDPE matrix by the starch particles [27].

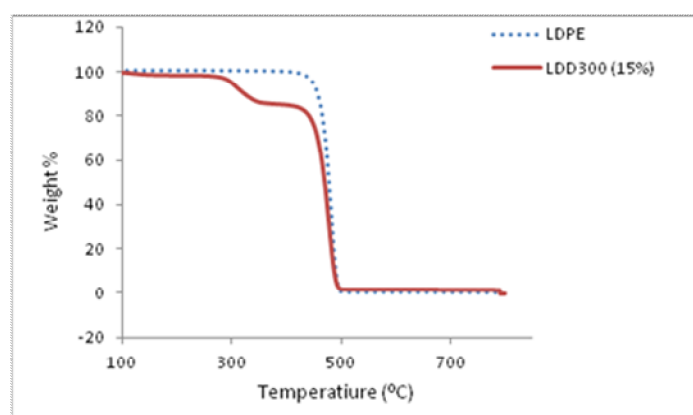
3.2.7 Thermogravimetric analysis

Figure 3.17 shows typical thermograms of LDPE and LDPE-biopolymer (15 weight %) blends. From figure it can be seen that the weight loss of LDPE occurred in a one-step degradation process which starts at 420 °C and reaches a maximum at 482 °C. At this temperature thermal decomposition of the C-C covalent bonds take place, resulting in breakdown of the main chain, which is due to generation of free radicals [28]. The onset of degradation temperature, the temperature at which weight loss is maximum (T_{\max}), and residual weight in percentage are given in Table 3.14.

The thermal degradation of the LDPE-starch blend occurred in a two-step degradation process. Similar degradation behaviour was observed in the case of LDPE-dextrin blend too. There is considerable decrease in weight during the temperature range of 250 °C-350 °C which corresponds to the loss of biopolymer as this is the decomposition temperature for this filler [29]. After that, the thermal degradation step of LDPE is observed. This illustrates that the thermal degradation temperature of the biopolymer is lower than that of LDPE. The decline of T_{\max} from 482 °C to 477 °C shows that the addition of biopolymer marginally reduces the thermal stability of LDPE.



(a)



(b)

Figure 3.17 TGA thermograms of a) LDPE-starch and b) LDPE-dextrin blends

Table 3.14 Results of thermogravimetric analysis of LDPE, LDPE-starch and LDPE-dextrin blends

Sample	Temperature of onset of degradation ($^{\circ}\text{C}$)	T_{max} ($^{\circ}\text{C}$)	Rate of maximum degradation ($\%/^{\circ}\text{C}$)	Residual weight (%)
LDPE	420	482	3.514	0.6023
LDS100 (15%)	414	477	2.581	1.207
LDS300 (15%)	416	477	2.616	1.285
LDD100 (15%)	409	478	2.502	1.492
LDD200 (15%)	411	478	2.562	1.535
LDD300 (15%)	409	477	2.515	1.623

3.2.8 Differential scanning calorimetry

Differential scanning calorimetry monitors enthalpy associated with phase transitions and chemical reactions as a function of temperature [30]. DSC thermograms of LDPE, LDS300 (15%), and LDD300 (15%) blends are shown in Figure 3.18. A melting point of 142 °C and a melting heat of 286.7J/g have been reported for completely crystallized polyethylene. The ratio of the melting heat of the samples and the melting heat of completely crystallized polyethylene was used to calculate the degree of crystallization [31]. Table 3.15 shows the average values for the melting temperature (T_m), crystallization temperature (T_c), enthalpy of fusion (ΔH_f), enthalpy of crystallization (ΔH_c) and % crystallinity for LDPE and LDS300 (15%), and LDD300 (15%) blends.

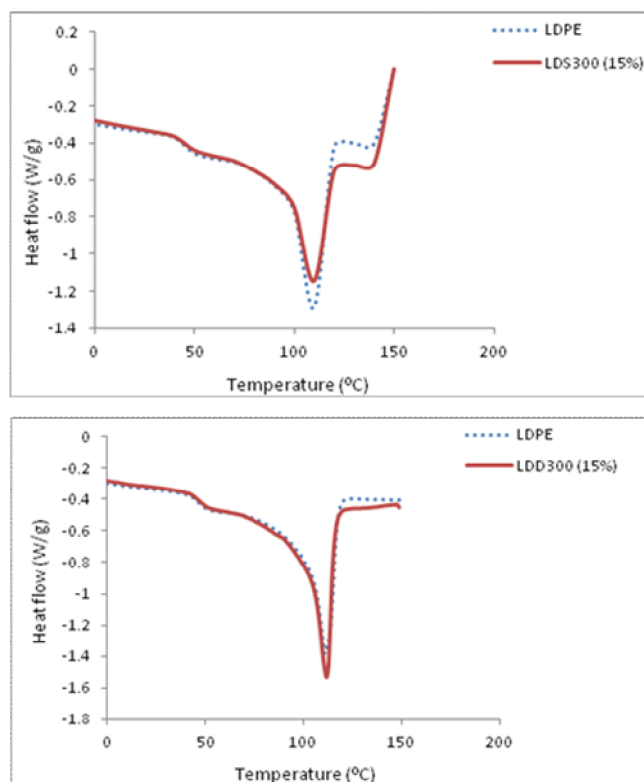


Figure 3.18 DSC thermograms of LDPE, LDPE-starch and LDPE-dextrin blends

Table 3.15 Results of differential scanning calorimetry

Sample	T _m (°C)	ΔH _f (J/g)	T _c (°C)	ΔH _c (J/g)	% crystallinity
LDPE	110	67	96	79	24
LDS300 (15%)	113	59	96	65	21
LDD300 (15%)	112	62	96	75	22

ΔH_f and ΔH_c values for the blends are lower compared to virgin LDPE. There is no significant decrease in crystallinity of LDPE in the blends which indicated that LDPE and biopolymer are incompatible. i.e., LDPE-starch and LDPE-dextrin interactions are weak. In addition to this, the melting and crystallization temperature of LDPE and blends are almost similar. This also suggests the incompatibility of LDPE and the fillers.

3.2.9 Morphological studies

SEM is a powerful technique used to evaluate the morphological changes of a degraded polymer [32]. Figure 3.19 show the scanning electron micrographs of the fractured surfaces of neat LDPE, LDS300 (15%), and LDD300 (15%). Figure 3.20 shows the SEM micrographs of the samples after immersing for eight weeks in the culture medium in a shake culture flask. The photomicrograph of the neat LDPE shows no significant change even after eight weeks. The micrographs of the LDS300 (15%), and LDD300 (15%) show a number of irregular cavities. This is a clear evidence of biodegradation in the case of biopolymer filled low density polyethylene.

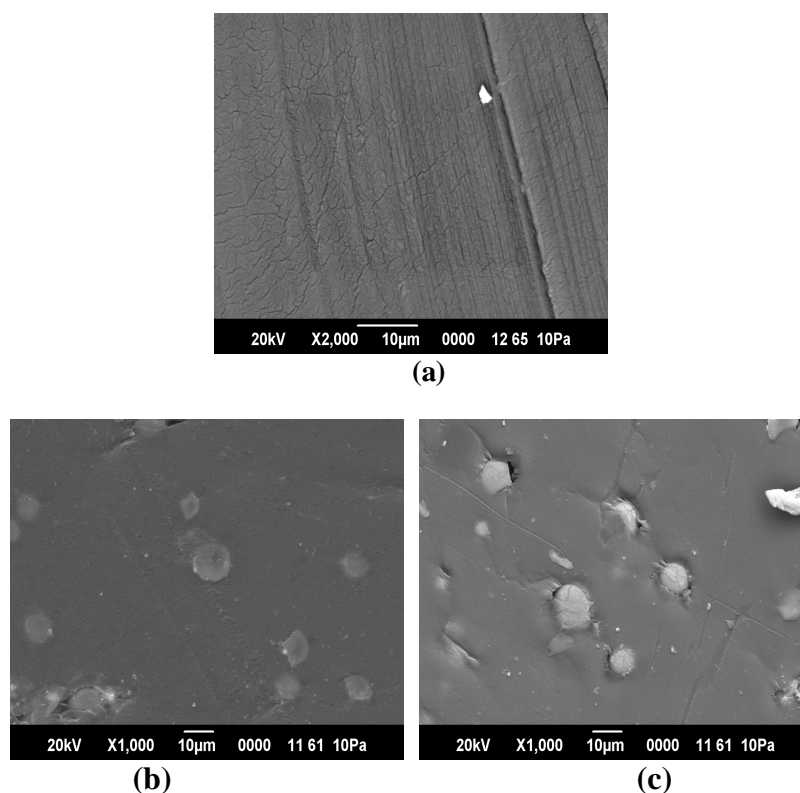


Figure 3.19 Scanning electron micrographs (before biodegradation) of: a)LDPE, b)LDPE-starch(LDS300) blend and c)LDPE-dextrin (LDD300) blend

As LDPE is nonpolar and starch and dextrin are polar in nature, they exhibit differences in polarity and surface free energy. The resulting large interfacial free energy leads to slight interactions in the interface of the two components in the blends [33] and it apparently causes reduction in tensile strength and elastic modulus. Spherical dispersed phase particles in the LDPE-biopolymer blends suggest that the biopolymer is incompatible with the matrix LDPE and there is poor adhesion resulting in starch particles being pulled out during fracture.

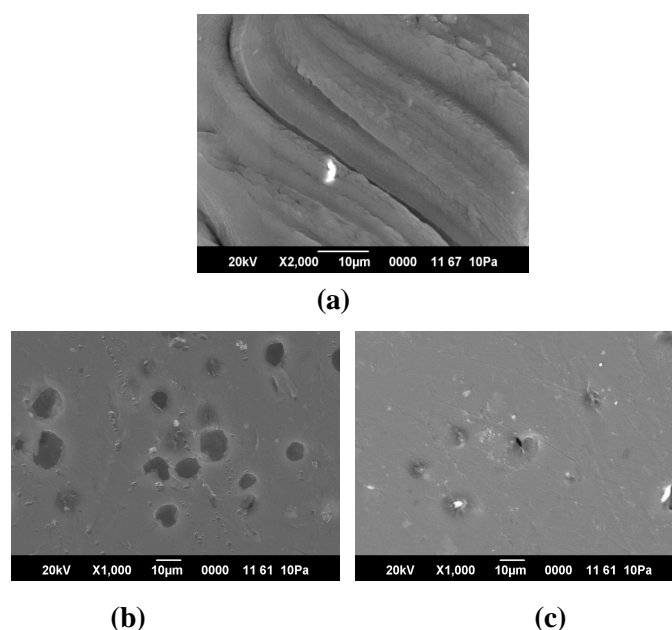


Figure 3. 20 Scanning electron micrographs of: a) LDPE, b) LDPE-starch and c) LDPE-dextrin blend after biodegradation in culture medium for eight weeks

Cavities present in the micrograph reveal the removal of biopolymer by microorganisms. This weakens the polymer matrix as well as greatly increases the surface area of the plastic as evident in the deterioration in mechanical properties.

3.3 Conclusions

Various compositions of blends of low density polyethylene with different grades of tapioca starch and dextrin were prepared. The reduction in the tensile properties of LDPE on incorporation of biopolymer suggests that the filler has no reinforcing effect on LDPE. The blends show lower melt flow rates as compared to neat LDPE. The melt flow indices of the LDPE-biopolymer blends decreases as the biopolymer concentration increases apparently due to increased entanglement of the polymer chains of LDPE and biopolymer. The reduction in the tensile properties and

weight loss of the blends after biodegradability tests in the culture medium and soil suggests that blends are partially biodegradable. The water absorption values of the blends were higher indicating an enhanced affinity for microbial attack. FTIR peak intensities of LDPE-starch and LDPE-dextrin blends before and after biodegradation studies in shake culture flask reveal the biodegradation of the samples in presence of amylase producing *vibrios*. Dynamic mechanical analyses results show that pure LDPE has lower storage modulus as compared to the LDPE-biopolymer blend. The thermogravimetric studies indicate that the thermal stability of LDPE is marginally lowered by the incorporation of biopolymer. There is no significant decrease in crystallinity of LDPE in the blends, which shows that LDPE and biopolymer are incompatible. The evidence from scanning electron microscopic studies suggests that the newly prepared LDPE-biopolymer blends are partially biodegradable.

References

- [1] Pedroso, A. G.; Rosa, D.S.; Polym Adv Technol 2005, 16, 310.
- [2] Chiellini, E.; Corti, A .; Swift, G.; Polym Degrad Stab 2003, 81, 341.
- [3] Santonja-Blasco, L.; Contat-Rodrigo, L.; Moriana-Torro, R.; Ribes-Greus, A.; J Appl Polym Sci 2007, 106, 2218.
- [4] Griffin, G. J. L.; Adv Chem Ser 1974, 134, 114.
- [5] Lim, S.; Jane, J.; Biotechnol Progr 1992, 8, 51.
- [6] Averous, L.; Fringant, C.; Moro, L.; Starch/ Starke 2001, 53, 368.
- [7] Clarinval, A.; Halleux, J.; Classification of biodegradable polymers. In: Smith R (ed) Biodegradable Polymers for Industrial Applications. Woodhead, London, 2005.
- [8] Otey, F.H.; West Hoff, R. P.; Doane, W. M.; Ind Eng Chem Prod Res Dev 1980, 19. 592.

- [9] Griffin, G. J. L.; Am Chem Sec Div Org Coat Plast Chem 1973, 33, 88.
- [10] Evangelista, R. L.; Sung, W.; Jane, J.; Gelina, R. J.; Nikolov, Z. L.; Ind Eng Chem Res 1991, 30 1841.
- [11] Ahamed, N. T.; Singhal, R. S.; Kulkarni, P. R.; Kale, D.D.; Pal, M.; Carbohydr Polym 1996, 31, 157.
- [12] Thakore, I. M.; Iyer, S.; Desai, A.; Lele, V.; Devi, S.; J Appl Polym Sci 1999, 74, 2791.
- [13] Strong, B. A.; Plastics Materials and Processing, 2nd edn. Prentice Hall, New Jersey, USA, 108, 1996.
- [14] Jang, B. C.; Huh, S. Y.; Jang, J. G.; Bae, Y. C.; J Appl Polym Sci 2001, 82, 3313.
- [15] Rutkowska, M.; Heimowska, A.; Krasowska, K.; Janik, H.; Pol J Environ Stud 2002, 11, 267.
- [16] Bikiaris, D.; Prinos, J.; Panayiotou, C.; Polym Degrad Stab 1997, 58, 215.
- [17] Danjaji, I.D.; Nawang, R.; Ishiaku, U.S.; Ismail, H.; Mohd Ishak, Z.A.; Polym Test 2002, 21, 75.
- [18] Zhang, M.; Li, X. H.; Gong, Y. D.; Zhao, N. M.; Zhang, X. F.; Biomaterials 2002, 23, 2641.
- [19] Chandra, R.; Rustgi, R.; Polym Degrad Stab 1997, 56, 185.
- [20] Wang, H. R.; Chen, K. M.; Colloids and Surfaces A: Physicochemical and Engineering Aspects, 281, Issues 1-3, 190, 2006.
- [21] Lin, S. C.; Bulkin, B. J.; Pearce, E. M.; J Polym Sci (Polym Chem Ed) 1979, 17, 3121.
- [22] Coleman, M. M.; Painter, P. C.; In: Bram Jr, E. G.(ed) Applications of Polymer Spectroscopy, Academic Press, New York, 135, 1978.
- [23] Coleman, M. M.; Painter, P. C.; J Macromol Sci Revs Macromol Chem 1978, C16, 2, 197.
- [24] Frubing, P.; Blischke, D.; Gerhard-Multhaupt, R.; Salah Khalil, M.; J Phys D: Appl Phys 2001, 34, 3051.

- [25] Dascalu, M.C.; Vasile, C.; Silvestre, C.; Pascu, M.; European Polym J 2005, 41, 1391.
- [26] Bikiaris, D.; Aburto, J.; Alric, I.; Borredon, E.; Botev, M.; Betchev, C.; Panayiotou, C.; J Appl Polym Sci 1999, 71, 1089.
- [27] Smit, P. P. A.; Rheol Acta 1966, 5, 277.
- [28] Jana, R.N.; Mukunda, P.G.; Nando, G.B.; Polym Degrad Stab 2003, 80, 75.
- [29] Moriana-Torro, R.; Contat-Rodrigo, L.; Santonja-Blasco, L.; Ribes-Greus, A.; J Appl Polym Sci 2008, 109, 1177.
- [30] Vyas, H.; Shrinet, V.; Murthy, C. N.; Jain, R. C.; Singh, A. K.; Polym-Plast Technol Eng 2008, 47, 1231.
- [31] Shogren, R.L.; Thompson, A. R.; Felker, F. C.; Harry-O’Kuru, R. E.; Gordon, S. H.; Greene, R. V.; Gould, J. M.; J Appl Polym Sci 1992, 44,1971.
- [32] Sawyer, L. C.; Grubb, D. T.; Polymer Microscopy, Chapman and Hall, 2-6 Boundary Row, London, 2, 229, 1996.
- [33] Fu, X.; Chen, X.; Wen, R.; He, X.; Shang, X.; Liao, Z.; Yang, L.; Polym Res 2007, 14, 297.



COMPATIBILIZED LOW DENSITY POLYETHYLENE-STARCH BLENDS

Contents	4.1	<i>Introduction</i>
	4.2	<i>Results and discussion</i>
	4.3	<i>Conclusions</i>

Blends of starch and low density polyethylene compatibilized with zinc salt of polyethylene-co-methacrylic acid (EMA-Zn), sodium salt of polyethylene-co-methacrylic acid (EMA-Na) and maleic anhydride (MA) were prepared. The compatibility behaviour of blends was studied by evaluating mechanical properties, melt flow measurements, spectroscopy, thermal analysis and scanning electron microscopy. Blends without compatibilizer show poor properties characteristic of incompatible polymer blends. Both spectroscopic and morphological features indicated that the ionomer is an efficient compatibilizer for low density polyethylene-starch blends. The biodegradability tests on the blends indicate that the blends are partially biodegradable.

4.1 Introduction

Low density polyethylene (LDPE) is popular as a packaging material because of its low cost, ease of processability, insensitivity to moisture, and flexibility. However LDPE is not biodegradable in nature [1]. Biopolymers, such as starch are relatively inexpensive and possess renewability and biodegradability [2]. The addition of small amount of starch to low density polyethylene can enhance the biodegradable properties of the resulting blends. Therefore blending of low density polyethylene with biopolymers offers an interesting route to obtain new materials with tailored properties.

Most of the polymer blends are found to be immiscible and incompatible. In the case of miscible blends, the overall physico-mechanical properties depend on two structural parameters: (a) proper interfacial tension which leads to a phase size small enough to allow the material to be considered as macroscopically homogenous and (b) an interphase adhesion strong enough to assimilate stresses and strains without disruption of the established morphology [3].

Starch and low density polyethylene form immiscible blends, in which weak interfacial adhesion and large interfacial tension lead to large particles in the dispersed phase. When these immiscible blends are subjected to stress, the stress concentration at the polymer-polymer interface is weak and unable to transfer the stress between the continuous and dispersed phases. This incompatibility results in blends with poor mechanical properties [4-5]. Numerous investigations have cited the use of compatibilization, ranging from modification of one of the blend components [6-7] to incorporation of a minor-component compatibilizer

[8-12] to improve the blend properties. By the introduction of a compatibilizer, an increase in stress transfer between the continuous and dispersed phases is produced, improving the mechanical properties of the blend [13].

Various studies have been published regarding the improvement of the morphology and the mechanical properties of LDPE blends by means of compatibilizers. Maleic anhydride grafted polyethylene has been reported as a compatibilizer in blends of LDPE [14]. Glycidyl methacrylate-grafted LDPE too has been used as a compatibilizer in LDPE blends [15].

Ionomers are ionic polymers having a hydrocarbon backbone containing pendant acid groups which are neutralized at least partially to form salt groups [16-17]. The unique properties of ionomers are sources of growing industrial and academic interest. The studies of ionic interaction in macromolecular systems represent one of the liveliest areas of research activity in modern polymer science. Ionomers have the unique ability to compatibilize certain incompatible blends, such as LDPE/Nylon-6 [18-19], PP/EVOH [20], HDPE/Nylon-6 [21], HDPE/Nylon-66 [22], and so on. In the literature, various ionomers, such as poly(ethylene-co-sodium methacrylate) [19], poly(styrene-co-sodium methacrylate) [23], and metal salts of sulfonated PET [24] were successfully used to compatibilize incompatible blends. When ionomers are added to the binary blend, they form ionic cross-links at the interface of the blends and thus homogeneity is improved [25].

This chapter reports the results of studies on the use of ionomers (zinc salt of polyethylene-co-methacrylic acid (EMA-Zn), sodium salt of polyethylene-co-methacrylic acid (EMA-Na)) and maleic anhydride

(MA) as compatibilizers for blends of low density polyethylene and starch. Maleic anhydride has been widely used as a compatibilizing agent for this type of systems and is used as a reference in this work. Designations of the samples used in this chapter and their descriptions are given in Table 4.1.

Table 4.1 Description of sample designations

Sample designation	Description
C5M	LDPE-20% starch-5% MA
C5Z	LDPE-20% starch-5% (EMA-Zn)
C5S	LDPE-20% starch-5% (EMA-Na)
LDS(x)-MA(y)	LDPE- x% starch-y% MA
LDS(x)-Zn(y)	LDPE- x% starch-y% (EMA-Zn)
LDS(x)-Na(y)	LDPE- x% starch-y% (EMA-Na)

4.2 Results and discussion

4.2.1 Mechanical properties

The mechanical properties of the compatibilized as well as uncompatibilized LDPE-starch blends are shown in the figures 4.1, 4.2 and 4.3. The tensile strength decreased with increase in concentration of starch due to the weak interfacial adhesion between hydrophilic starch and hydrophobic LDPE [26-27]. Samples with maleic anhydride, EMA-Zn and EMA-Na as compatibilizing agents show higher tensile strength compared to uncompatibilized blends. In the case of the MA-compatibilized blends, 2% addition of MA gives maximum tensile strength while for ionomer-compatibilized blends, 5% addition of ionomer gives maximum tensile strength both in the case of EMA-Zn and EMA-Na. The changes in tensile strength are apparently due to the changes in phase behaviour. Addition of

compatibilizer increases the interfacial adhesion which facilitates efficient stress transfer from one phase to other, due to which compatibility between LDPE and starch increases.

The ductility, as measured by the elongation at break of the blends, is shown in figure 4.2. The ductility of the LDPE-starch blends is also shown as a reference and as a measure of the compatibilization effect. The elongation at break for all the compatibilized blends increased compared to the uncompatibilized blend. The increase in ductility is attributed to the higher interfacial adhesion and the particle size decrease and also proves that compatibilization has occurred.

In contrast, elastic modulus increases as the starch loading is increased (figure 4.3). Starch incorporated into LDPE apparently retained their granular shape after processing. These granules are stiff and act as rigid fillers. In general, modulus is closely related to the hard domain of the material. As the starch content increases, the hard domain content increases, as does the tensile modulus of the blend. But the elastic moduli of the compatibilized blends are lower than that of the uncompatibilized blends due to the flexibilization of the blends.

Addition of MA to LDPE-starch blends, showed a significant changes in mechanical properties of the blends, since anhydride groups could react with hydroxyl groups in starch to produce chemical bonding, thus improving the dispersion of starch, the interfacial adhesion, and subsequently the mechanical properties of the blends [28].

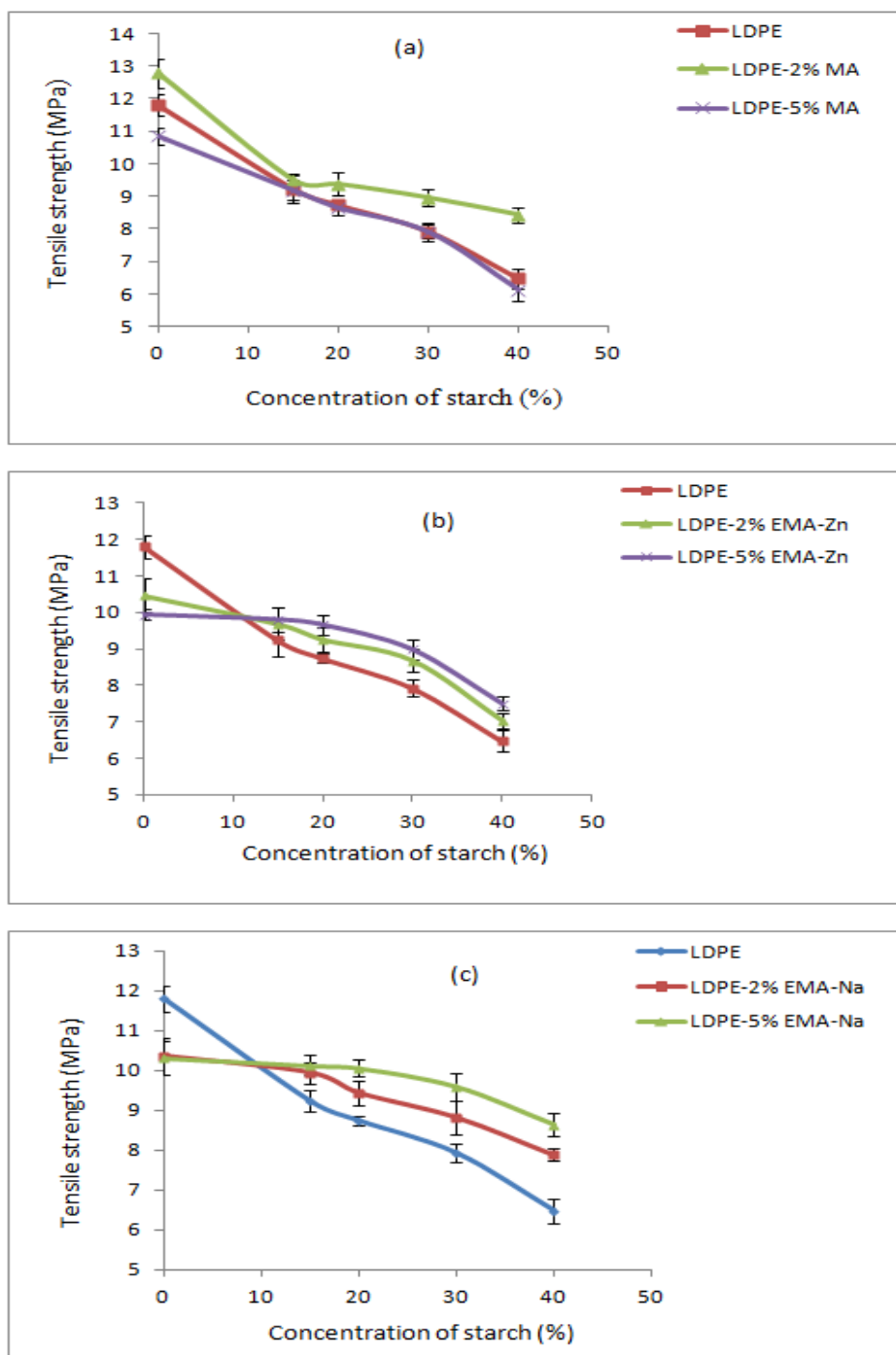


Figure 4.1 Variation of tensile strength with the concentration of starch for: (a) LDPE-starch-MA blends, (b) LDPE-starch-(EMA-Zn) blends and (c) LDPE-starch-(EMA-Na) blends

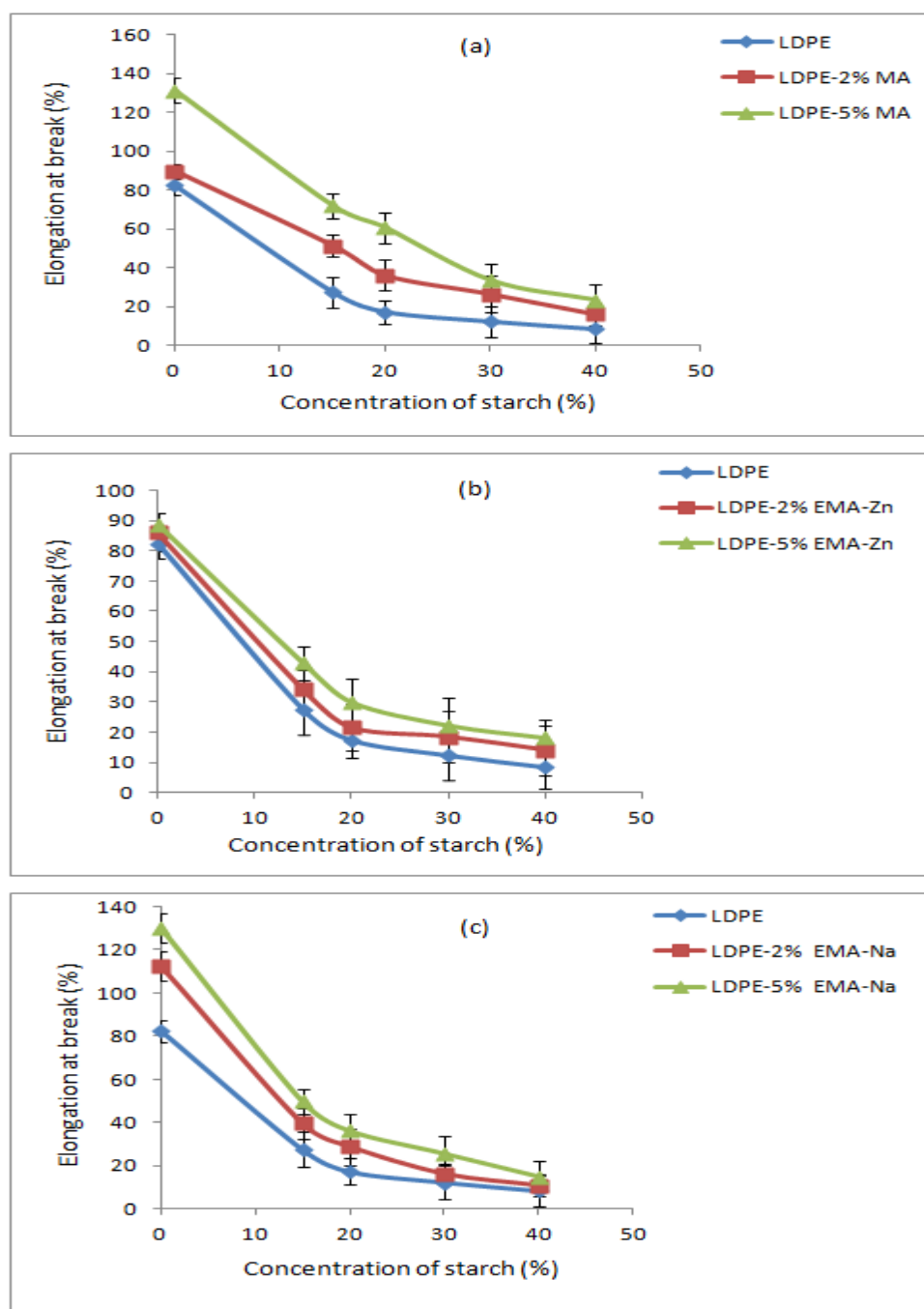


Figure 4.2 Variation of elongation at break with the concentration of starch for: (a) LDPE-starch -MA blends, (b) LDPE-starch-(EMA-Zn) blends and (c) LDPE-starch-(EMA-Na) blends

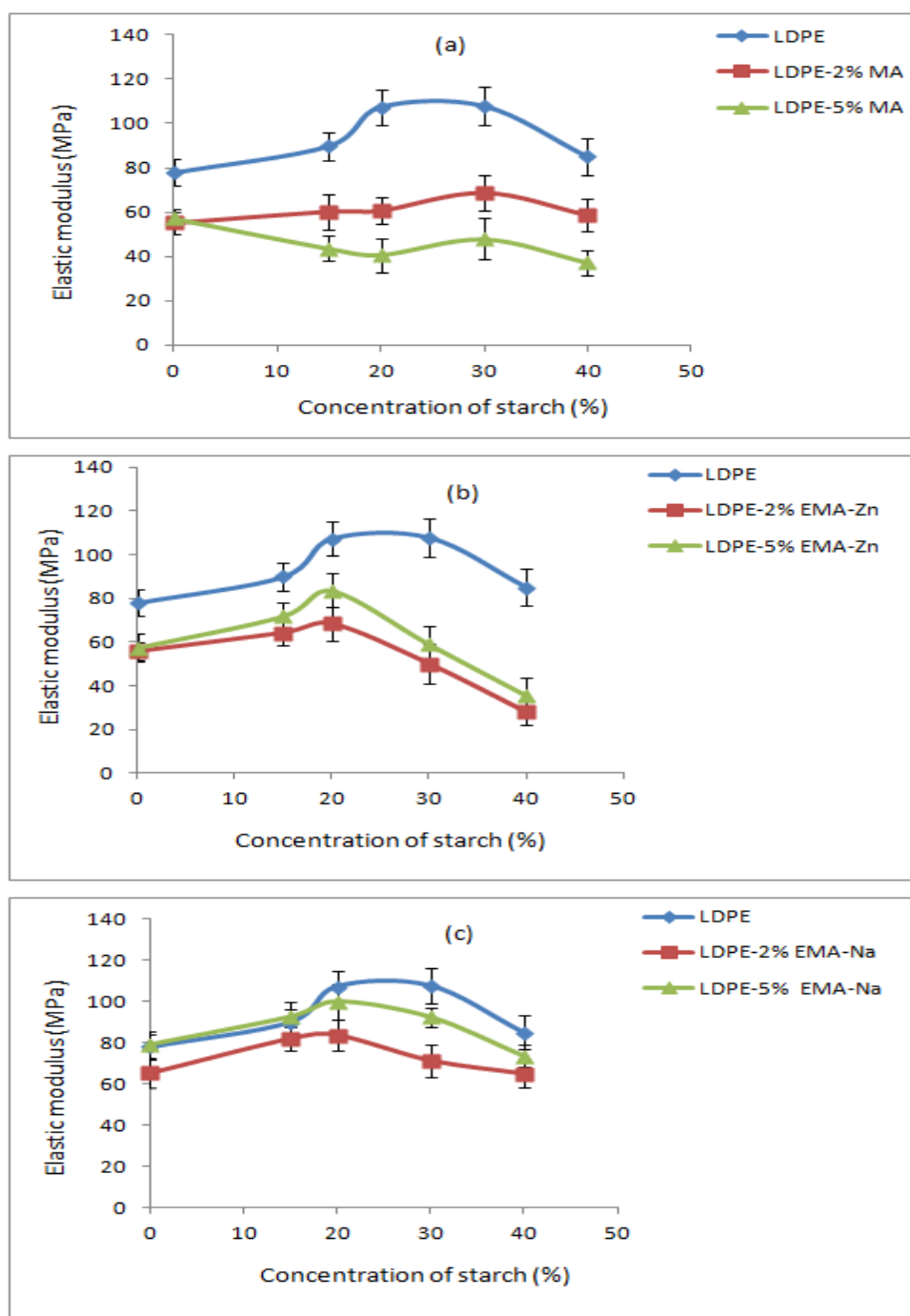


Figure 4.3 Variation of elastic modulus with the concentration of starch for: (a) LDPE-starch-MA blends, (b) LDPE-starch-(EMA-Zn) blends and (c) LDPE-starch-(EMA-Na) blends

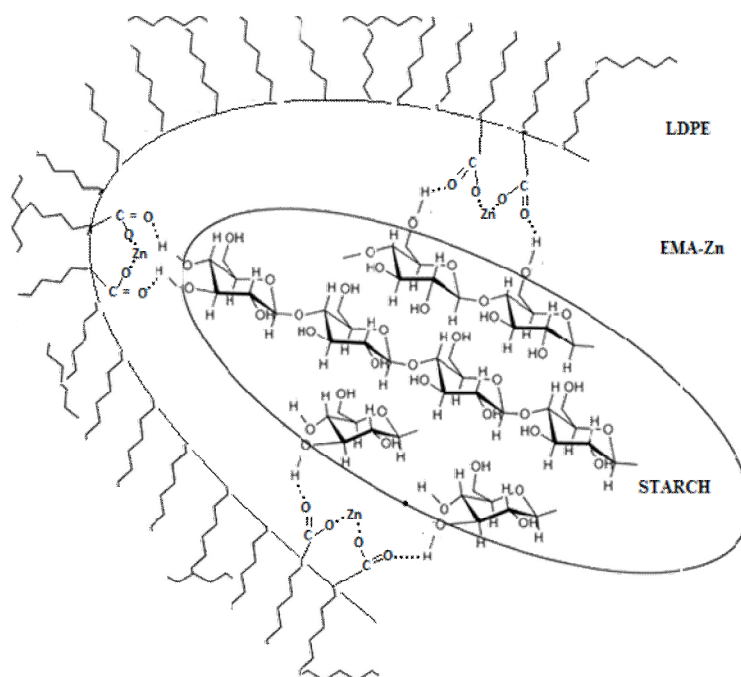


Figure 4.4a Proposed schematic representation of the interaction between starch, EMA-Zn and LDPE

When ionomers are added to the binary blend, they apparently form ionic cross-links at the interface of the blends and homogeneity is improved. The ionomers used in this study have two distinct regions—a polyethylene rich domain and a region predominantly composed of metal cation-carboxylate anion pair. The carboxyl groups of the ionomers may be interacting with the hydroxyl groups of starch through polar-polar interactions as proposed in figures 4.4a and 4.4b. The nonpolar polyethylene domain of the ionomers and the LDPE are compatible. The polyethylene domain of the ionomers and the LDPE are believed to associate through co-crystallization, amorphous chain entanglement or both (figures 4.4a and 4.4b) [29-30]. While the interactions involving nonpolar LDPE molecular chains and the nonpolar region of the ionomers is of weak van der Waals type, the same due to carboxyl groups of the ionomer and the hydroxyl groups of starch could be of much stronger type as proposed in the figures.

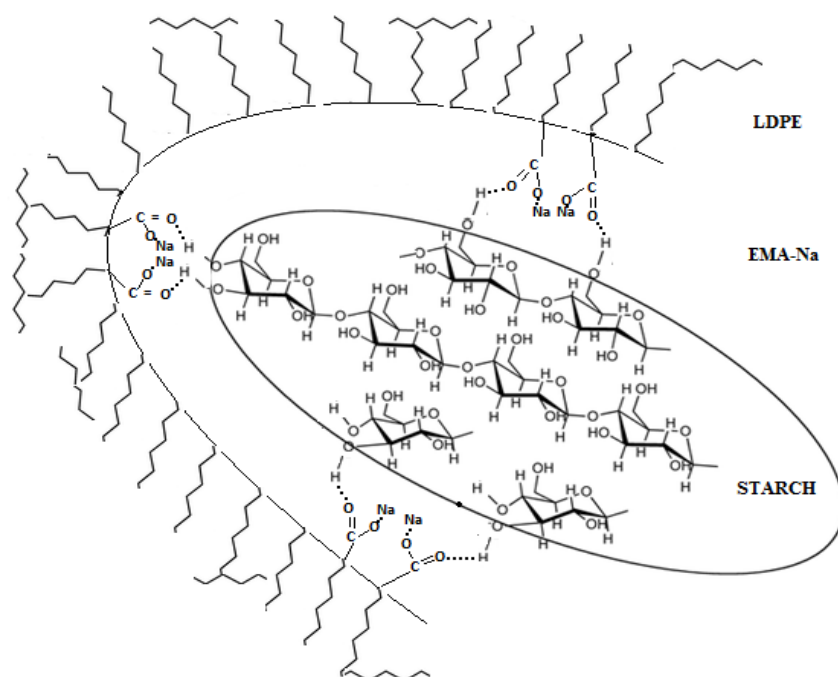


Figure 4.4b Proposed schematic representation of the interaction between starch, EMA-Na and LDPE

The effect of the addition of the ionomer as compatibilizer on the tensile strength of LDPE- starch blends is shown in figures 4.5a and 4.5b. The tensile strength increases with increase in ionomer content up to 5 weight %. The additions of more than 5 weight % ionomer do not result in further improvement in tensile strength. This suggests that the tensile strength of a compatibilized blend is determined not only by the interfacial adhesion but also by the strength of the matrix that is highly affected by the quantity of the compatibilizer in the blend [31]. The lack of improvement in properties with higher ionomer concentration in the blend may be due to the limited solubility of the ionomer in the blend, or the limit on the migration of ionomer to the interface during processing [32].

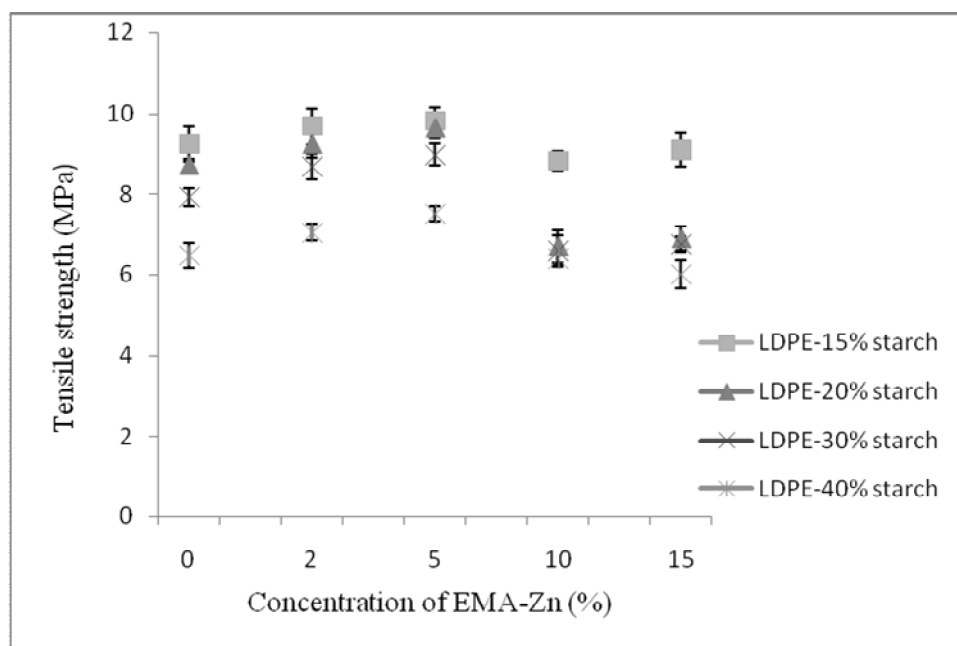


Figure 4.5a Effect of concentration of EMA-Zn as compatibilizer on the tensile strength of LDPE- starch blends

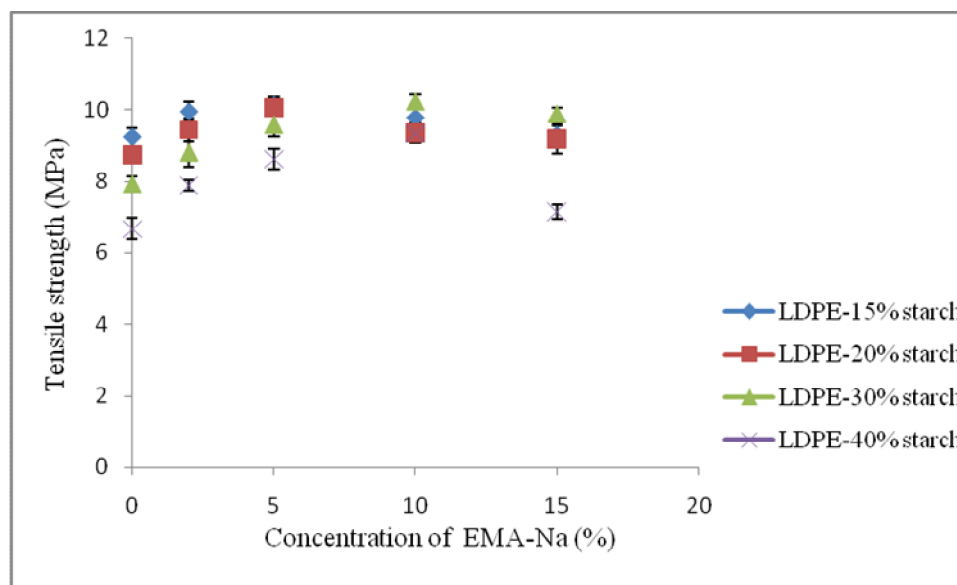


Figure 4.5b Effect of concentration of EMA-Na as compatibilizer on the tensile strength of LDPE- starch blends

4.2.2 Melt flow measurements

Figures 4.6a and 4.6b show the variations of melt flow indices with varying concentration of starch in the case of LDPE-starch-(EMA-Zn) blends and LDPE-starch-(EMA-Na) blends. Melt flow index is a measure of average molecular mass and is an inverse measure of the melt viscosity. All the samples containing starch show a reduction in MFI values as compared to the samples without starch. The MFI values decreased as the concentration of starch increased. This may be due to a higher viscosity associated with increase in concentration of the spherical starch particles in the LDPE matrix. It was observed that the melt flow increased in the case of all the LDPE-starch-ionomer blends as the ionomer content increased from 2 weight % to 15 weight %. Though ionomers generally show higher melt viscosity as compared to their base polymers, in the case of the ionomers used in this study the increase in melt flow may be due to the low molecular weight of their backbone [33]. This clearly proves the favourable effect of ionomer as a compatibilizer.

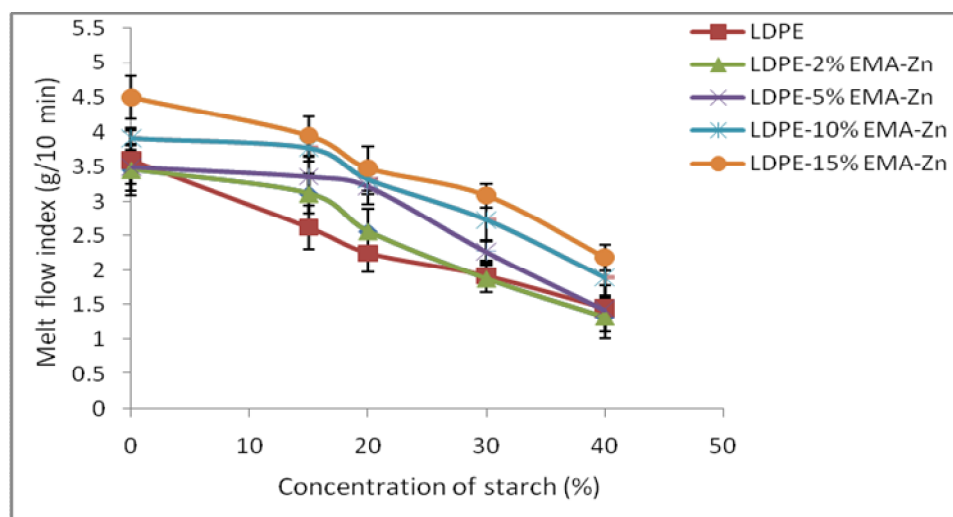


Figure 4.6a Variation of melt flow index with the concentration of starch in LDPE-starch-(EMA-Zn) blends

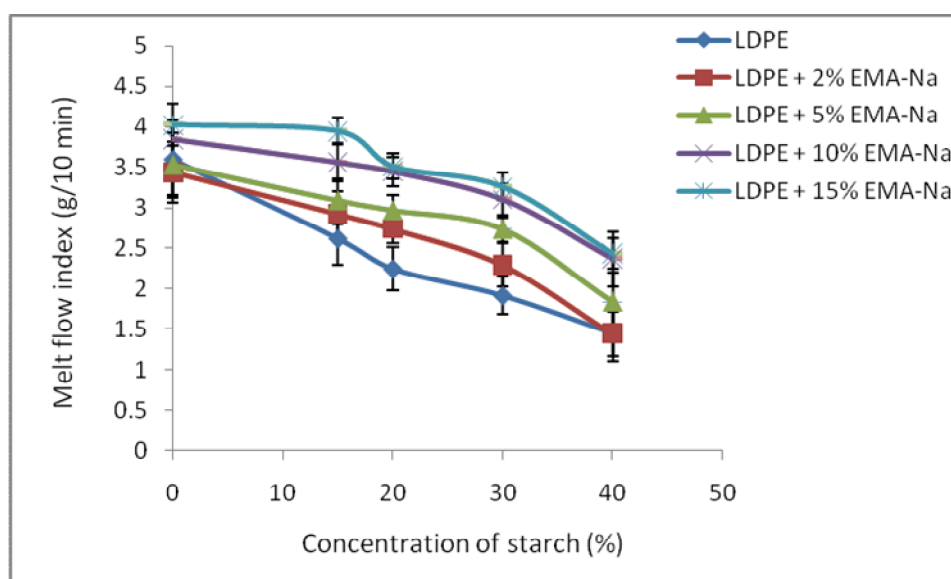


Figure 4.6b Variation of melt flow index with the concentration of starch in LDPE-starch-(EMA-Na) blends

4.2.3 Biodegradation studies

Figure 4.7 exhibits the tensile properties of LDPE-20% starch-compatible blends after biodegradation in culture medium. As shown in the figure there is a significant reduction in tensile strength after biodegradation for all the blends. The reason for this reduction is the consumption of starch by microorganisms. For the blends with higher starch content apparently starch is more exposed and as a result, a greater portion of it is consumed by microorganisms as evident from the higher drop in stress-strain properties after biodegradation in the case of these blends. For the blends containing lower quantity of starch, the starch may be almost completely covered by LDPE and therefore not accessible to the microorganisms [34].

After biodegradation in culture medium for four months the tensile properties of the uncompatibilized blend films were lower than those of the compatibilized blend films. For the uncompatibilized blends, apparently the LDPE matrix encapsulates the starch granules without any bonding.

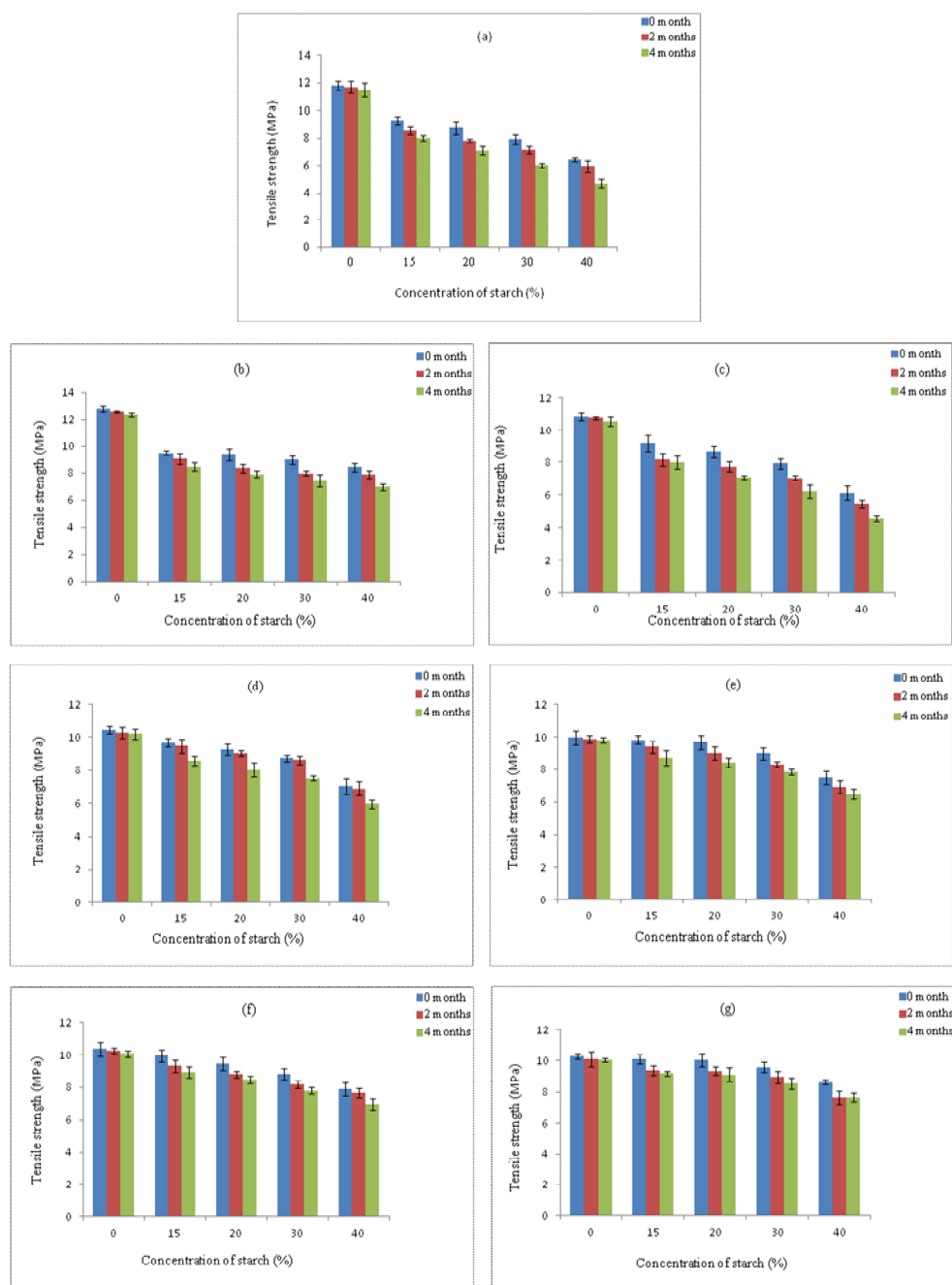


Figure 4.7 Biodegradation of: (a) LDPE-starch blends, (b) LDPE-starch-2% MA blends, (c) LDPE-starch-5 % MA blends, (d) LDPE-starch-2% (EMA-Zn) blends, (e) LDPE-starch-5% (EMA-Zn) blends, (f) LDPE-starch-2% (EMA-Na) blends and (g) LDPE-starch-5% (EMA-Na) blends

Table 4.2 Percentage decrease in weight of LDPE-starch-MA blends after biodegradation in culture medium for four months

Sample	Initial weight (g)	Weight after four months (g)	% weight loss
LDS(0)-MA(2)	0.3042	0.3041	0.03
LDS(0)-MA(5)	0.2254	0.2253	0.04
LDS(15)-MA(2)	0.2411	0.2320	3.77
LDS(15)-MA(5)	0.2769	0.2659	3.97
LDS(20)-MA(2)	0.2155	0.2056	4.59
LDS(20)-MA(5)	0.2858	0.2669	6.61
LDS(30)-MA(2)	0.1888	0.1718	9.00
LDS(30)-MA(5)	0.1583	0.1409	10.99
LDS(40)-MA(2)	0.3141	0.2445	22.16
LDS(40)-MA(5)	0.1552	0.1095	29.45

Table 4.3 Percentage decrease in weight of LDPE-starch-(EMA-Zn) blends after biodegradation in culture medium for four months

Sample	Initial weight (g)	Weight after four months (g)	% weight loss
LDS(0)-Zn(2)	0.2269	0.2268	0.04
LDS(0)-Zn(5)	0.2765	0.2764	0.04
LDS(15)-Zn(2)	0.1625	0.1580	2.77
LDS(15)-Zn(5)	0.1863	0.1831	1.72
LDS(20)-Zn(2)	0.1133	0.1083	4.41
LDS(20)-Zn(5)	0.1453	0.1405	3.30
LDS(30)-Zn(2)	0.2687	0.2486	7.48
LDS(30)-Zn(5)	0.1862	0.1755	5.75
LDS(40)-Zn(2)	0.1054	0.0895	15.09
LDS(40)-Zn(5)	0.2093	0.1860	11.13

This results in porosity of the LDPE matrix favoring the attack by microorganisms. For the LDPE-starch film with compatibilizer, the interfacial adhesion between the two components may make the removal of starch granules from the films more difficult.

Tables 4.2, 4.3 and 4.4 illustrate the weight loss of compatibilized LDPE-starch blends after biodegradation in culture medium for four months. All the compositions show reduction in weight due to the consumption of starch by microorganisms. LDPE in culture medium did not show any significant weight loss, whereas its blends with starch exhibited greater weight loss. It was observed that the biodegradation rate rapidly increased for the blend with 40% starch.

Table 4.4 Percentage decrease in weight of LDPE-starch-(EMA-Na) blends after biodegradation in culture medium for four months

Sample	Initial weight (g)	Weight after four months (g)	% weight loss
LDS(0)-Na(2)	0.2688	0.2687	0.04
LDS(0)-Na(5)	0.3144	0.3143	0.03
LDS(15)-Na(2)	0.2665	0.2601	2.40
LDS(15)-Na(5)	0.1486	0.1466	1.35
LDS(20)-Na(2)	0.2168	0.2074	4.34
LDS(20)-Na(5)	0.2969	0.2874	3.20
LDS(30)-Na(2)	0.2154	0.2001	7.10
LDS(30)-Na(5)	0.2761	0.2604	5.69
LDS(40)-Na(2)	0.2092	0.1794	14.25
LDS(40)-Na(5)	0.1902	0.1696	10.83

The table suggests that the degradation rate of the ionomer compatibilized films was lower than that of the MA compatibilized films. It might be implied that the compatibilizer has an inhibiting effect on the biodegradation of the film. This ionomer effect may be due to the polar-polar interactions between the carboxyl groups of ionomer and the hydroxyl groups of starch, which obstructs the consumption of starch by microorganisms [35].

4.2.4 Water absorption studies

Table 4.5 Water absorption of LDPE-starch-(EMA-Zn) blends

Sample	Initial weight (g)	Weight after 24 hours (g)	% water absorption
LDS(0)-Zn(2)	0.2999	0.3001	0.07
LDS(0)-Zn(5)	0.2537	0.2538	0.04
LDS(15)-Zn(2)	0.2432	0.2453	0.86
LDS(15)-Zn(5)	0.2996	0.3016	0.67
LDS(20)-Zn(2)	0.3722	0.3771	1.32
LDS(20)-Zn(5)	0.4332	0.4387	1.27
LDS(30)-Zn(2)	0.3080	0.3156	2.47
LDS(30)-Zn(5)	0.4317	0.4373	1.30
LDS(40)-Zn(2)	0.3721	0.3870	4.00
LDS(40)-Zn(5)	0.4072	0.4201	3.17

Table 4.6 Water absorption of LDPE-starch-(EMA-Na) blends

Sample	Initial weight (g)	Weight after 24 hours (g)	% water absorption
LDS(0)-Na(2)	0.3682	0.3684	0.05
LDS(0)-Na(5)	0.3773	0.3774	0.03
LDS(15)-Na(2)	0.3021	0.3043	0.73
LDS(15)-Na(5)	0.5418	0.5450	0.59
LDS(20)-Na(2)	0.3436	0.3480	1.28
LDS(20)-Na(5)	0.5418	0.5485	1.25
LDS(30)-Na(2)	0.4653	0.4723	1.50
LDS(30)-Na(5)	0.3344	0.3389	1.35
LDS(40)-Na(2)	0.2395	0.2473	3.26
LDS(40)-Na(5)	0.3513	0.3579	1.88

Tables 4.5 and 4.6 show the water uptake of LDPE-starch-ionomer blends after 24 hours of immersion. The water uptake of blends increases with the starch proportion because the water absorption of starch is very high compared to that of LDPE [36]. However the addition of ionomer decreases

the water absorption with lower water absorption observed at higher ionomer contents. This could be due to the decrease in void volume in ionomer compatibilized blends, resulting in enhanced adhesion of the blend components which restricts water penetration and storage at the interface.

4.2.5 Fourier transform infrared spectroscopic analysis



Figure 4.8 FTIR spectra of LDPE-starch-compatible blends

Figure 4.8 gives the FTIR spectra of LDPE-starch-compatible blends. The spectra show characteristic absorption peaks which are reported in Table 4.7. The peaks between 3700 and 3000 cm^{-1} is attributed to the stretching vibration of intermolecularly hydrogen-bonded hydroxyl groups in all the blends. In C5Z and C5S blends, the absorptions at 3450 , 3300 and 3200 cm^{-1} show variation in intensity (reinforcement of the 3450 cm^{-1} band as compared to the spectrum C5M) due to dilution effects with ionomer addition [37]. The bands at 2910 – 2860 cm^{-1} and 1470 – 1450 cm^{-1} are caused by the alkane component of the modified polyolefins. In the case of ionomer compatibilized blends, peak at 1735 cm^{-1} was an indication of ester group formed through reactions between the carboxyl groups in the compatibilizer

(ionomer) and the hydroxyl groups in starch. The blends show a peak at 1700cm^{-1} derived from carboxylic groups that most probably formed hydrogen bonds with starch. The carbonyl group stretching vibration of the ester, the carboxylic acid and the carboxylate anion gives rise to absorptions at 1735 , 1700 and 1586 cm^{-1} , respectively [38]. A comparison of these spectra with the spectrum of uncompatibilized LDPE-starch blend (chapter 3, figure 3.14(i)), clearly indicates the role of maleic anhydride, EMA-Zn and EMA-Na as compatibilizers.

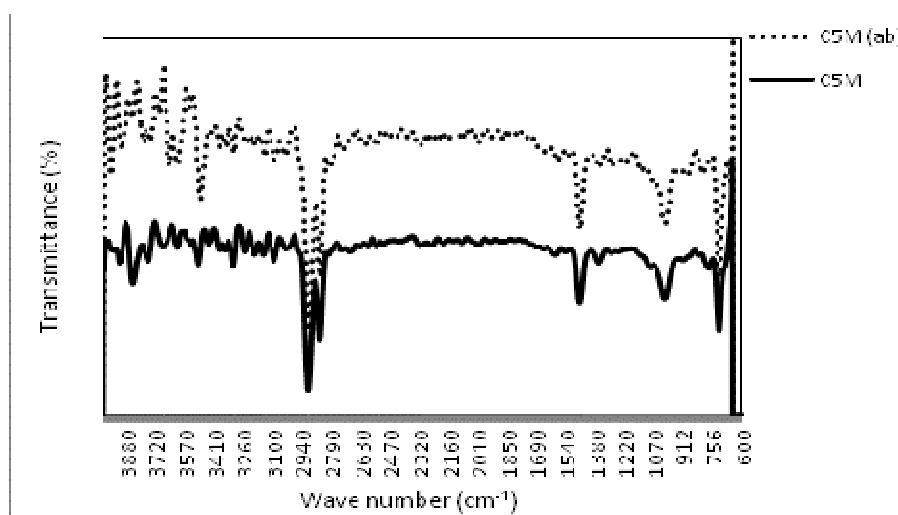


Figure 4.9a FTIR spectra of LDPE-starch-MA blends before and after (ab) biodegradation

The FTIR spectra of LDPE-starch-compatibilizer blends before and after biodegradation for four months are shown in figures 4.9a, 4.9b and 4.9c. The increase in the intensity of peaks at $2921\text{--}2848\text{ cm}^{-1}$, $1473\text{--}1463\text{ cm}^{-1}$, $1156\text{--}1028\text{ cm}^{-1}$ and $730\text{--}720\text{ cm}^{-1}$ after degradation may be due to the fracture of the polyethylene chain in degradable environments, which resulted in increase in the terminal group numbers. Comparison of the spectra of C5M blend before and after biodegradation shows notable

differences in the C-O stretching absorbance at 1260-1000 cm^{-1} region, indicating the removal of starch from the plastic film.

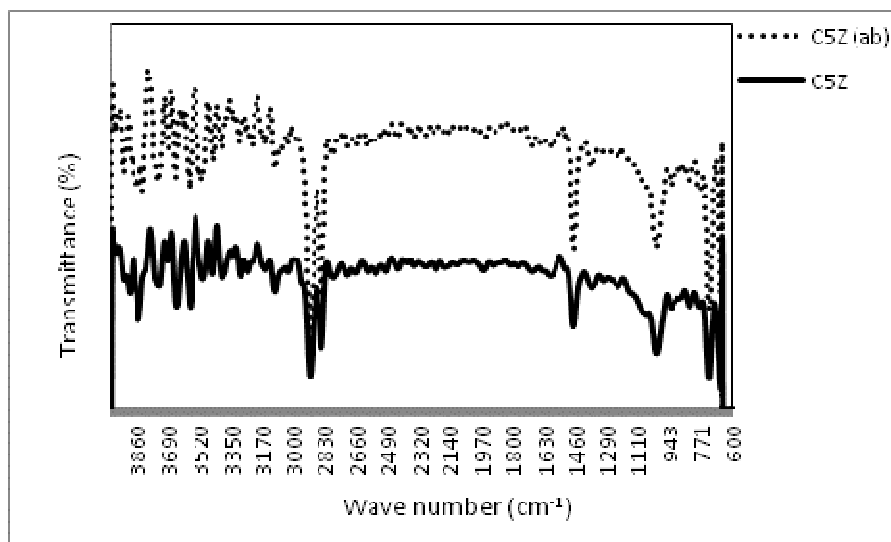


Figure 4.9b FTIR spectra of LDPE-starch-(EMA-Zn) blends before and after (ab) biodegradation

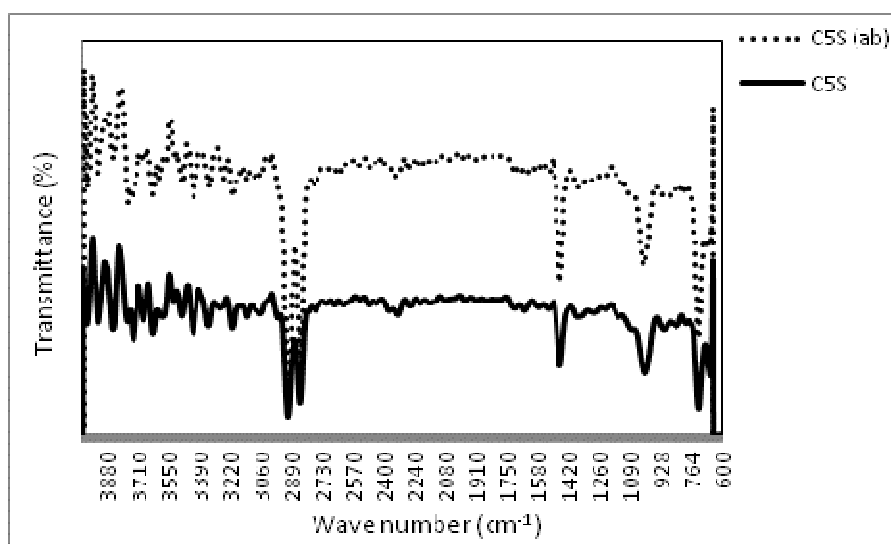


Figure 4.9c FTIR spectra of LDPE-starch-(EMA-Na) blends before and after (ab) biodegradation

But these differences are not much pronounced in C5Z and C5S blends, which may be due to the better phase adhesion between starch and ionomer. After biodegradation, slight decrease in intensities of broad O-H stretching peak at 3700-3000 cm^{-1} region and O-H bending peak at 1640 cm^{-1} observed in the spectra of C5M and C5Z blends confirmed the loss of absorbed water as starch is removed by microorganisms.

Table 4.7 Characteristic FTIR spectral peaks in C5M, C5Z and C5S

Sample	Peak position (cm^{-1})	Characteristic group
C5M	2913, 2847	C-H stretching
	1790	C=O stretching
	1591	C=O stretching
	1463	CH ₂ scissor and asymmetric bending
	1361	C-H bending
	1011	O-C stretching
	916	O-H deformation
	722	CH ₂ rocking
C5Z	2913, 2846	C-H stretching
	1790	C=O stretching
	1700, 1591	C=O stretching
	1463	CH ₂ scissor and asymmetric bending
	1366	C-H bending
	1011	O-C stretching
	928	O-H deformation
	722	CH ₂ rocking
C5S	2913, 2848	C-H stretching
	1735	C=O stretching
	1700, 1522	C=O stretching
	1463	CH ₂ scissor and asymmetric bending
	1364	C-H bending
	1010	O-C stretching
	911	O-H deformation
	721	CH ₂ rocking

4.2.6 Dynamic mechanical analysis

The DMA plots in terms of storage modulus and loss factor ($\tan \delta$) in the temperature region 40 °C-100 °C are given in figure 4.10. It is observed that the storage modulus decreases on addition of all the three compatibilizers leading to the flexibilization of the blends [39].

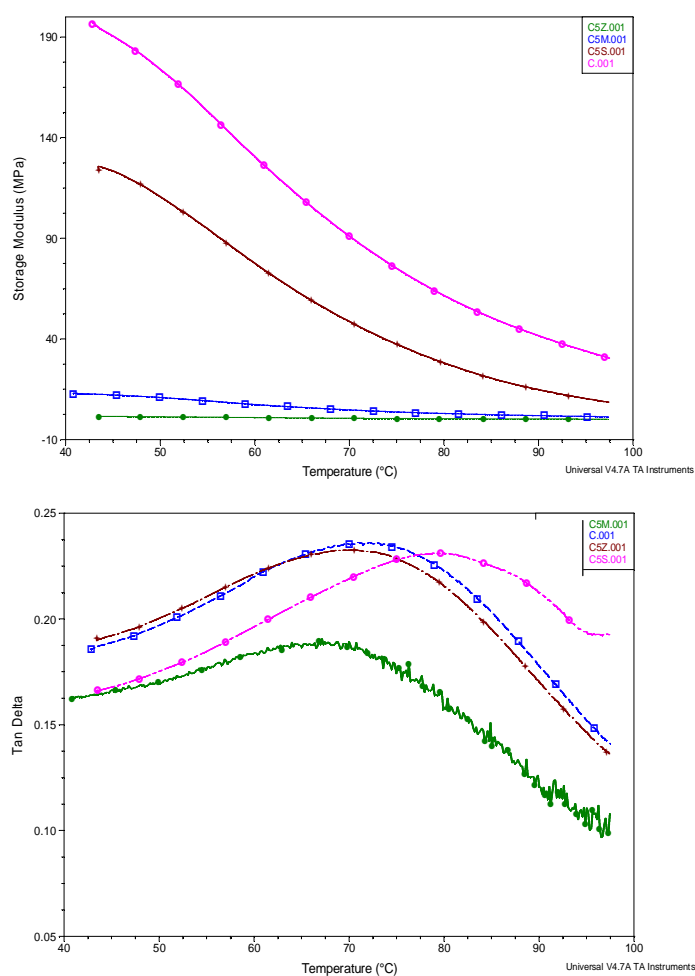


Figure 4.10 DMA plots of LDPE-starch and LDPE- starch-compatibilizer blends

The results of DMA analysis are summarized in Table 4.8. The damping peak broadens and the peak position shifts if there are strong interactions

between the matrix polymer and the filler [40]. As can be seen from the figure 4.9 the peak amplitude is decreased with the addition of compatibilizers. The decrease of amplitude indicates that the number of molecular segments involved have decreased due to improved adhesion between starch and LDPE [41]. The LDPE-starch blend containing EMA-Na shows the $\tan \delta$ peak at a higher temperature than those of pure LDPE and uncompatibilized blend (C), thus confirming better compatibility of the blend components.

Table 4.8 Dynamic mechanical analysis of LDPE-starch-compatibilizer blends

Sample	T ($^{\circ}\text{C}$)	Tan δ at T
A	73.85	0.253
C	70.71	0.236
C5M	67.10	0.191
C5Z	70.50	0.233
C5S	79.64	0.231

(A = LDPE; C = LDPE-20% starch; T = Temperature at which $\tan \delta$ is maximum)

4.2.7 Thermogravimetric analysis

Figure 4.11 shows the comparative thermograms of LDPE-starch (80/20) blends with MA and ionomers as compatibilizers. A minor weight loss due to loss of moisture from starch is noted initially, followed by a considerable weight loss in the temperature range 250°C - 350°C due to the decomposition of starch. The thermal stability of the uncompatibilized blend is lower and shows a maximum degradation temperature at 477°C as shown in figure 3.17(a). Table 4.9 summarizes the temperature of onset of degradation, temperature at which rate of weight loss is maximum (T_{max}), rate of maximum degradation and the weight of residue for compatibilized LDPE-starch blends. It can be seen that the addition of compatibilizer increases the thermal stability of the blends. LDPE-starch blend with MA as compatibilizer shows T_{max} at 489.56°C , meanwhile the weight loss of

blends with ionomer as compatibilizer achieved a maximum during the range 490 °C-492 °C. This increase in T_{\max} for compatibilized blends could be related to the induced thermal stability due to the better dispersion of filler in the matrix. This result confirms the effect of ionomer on the thermal stability of the LDPE-starch blends. Among the three blends the LDPE-starch blends compatibilized with EMA-Na show the highest thermal stability.

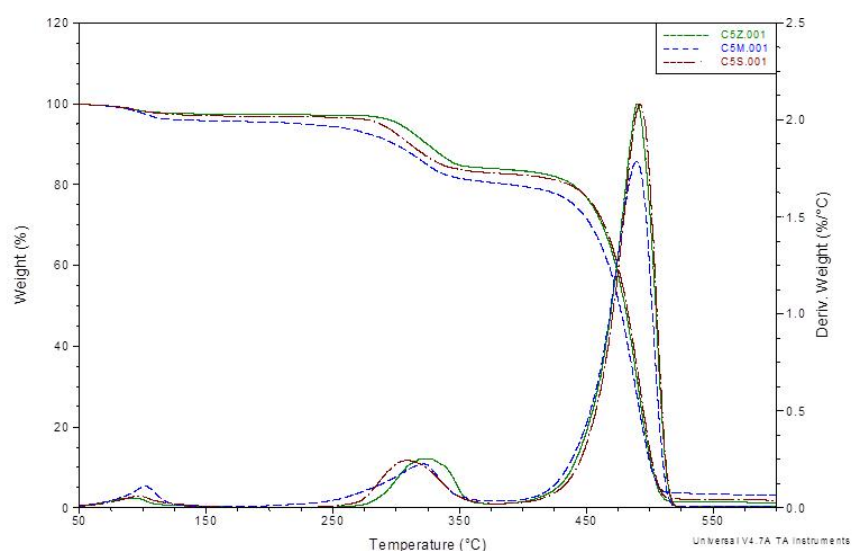


Figure 4.11 TGA thermograms of LDPE-starch-Compatibilizer blends

Table 4.9 Results of thermogravimetric analysis

Sample	Temperature of onset of degradation (°C)	T_{\max} (°C)	Rate of maximum degradation (%/°C)	Residual weight (%)
C	416.00	477.00	2.616	1.285
C5M	420.25	489.56	1.784	2.983
C5Z	431.28	490.07	2.082	1.209
C5S	430.41	492.37	2.079	1.87

(C = LDPE-20% starch; T_{\max} = temperature at which rate of weight loss is maximum)

4.2.8 Differential scanning calorimetry

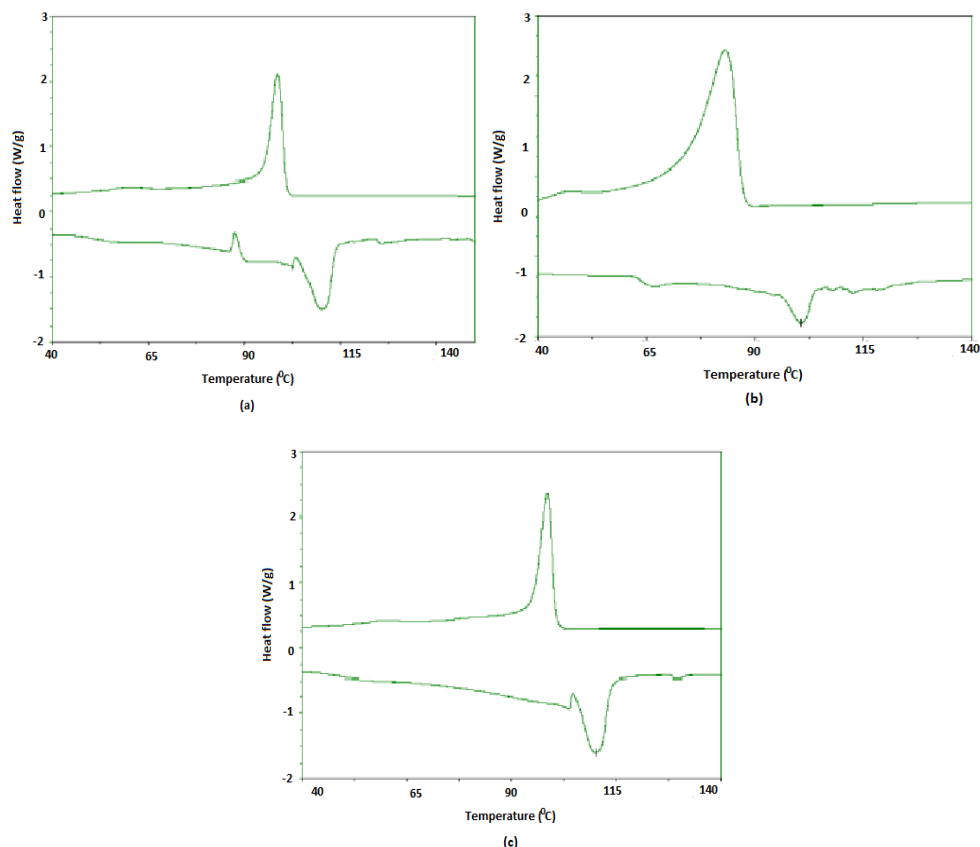


Figure 4.12 DSC thermograms of LDPE-starch-compatibilizer blends: (a) C5M (b) C5Z and (c) C5S

DSC thermograms for LDPE-starch-MA, LDPE-starch-(EMA-Zn) and LDPE-starch-(EMA-Na) blends are shown in figure 4.12. Compared to the melting temperature of pure LDPE film, there was no change in the melting temperature of the LDPE phase in the blends. An endothermic transition observed in the DSC thermograms of the LDPE-starch blends does not mean that the blends are compatible, because starch has no melting temperature, but shows gelatinization and degradation temperature. The endothermic transition that is due to the LDPE phase [42].

The melting temperature (T_m), crystallization temperature (T_c), heat of fusion (ΔH_f), heat of crystallization (ΔH_c) and the percentage of crystallinity of the LDPE phase in the blends determined from the DSC thermograms are given in Table 4.10. Generally, the heat of transition decreases as compatibilization increases - the larger variations being observed for blends containing ionomer. This may be ascribed to the effect of miscibility of ionomer with the LDPE phase and the interactions of the ionomer functional groups with starch in the melt, which can influence the crystallization process and the crystalline structure of the phase. For compatibilized blends, the percentage of crystallinity is lower, and the reduction is higher for LDPE-starch blends with ionomer as compatibilizer. This decrease may be due to the presence of an interaction between LDPE and starch in presence of ionomer which reduce chain mobility, and this in turn should reduce crystallization [18].

Table 4.10 Thermal properties of LDPE, LDPE-starch and LDPE-starch - compatibilizer blends before biodegradation

Sample	T_m ($^{\circ}\text{C}$)	ΔH_f (J/g)	T_c ($^{\circ}\text{C}$)	ΔH_c (J/g)	% Crystallinity
LDPE	110.00	67.00	96.00	79.00	23.4
C	113.00	59.00	96.00	65.00	20.6
C5M	110.63	38.7	93.17	60.89	13.5
C5Z	110.49	33.3	98.6	50.6	11.6
C5S	110.17	32.75	98.51	57.9	11.4

4.2.9 Morphological studies

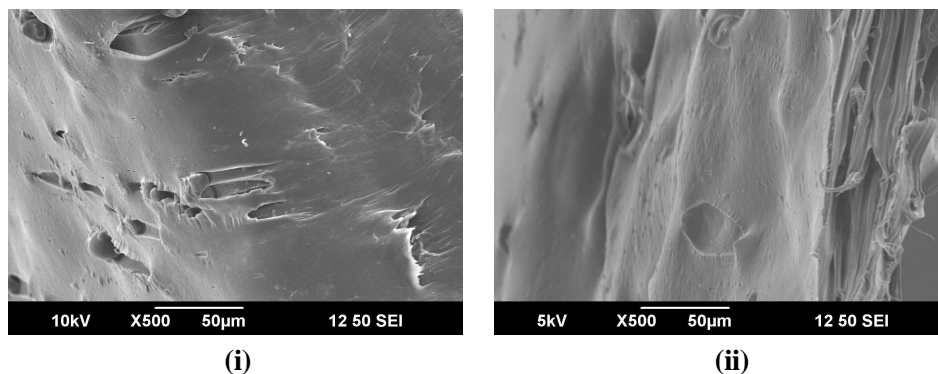


Figure 4.13a Scanning electron micrographs of LDPE-starch-MA (75/20/5) blend: (i) before biodegradation and (ii) after biodegradation for four months

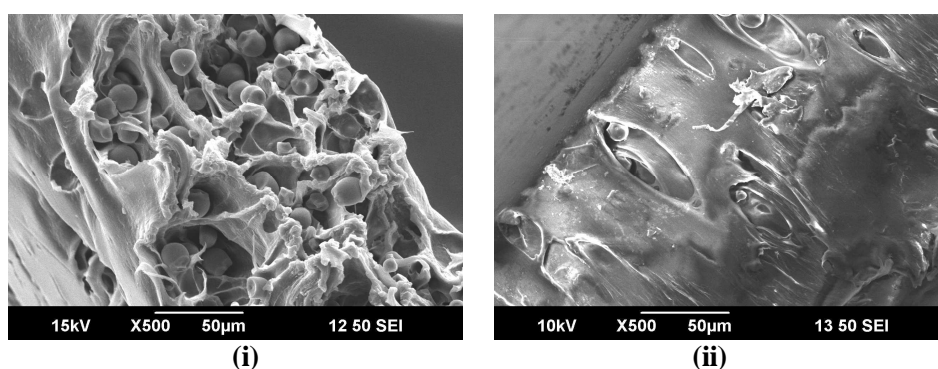


Figure 4.13b Scanning electron micrographs of LDPE-starch-(EMA-Zn) (75/20/5) blend: (i) before biodegradation and (ii) after biodegradation for four months

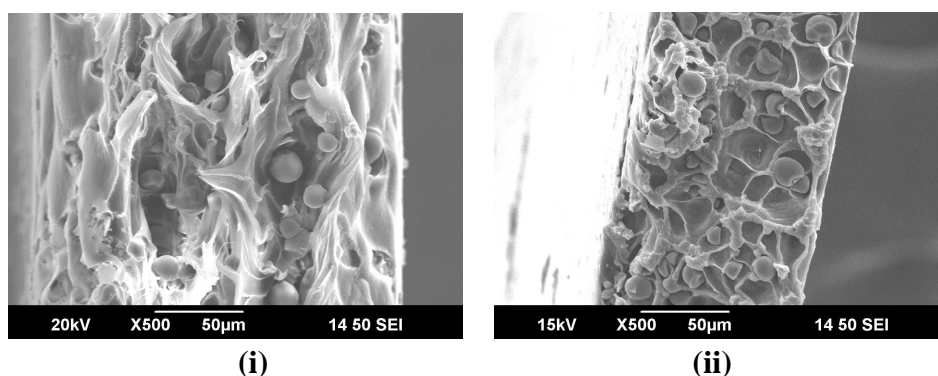


Figure 4.13c. Scanning electron micrographs of LDPE-starch-(EMA-Na) (75/20/5) blend: (i) before biodegradation and (ii) after biodegradation for four months

The effect of compatibilizing agents on the morphology of the blends was studied by scanning electron microscopy. Figures 4.13a, 4.13b and 4.13c show the SEM microphotographs of the fractured surfaces of the compatibilized LDPE-starch blends (75/20/5). Micrographs of the LDPE-starch blends without compatibilizer in figure 3.19 (b) in the previous chapter clearly indicate the heterogeneous morphology of the blends, where deformed starch particles are dispersed in the continuous LDPE matrix as fillers. Figures denoted by (i) show the morphology of the LDPE-starch-Compatibilizer (75/20/5) blends where the two phase morphology, even though appears very similar to that of the uncompatibilized blend, exhibits some starch particles that were broken after the cryogenic fracture as well as some plastic deformation at the interfaces indicating enhanced interactions between the two phases. Figures show that addition of compatibilizer has a clear effect on the morphology by reducing the dimensions of the dispersed phase and improving its dispersion into the LDPE matrix. This reduction in size suggests that the size of the starch agglomerates is reduced. Hence the addition of ionomers gives rise to well-dispersed, starch particles. The particle size distribution is more homogeneous and the overall size is smaller, indicating that compatibilization and a decrease in interfacial tension occurred.

SEM micrographs of LDPE-starch-Compatibilizer blends after biodegradation are given in figures denoted by (ii). Black pores in the micrographs prove the biodegradation of LDPE-starch blends. The entire amount of starch is not removed during the biodegradability experiments. The uncompatibilized film has more surface area to be attacked by microorganisms; therefore, it has more microscopic holes randomly scattered in the film than the compatibilized one. Increased interfacial adhesion of starch

into LDPE matrix due to the presence of compatibilizer makes the removal of starch granules from the films more difficult.

4.3 Conclusions

Melt-mixed blends of low density polyethylene and starch can be compatibilized using the sodium or zinc salt of polyethylene-co-methacrylic acid ionomer. The addition of the ionomer as a compatibilizer improved the stress-strain properties of the blends. Among the various dosages of ionomers used in this study as compatibilizers, 5 weight % show maximum improvement in mechanical properties in the case of both EMA-Zn and EMA-Na. An increase in the melt flow of the blends was also realized by the addition of the ionomer. Biodegradation studies suggested that the degradation rate of the ionomer compatibilized films was marginally lower than that of the MA compatibilized films. Dynamic mechanical analyses indicated that the storage modulus decreases on addition of all the three compatibilizers leading to the flexibilization of the blends. Spectroscopic studies indicate interaction between starch and ionomer. Results of thermogravimetric analyses show improved thermal stability in the case of the compatibilized blends using ionomers as compared to the compatibilized blends using maleic anhydride and the uncompatibilized blends. The results of differential scanning calorimetry show decrease in crystallinity on incorporating ionomers as compatibilizers in LDPE-starch blends. Morphological studies show improved dispersion of starch particles in the blend in presence of ionomers as compatibilizers.

References

- [1] Sinthavathavorn, W.; Nithitanakul, M.; Magaraphan, R.; Grady, B. P.; J Appl Polym Sci 2007, 107, 3090.
- [2] Averous, L.; Fringant, C.; Moro, L.; Starch/ Starke 2001, 53, 368.
- [3] Polymer Blends Vol 2; Paul, D. R., Newman, S., Eds.; Academic Press, New York, 1978, 167.
- [4] Paul, D. R.; Vincen, C. E.; Locke, C. E.; Polym Eng Sci 1972, 12, 157.
- [5] Hallden, A.; Ohisson, B.; Wesslen, B.; J Appl Polym Sci 2000, 78, 2416.
- [6] John, J.; Bhattacharya, M.; Polym Int 2000, 203, 1614.
- [7] Weiss, R. A.; U. S. Patent 5 1995, 422, 398.
- [8] Zheng, X.; Zhang, J.; He, J.; J Appl Polym Sci 2003, 87, 1452.
- [9] Dutta, D.; Weiss, R. A.; He, J.; Polymer 1996, 37, 429.
- [10] Castellano, M.; Nebbia, D.; Turturro, A.; Valenti, B.; Costa, G.; Falqui, L.; Macromol Chem Phys 2002, 203, 1614.
- [11] Huang, C. C.; Chang, F. C.; Polymer 1997, 38, 2135.
- [12] Samios, C. K.; Kalfoglou, N. K.; Polymer 1999, 40, 4811.
- [13] Utracki, L. A.; Polymer Alloys and Blends, Hanser Publishers, New York, 1990.
- [14] Sanchez, S.; Lopez, M. L.; Ramirez, E.; Medellin, F. J.; Gutierrez, J. M.; Macromol Mater Eng 2006, 291, 128.
- [15] Sailaja, R. R. N.; Reddy, A. P.; Chanda, M.; Polym Int 2001, 50, 1352.
- [16] Ma, X.; Sauer, J. A.; Hara, M.; Macromolecules 1995, 28, 3953.
- [17] Holliday, L.; (Ed), Ionic Polymers, Applied Science, London, 1975.
- [18] Leewajanakul, P.; Pattanaolarn, R.; Ellis, J. W.; Nithitanakul, M.; Grady, B. P.; J Appl Polym Sci 2003, 89, 620.

- [19] Lahor, A.; Nithitanakul, M.; Grady, B. P.; Eur Polym J 2004, 40, 2409.
- [20] Abad, M. J.; Ares, A.; Barral, L.; Eguiazabal, J. I.; Polym Int 2005, 54, 673.
- [21] Gonzalez-Nunnez, R.; Padilla, H.; De Kee, B.; Favis, B. D.; Polym Bull 2001, 46, 323.
- [22] Baouz, T.; Fellahi, S.; J Appl Polym Sci 2005, 98, 1748.
- [23] Villarreal, M. E.; Tapia, M.; Nuno-Donlucas, S. M.; Puig, J. E.; Gonzalez-Nunez, R.; J Appl Polym Sci 2004, 92, 2545.
- [24] Gemeinhardt, G. C.; Moore, A. A.; Moore, R. B.; Polym Eng Sci 2004, 44, 1721.
- [25] Vyas, H.; Shrinet, V.; Murthy, C. N.; Jain, R. C.; Singh, A. K.; Polym-Plast Technol Eng 2008, 47, 1231.
- [26] Ahamed, N. T.; Singhal, R. S.; Kulkarni, P. R.; Kale, D.D.; Pal, M.; Carbohydr Polym 1996, 31, 157.
- [27] Thakore, I. M.; Iyer, S.; Desai, A.; Lele, V.; Devi, S.; J Appl Polym Sci 1999, 74, 2791.
- [28] Yoo, S. I.; Lee, T. Y.; Yoon, J.; Lee, I.; Kim, M.; Lee, H. S.; J Appl Polym Sci 2002, 83, 767.
- [29] Magaraphan, R.; Skularriya, R.; Kohjiya, S.; J Appl Polym Sci 2007, 105, 1914.
- [30] Sinthavathavorn, W.; Nithitanakul, M.; Grady, B. P.; Magaraphan, R.; Polym Bull 2009, 63, 23.
- [31] Chen, B.; Li, Z.; Xu, S.; Tang, T.; Zhou, B.; Huang, B.; Polymer 2002, 43, 953.
- [32] Younggon, S.; Weiss, R. A.; J Appl Polym Sci 2003, 87, 564.
- [33] Molnar, A.; Eisenberg, A.; Macromolecules 1992, 25, 5774.
- [34] Ratanakamnuan, U.; Aht-Ong, D.; J Appl Polym Sci 2006, 100, 2725.
- [35] Park, H.; Lee, S.; Chowdhury, S. R.; Kang, T.; Kim, H.; Park, S.; Ha, C.; J Appl Polym Sci 2002, 86, 2907.

- [36] Acierno, S.; Puyvelde, V. P.; J Appl Polym Sci 2005, 97, 666.
- [37] Dyer, J. R.; Applications of Absorption Spectroscopy of Organic Compounds, Prentice-Hall, Inc., NJ, 1965.
- [38] Samios, C. K.; Kalfoglou, N. K.; Polymer 1998, 39, 3863.
- [39] Dascalu, M. C.; Vasile, C.; Silvestre, C.; Pascu, M.; Europ Polym J 2005, 41, 1391.
- [40] Nielsen, L. E.; Mechanical Properties of Polymers and Composites, Vol. 2, Marcel Dekker, New York, 1974.
- [41] Wang, Y.; Yeh, F.; Lai, S.; Chan, H.; Shan, H.; Polym Eng Sci 2003.
- [42] Aht-Ong, D.; Charoenkongthum, K.; J Metals, Materials and Minerals 2002, 12, 1.



PRO-OXIDANT FILLED LOW DENSITY POLYETHYLENE

Contents	5.1	<i>Introduction</i>
	5.2	<i>Results and discussion</i>
	5.3	<i>Conclusions</i>

Various metal oxides (iron oxide, manganese dioxide, titanium dioxide (rutile and anatase grades)) and metal stearates (ferric stearate, manganese stearate, cupric stearate, magnesium stearate and zinc stearate) have been mixed with low density polyethylene to enhance its photodegradability. The studies include the evaluation of mechanical properties, measurement of melt flow indices, water absorption, spectroscopy, thermal analyses and morphological studies. The effect of metal oxides and metal stearates on the photodegradability of LDPE was evaluated by exposing the test specimens under a 30 watt shortwave ultraviolet (UV) lamp for one month. The tensile strength of the test specimens were measured before and after exposure to UV light. The studies show that the presence of metal oxides and metal stearates accelerate the photodegradation of LDPE.

5.1 Introduction

Low density polyethylene, the major polymer consumed worldwide, is the most common polymer present in the plastic wastes. Low surface area, high molecular weight and impermeability to water and oxygen are believed to be the major reasons for the resistance of low density polyethylene to degradation. It is known that the photo-oxidation is an important first degradation step for non-hydrolysable materials such as polyethylene. Photodegradation involves the natural tendency of most of the plastics to undergo a gradual reaction with atmospheric oxygen in the presence of light. Photo-oxidation increases the amount of low molecular weight material by breaking bonds and increasing the surface area and can assist rapid disintegration of plastics into a powdery residue with a much reduced visual impact [1-3]. During UV irradiation of polymers, activated molecules are formed in first step of the degradation reaction followed by various processes, such as chain scission, cross-linking and oxidation [4-7]. Among the many approaches used to induce degradation in polyethylene, use of pro-oxidants has been gaining popularity recently [8] which induces abiotic oxidation, leading to the reduction of molecular mass to levels where the material becomes susceptible to microbial attack [9-12]. Pro-oxidants help in the insertion of oxygen atom into the polymer chain. Increased surface area as well as increased oxygen permeability can enhance degradation. The transition metal complexes, especially in the form of oxides and stearates, possess remarkable ability to decompose the hydroperoxides formed during the oxidation of polymers [13-14].

Low density polyethylene containing 0.5 and 1 weight percent of pro-oxidants, viz., metal oxides (iron oxide, manganese dioxide and titanium dioxide (anatase and rutile grades)) and metal stearates (ferric stearate,

manganese stearate, copper stearate, magnesium stearate and zinc stearate) were prepared by melt mixing. Designations of the samples used in this chapter and their descriptions are given in Table 5.1. These samples were exposed to UV light for one month. The mechanical properties, melt flow characteristics, photodegradability, water absorption, FTIR spectra, thermal properties and morphology of the pro-oxidant mixed LDPE were compared with those of the neat LDPE.

Table 5.1 Description of sample designations

Sample designation	Description
LDFeO	LDPE-Fe ₂ O ₃
LDMnO	LDPE-MnO ₂
LDRu	LDPE-TiO ₂ (rutile)
LDA _n	LDPE-TiO ₂ (anatase)
LDFeS	LDPE-ferric stearate
LDMnS	LDPE- manganese stearate
LDCuS	LDPE-cupric stearate
LDMgS	LDPE-magnesium stearate

5.2 Results and discussion

5.2.1 Metal oxides as pro-oxidants

5.2.1.1 Mechanical properties

Figure 5.1 shows the effect of metal oxides on the mechanical properties of LDPE. From the figures, it can be seen that the stress-strain properties of LDPE containing metal oxides are in the same range as that of pure LDPE, thereby indicating that the metal oxides do not affect the stress-strain properties of LDPE adversely. Figures show that among metal oxides used in this study, incorporation of 1% ferric oxide gives the minimum variation in tensile strength as compared to neat LDPE.

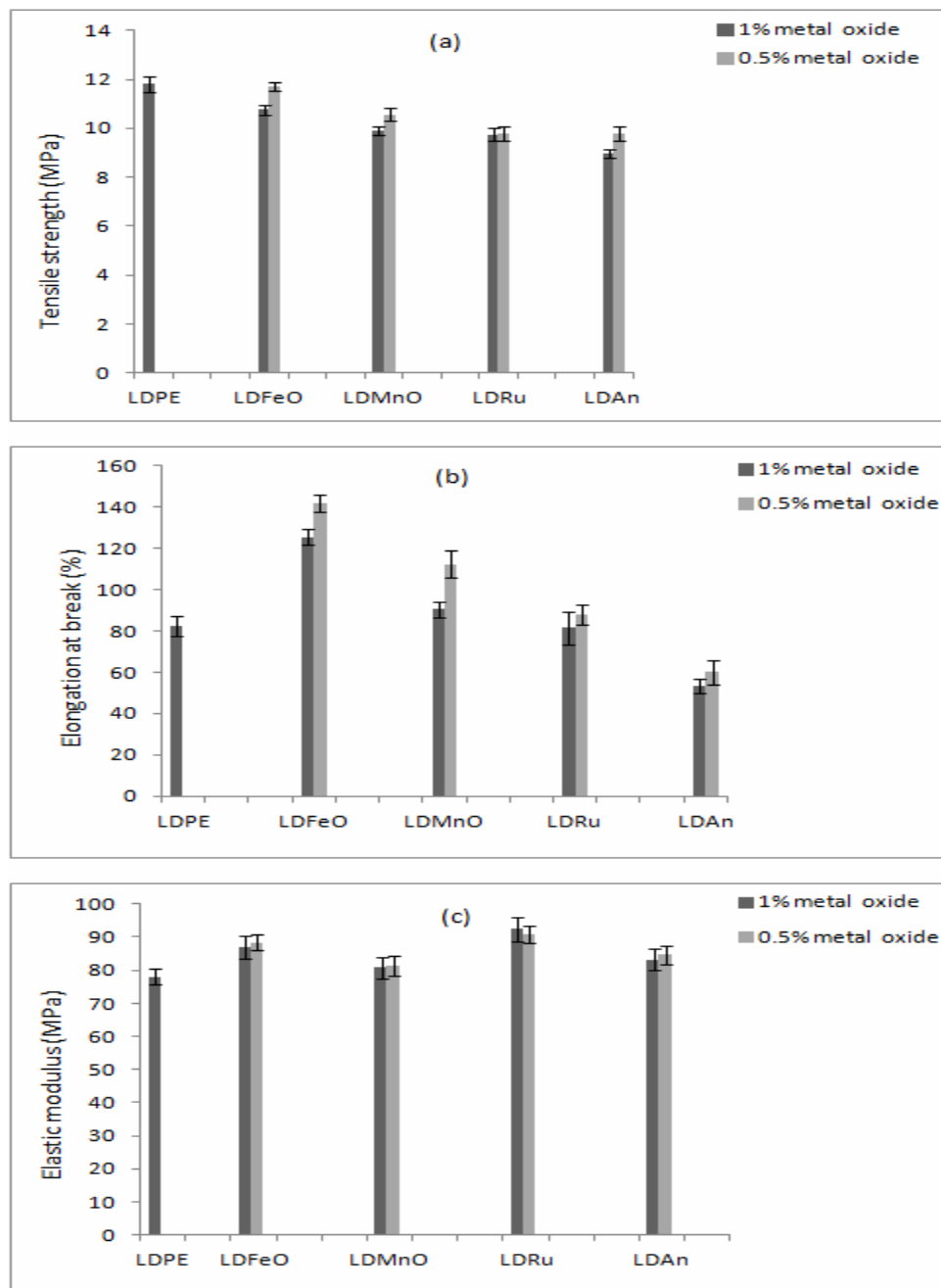


Figure 5.1 Effect of metal oxides on the mechanical properties of LDPE

5.2.1.2 Melt flow measurements

The melt flow rates of neat LDPE and the LDPE-metal oxide mixes are shown in figure 5.2. All the samples except the composition containing MnO_2 show melt flow values almost similar to that of neat LDPE. The results show that the processing of LDPE in the presence of these metal oxides does not lead to high level of chain scission or crosslinking so as to cause a change in the melt flow indices [15]. A slight increase in MFI of LDPE containing MnO_2 was observed which indirectly reflects upon the lowering of molecular weight.

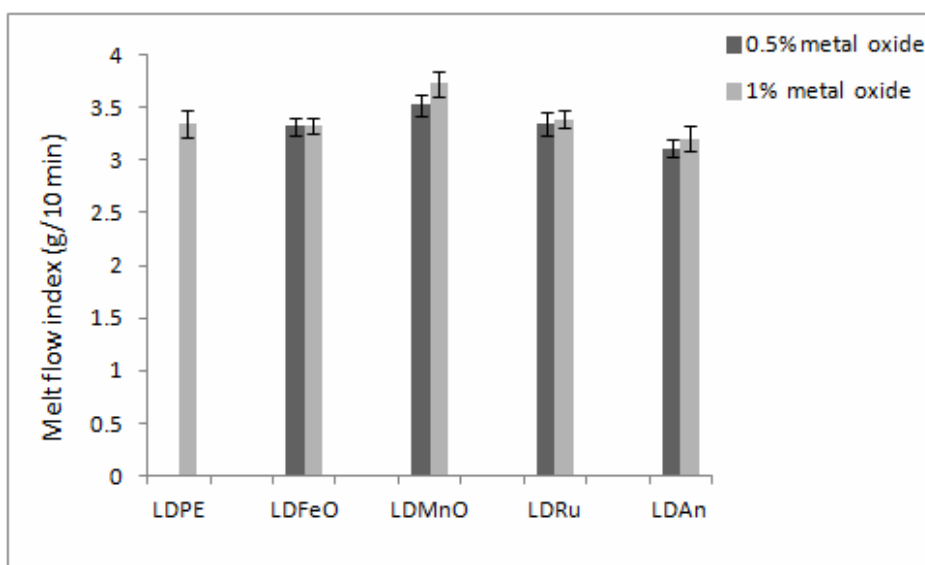


Figure 5.2 Effect of metal oxides on the melt flow index of LDPE

5.2.1.3 Photodegradation studies

Figure 5.3 presents the effect of UV exposure for one month on the tensile strength of LDPE containing metal oxides. The tensile strength of all the LDPE-metal oxide compositions decreased after one month of exposure to UV radiation. Among various metal oxides used, the maximum reduction in tensile strength was observed in the case of the film containing

1% Fe₂O₃. Addition of the metal oxides enhanced the rate of photodegradation in the order FeO > MnO > Ru > An.

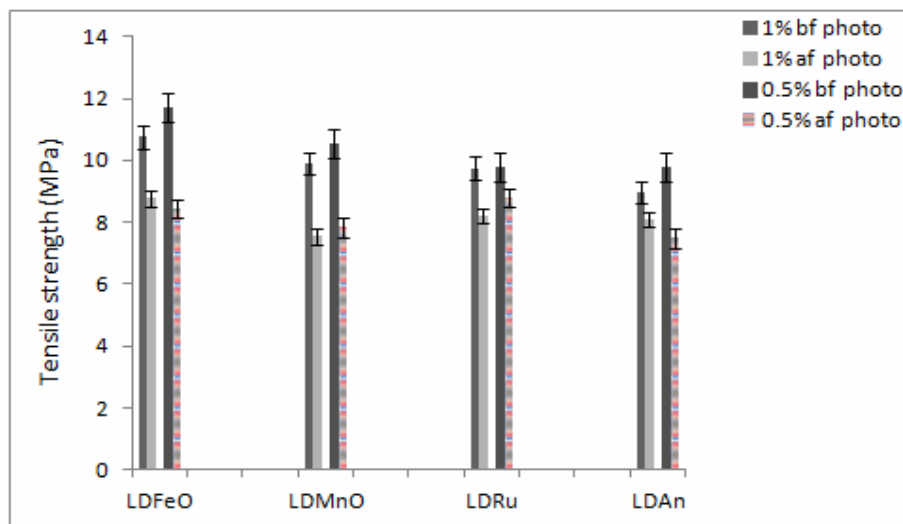
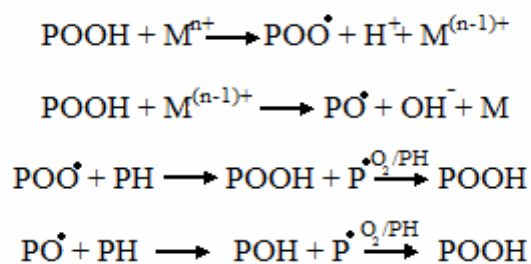


Figure 5.3 Effect of photodegradation on the tensile strength of LDPE containing metal oxides

During UV irradiation of polymers, M^{n+} ions present in pro-oxidants affect the rate of degradation of polymeric matrix by reducing to $M^{(n-1)+}$ ions by redox catalysis of the hydroperoxide decomposition reaction. The POO^\bullet and PO^\bullet radicals in polymer enhance the alkyl radical and peroxide formations in the polymer matrix, which enhance the photo-oxidation process according to the reaction shown in scheme 5.1. [16-17].



(PH-hydrocarbon polymer; POOH-polymer hydroperoxide)

Scheme 5.1 Pro-oxidant catalyzed photo-oxidation reaction

Tables 5.2 and 5.3 show the loss in tensile strength (%) and loss in weight (%) of LDPE containing metal oxides after exposure to UV radiation for one month. It was observed that all the samples show a slight rise in weight loss after photodegradation and the weight loss was found to increase with increase in concentration of metal oxides.

Table 5.2 Percentage decrease in tensile strength of LDPE-metal oxides after UV exposure for one month

Sample*	Initial tensile strength (MPa)	Tensile strength after UV irradiation for one month (MPa)	% decrease in tensile strength
LDPE	11.81	11.78	0.25
LD(0.5)FeO	11.72	9.23	21.25
LD(1)FeO	10.75	8.05	25.11
LD(0.5)MnO	10.56	8.35	20.92
LD(1)MnO	9.89	7.64	22.75
LD(0.5)Ru	9.80	8.15	16.85
LD(1)Ru	9.75	8.02	17.77
LD(0.5)An	9.78	8.22	15.95
LD(1)An	8.97	7.46	16.83

* Number given in paranthesis denotes the weight percentage of metal oxides in the blend

Table 5.3 Percentage weight loss of LDPE-metal oxides after UV exposure for one month

Sample	Initial weight (g)	Weight after one month (g)	% weight loss
LDPE	0.5185	0.5184	0.02
LD(0.5)FeO	0.5459	0.5452	0.13
LD(1)FeO	0.4492	0.4480	0.27
LD(0.5)MnO	0.4213	0.4209	0.10
LD(1)MnO	0.4790	0.4780	0.21
LD(0.5)Ru	0.1648	0.1647	0.06
LD(1)Ru	0.1376	0.1375	0.07
LD(0.5)An	0.4925	0.4923	0.04
LD(1)An	0.5992	0.5989	0.05

5.2.1.4 Water absorption studies

The extent of hydrophilicity of LDPE containing metal oxides was established by water absorption measurements. The water uptake of the neat LDPE and LDPE-metal oxide compositions are tabulated in Table 5.4. Absence of marginal change in water absorption after 24 hours of immersion in water indicated the hydrophobic character of the blends.

Table 5.4 Water absorption for LDPE and LDPE containing metal oxides

Sample	Initial weight (g)	Weight after 24 hours (g)	% water absorption
LDPE	0.3337	0.3338	0.03
LD(0.5)FeO	0.2394	0.2396	0.08
LD(1)FeO	0.2623	0.2628	0.19
LD(0.5)MnO	0.2270	0.2271	0.04
LD(1)MnO	0.2247	0.2250	0.13
LD(0.5)Ru	0.2537	0.2538	0.04
LD(1)Ru	0.2999	0.3001	0.07
LD(0.5)An	0.3512	0.3513	0.03
LD(1)An	0.2124	0.2125	0.05

5.2.1.5 FTIR spectroscopy

Figure 5.4 shows the changes in the FTIR spectra of LD(1)FeO after exposure to UV radiation for one month. The spectrum of LD(1)FeO shows characteristic absorption peaks which are reported in Table 5.5. As compared to the spectrum of LD(1)FeO before exposure to the UV radiation, the spectrum of the sample after exposure to UV radiation shows significant changes in the carbonyl ($1785 - 1700 \text{ cm}^{-1}$), amorphous (1364 cm^{-1}) and hydroxyl regions (3400 cm^{-1}). The difference in peak intensities at 1463 cm^{-1} and 932 cm^{-1} reveals the auto-oxidation of LDPE in presence

of Fe_2O_3 . The absorption peak due to stretching of carbonyl group indicates the presence of numerous oxidation products like H-bonded carboxylic acids (1711 cm^{-1}), esters (1736 cm^{-1}) and γ lactones (1780 cm^{-1}). The degradation is also monitored by measuring the carbonyl index (CI). Carbonyl index is defined as the ratio of absorbance of carbonyl band at 1714 cm^{-1} to an internal thickness band at 2020 cm^{-1} [18-19]. As compared to the spectrum of LD(1)FeO before exposure to the UV radiation, the spectrum of the sample after exposure to UV radiation show an increase in the value of CI indicating photodegradation.

Absorptions at 1410 and 1240 cm^{-1} are assigned to carboxylic acids and those at 1640 and 932 cm^{-1} are assigned to $\text{C}=\text{C}$ groups [20]. There is slight difference in the intensity of peaks at 1364 cm^{-1} and 721 cm^{-1} probably due to the degradation of LDPE. This shows that the presence of Fe_2O_3 enhances the auto-oxidation of LDPE and thus accelerates the photodegradation process.

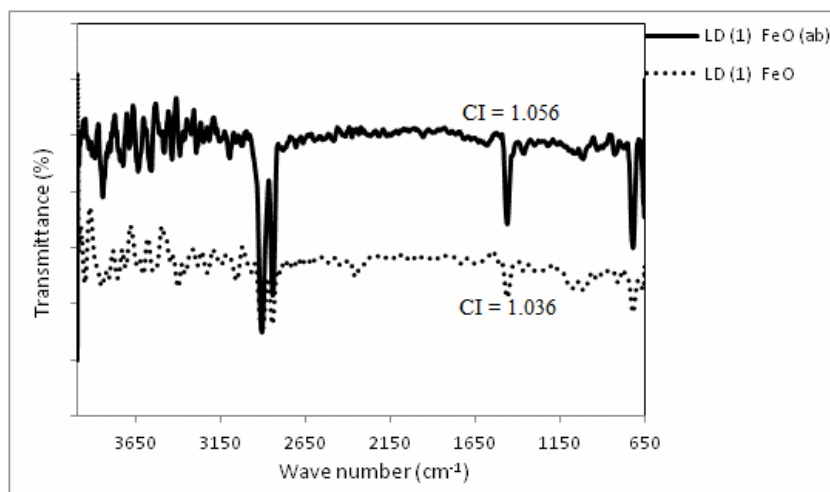


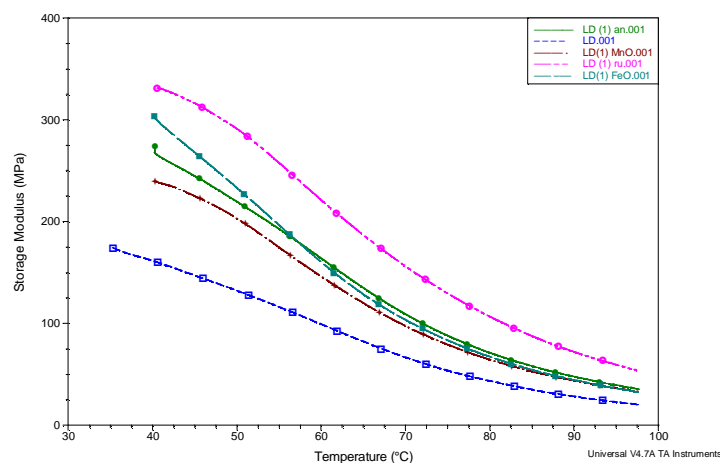
Figure 5.4 FTIR spectra of LD(1)FeO:
(..) before degradation and (-) after degradation (ab)

Table 5.5 Characteristic FTIR spectral peaks in LD(1)FeO

Peak position (cm ⁻¹)	Characteristic group
3400	O-H stretching
2912, 2847	C-H stretching
1637	O-H bending
1463	CH ₂ scissor and asymmetric bending
1454	H-C-OH deformation
1364	C-H bending
1149	C-O stretching
1015	C-O stretching
932	O-H deformation
721	CH ₂ rocking

5.2.1.6 Dynamic mechanical analysis

Figure 5.5 shows the variation in storage modulus of LDPE and LDPE containing metal oxides measured over the temperature range from 40 °C to 100 °C. Incorporation of metal oxides resulted in an increase in storage modulus. This is attributed to the stiffening of the LDPE matrix imparted by the presence of the metal oxides [21].

**Figure 5.5 DMA curves of LDPE and LDPE containing 1% metal oxides**

5.2.1.7 Differential scanning calorimetry (DSC)

Figure 5.6 presents the DSC thermogram of LD(1)FeO. The melting temperature (T_m), crystallization temperature, heat of fusion, heat of crystallization and the degree of crystallization of pure LDPE and LD(1)FeO were determined and summarized in Table 5.6. For LDPE, the melting point was observed at 110°C and addition of Fe_2O_3 did not produce any change in melting point. However, the heat of transitions increase upon the addition of Fe_2O_3 , which is indicative of increased crystallinity. An increase in crystallinity observed in the case of the blend, may be due to the role of the filler particles as nucleating agents for the formation of crystallites [22].

Table 5.6 Results of DSC analysis of LDPE and LDPE containing 1% ferric oxide

Sample	$T_m (^{\circ}\text{C})$	$\Delta H_f (\text{J/g})$	$T_c (^{\circ}\text{C})$	$\Delta H_c (\text{J/g})$	% crystallinity
LDPE	110.00	67.00	96.00	79	23.4
LD(1)FeO	110.53	89.21	98.72	80	31.1

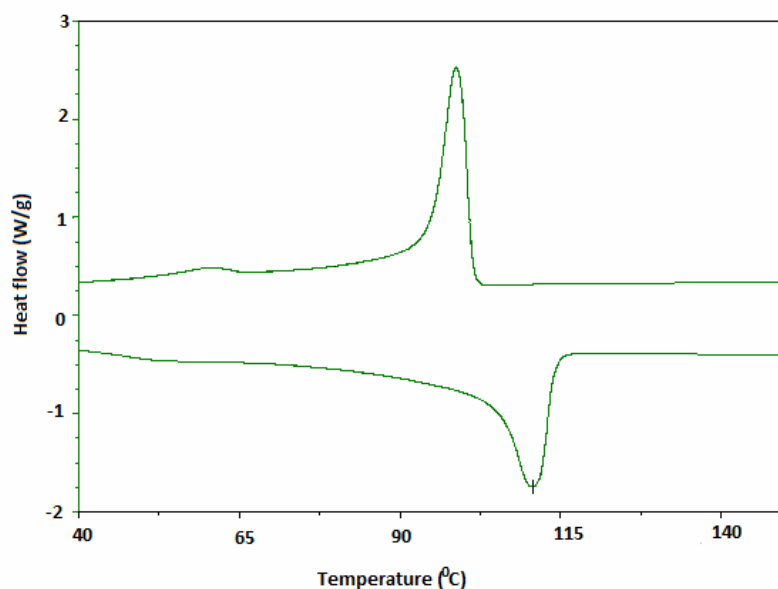
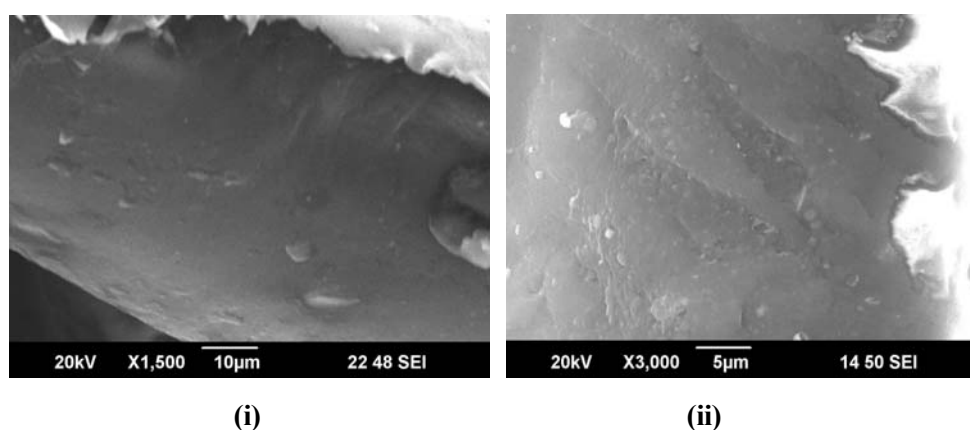


Figure 5.6 DSC thermogram of LD(1)FeO

5.2.1.8 Morphological studies

Figure 5.7 shows the SEM micrographs of LD(1)FeO before and after exposure to UV radiation for one month. The surface of nondegraded film is smooth. The roughness observed on the surface of the film after UV irradiation for one month is due to the degradation of LDPE.



**Figure 5.7 Scanning electron micrographs of LD(1)FeO:
(i) before degradation and (ii) after degradation**

5.2.2 Metal stearates as pro-oxidants

5.2.2.1 Mechanical properties

Figure 5.8 depicts the effect of addition of metal stearates on the stress-strain properties of LDPE. As compared to the neat LDPE the samples containing metal stearates as pro-oxidants exhibit marginal deterioration in mechanical properties. The results show that the presence of small quantities of metal stearates do not lead to severe degradation of LDPE during the processing.

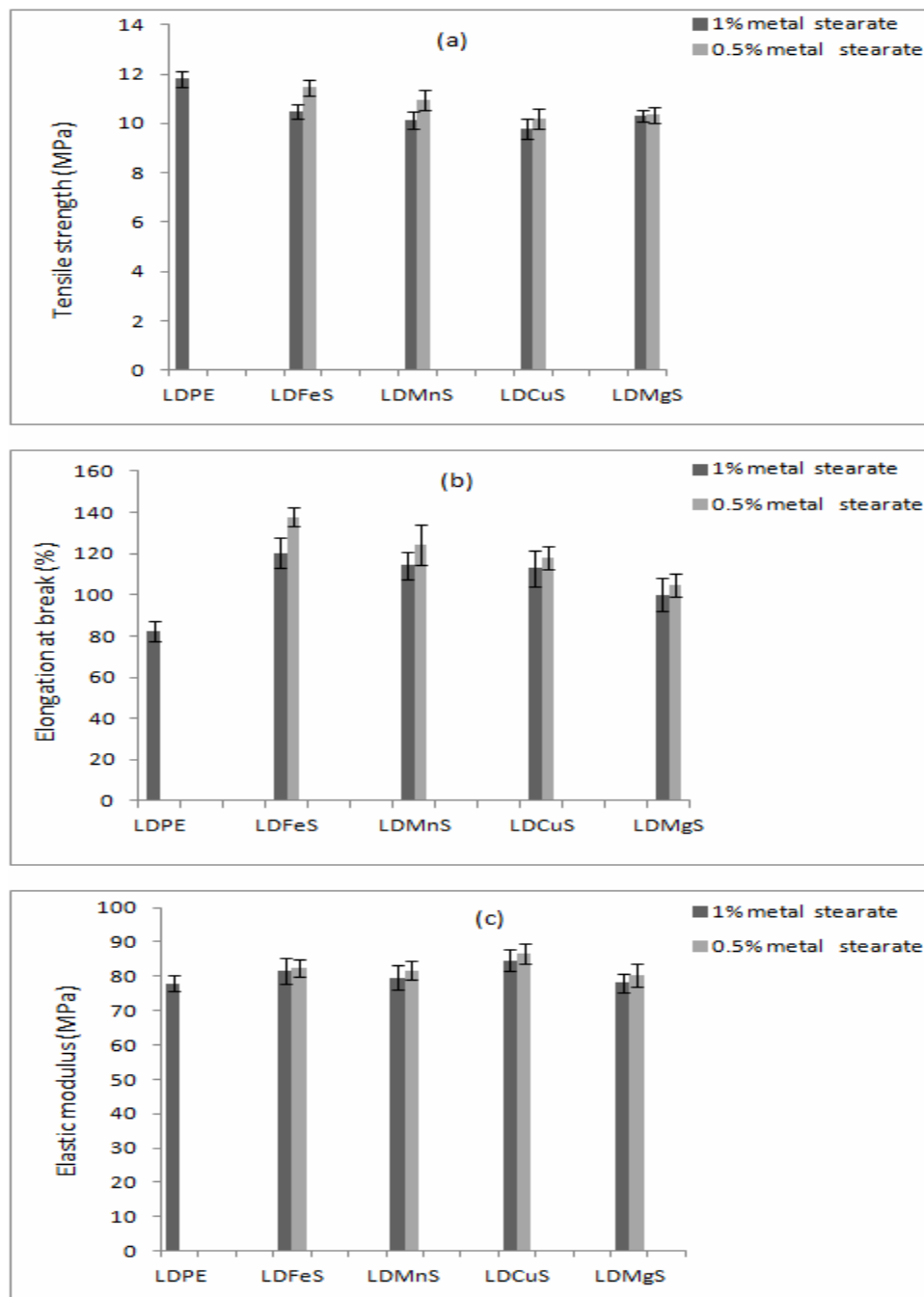


Figure 5.8 Effect of metal stearates on the mechanical properties of LDPE

5.2.2.2 Melt flow measurements

The met flow indices of neat LDPE and the LDPE-metal stearate mixes are shown in figure 5.9. Figure shows that the melt flow indices of the LDPE samples containing metal stearates as pro-oxidants are marginally higher compared to neat LDPE. The pro-oxidant additives may be contributing to the initiation and the propagation of the radical reactions and chain scission [23].

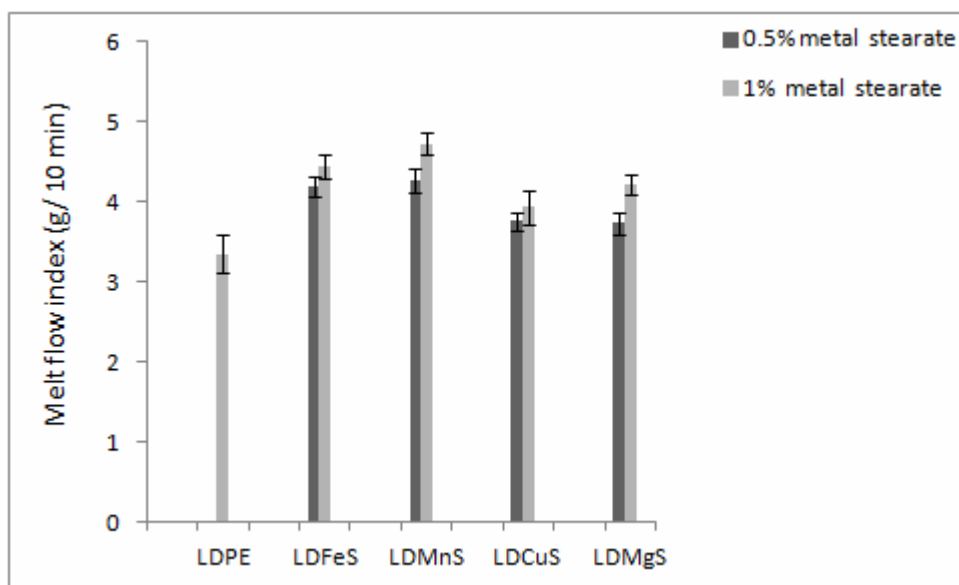


Figure 5.9 Effect of metal stearates on the melt flow index of LDPE

5.2.2.3 Photodegradation studies

Figure 5.10 shows the changes in the tensile strength of LDPE containing metal stearates after UV exposure for one month. LD(1)FeS exhibit a rapid loss in mechanical properties (28.32%). Table 5.7 summarizes the percentage decrease in tensile strength of LDPE containing metal stearates after UV exposure for one month. On absorption of energy in the form of light, the stearates undergo decomposition leading to the formation of free

radicals[24-25].These generate radicals on the main chains in the polymer matrix leading to chain scission which affects the mechanical properties.

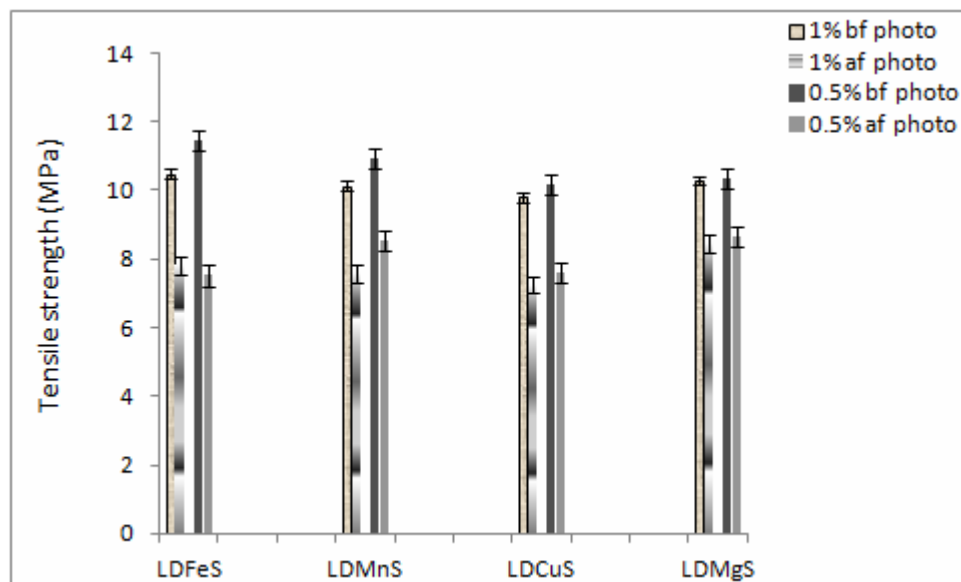


Figure 5.10 Effect of photodegradation on the tensile strength of LDPE containing metal stearates

Table 5.7 Percentage decrease in tensile strength of LDPE-metal stearates after UV exposure for one month

Sample*	Initial tensile strength (MPa)	Tensile strength after UV irradiation for one month (MPa)	% decrease in tensile strength
LDPE	11.81	11.78	0.25
LD(0.5)FeS	11.46	8.52	25.67
LD(1)FeS	10.48	7.51	28.32
LD(0.5)MnS	10.94	8.15	25.50
LD(1)MnS	10.13	7.38	27.11
LD(0.5)CuS	10.17	7.62	25.07
LD(1)CuS	9.80	7.25	26.02
LD(0.5)MgS	10.35	8.65	16.43
LD(1)MgS	10.29	8.46	17.78

* Number given in paranthesis denotes the weight percentage of metal oxides in the blend

Table 5.8 Percentage weight loss of LDPE-metal stearates after UV exposure for one month

Sample	Initial weight (g)	Weight after one month (g)	% weight loss
LDPE	0.5185	0.5184	0.02
LD(0.5)FeS	0.5777	0.5766	0.19
LD(1)FeS	0.5735	0.5712	0.40
LD(0.5)MnS	0.6238	0.6230	0.13
LD(1)MnS	0.8292	0.8265	0.33
LD(0.5)CuS	0.5559	0.5552	0.13
LD(1)CuS	0.4410	0.4397	0.30
LD(0.5)MgS	0.5234	0.5230	0.08
LD(1)MgS	0.5200	0.5189	0.21

In almost all the cases, LDPE films containing the stearates show considerable reduction in their tensile strength after the UV irradiation for one month clearly indicating photodegradation. Addition of the metal stearates enhances the rate of photodegradation in the order FeS > MnS > CuS > MgS. Table 5.8 shows that exposure to UV radiation did not produce any significant loss in weight of LDPE containing metal stearates.

5.2.2.4 Water absorption studies

Table 5.9 shows the water absorption of LDPE and LDPE containing metal stearates. In presence of the metal stearates the change in water absorption is very marginal thus indicating the hydrophobic nature of the samples.

Table 5.9 Water absorption of LDPE and LDPE containing metal stearates

Sample	Initial weight (g)	Weight after 24 hours (g)	% water absorption
LDPE	0.3337	0.3338	0.03
LD(0.5)FeS	0.2501	0.2502	0.04
LD(1)FeS	0.4736	0.4740	0.09
LD(0.5)MnS	0.2385	0.2386	0.04
LD(1)MnS	0.2748	0.2750	0.07
LD(0.5)CuS	0.3777	0.3778	0.03
LD(1)CuS	0.3252	0.3254	0.06
LD(0.5)MgS	0.2432	0.2433	0.04
LD(1)MgS	0.2395	0.2397	0.08

5.2.2.5 FTIR spectroscopy

Figure 5.11 shows the FTIR spectra of LD(1)FeS before and after exposure to UV radiation for one month. The spectrum of LD(1)FeS show characteristic absorption peaks which are reported in Table 5.10. The spectrum of LD(1)FeS reveals additional peaks at 1642 cm^{-1} and 1463 cm^{-1} due to absorption of aromatic groups along with absorption of carboxylic groups at 1711 cm^{-1} (C=O) and at 1409 cm^{-1} (C-O), present in the spectrum of stearic acid [26]. The spectrum shows absorbance at 1534 cm^{-1} due to asymmetric stretching vibration of the carboxylic group coordinated to the metal ion.

As compared to the spectrum of LD(1)FeS before exposure to the UV radiation, the spectrum of the sample after exposure to UV radiation shows significant changes in the carbonyl ($1785\text{--}1700\text{ cm}^{-1}$), amorphous (1364 cm^{-1}) and hydroxyl regions (3400 cm^{-1}). The difference in peak intensities at 1463 cm^{-1} and 932 cm^{-1} reveals the auto-oxidation of LDPE in presence of ferric stearate. The absorption band due to stretching of carbonyl group,

which is centered around 1711 cm^{-1} grow in intensity and at the same time, a band broadening is observed which indicates the presence of numerous oxidation products like aldehydes (1733 cm^{-1}), carboxylic acid groups (1700 cm^{-1}) and γ lactones (1780 cm^{-1}) [27].

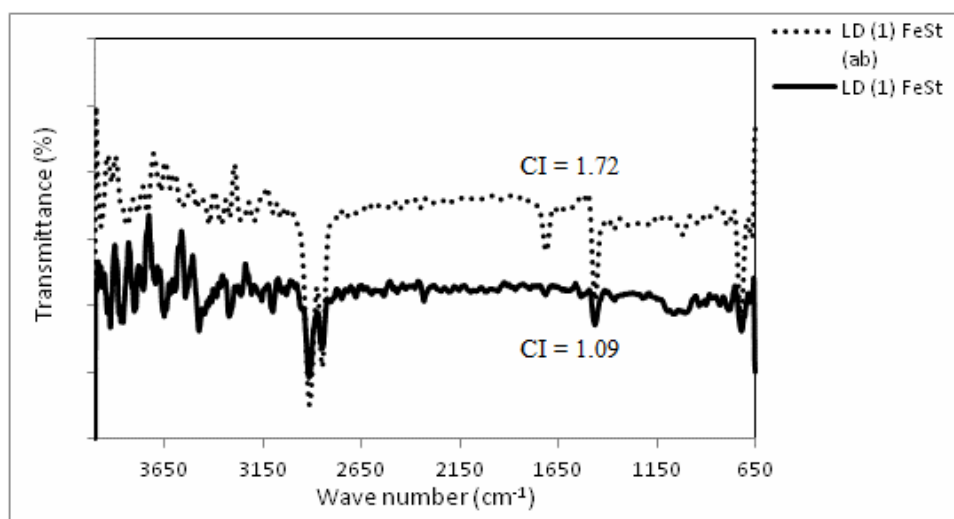


Figure 5.11 FTIR spectra of LD(1)FeS:
(-) before degradation and (..) after degradation

Table 5.10 Characteristic FTIR spectral peaks in LD(1)FeS

Peak position (cm^{-1})	Characteristic group
3400	O-H stretching
2912, 2848	C-H stretching
1711	O-H bending
1534	COO^- asymmetric stretching
1463	CH_2 scissor and asymmetric bending
1454	H-C-OH deformation
1368	C-H bending
932	O-H deformation
723	CH_2 rocking

5.2.2.6 Dynamic mechanical analysis

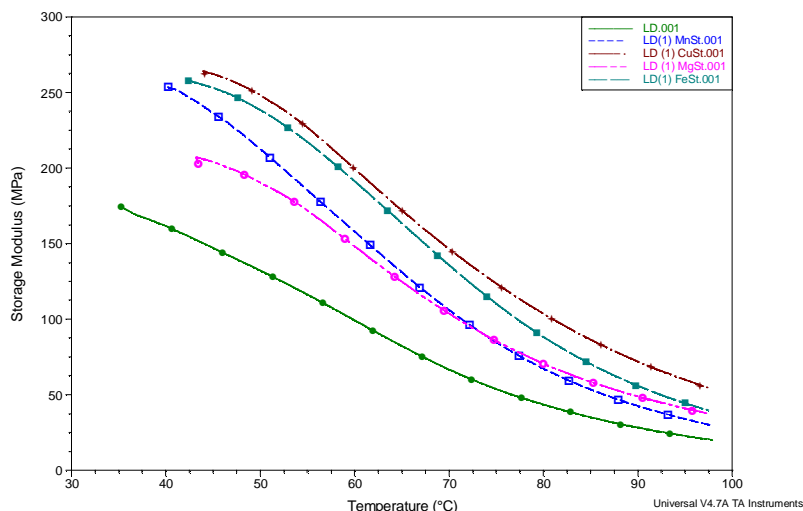


Figure 5.12 DMA curves of LDPE and LDPE containing 1% metal stearates

Figure 5.12 shows the variation in storage modulus of LDPE and LDPE containing metal stearates measured over the temperature range from 40 °C to 100 °C. For all the samples, the addition of metal stearates increased the storage modulus, indicating the stiffening imparted by the metal stearates.

5.2.2.7 Differential scanning calorimetry (DSC)

The DSC thermograms of LD(1)FeS blends are presented in figure 5.13. The melting point of LDPE was observed at 110 °C. It was observed that the melting point increased to 113.14 °C after the addition of ferric stearate with increase in the area under the melting endotherm which is indicative of increased crystallinity. An increase in crystallinity observed in the case of the blend, may be due to the role of the filler particles as nucleating agents for the formation of crystallites (Table.5.11) [28].

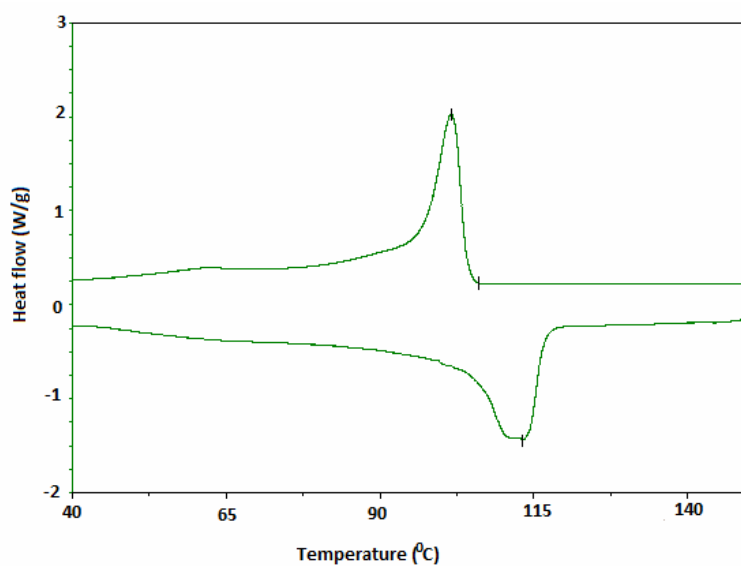


Figure 5.13 DSC curve of LD(1)FeS

Table 5.11 Results of DSC analysis of LDPE and LDPE containing 1% ferric stearate

Sample	T_m ($^{\circ}\text{C}$)	ΔH_f (J/g)	T_c ($^{\circ}\text{C}$)	ΔH_c (J/g)	% Crystallinity
LDPE	110.00	67.00	96.00	79.0	23.4
LD(1)FeS	113.14	87.40	101.58	72.56	30.5

5.2.2.8 Morphological studies

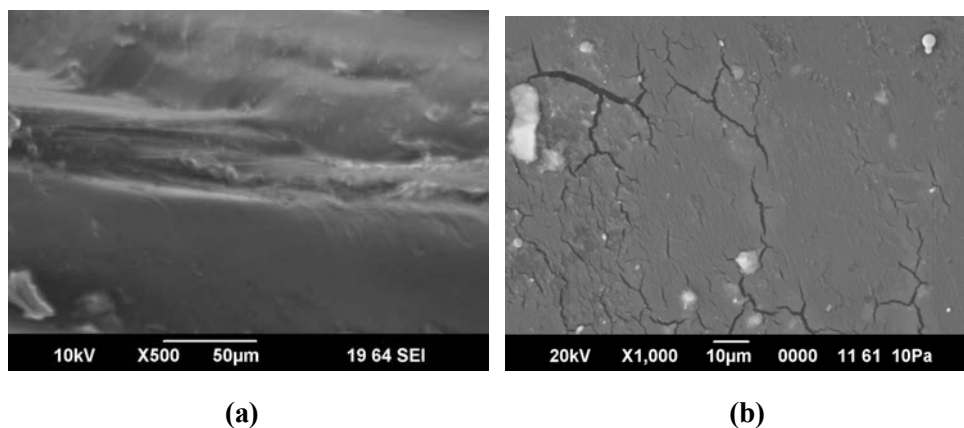


Figure 5.14 Scanning electron micrographs of LD(1)FeS:

a) before degradation and b) after degradation for one month

Figure 5.14 shows the SEM micrographs of LDPE containing ferric stearate before and after UV exposure for one month. The surface of nondegraded film is smooth. The roughness observed on the surface of the film after UV irradiation for one month is due to the degradation of LDPE.

5.3 Conclusions

Addition of small quantities of metal oxides (iron oxide, manganese dioxide, titanium dioxide (rutile and anatase grades)) and metal stearates (ferric stearate, manganese stearate, cupric stearate, magnesium stearate and zinc stearate) as pro-oxidants causes only marginal changes in the mechanical properties of LDPE. The change in the melt flow index of LDPE was marginal on incorporation of small quantities of metal oxides. However the incorporation of small quantities of metal stearates results in an increase in melt flow index of LDPE. The presence of small quantities of both metal oxides and metal stearates induces degradation of LDPE on exposure to UV radiation. Addition of the metal oxides enhanced the rate of photodegradation in the order $\text{FeO} > \text{MnO} > \text{Ru} > \text{An}$ and addition of the metal stearates enhances the rate of photodegradation in the order $\text{FeS} > \text{MnS} > \text{CuS} > \text{MgS}$. The results of the spectroscopic studies reveal the presence of oxidation products after photodegradation. For all the samples, the addition of small quantities of pro-oxidants increased the storage modulus, indicating stiffening. Addition of small quantities of the pro-oxidants results in an enhancement in crystallinity. SEM micrographs of LDPE containing small quantities of ferric oxide and ferric stearate validate photodegradation on exposure to UV radiation for one month.

References

- [1] Gilead, D.; Polym Degrad Stab 1990, 29, 65.
- [2] Jakubowicz, I.; Polym Degrad Stab 2003, 80, 39.
- [3] Wiles, D. M.; Scott, G.; Polym Degrad Stab 2006, 91, 92.
- [4] Albertsson, A. C.; Barenstedt, C.; Karlsson, S.; Lindburg, T.; Polymer 1995, 36, 83.
- [5] Hasan, F.; Shah, A. A.; Hameed, A.; Ahmed, S.; J Appl Polym Sci 2007, 105, 70.
- [6] Weiland, M.; Daro, A.; David, C.; Polym Degrad Stab 1995, 48, 89.
- [7] Tse, K. C. C.; Ng, F. M. F.; Yu, K. N.; Polym Degrad Stab 2006, 91, 2380.
- [8] Roy, P. K.; Surekha, P.; Rajagopal, C.; Choudhary, V.; Polym Degrad Stab 2006, 91, 8.
- [9] Scott, G.; Wiles, D. M.; Biomacromolecules 2001, 2, 22.
- [10] Kyrikou, I.; Briassoulis, D.; J Polym Environ 2007, 15, 50.
- [11] Roy, P. K.; Titus, S.; Surekha, P.; Tulsi, E.; Deshmukh, C.; Rajagopal, C.; Polym Degrad Stab 2008, 93, 22.
- [12] Ojeda, T. F. M.; Dalmolin, E.; Forte, M. M. C.; Jacques, R. J. S.; Bento, F. M.; Camargo, F. A. O.; Polym Degrad Stab 2009, 94, 70.
- [13] Albertsson, A. C.; Barenstedt, C.; Karlsson, S.; Acta Polym 1994, 45, 97.
- [14] Kemp, T. J.; McIntyre, R. A.; Polym Degrad Stab 2006, 91, 3020.
- [15] Roy, P. K.; Surekha, P.; Raman, R.; Rajagopal, C.; Polym Degrad Stab 2009, 94, 1033.
- [16] Scott, G.; Wiles, D.M.; Biomacromolecules 2001, 2, 615.
- [17] Kumnayaka, T.O.; Parthasarathay, R.; Jollands, M.; Ivanov, I.; Korea-Australia Rheol J 2010, 22, 173.
- [18] Lacoste, J.; Vaillant, D.; Carlsson, D. J.; J Polym Sci A- Chem 1993, 31, 715.

- [19] Wilhelm, C.; Gardette, J. L.; J Appl Polym Sci 1994, 51, 1411.
- [20] Jinguang, W.; Technique and application of advanced Fourier transform infrared spectroscopy, Technological Literature Press, Beijing, 1994, pp. 607-20.
- [21] Pablos, J. L.; Abrusci, C.; Marin, I.; Lopez-Marin, J.; Catalina, F.; Espi, E.; Corrales, T.; Polym Degrad Stab 2010, 95, 2057.
- [22] Sanchez-Solis, A.; Estrada, M. R.; Polym Degrad Stab 1996, 52, 305.
- [23] Koutny, M.; Lemaire, J.; Delort, A. M.; Chemosphere 2006, 64, 52.
- [24] Guthrie, J. T.; Surface Coatings International Part B: Coatings Transactions 2002, 85(B1), 27.
- [25] Chapiro, A.; In: Mark, H. F.; Gaylord, N. G.; (Eds), Encyclopedia of Polymer Science & Technology, John Wiley & Sons, New York, 1969, 11, 702.
- [26] Rivas, B. L.; Seguel, G. V.; Geckeler, K. E.; J Appl Polym Sci 2001, 81, 1310.
- [27] Gulmine, J. V.; Janissek, P. R.; Heise, H. M.; Akcelrud, L.; Polym Degrad Stab 2003, 79, 385.
- [28] Hinsken, H.; Moss, S.; Pauquet, J. R.; Zweifel, H.; Polym Degrad Stab 1991, 34, 279.



EFFECT OF METAL OXIDES AS PRO-OXIDANTS ON IONOMER COMPATIBILIZED LOW DENSITY POLYETHYLENE-STARCH BLENDS

Contents**6.1 Introduction****6.2 Results and discussion****6.3 Conclusions**

Various compositions (0.5 and 1 weight %) of the metal oxides (iron oxide, manganese dioxide, titanium dioxide (anatase and rutile grades)) were incorporated into EMA-Zn (5%) and EMA-Na (5%) compatibilized low density polyethylene-starch blends. The role of small quantities of the metal oxides as pro-oxidants in the blends were evaluated by measuring mechanical properties, melt flow indices, biodegradability, photodegradability, photobiodegradability, water absorption, infrared spectroscopy, dynamic mechanical analysis, thermogravimetry, differential scanning calorimetry and scanning electron microscopy. The blends showed changes in mechanical properties with the addition of metal oxides. Thermal characterization using TGA and DSC showed that there were changes in thermal stability and crystallinity with the incorporation of metal oxides. Various degradative studies show that the addition of metal oxides enhances the degradability of the blends.

6.1 Introduction

Nowadays oxo-biodegradation of polymers used in packaging applications is receiving ever increasing attention. Low density polyethylene is one of the most widely used polyolefin polymer for packaging applications. In order to overcome the intrinsic recalcitrance of low density polyethylene to biological attack, the major strategies are focused on: (i) introduction of functional groups in the polyethylene backbone, and (ii) blending polyethylene with photo initiating pro-oxidants capable of promoting the formation of free radical precursor moieties by photo-oxidation to induce cleavage of macromolecular backbone [1-4]. Photo-oxidation of low density polyethylene-starch blends containing pro-oxidants leads to an increase in the low molecular weight fraction by chain scission, thereby facilitating biodegradation [5-7]. It also leads to an increase in the surface area through embrittlement and subsequent track formation. In addition, the formation of carbonyl groups on the surface increases the hydrophilicity of polyethylene [8]. Transition metals have been reported to act as effective photoinitiators for polyethylene [9]. Transition metals, especially iron and manganese possess remarkable ability to decompose the hydroperoxides formed during the oxidation process of polymers and therefore they are used in most of the commercial photodegradable compositions [10-12]. TiO_2 has become another choice as photocatalyst due to its superb characteristics such as inexpensiveness, non-toxicity, stability and high photoactiveness, [13-14].

This chapter explores the possibility of using metal oxides, namely ferric oxide, manganese dioxide and titanium dioxide (anatase and rutile grades) for improving the degradative properties of ionomer compatibilized low density polyethylene-starch blends. Designations of the samples used in this chapter and their descriptions are given in Table 6.1. The films were

characterized by mechanical properties, infrared spectroscopy, thermal properties and scanning electron microscopy. The biodegradability, photodegradability and photobiodegradability of the films were also carried out.

Table 6.1 Description of sample designations

Sample designation	Description
LDS-Zn	LDPE-20% starch-5% (EMA-Zn)
LDS-Zn-Fe	LDPE-20% starch-5% (EMA-Zn)-Fe ₂ O ₃
LDS-Zn-Mn	LDPE-20% starch-5% (EMA-Zn)-MnO ₂
LDS-Zn-Ru	LDPE-20% starch-5% (EMA-Zn)-TiO ₂ (rutile)
LDS-Zn-An	LDPE-20% starch-5% (EMA-Zn)- TiO ₂ (anatase)
LDS-Na	LDPE-20% starch-5% (EMA-Na)
LDS-Na-Fe	LDPE-20% starch-5% (EMA-Na)-Fe ₂ O ₃
LDS-Na-Mn	LDPE-20% starch-5% (EMA-Na)-MnO ₂
LDS-Na-Ru	LDPE-20% starch-5% (EMA-Na)-TiO ₂ (rutile)
LDS-Na-An	LDPE-20% starch-5% (EMA-Na)- TiO ₂ (anatase)

6.2 Results and discussion

6.2.1 Mechanical properties

The mechanical properties of neat LDPE, LDPE-starch-(EMA-Zn) blend, LDPE-starch-(EMA-Na) blend and the blends containing the metal oxides as pro-oxidants are shown in figures 6.1A and 6.1B. In the case of LDPE-starch-(EMA-Zn) blends and LDPE-starch-(EMA-Na) blends, all the samples containing metal oxides exhibit tensile strength in the same range as that of neat LDPE thereby signifying that processing of these materials has not promoted premature degradation reactions [15].

In all the compositions containing metal oxides there was a drastic reduction in the elongation at break as compared to neat LDPE. Figures 6.1A(c) and 6.1B(c) show that elastic modulus of the blends increased with the incorporation of metal oxides. The elastic moduli for all the blends were greater than the value for LDPE thus indicating an increase in rigidity [16].

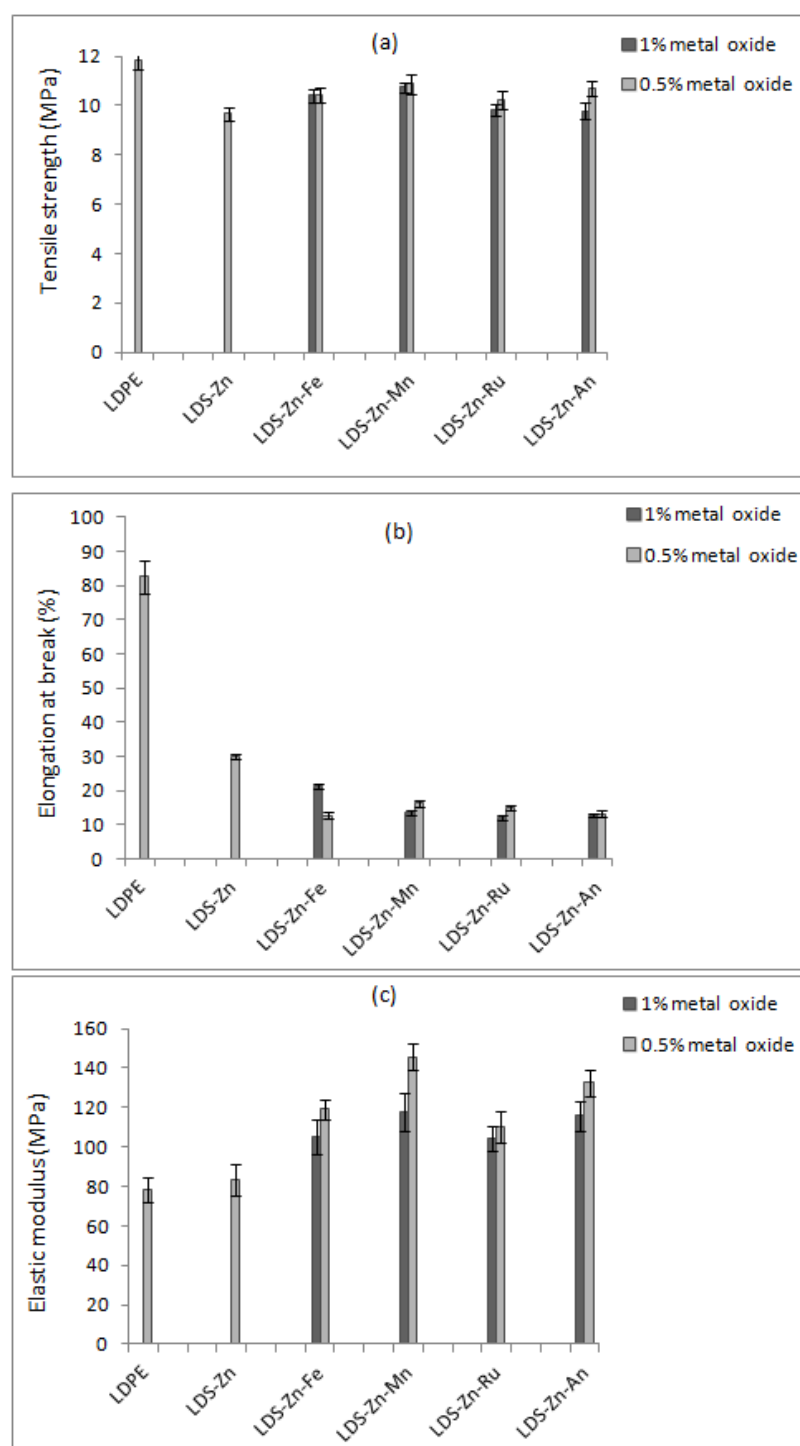


Figure 6.1A Effect of metal oxides on the mechanical properties of LDPE-starch-(EMA-Zn) blends

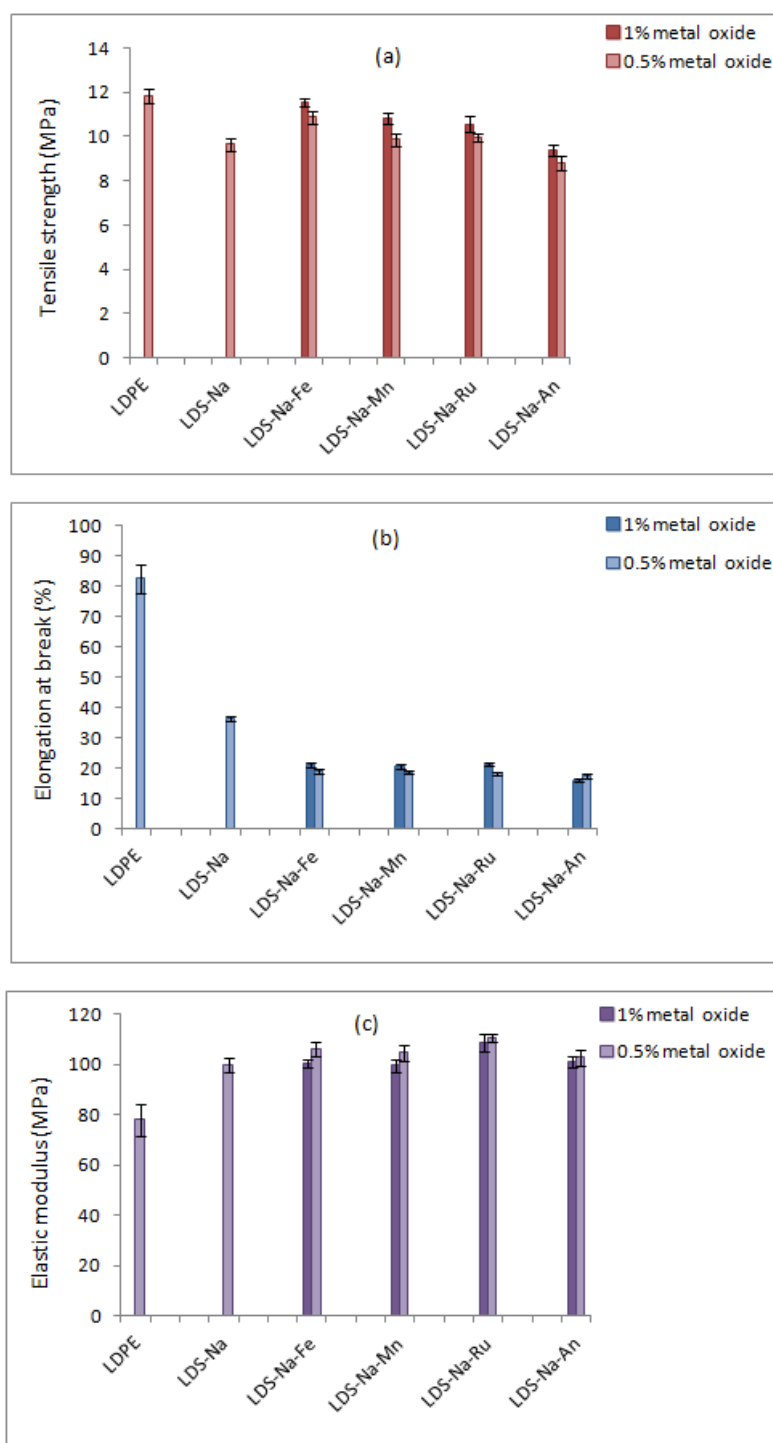


Figure 6.1B Effect of metal oxides on the mechanical properties of LDPE-starch-(EMA-Na) blends

6.2.2 Melt flow measurements

Figures 6.2A and 6.2B show the effect of metal oxides on the melt flow indices of LDPE-starch-ionomer blends.

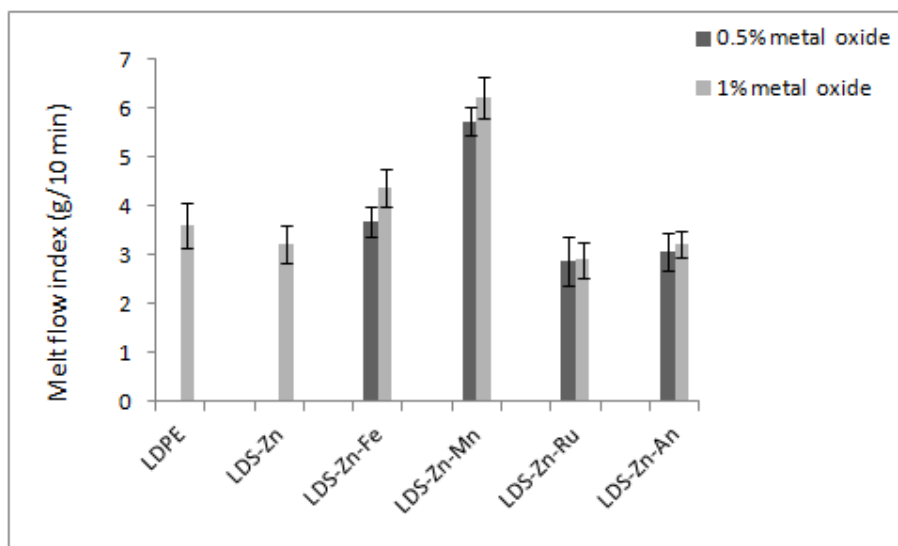


Figure 6.2A Effect of metal oxides on the melt flow indices of LDPE-starch-(EMA-Zn) blends

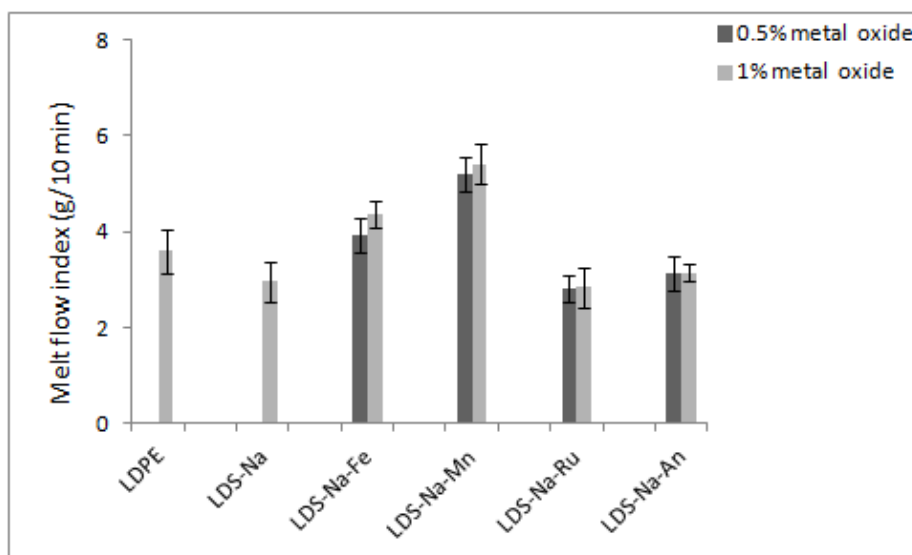


Figure 6.2B Effect of metal oxides on the melt flow indices of LDPE-starch-(EMA-Na) blends

The samples of LDPE-starch-(EMA-Zn) blends containing metal oxides with the exception of Fe_2O_3 and MnO_2 exhibited an MFI value nearly equal to the value of LDPE indicating that processing in the presence of pro-oxidants does not lead to either chain scission or crosslinking so as to cause a remarkable change in the melt indices [17]. A notable increase in the MFI of LDPE-starch-ionomer blends containing Fe_2O_3 and MnO_2 demonstrates a significant chain scission.

6.2.3 Biodegradation studies

Figures 6.3A and 6.3B exhibit the tensile properties of LDPE-starch-(EMA-Zn)-metal oxide blends and LDPE-starch-(EMA-Na)-metal oxide blends after biodegradation in culture medium for two months. Tables 6.2 and 6.3 show the percentage decrease in tensile strength of LDPE-starch-(EMA-Zn)-metal oxide blends and LDPE-starch-(EMA-Na)-metal oxide blends respectively. As shown, there was a significant reduction in tensile strength after biodegradation for all the blends. The reason for this reduction is the starch consumption by microorganisms. These changes are reflected in the tensile properties of the blend films which suggest that the blends are partially biodegradable.

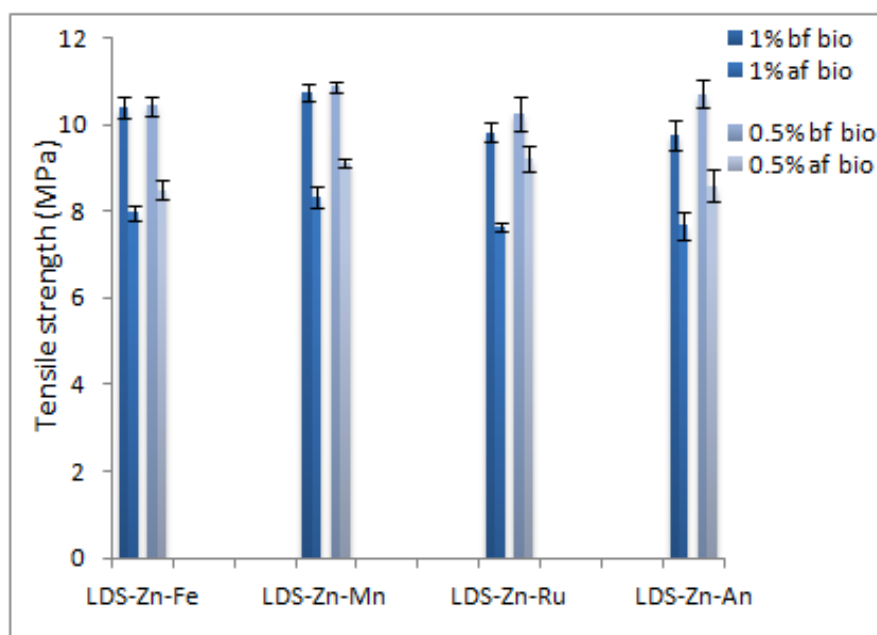


Figure 6.3A Biodegradation of LDPE-starch-(EMA-Zn)-metal oxide blends after immersion of plastic strips in culture medium for two months (Evident from tensile strength)

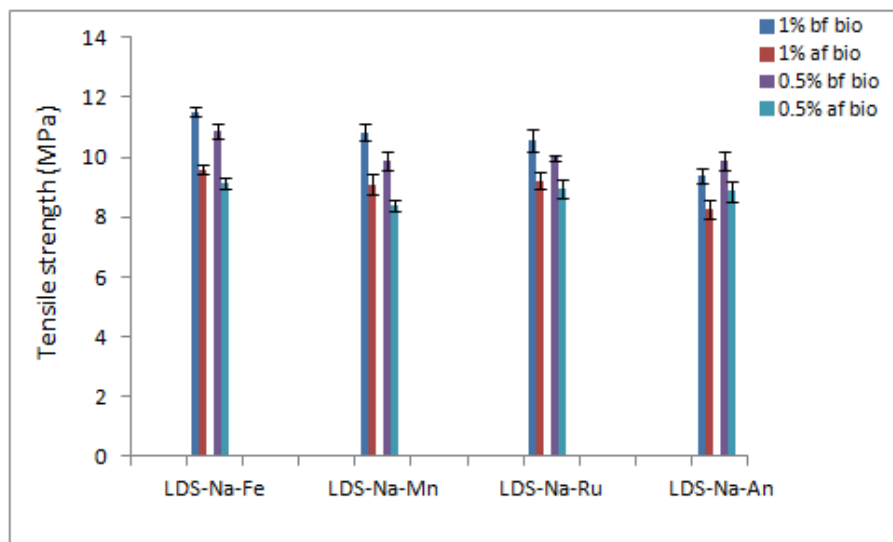


Figure 6.3B Biodegradation of LDPE-starch-(EMA-Na)-metal oxide blends after immersion of plastic strips in culture medium for two months (Evident from tensile strength)

Table 6.2 Percentage decrease in tensile strength of LDPE-starch-(EMA-Zn)-metal oxide blends after biodegradation in culture medium for two months

Sample	Initial tensile strength (MPa)	Tensile strength after biodegradation for two months (MPa)	% decrease in tensile strength
LDS-Zn(1)Fe*	10.4 ± 0.24	7.96 ± 0.15	23.46
LDS-Zn(0.5)Fe	10.4 ± 0.32	8.50 ± 0.23	18.29
LDS-Zn(1)Mn	10.7 ± 0.20	8.32 ± 0.26	22.24
LDS-Zn(0.5)Mn	10.9 ± 0.41	9.11 ± 0.09	16.42
LDS-Zn(1)Ru	9.8 ± 0.21	7.65 ± 0.10	22.11
LDS-Zn(0.5)Ru	10.2 ± 0.38	9.21 ± 0.30	9.71
LDS-Zn(1)An	9.77 ± 0.35	7.68 ± 0.32	21.39
LDS-Zn(0.5)An	10.7 ± 0.31	8.58 ± 0.37	19.81

* Number given in paranthesis denotes the weight percentage of metal oxides in the blend

Table 6.3 Percentage decrease in tensile strength of LDPE-starch-(EMA-Na)-metal oxide blends after biodegradation in culture medium for two months

Sample	Initial tensile strength (MPa)	Tensile strength after biodegradation for two months (MPa)	% decrease in tensile strength
LDS-Na(1)Fe	11.5 ± 0.17	9.59 ± 0.15	16.79
LDS-Na(0.5)Fe	10.9 ± 0.26	9.15 ± 0.18	15.77
LDS-Na(1)Mn	10.8 ± 0.26	9.10 ± 0.32	16.05
LDS-Na(0.5)Mn	9.86 ± 0.31	8.37 ± 0.18	15.09
LDS-Na(1)Ru	10.6 ± 0.35	9.21 ± 0.29	12.87
LDS-Na(0.5)Ru	9.99 ± 0.08	8.95 ± 0.33	10.39
LDS-Na(1)An	9.38 ± 0.23	8.24 ± 0.31	12.11
LDS-Na(0.5)An	9.91 ± 0.31	8.86 ± 0.37	10.57

Table 6.4 Percentage decrease in weight of LDPE-starch-(EMA-Zn)-metal oxide blends after biodegradation in culture medium for two months

Sample	Initial weight (g)	Weight after two months (g)	% weight loss
LDS-Zn(1)Fe	0.5583	0.5434	2.666
LDS-Zn(0.5)Fe	0.5684	0.5547	2.402
LDS-Zn(1)Mn	0.6881	0.6720	2.334
LDS-Zn(0.5)Mn	0.6480	0.6332	2.283
LDS-Zn(1)Ru	0.5246	0.5150	1.824
LDS-Zn(0.5)Ru	0.5099	0.5003	1.703
LDS-Zn(1)An	0.5803	0.5710	1.613
LDS-Zn(0.5)An	0.6611	0.6511	1.505

Table 6.5 Percentage decrease in weight of LDPE-starch-(EMA-Na)-metal oxide blends after biodegradation in culture medium for two months

Sample	Initial weight (g)	Weight after two months (g)	% weight loss
LDS-Na(1)Fe	0.4633	0.4510	2.669
LDS-Na(0.5)Fe	0.6113	0.5957	2.552
LDS-Na(1)Mn	0.4724	0.4598	2.674
LDS-Na(0.5)Mn	0.5065	0.4944	2.398
LDS-Na(1)Ru	0.5544	0.5404	2.534
LDS-Na(0.5)Ru	0.6442	0.6295	2.283
LDS-Na(1)An	0.4953	0.4870	1.674
LDS-Na(0.5)An	0.4335	0.4268	1.559

Weight loss is one of the main parameters which determine the biodegradation of a polymer. The percentage weight loss of the blends after biodegradation in culture medium is summarized in Tables 6.4 and 6.5. All the samples exhibit a significant weight loss after degradation in

culture medium which indicates that the LDPE-starch-ionomer blends containing metal oxides are partially biodegradable.

6.2.4 Photodegradation studies

Figures 6.4A and 6.4B show the tensile properties of LDPE-starch-(EMA-Zn)-metal oxide blends and LDPE-starch-(EMA-Na)-metal oxide blends after UV exposure for one month. Tables 6.6 and 6.7 show the percentage decrease in tensile strength of LDPE-starch-(EMA-Zn)-metal oxide blends and LDPE-starch-(EMA-Na)-metal oxide blends respectively. There is significant reduction in tensile strength after one month of exposure to UV radiation. The changes in chemical structure of the blend, after exposure to ultraviolet radiation result in the formation of new groups in the polymer chain, mainly in the amorphous region of material and this may be the reason for the reduction in tensile strength [17].

Table 6.6 Percentage decrease in tensile strength of LDPE-starch-(EMA-Zn)-metal oxide blends after UV exposure for one month

Sample	Initial tensile strength (MPa)	Tensile strength after UV exposure for one month (MPa)	% decrease in tensile strength
LDS-Zn(1)Fe	10.4 ± 0.24	7.23 ± 0.32	30.48
LDS-Zn(0.5)Fe	10.4 ± 0.32	7.43 ± 0.15	28.52
LDS-Zn(1)Mn	10.7 ± 0.20	7.66 ± 0.26	28.41
LDS-Zn(0.5)Mn	10.9 ± 0.41	7.91 ± 0.11	27.41
LDS-Zn(1)Ru	9.8 ± 0.21	7.92 ± 0.13	19.35
LDS-Zn(0.5)Ru	10.2 ± 0.38	8.39 ± 0.17	17.75
LDS-Zn(1)An	9.77 ± 0.35	8.05 ± 0.16	17.61
LDS-Zn(0.5)An	10.7 ± 0.31	8.87 ± 0.28	17.22

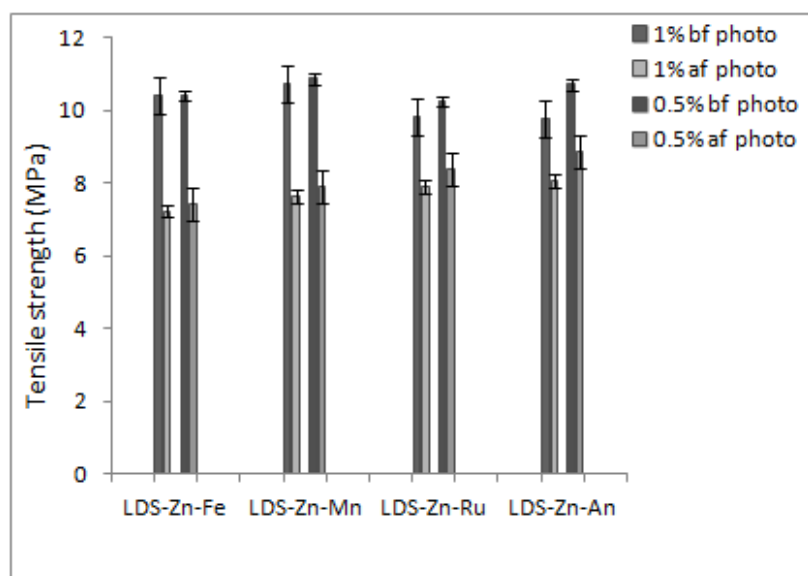


Figure 6.4A Photodegradation of LDPE-starch-(EMA-Zn)-metal oxide blends after UV exposure for one month (Evident from tensile strength)

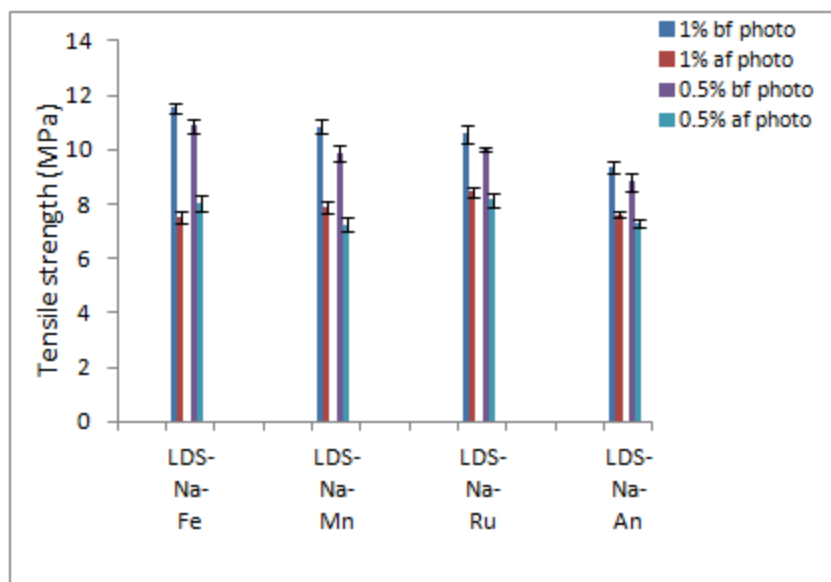


Figure 6.4B Photodegradation of LDPE-starch-(EMA-Na)-metal oxide blends after UV exposure for one month (Evident from tensile strength)

Table 6.7 Percentage decrease in tensile strength of LDPE-starch-(EMA-Na)-metal oxide blends after UV exposure for one month

Sample	Initial tensile strength (MPa)	Tensile strength after UV exposure for one month (MPa)	% decrease in tensile strength
LDS-Na(1)Fe	11.5 ± 0.17	7.52 ± ± 0.25	34.61
LDS-Na(0.5)Fe	10.9 ± 0.26	8.02 ± 0.30	26.17
LDS-Na(1)Mn	10.8 ± 0.26	7.86 ± 0.23	27.49
LDS-Na((0.5)Mn	9.86 ± 0.31	7.34 ± 0.28	25.54
LDS-Na(1)Ru	10.6 ± 0.35	8.45 ± 0.19	20.06
LDS-Na(0.5)Ru	9.99 ± 0.08	8.15 ± 0.28	18.40
LDS-Na(1)An	9.38 ± 0.23	7.61 ± 0.12	18.83
LDS-Na(0.5)An	8.81 ± 0.31	7.27 ± 0.15	17.45

Table 6.8 Percentage decrease in weight of LDPE-starch-(EMA-Zn)-metal oxide blends after UV exposure for one month

Sample	Initial weight (g)	Weight after one month (g)	% weight loss
LDS-Zn(1)Fe	0.5690	0.5668	0.387
LDS-Zn(0.5)Fe	0.6007	0.5990	0.283
LDS-Zn(1)Mn	0.5680	0.5662	0.317
LDS-Zn(0.5)Mn	0.6657	0.6639	0.270
LDS-Zn(1)Ru	0.5197	0.5185	0.231
LDS-Zn(0.5)Ru	0.6196	0.6185	0.178
LDS-Zn(1)An	0.5319	0.5309	0.188
LDS-Zn(0.5)An	0.6676	0.6667	0.135

Tables 6.8 and 6.9 show the percentage weight loss for LDPE-starch-ionomer-metal oxide blends after UV exposure for one month. It was observed that all the samples show a slight decrease in weight after photodegradation and the weight loss is found to increase with increase in concentration of metal oxides.

Table 6.9 Percentage decrease in weight of LDPE-starch-(EMA-Na)-metal oxide blends after UV exposure for one month

Sample	Initial weight (g)	Weight after one month (g)	% weight loss
LDS-Na(1)Fe	0.5950	0.5930	0.336
LDS-Na(0.5)Fe	0.5333	0.5326	0.244
LDS-Na(1)Mn	0.4634	0.4621	0.281
LDS-Na(0.5)Mn	0.4785	0.4774	0.230
LDS-Na(1)Ru	0.6540	0.6527	0.199
LDS-Na(0.5)Ru	0.4408	0.4403	0.113
LDS-Na(1)An	0.6010	0.5999	0.183
LDS-Na(0.5)An	0.5495	0.5489	0.109

6.2.5 Photobiodegradation studies

Figures 6.5A and 6.5B show the tensile properties of LDPE-starch-(EMA-Zn)-metal oxide blends and LDPE-starch-(EMA-Na)-metal oxide blends after photobiodegradation studies. Photobiodegradation was investigated by exposure of the samples to UV radiation for one month followed by the immersion of the photodegraded samples in culture medium containing amylase producing *vibrios*, which were isolated from marine benthic environment, for one month. Tables 6.10 and 6.11 show the percentage decrease in tensile strength of LDPE-starch-(EMA-Zn)-metal oxide blends and LDPE-starch-(EMA-Na)-metal oxide blends respectively. There is significant reduction in tensile strength after two months of photobiodegradation. This is because of the photo-oxidation of polyethylene-starch-ionomer blends containing pro-oxidants which leads to an increase in the low molecular weight fraction by chain scission, thereby facilitating biodegradation [6].

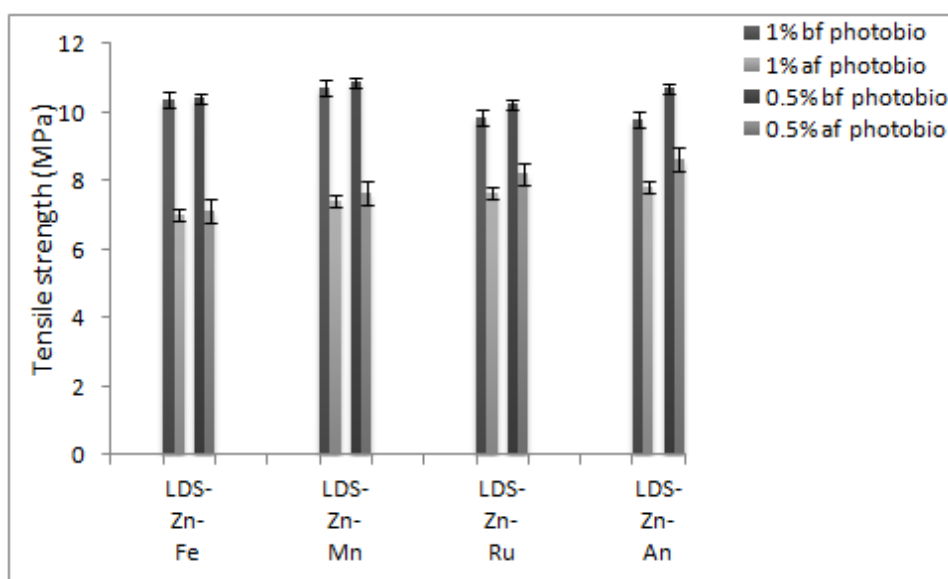


Figure 6.5A Variation in tensile strength of LDPE-starch-(EMA-Zn)-metal oxide blends after UV exposure for one month followed by biodegradation in culture medium for one month

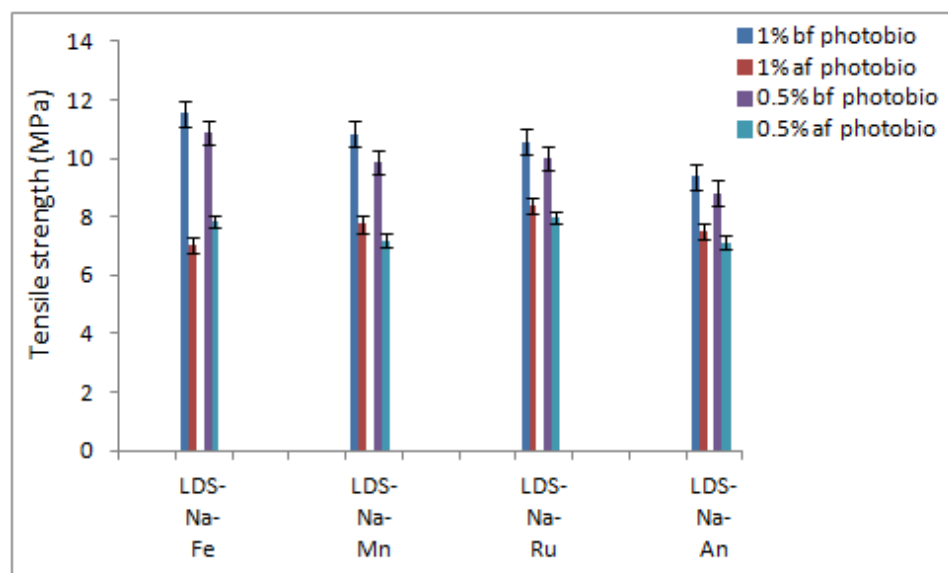


Figure 6.5B Variation in tensile strength of LDPE-starch-(EMA-Na)-metal oxide blends after UV exposure for one month followed by biodegradation in culture medium for one month

Table 6.10 Percentage decrease in tensile strength of LDPE-starch-(EMA-Zn)-metal oxide blends after photobiodegradation

Sample	Initial tensile strength (MPa)	Tensile strength after photobiodegradation for two months (MPa)	% decrease in tensile strength
LDS-Zn(1)Fe	10.4 \pm 0.24	7.01 \pm 0.18	32.58
LDS-Zn(0.5)Fe	10.4 \pm 0.32	7.12 \pm 0.35	31.59
LDS-Zn(1)Mn	10.7 \pm 0.20	7.43 \pm 0.19	30.54
LDS-Zn(0.5)Mn	10.9 \pm 0.41	7.66 \pm 0.43	29.75
LDS-Zn(1)Ru	9.8 \pm 0.21	7.66 \pm 0.18	21.99
LDS-Zn(0.5)Ru	10.2 \pm 0.38	8.21 \pm 0.41	19.82
LDS-Zn(1)An	9.77 \pm 0.35	7.83 \pm 0.36	19.88
LDS-Zn(0.5)An	10.7 \pm 0.31	8.64 \pm 0.41	19.22

Table 6.11 Percentage decrease in tensile strength of LDPE-starch-(EMA-Na)-metal oxide blends after photobiodegradation

Sample	Initial tensile strength (MPa)	Tensile strength after photobiodegradation for two months (MPa)	% decrease in tensile strength
LDS-Na(1)Fe	11.5 \pm 0.17	7.01 \pm 0.15	39.04
LDS-Na(0.5)Fe	10.9 \pm 0.26	7.83 \pm 0.11	28.17
LDS-Na(1)Mn	10.8 \pm 0.26	7.75 \pm 0.16	28.24
LDS-Na((0.5)Mn	9.86 \pm 0.31	7.18 \pm 0.10	27.17
LDS-Na(1)Ru	10.6 \pm 0.35	8.37 \pm 0.18	21.11
LDS-Na(0.5)Ru	9.99 \pm 0.08	7.98 \pm 0.11	20.10
LDS-Na(1)An	9.38 \pm 0.23	7.49 \pm 0.16	20.11
LDS-Na(0.5)An	8.81 \pm 0.31	7.12 \pm 0.12	19.16

The percentage weight loss of the blends after biodegradation in culture medium is summarized in Tables.6.12 and 6.13. All the samples exhibited a significant weight loss after photobiodegradation. This is because of the microbial degradation of the oxidation products.

Table 6.12 Percentage decrease in weight of LDPE-starch-(EMA-Zn)-metal oxide blends after photobiodegradation for two months

Sample	Initial weight (g)	Weight after two months (g)	% weight loss
LDS-Zn(1)Fe	0.5690	0.5572	2.074
LDS-Zn(0.5)Fe	0.6007	0.5915	1.532
LDS-Zn(1)Mn	0.5680	0.5592	1.550
LDS-Zn(0.5)Mn	0.6657	0.6562	1.427
LDS-Zn(1)Ru	0.5319	0.5238	1.523
LDS-Zn(0.5)Ru	0.6676	0.6601	1.123
LDS-Zn(1)An	0.5197	0.5141	1.078
LDS-Zn(0.5)An	0.6196	0.6133	1.017

Table 6.13 Percentage decrease in weight of LDPE-starch-(EMA-Na)-metal oxide blends after photobiodegradation for two months

Sample	Initial weight (g)	Weight after two months (g)	% weight loss
LDS-Na(1)Fe	0.5950	0.5867	1.395
LDS-Na(0.5)Fe	0.5333	0.5272	1.144
LDS-Na(1)Mn	0.4634	0.4575	1.273
LDS-Na(0.5)Mn	0.4785	0.4725	1.254
LDS-Na(1)Ru	0.6010	0.5943	1.115
LDS-Na(0.5)Ru	0.5495	0.5436	1.074
LDS-Na(1)An	0.6540	0.6468	1.101
LDS-Na(0.5)An	0.4408	0.4361	1.066

6.2.6 Water absorption studies

The extent of hydrophilicity of LDPE-starch-ionomer-metal oxide blends was established by % water absorption measurements. The water absorption characteristics of LDPE-starch-ionomer-metal oxide blends are shown in Tables 6.14 and 6.15. As compared to the blends without metal

oxides (chapter 4, Tables 4.5 and 4.6), the water uptake of the blend with metal oxides remain unchanged. For films containing 1% metal oxides the % water absorption was observed in the order LDS-(1)Fe > LDS-(1)Mn > LDS-(1)Ru > LDS-(1)An in both EMA-Zn and EMA-Na compatibilized blends.

Table 6.14 Water absorption of LDPE-starch-(EMA-Zn)-metal oxide blends

Sample	Initial weight (g)	Weight after 24 hours (g)	% water absorption
LDS-Zn(1)Fe	0.3552	0.3596	1.239
LDS-Zn(0.5)Fe	0.3045	0.3082	1.215
LDS-Zn(1)Mn	0.2764	0.2799	1.27
LDS-Zn(0.5)Mn	0.4014	0.406	1.146
LDS-Zn(1)Ru	0.5558	0.5624	1.188
LDS-Zn(0.5)Ru	0.3295	0.3330	1.062
LDS-Zn(1)An	0.4321	0.4372	1.180
LDS-Zn(0.5)An	0.3741	0.3780	1.043

Table 6.15 Water absorption of LDPE-starch-(EMA-Na)-metal oxide blends

Sample	Initial weight (g)	Weight after 24 hours (g)	% water absorption
LDS-Na(1)Fe	0.3912	0.3960	1.227
LDS-Na(0.5)Fe	0.2691	0.2723	1.189
LDS-Na(1)Mn	0.2959	0.2994	1.183
LDS-Na(0.5)Mn	0.2884	0.2918	1.179
LDS-Na(1)Ru	0.3278	0.3315	1.129
LDS-Na(0.5)Ru	0.2427	0.2451	0.989
LDS-Na(1)An	0.3363	0.3396	0.981
LDS-Na(0.5)An	0.2913	0.2940	0.927

6.2.7 FTIR spectroscopy

Figure 6.6A shows the FTIR spectra of the LDPE- starch-(EMA-Zn)- Fe_2O_3 films before and after biodegradation. The spectrum of LDPE- starch-(EMA-Zn)- Fe_2O_3 film shows characteristic absorption peaks which are reported in Table 6.16. The peaks at $2921\text{--}2848\text{ cm}^{-1}$, $1473\text{--}1463\text{ cm}^{-1}$ and $730\text{--}720\text{ cm}^{-1}$ are due to symmetrical stretching vibration of C-H bonds, bending vibration of C-H bonds and the characteristic absorption of the crystalline and amorphous bands. As shown in figure, peak intensities of films at $2921\text{--}2848\text{ cm}^{-1}$, $1473\text{--}1463\text{ cm}^{-1}$, $1156\text{--}1028\text{ cm}^{-1}$ and $730\text{--}720\text{ cm}^{-1}$ were all improved greatly after biodegradation in culture for two months. The increase in the intensity of peaks is due to the fracture of the polyethylene chain in degradable environments, which resulted in increase in the terminal group numbers. In addition, the peak at 1706 cm^{-1} after degradation was caused by the carbonyl group due to the oxidation of polyethylene.

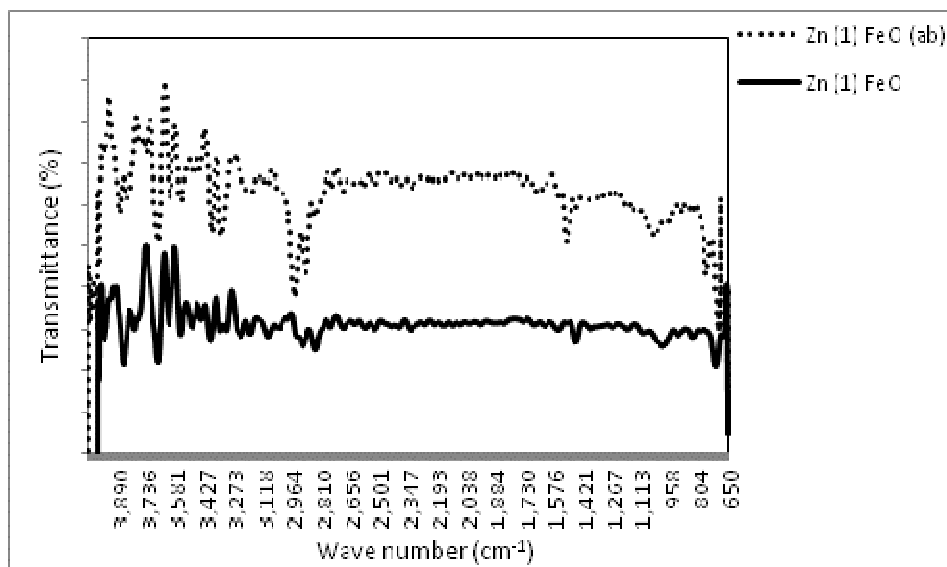


Figure 6.6A FTIR spectra of LDPE-starch-(EMA-Zn)- Fe_2O_3 blend: (—) before biodegradation and (...) after biodegradation

The peaks at 1156 cm^{-1} and 1028 cm^{-1} are attributed to C-O-C bond stretching of starch, and the peak near 1001 cm^{-1} is the characteristic peak of the anhydroglucose ring O-C stretch. The degradation of starch led to the increase in the intensity of these peaks which indicates that addition of ferric oxide does not produce any adverse effects on the biodegradation of LDPE-starch-(EMA-Zn) blends.

Table 6.16 Characteristic FTIR spectral peaks

Sample	Peak position (cm^{-1})	Characteristic group
LDPE- starch-(EMA-Zn)-Fe_2O_3 film	2911, 2845	C-H stretching
	1557	C=O stretching
	1461	CH_2 scissor and asymmetric bending
	1368	C-H bending
	1001	O-C stretching
	932	O-H deformation
	721	CH_2 rocking
LDPE- starch-(EMA-Na)-Fe_2O_3 film	2912, 2847	C-H stretching
	1537	C=O stretching
	1463	CH_2 scissor and asymmetric bending
	1368	C-H bending
	1008	O-C stretching
	918	O-H deformation
	721	CH_2 rocking

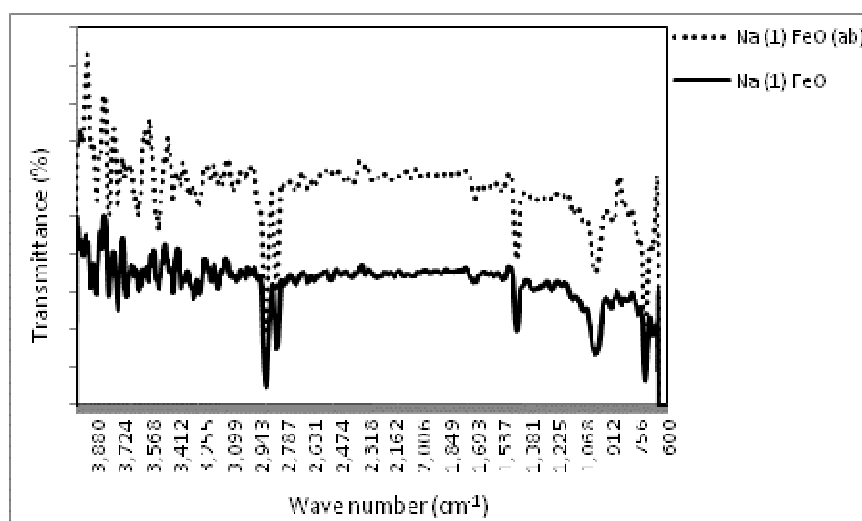


Figure 6.6B FTIR spectra of LDPE-starch-(EMA-Na)-1% Fe_2O_3 blend: (-) before biodegradation and (...) after biodegradation

The FTIR spectra of LDPE-starch-(EMA-Na)- Fe_2O_3 blend before and after biodegradation process are shown in figure 6.6B. The characteristic absorption peaks in the spectrum of LDPE- starch-(EMA-Na)- Fe_2O_3 film are given in Table 6.16. Peak intensity of starch and polyethylene too improved a little. This demonstrates that LDPE-starch-(EMA-Na)- Fe_2O_3 blends are more compatible than LDPE-starch-(EMA-Zn)- Fe_2O_3 blends.

6.2.8 Dynamic mechanical analysis

Figures 6.7A and 6.7B show the variation in storage modulus of LDPE-starch-(EMA-Zn) blends and LDPE-starch-(EMA-Na) blends containing metal oxides measured over the temperature range from 40 °C to 100 °C. The addition of metal oxides increased the storage modulus values, indicating that there was an improvement in the interfacial interaction between the phases of the blends [18].

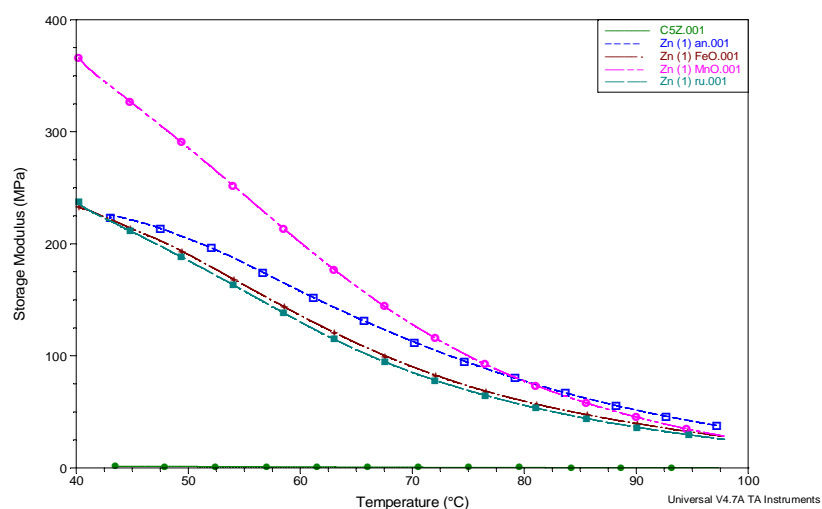


Figure 6.7A DMA curves of LDPE-starch-(EMA- Zn)-1% metal oxide blends

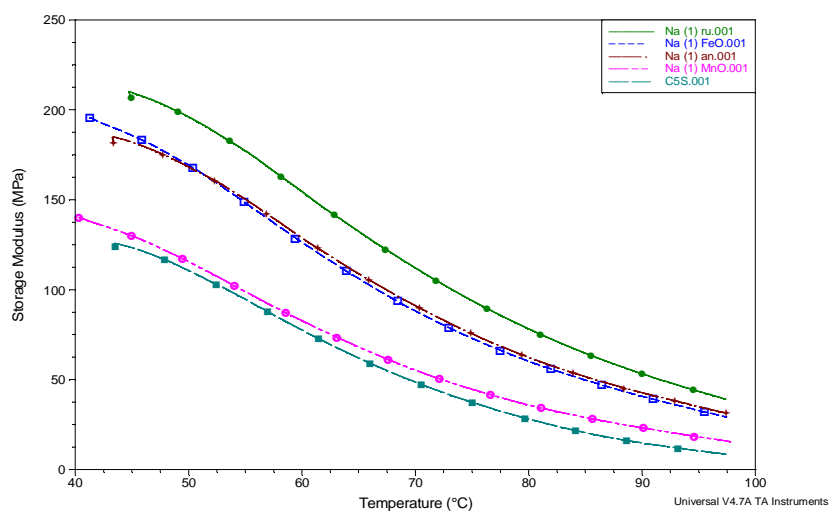


Figure 6.7B DMA curves of LDPE-starch-(EMA- Na)-1% metal oxide blends

6.2.9 Thermogravimetric analysis (TGA)

Table 6.17 TGA results for LDPE-starch-(EMA-Zn)-1% metal oxide blends

Sample	Temperature of onset of degradation ($^{\circ}\text{C}$)	T_{max} ($^{\circ}\text{C}$)	Rate of maximum degradation ($\%/^{\circ}\text{C}$)	Residual weight (%)
LDS-Zn	431.28	490.07	2.082	1.209
LDS-Zn(1)Fe	421.57	488.53	1.779	2.417
LDS-Zn(1)An	424.32	490.88	1.857	2.603

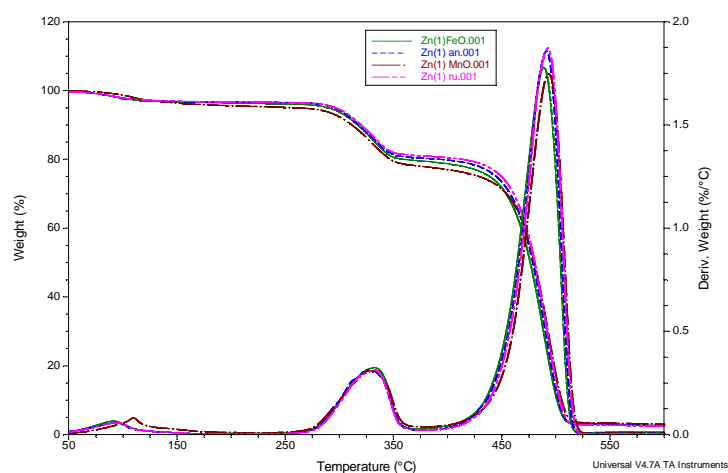


Figure 6.8A TGA thermograms of LDPE-starch-(EMA-Zn)-1% metal oxide blends

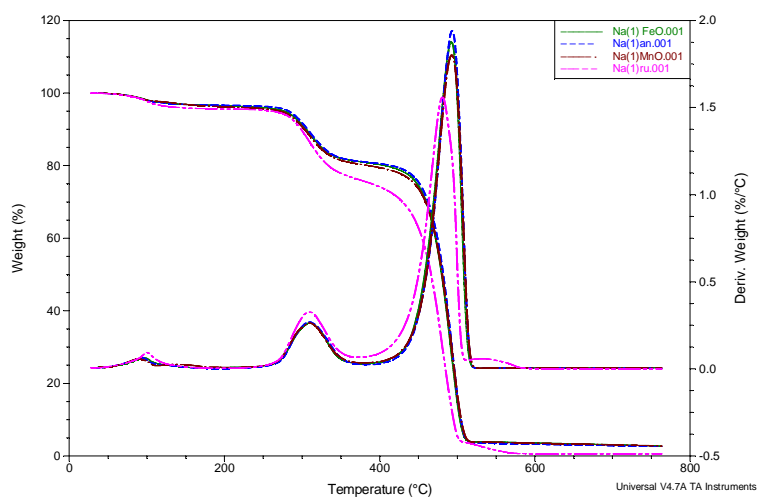


Figure 6.8B TGA thermograms of LDPE-starch-(EMA-Na)-1% metal oxide blends

Figure 6.8A and 6.8B show the thermograms of LDPE-starch-(EMA-Zn)-1% metal oxide and LDPE-starch-(EMA-Na)-1% metal oxide blends that display several decomposition regions. The first weight loss region (around 100 °C), can be assigned to the thermal decomposition of the low molecular weight compounds present in the blend. The second weight loss region (225 °C-350 °C) may be attributed to the thermal degradation of the most part

of the starch. The third weight loss region located between 420 °C and 525 °C is the main decomposition region assigned to the thermal decomposition of the backbone chains of pure polyethylenes. Thermogravimetric parameters of the blends are summarized in Tables 6.17 and 6.18. The results show that addition of metal oxides decrease the thermal stability of LDPE-starch-ionomer blends.

Table 6.18 Results of thermogravimetric analysis of LDPE-starch-(EMA-Na)-1% metal oxide blends

Sample	Temperature of onset of degradation (°C)	T _{max} (°C)	Rate of maximum degradation (%/°C)	Residual weight (%)
LDS-Na	430.41	492.37	2.079	1.870
LDS-Na(1)Fe	423.23	491.78	1.878	2.747
LDS-Na(1)Mn	420.50	492.14	1.802	2.773
LDS-Na(1)Ru	411.48	480.41	1.558	0.5767
LDS-Na(1)An	422.82	492.75	1.940	2.577

6.2.10 Differential scanning calorimetry (DSC)

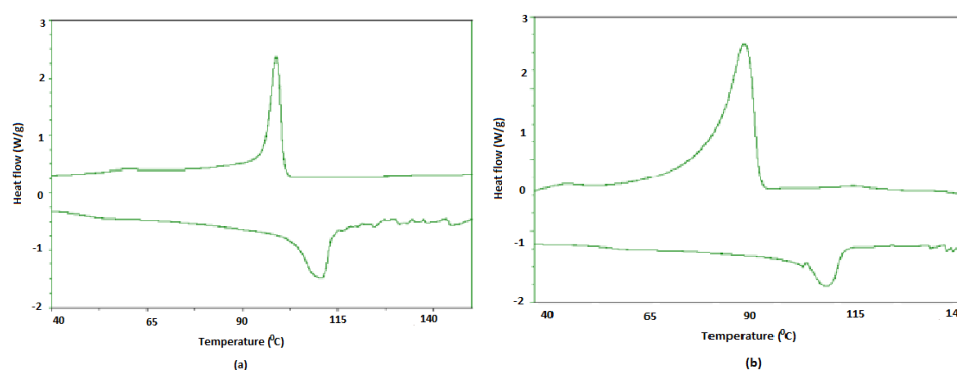
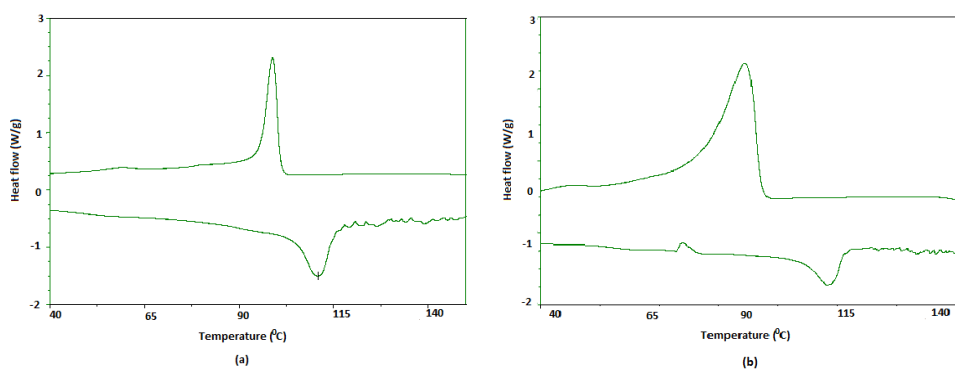


Figure 6.9A DSC curves of LDPE-starch-(EMA- Zn)-1% ferric oxide blend: a) before biodegradation and b) after biodegradation

Table 6.19 Results of DSC analysis of LDPE-starch-(EMA-Zn)-1% ferric oxide blend

Sample	T _m (°C)	ΔH _f (J/g)	T _c (°C)	ΔH _c (J/g)	% crystallinity
LDPE	110.00	67.00	96.00	79.00	23.4
LDS-Zn(1)Fe	110.50	49.83	98.82	54.55	17.4
LDS-Zn(1)Fe(ab)	110.91	24.14	93.51	53.89	8.4

Tables 6.19 and 6.20 and figures 6.9A and 6.9B show the thermal behaviour of LDPE-starch- ionomer-ferric oxide (74/20/5/1) blends before and after biodegradation. The results indicate that the incorporation of ferric oxide did not significantly alter the melting temperature (T_m) of pure LDPE. Incorporation of ferric oxide reduces the crystallinity of LDPE in LDPE-starch-(EMA-Zn)-ferric oxide blend. This reduction might have enhanced the biodegradation of the samples through the presence of an amorphous phase. The reduction in the crystallinity after biodegradation for two months could be attributed to the initial changes associated with degradation occurring in the amorphous phase of the polymer [19-20].



**Figure 6.9B DSC curves of LDPE-starch-(EMA-Na)-1% ferric oxide blend:
a) before biodegradation and b) after biodegradation**

Table 6.20 Results of DSC analysis of LDPE-starch-(EMA-Na)-1% ferric oxide blend

Sample	T _m (°C)	ΔH _f (J/g)	T _c (°C)	ΔH _c (J/g)	% crystallinity
LDPE	110	67	96	79	23.4
LDS-Na(1)Fe	110.86	51.41	98.83	57.26	17.9
LDS-Na(1)Fe(ab)	110.57	46.08	93.01	58.31	16.1

6.2.11 Morphological studies

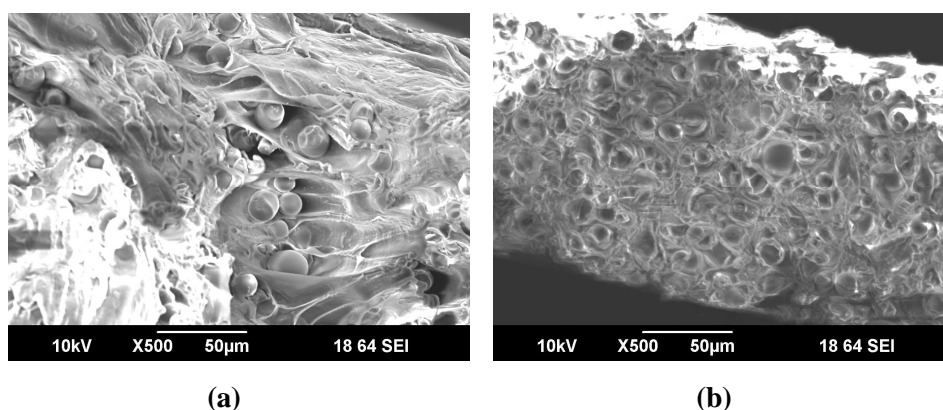


Figure 6.10A Scanning electron micrographs of LDPE-starch-(EMA-Zn) blend containing 1% Fe₂O₃ as pro-oxidant:
(a) before biodegradation and (b) after biodegradation for two months

Scanning electron micrographs of fractured surfaces of LDPE-starch-(EMA-Zn) blend containing 1% ferric oxide before and after they have been subjected to biodegradation in culture medium for two months are shown in figure 6.10A. After two months of biodegradation a number of small cavities are visible on the LDPE-starch-(EMA-Zn)-ferric oxide blend which indicates the removal of starch by microorganisms. But the number of cavities are less in ferric oxide incorporated blend as compared to the film prepared from LDPE-starch blend (chapter III, figure 3.20 (b)). This is because of the presence of compatibilizer and indicates that the interfacial adhesion of blend samples containing ionomer is appreciably improved.

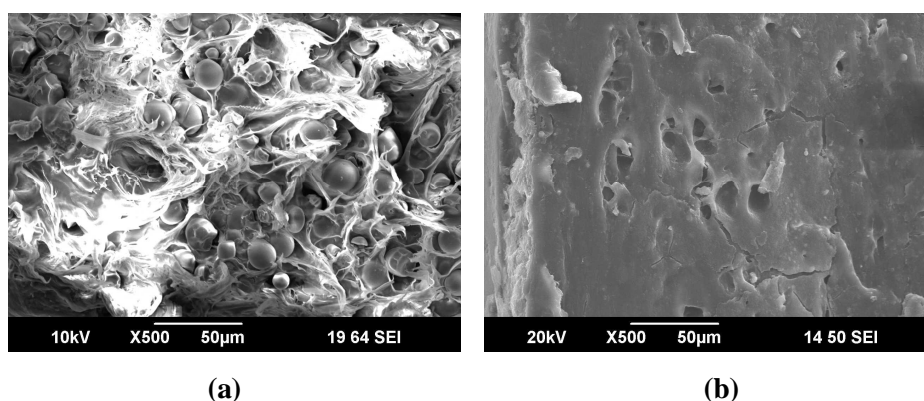


Figure 6.10B Scanning electron micrographs of LDPE-starch-(EMA-Na) (75/20/5) blend containing 1% Fe_2O_3 as pro-oxidant: (a) before biodegradation and (b) after biodegradation for two months

Figure 6.10B shows the SEM micrographs of fractured surfaces of LDPE-starch-(EMA-Na) (75/20/5) blend containing 1% ferric oxide before and after biodegradation for two months. After biodegradation cracks and pits are clearly visible on the surface of the films which indicate surface deterioration.

6.3 Conclusions

Incorporation of small quantities of metal oxides (ferric oxide, manganese dioxide, titanium dioxide (rutile and anatase grades)) in ionomer compatibilized LDPE-starch blends results in marginal changes in the mechanical properties of LDPE. The change in the melt flow index of LDPE was marginal on incorporation of small quantities of titanium dioxide (rutile and anatase grades). However the incorporation of small quantities of ferric oxide and manganese dioxide results in increase in melt flow index of LDPE. There was significant reduction in the tensile strength of all the samples after immersion in culture medium indicating biodegradation of the blends by microorganisms which is also confirmed

from IR spectroscopy. The presence of small quantities of metal oxides induces degradation of LDPE-starch-ionomer blends on exposure to UV radiation. All the samples exhibited a significant reduction in tensile strength and weight after photobiodegradation. Addition of the metal oxides enhanced the rate of degradation in the order $\text{FeO} > \text{MnO} > \text{Ru} > \text{An}$. For all the samples, the addition of small quantities of metal oxides increased the storage modulus, indicating the stiffening. Addition of small quantities of the metal oxides reduces the thermal stability and crystallinity of LDPE. SEM micrographs confirm the biodegradation of the pro-oxidant incorporated blend samples.

References

- [1] Ammala, A.; Bateman, S.; Dean, K.; Petinakis, S.; Sangwan, P.; Wong, S.; Yuan, Q.; Yu, L.; Prog Polym Sci 2010, doi:10.1016/j.progpolymsci. 2010. 12.002.
- [2] Ammala, A.; Hill, A. J.; Meakin, P.; Pas, S. J.; Turney, T. W.; J Nanopart Res 2002, 4, 167.
- [3] Hill, A. J.; Turney, T.; Ammala, A.; PMSE, 2003, 89, 719.
- [4] Rabek, J. F.; editor. Polymer Photodegradation, Chapman & Hall, London, 1995.
- [5] Chiellini, E.; Corti, A.; Swift, G.; Polym Degrad Stab 2003, 81, 341.
- [6] Albertson, A. C.; Andersson, S. O.; Karlsson, S.; Polym Degrad Stab 1987, 18, 73.
- [7] Vasile, C.; Degradation and decomposition, in: Vasile, C.; Seymour, R. B. (Eds.) Handbook of polyolefins synthesis and properties, Marcel Dekker Inc, New York, 1993, pp. 479-506.
- [8] Jakubowicz, I.; Polym Degrad Stab 2003, 80, 39.
- [9] Osawa, Z.; Kurisu, N.; Nagashima, K.; Nankano, K.; J Appl Polym Sci 1979, 23, 3583.

- [10] Roy, P. K.; Surekha, P.; Rajagopal, C.; Choudhary, V.; Polym Degrad Stab 2006, 91, 8.
- [11] Roy, P. K.; Titus, S.; Surekha, P.; Tulsi, E.; Deshmukh, C.; Rajagopal, C.; Polym Degrad Stab 2008, 93, 22.
- [12] Qin, H.; Zhao, C.; Zhang, S.; Chen, G.; Yang, M.; Polym Degrad Stab 2003, 81, 497.
- [13] Zhao, X.; Li, Z.; Chen, Y.; Shi, L.; Zhu, Y.; J Mole Cata A: Chem 2007, 268, 101.
- [14] Osman, M. A.; Atallah, U.; Suter, U. W.; Polymer 2004, 45, 1177.
- [15] Rosa, D. S.; Grillo, D.; Bardi, M. A. G.; Calil, M. R.; Guedes, C. G. F.; Ramires, E. C.; Frollini, E.; Polym Test 2009, 28, 836.
- [16] Roy, P. K.; Surekha, P.; Raman, R.; Rajagopal, C.; Polym Degrad Stabil 2009, 94, 1033.
- [17] Coelho, N. S.; Almeida, Y. M. B.; Vinhas, G. M.; Polimeros Cienc Technol 2008, 18, 270.
- [18] Pedroso, A. G.; Rosa, D. S.; Polym Adv Technol 2005, 16, 310.
- [19] Albertson, A. C.; Karlsson, S.; Prog in Polym Sci 1990, 15, 177.
- [20] Rosa, D. S.; Grillo, D.; Bardi, M. A. G.; Calil, M. R.; Guedes, C. G. F.; Ramires, E. C.; Frollini, E.; Polym Test 2009, 28, 836.



EFFECT OF METAL STEARATES AS PRO-OXIDANTS ON IONOMER COMPATIBILIZED LOW DENSITY POLYETHYLENE-STARCH BLENDS

Contents	7.1	<i>Introduction</i>
	7.2	<i>Results and discussion</i>
	7.3	<i>Conclusions</i>

Various compositions (0.5 and 1 weight %) of the metal stearates (ferric stearate, manganese stearate, cupric stearate, magnesium stearate and zinc stearate) were incorporated into EMA-Zn (5%) and EMA-Na (5%) compatibilized low density polyethylene-starch blends. The role of small quantities of the metal stearates as pro-oxidants in the blends were evaluated by measuring mechanical properties, melt flow indices, biodegradability, photodegradability, photobiodegradability, water absorption, infrared spectroscopy, dynamic mechanical analysis, thermogravimetry, differential scanning calorimetry and scanning electron microscopy. The blends show changes in mechanical properties with the addition of metal stearates. Thermal characterization using TGA and DSC shows changes in thermal stability and crystallinity with the incorporation of metal stearates. The results of the studies show that the addition of metal stearates enhances the biodegradability, photodegradability and photobiodegradability of the blends.

7.1 Introduction

Among the many approaches used to induce degradation in polyethylene, photodegradation by the incorporation of pro-oxidants has been gaining more popularity recently. Polyolefins generally show very low degree of degradation when exposed to sunlight [1]. Photodegradation is one of the most efficient abiotic degradation processes occurring in the open environment. In this process the polymers undergo degradation from the action of sunlight on exposure of the polymer in the outdoor [2-4]. Pro-oxidants are transition metal ion complexes, which catalyze the oxidation of polyethylene and lead to its molecular weight reduction. The pro-oxidants facilitate biodegradation too [5-7]. Common pro-oxidants presently being used for the preparation of oxo-degradable films are oxides and stearates of transition metals, particularly iron and manganese [8-13].

This chapter presents an attempt to understand the effect of metal stearates namely ferric stearate, manganese stearate, cupric stearate, magnesium stearate and zinc stearate on the degradation behaviour of ionomer compatibilized low density polyethylene-starch blends. Designations of the samples used in this chapter and their descriptions are given in Table 7.1. The studies include the evaluation of mechanical properties, melt flow indices, biodegradability, photodegradability, photobiodegradability, water absorption, infrared spectroscopy, dynamic mechanical analysis, thermogravimetry, differential scanning calorimetry and scanning electron microscopy.

Table 7.1 Description of sample designations

Sample designation	Description
LDS-Zn	LDPE-20% starch-5% (EMA-Zn)
LDS-Zn-Fe	LDPE-20% starch-5% (EMA-Zn)- ferric stearate
LDS-Zn-Mn	LDPE-20% starch-5% (EMA-Zn)- manganese stearate
LDS-Zn-Cu	LDPE-20% starch-5% (EMA-Zn)- cupric stearate
LDS-Zn-Mg	LDPE-20% starch-5% (EMA-Zn)- magnesium stearate
LDS-Zn-Zn	LDPE-20% starch-5% (EMA-Zn)- zinc stearate
LDS-Na	LDPE-20% starch-5% (EMA-Na)
LDS-Na-Fe	LDPE-20% starch-5% (EMA-Na)- ferric stearate
LDS-Na-Mn	LDPE-20% starch-5% (EMA-Na)- manganese stearate
LDS-Na-Cu	LDPE-20% starch-5% (EMA-Na)- cupric stearate
LDS-Na-Mg	LDPE-20% starch-5% (EMA-Na)- magnesium stearate
LDS-Na-Zn	LDPE-20% starch-5% (EMA-Na)- zinc stearate

7.2 Results and discussion

7.2.1 Mechanical properties

The tensile strength, elongation at break and elastic modulus of neat LDPE, LDPE-starch-(EMA-Zn) blend, LDPE-starch-(EMA-Na) blend and the blends containing the metal stearates as pro-oxidants are shown in figures 7.1A and 7.1B. In the case of LDPE-starch-(EMA-Zn) blends containing metal stearates, the blend containing ferric stearate shows marginal improvement in tensile strength as compared to LDPE-starch-(EMA-Zn) blend. In the case of the compositions containing the other metal stearates (figure 7.1A(a)) the tensile strength was almost similar to that of LDPE-starch-(EMA-Zn). In LDPE-starch-(EMA-Na) blends, the samples with ferric stearate and magnesium stearate show an improvement in tensile strength whereas the samples with other metal stearates show a reduction in the tensile strength.

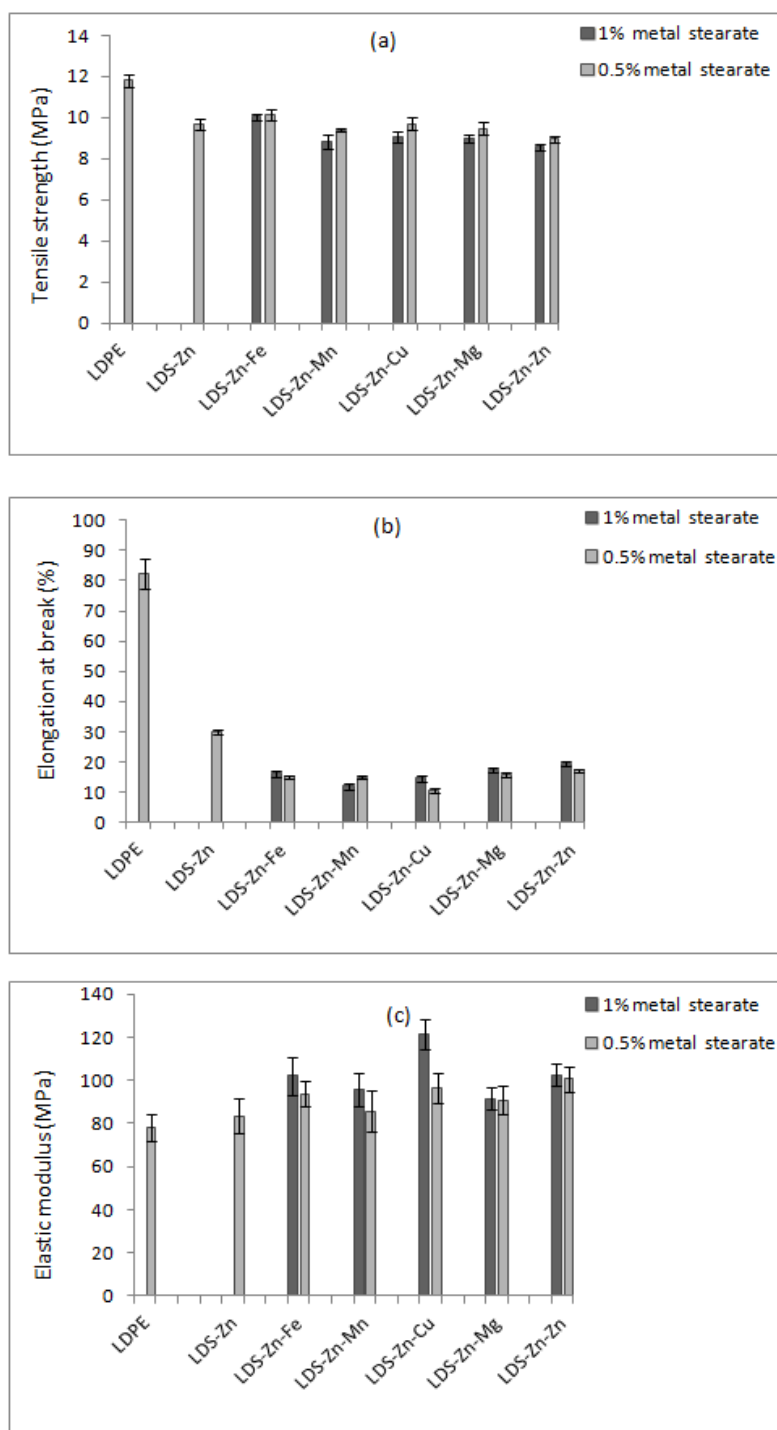


Figure 7.1A Effect of metal stearates on the mechanical properties of LDPE-starch-(EMA-Zn) blends

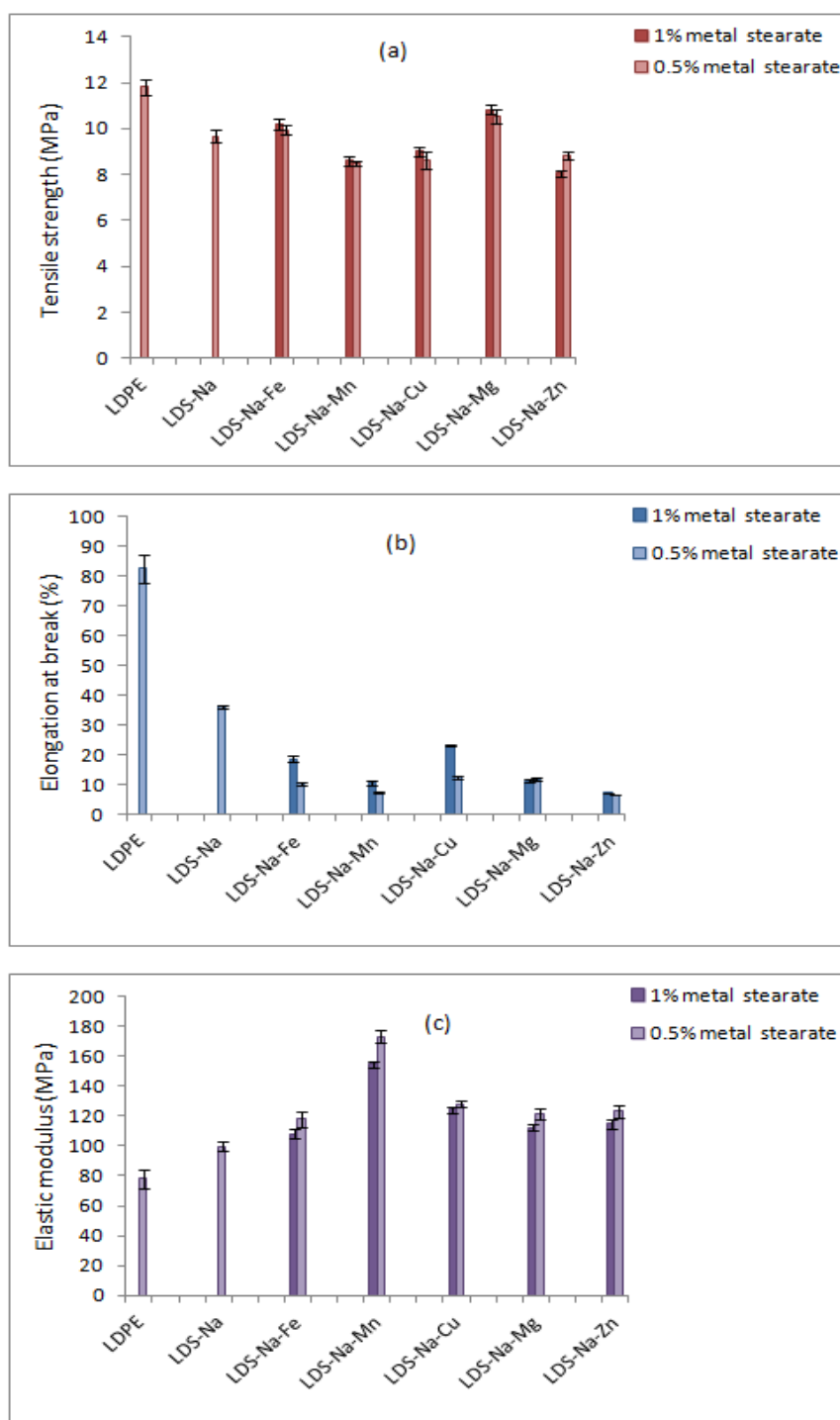


Figure 7.1B Effect of metal stearates on the mechanical properties of LDPE-starch-(EMA-Na) blends

Figures 7.1A(b) and 7.1B(b) show that there was a reduction in the elongation at break with the incorporation of metal stearates as compared to the base material (LDPE-starch-ionomer blends). Figures 7.1A(c) and 7.1B(c) show that elastic modulus of the blends containing metal stearates increased, with the values for all blends being greater than the value for LDPE-starch-ionomer blend. This is a reflection of the presence of rigid materials and the degree of compatibility [13].

7.2.2 Melt flow measurements

The melt flow index (MFI) of a polymer is related to its molecular weight distribution and is often used to characterize the processability [14]. Figure 7.2A shows the effect of metal stearates on the melt flow indices of LDPE-starch-(EMA-Zn) blends. The MFI of all the samples increased as compared to the MFI value of neat LDPE, which is an indication of chain scission in presence of metal stearates, at high temperature. The results show that LDPE-starch-(EMA-Zn) blends containing metal stearates are more susceptible to degradation.

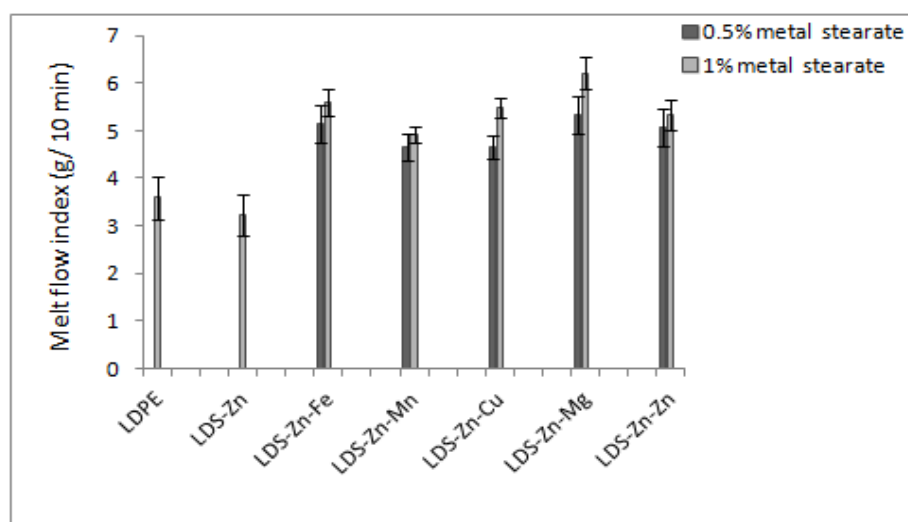


Figure 7.2A Effect of metal stearates on the melt flow indices of LDPE-starch-(EMA-Zn) blends

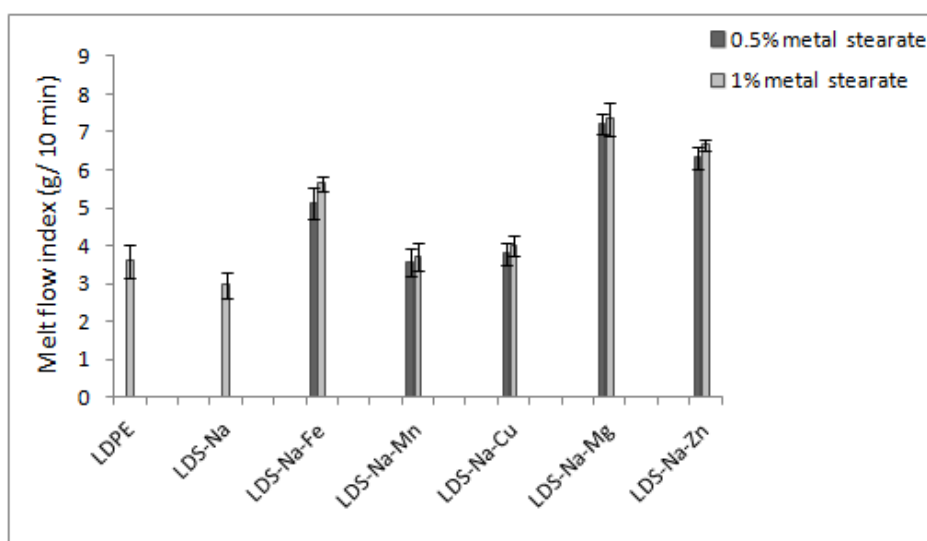


Figure 7.2B Effect of metal stearates on the melt flow indices of LDPE-starch-(EMA-Na) blends

Figure 7.2B shows the effect of metal stearates on the melt flow indices of LDPE-starch-(EMA-Na) blends. All the samples show an increase in MFI value as compared to LDPE-starch-(EMA-Na) blend. Among the samples containing the pro-oxidants studied the samples with magnesium stearate, ferric stearate and zinc stearate shows significant improvement in MFI which is an indication of massive chain scission.

7.2.3 Biodegradation studies

Figures 7.3A and 7.3B show the tensile properties of LDPE-starch-(EMA-Zn)-metal stearate blends and LDPE-starch-(EMA-Na)-metal stearate blends after biodegradation in culture medium for two months. Tables 7.2 and 7.3 show the percentage decrease in tensile strength of LDPE-starch-(EMA-Zn)-metal stearate blends and LDPE-starch-(EMA-Na)-metal stearate blends respectively. There is significant reduction in tensile strength after biodegradation for all the blends.

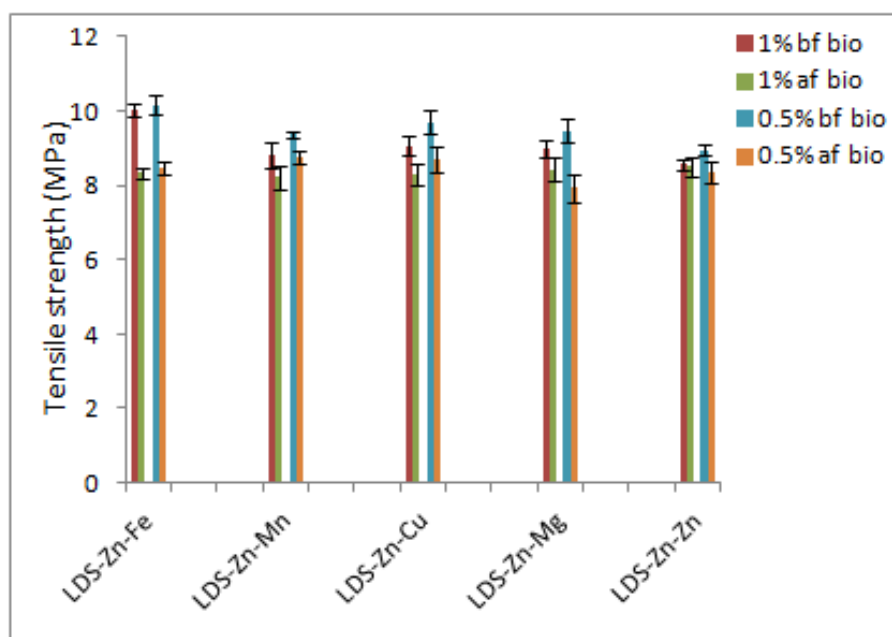


Figure 7.3A Biodegradation of LDPE-starch-(EMA-Zn)-metal stearate blends after biodegradation in culture medium for two months (Evident from tensile strength)

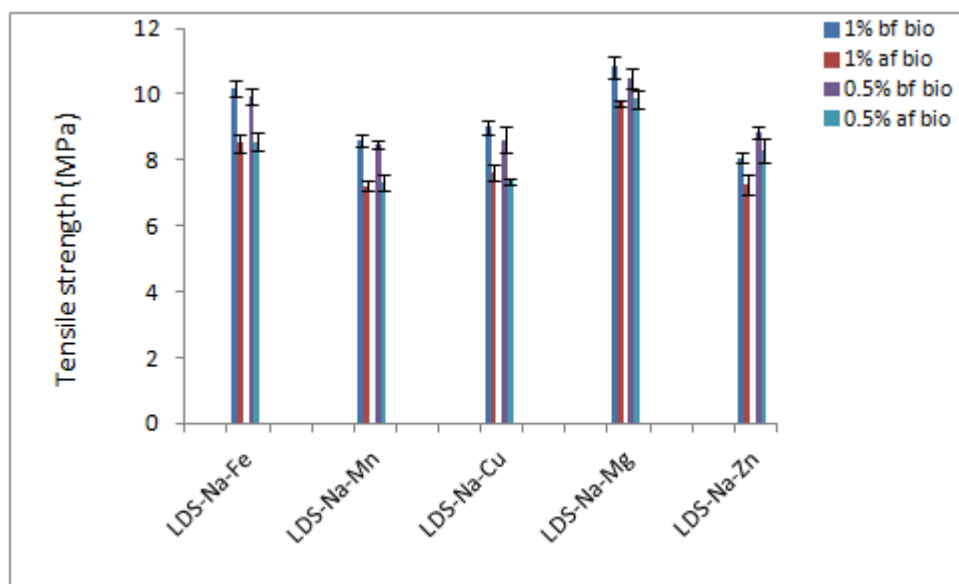


Figure 7.3B Biodegradation of LDPE-starch-(EMA-Na)-metal stearate blends after biodegradation in culture medium for two months (Evident from tensile strength)

Table 7.2 Percentage decrease in tensile strength of LDPE-starch-(EMA-Zn)-metal stearate blends after biodegradation in culture medium for two months

Sample	Initial tensile strength (MPa)	Tensile strength after biodegradation for two months (MPa)	% decrease in tensile strength
LDS-Zn(1)Fe*	10.1 ± 0.17	8.33 ± 0.15	17.53
LDS-Zn((0.5))Fe	10.2 ± 0.26	8.46 ± 0.18	17.06
LDS-Zn(1)Mn	8.90 ± 0.35	7.62 ± 0.31	14.38
LDS-Zn(0.5)Mn	9.38 ± 0.08	8.26 ± 0.16	11.94
LDS-Zn(1)Cu	9.06 ± 0.26	7.68 ± 0.30	15.28
LDS-Zn(0.5)Cu	9.71 ± 0.31	8.51 ± 0.33	12.36
LDS-Zn(1)Mg	8.98 ± 0.23	8.12 ± 0.32	9.58
LDS-Zn(0.5)Mg	9.48 ± 0.31	8.73 ± 0.35	7.91
LDS-Zn(1)Zn	8.56 ± 0.15	7.96 ± 0.22	7.01
LDS-Zn(0.5)Zn	8.96 ± 0.16	8.370 ± 0.28	6.59

* Number given in paranthesis denotes the weight percentage of metal oxides in the blend

Table 7.3 Percentage decrease in tensile strength of LDPE-starch-(EMA-Na)-metal stearate blends after biodegradation in culture medium for two months

Sample	Initial tensile strength (MPa)	Tensile strength after biodegradation for two months (MPa)	% decrease in tensile strength
LDS-Na(1)Fe	10.2 ± 0.24	8.53 ± 0.27	16.19
LDS-Na((0.5))Fe	9.94 ± 0.22	8.56 ± 0.28	13.90
LDS-Na(1)Mn	8.60 ± 0.20	7.21 ± 0.15	16.10
LDS-Na(0.5)Mn	9.09 ± 0.12	7.31 ± 0.23	13.79
LDS-Na(1)Cu	9.00 ± 0.21	7.64 ± 0.26	15.16
LDS-Na(0.5)Cu	8.63 ± 0.38	7.38 ± 0.09	14.49
LDS-Na(1)Mg	10.8 ± 0.35	9.73 ± 0.10	10.18
LDS-Na(0.5)Mg	10.5 ± 0.31	9.85 ± 0.30	6.26
LDS-Na(1)Zn	8.06 ± 0.15	7.25 ± 0.32	10.09
LDS-Na(0.5)Zn	8.84 ± 0.16	8.31 ± 0.37	5.97

The reason for the reduction is the starch consumption by microorganisms. These changes are reflected in the tensile properties of the

blend films which suggest that the blends are partially biodegradable. The percentage weight loss of the blends after biodegradation in culture medium is summarized in Tables.7.4 and 7.5. All the samples exhibited a significant weight loss after degradation in culture medium which indicates that the LDPE-starch-ionomer blends containing metal stearates are partially biodegradable.

Table 7.4 Percentage decrease in weight of LDPE-starch-(EMA-Zn)-metal stearate blends after biodegradation in culture medium for two months

Sample	Initial weight (g)	Weight after two months (g)	% weight loss
LDS-Zn(1)Fe	0.3905	0.3749	4.01
LDS-Zn((0.5))Fe	0.4808	0.4683	2.60
LDS-Zn(1)Mn	0.5420	0.5265	2.87
LDS-Zn(0.5)Mn	0.6531	0.6359	2.64
LDS-Zn(1)Cu	0.6057	0.5948	1.79
LDS-Zn(0.5)Cu	0.4397	0.4314	1.88
LDS-Zn(1)Mg	0.4950	0.4813	2.76
LDS-Zn(0.5)Mg	0.4834	0.4684	3.10
LDS-Zn(1)Zn	0.7460	0.7274	2.49
LDS-Zn(0.5)Zn	0.5202	0.5050	2.92

Table 7.5 Percentage decrease in weight of LDPE-starch-(EMA-Na)-metal stearate blends after biodegradation in culture medium for two months

Sample	Initial weight (g)	Weight after two months (g)	% weight loss
LDS-Na(1)Fe	0.4166	0.4039	3.05
LDS-Na((0.5))Fe	0.4808	0.4683	2.60
LDS-Na(1)Mn	0.6725	0.6497	3.39
LDS-Na(0.5)Mn	0.6265	0.5819	7.31
LDS-Na(1)Cu	0.5970	0.5820	2.51
LDS-Na(0.5)Cu	0.5360	0.5231	2.40
LDS-Na(1)Mg	0.6553	0.6359	2.98
LDS-Na(0.5)Mg	0.6931	0.6734	2.84
LDS-Na(1)Zn	0.4932	0.4799	2.70
LDS-Na(0.5)Zn	0.6545	0.6997	2.26

7.2.4 Photodegradation studies

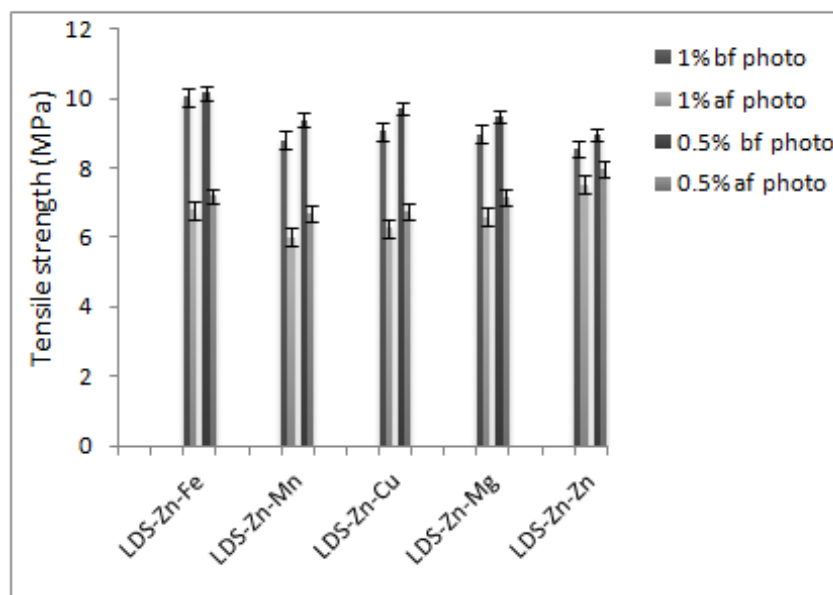


Figure 7.4A Photodegradation of LDPE-starch-(EMA-Zn)-metal stearate blends after UV exposure for one month (Evident from tensile strength)

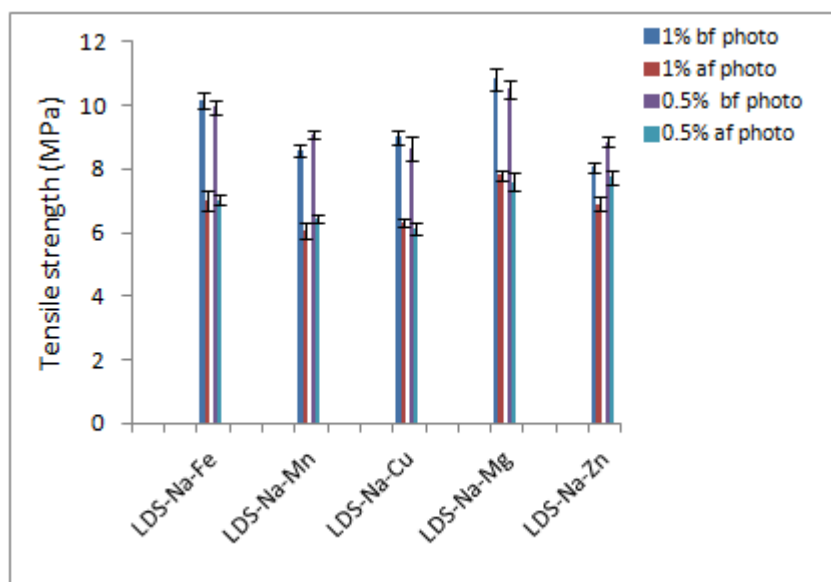


Figure 7.4B Photodegradation of LDPE-starch-(EMA-Na)-metal stearate blends after UV exposure for one month (Evident from tensile strength)

Table 7.6 Percentage decrease in tensile strength of LDPE-starch-(EMA-Zn)-metal stearate blends after UV exposure for one month

Sample	Initial tensile strength (MPa)	Tensile strength after UV exposure for one month (MPa)	% decrease in tensile strength
LDS-Zn(1)Fe	10.1 \pm 0.17	6.78 \pm 0.25	32.47
LDS-Zn((0.5))Fe	10.2 \pm 0.26	7.19 \pm 0.30	29.50
LDS-Zn(1)Mn	8.81 \pm 0.35	6.02 \pm 0.23	31.67
LDS-Zn(0.5)Mn	9.38 \pm 0.08	6.68 \pm 0.28	28.79
LDS-Zn(1)Cu	9.06 \pm 0.26	6.26 \pm 0.19	30.91
LDS-Zn(0.5)Cu	9.71 \pm 0.31	6.76 \pm 0.28	30.38
LDS-Zn(1)Mg	8.98 \pm 0.23	6.59 \pm 0.12	26.62
LDS-Zn(0.5)Mg	9.48 \pm 0.31	7.17 \pm 0.15	24.37
LDS-Zn(1)Zn	8.56 \pm 0.15	7.52 \pm 0.24	12.15
LDS-Zn(0.5)Zn	8.96 \pm 0.16	7.96 \pm 0.23	11.15

Table 7.7 Percentage decrease in tensile strength of LDPE-starch-(EMA-Na)-metal stearate blends after UV exposure for one month

Sample	Initial tensile strength (MPa)	Tensile strength after UV exposure for one month (MPa)	% decrease in tensile strength
LDS-Na(1)Fe	10.2 \pm 0.24	7.01 \pm 0.32	31.11
LDS-Na((0.5))Fe	9.94 \pm 0.22	7.02 \pm 0.15	29.38
LDS-Na(1)Mn	8.60 \pm 0.20	6.08 \pm 0.26	29.25
LDS-Na(0.5)Mn	9.09 \pm 0.12	6.45 \pm 0.11	29.05
LDS-Na(1)Cu	9.00 \pm 0.21	6.31 \pm 0.13	29.90
LDS-Na(0.5)Cu	8.63 \pm 0.38	6.12 \pm 0.17	29.04
LDS-Na(1)Mg	10.8 \pm 0.35	7.82 \pm 0.16	27.81
LDS-Na(0.5)Mg	10.5 \pm 0.31	7.59 \pm 0.28	27.77
LDS-Na(1)Zn	8.06 \pm 0.15	6.91 \pm 0.24	14.27
LDS-Na(0.5)Zn	8.84 \pm 0.16	7.75 \pm 0.23	12.34

Figures 7.4A and 7.4B show the tensile properties of LDPE-starch-(EMA-Zn)-metal stearate blends and LDPE-starch-(EMA-Na)-metal stearate blends after UV exposure for one month. Tables 7.6 and 7.7 show the

percentage decrease in tensile strength of LDPE-starch-(EMA-Zn)-metal stearate blends and LDPE-starch-(EMA-Na)-metal stearate blends

Table 7.8 Percentage decrease in weight of LDPE-starch-(EMA-Zn)-metal stearate blends after UV exposure for one month

Sample	Initial weight (g)	Weight after one month (g)	% weight loss
LDS-Zn(1)Fe	0.5867	0.5826	0.699
LDS-Zn((0.5))Fe	0.8243	0.8217	0.315
LDS-Zn(1)Mn	0.5060	0.5013	0.929
LDS-Zn(0.5)Mn	0.5933	0.5910	0.388
LDS-Zn(1)Cu	0.5601	0.5592	0.161
LDS-Zn(0.5)Cu	0.5706	0.5700	0.105
LDS-Zn(1)Mg	0.4819	0.4804	0.311
LDS-Zn(0.5)Mg	0.5873	0.5872	0.017
LDS-Zn(1)Zn	0.6251	0.6231	0.320
LDS-Zn(0.5)Zn	0.7764	0.7744	0.258

Table 7.9 Percentage decrease in weight of LDPE-starch-(EMA-Na)-metal stearate blends after UV exposure for one month

Sample	Initial weight (g)	Weight after one month (g)	% weight loss
LDS-Na(1)Fe	0.5308	0.5302	0.113
LDS-Na((0.5))Fe	0.4437	0.4435	0.045
LDS-Na(1)Mn	0.4942	0.4934	0.162
LDS-Na(0.5)Mn	0.6044	0.6043	0.017
LDS-Na(1)Cu	0.4659	0.4640	0.408
LDS-Na(0.5)Cu	0.4955	0.4937	0.363
LDS-Na(1)Mg	0.6469	0.6466	0.046
LDS-Na(0.5)Mg	0.7792	0.7790	0.026

LDS-Na(1)Zn	0.5886	0.5877	0.153
LDS-Na(0.5)Zn	0.6660	0.6659	0.015

respectively. There is significant reduction in tensile strength after one month of exposure to UV radiation. The change in chemical structure of the blend, after exposure to ultraviolet radiation, results in the formation of new groups in the polymer chain, mainly in the amorphous region of material, and this may be one of the reasons for the decrease in tensile strength [15]. Tables 7.8 and 7.9 show the % weight loss for LDPE-starch-ionomer-metal stearate blends after UV exposure for one month. It was observed that all the samples show a slight decrease in weight after photodegradation and the weight loss is found to increase with increase in concentration of metal stearates.

7.2.5 Photobiodegradation studies

Figures 7.5A and 7.5B show the tensile properties of LDPE-starch-(EMA-Zn)-metal stearate blends and LDPE-starch-(EMA-Na)-metal stearate blends after photobiodegradation studies. Photobiodegradation was investigated by exposure of the samples to UV radiation for one month followed by the immersion of the photodegraded samples in culture medium containing amylase producing *Vibrios*, which were isolated from marine benthic environment, again for one month. Tables 7.10 and 7.11 show the percentage decrease in tensile strength of LDPE-starch-(EMA-Zn)-metal stearate blends and LDPE-starch-(EMA-Na)-metal stearate blends respectively. There is significant reduction in tensile strength after two months of photobiodegradation. This is because of the photo-oxidation of polyethylene-starch blend containing pro-oxidants which leads to an

increase in the low molecular weight fraction by chain scission, thereby facilitating biodegradation [4].

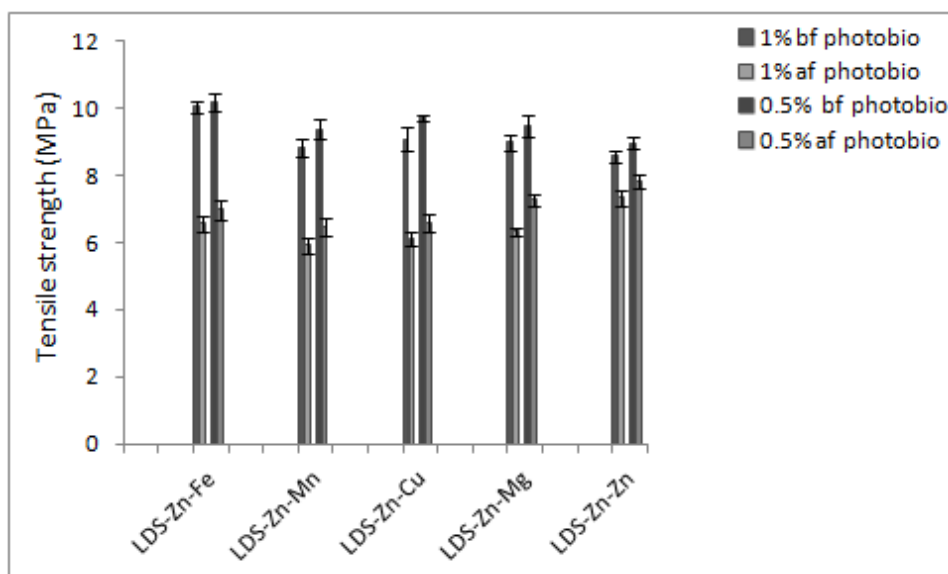


Figure 7.5A Variation in tensile strength of LDPE-starch-(EMA-Zn)-metal stearate blends after UV exposure for one month followed by biodegradation in culture medium for one month

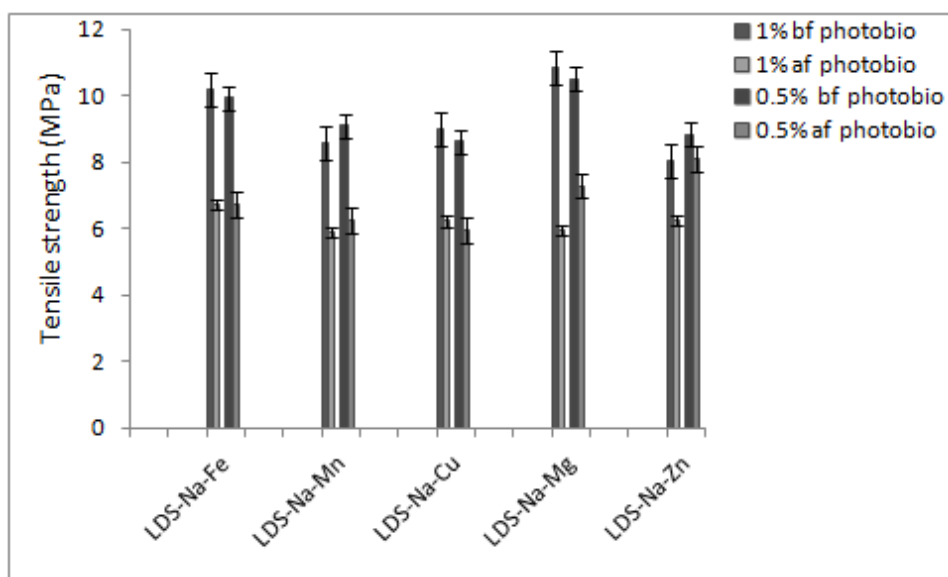


Figure 7.5B Variation in tensile strength of LDPE-starch-(EMA-Na)-metal stearate blends after UV exposure for one month followed by biodegradation in culture medium for one month

Table 7.10 Percentage decrease in tensile strength of LDPE-starch-(EMA-Zn)-metal stearate blends after UV exposure for one month followed by biodegradation in culture medium for one month

Sample	Initial tensile strength (MPa)	Tensile strength after photobiodegradation for two months (MPa)	% decrease in tensile strength
LDS-Zn(1)Fe	10.1 ± 0.17	6.56 ± 0.25	35.04
LDS-Zn((0.5))Fe	10.2 ± 0.26	6.98 ± 0.30	31.53
LDS-Zn(1)Mn	8.90 ± 0.35	5.91 ± 0.23	32.88
LDSs-Zn(0.5)Mn	9.38 ± 0.08	6.45 ± 0.28	31.20
LDS-Zn(1)Cu	9.06 ± 0.26	6.10 ± 0.19	32.65
LDS-Zn(0.5)Cu	9.71 ± 0.31	6.59 ± 0.28	32.10
LDS-Zn(1)Mg	8.98 ± 0.23	6.34 ± 0.12	29.40
LDS-Zn(0.5)Mg	9.48 ± 0.31	7.26 ± 0.15	23.41
LDS-Zn(1)Zn	8.56 ± 0.15	7.33 ± 0.24	14.43
LDS-Zn(0.5)Zn	8.96 ± 0.16	7.82 ± 0.23	12.78

Table 7.11 Percentage decrease in tensile strength of LDPE-starch-(EMA-Na)-metal stearate blends after UV exposure for one month followed by biodegradation in culture medium for one month

Sample	Initial tensile	Tensile strength after	% decrease
--------	-----------------	------------------------	------------

	strength (MPa)	photobiodegradation for two months (MPa)	in tensile strength
LDS-Na(1)Fe	10.2 ± 0.24	6.75 ± 0.12	33.65
LDS-Na((0.5))Fe	9.94 ± 0.22	6.75 ± 0.23	32.09
LDS-Na(1)Mn	8.60 ± 0.20	5.88 ± 0.11	31.58
LDS-Na(0.5)Mn	9.09 ± 0.12	6.25 ± 0.20	31.25
LDS-Na(1)Cu	9.00 ± 0.21	6.22 ± 0.11	30.90
LDS-Na(0.5)Cu	8.63 ± 0.38	5.94 ± 0.22	31.13
LDS-Na(1)Mg	10.8 ± 0.35	7.56 ± 0.13	30.21
LDS-Na(0.5)Mg	10.5 ± 0.31	7.29 ± 0.25	30.62
LDS-Na(1)Zn	8.06 ± 0.15	6.24 ± 0.12	22.58
LDS-Na(0.5)Zn	8.84 ± 0.16	8.09 ± 0.21	8.49

The percentage weight loss of the blends after biodegradation in culture medium is summarized in Tables.7.12 and 7.13. All the samples exhibited a significant weight loss after photobiodegradation. This is because of the microbial degradation of the oxidation products.

Table 7.12 Percentage decrease in weight of LDPE-starch-(EMA-Zn)-metal stearate blends after UV exposure for one month followed by biodegradation in culture medium for one month

Sample	Initial weight (g)	Weight after two months (g)	% weight loss
LDS-Zn(1)Fe	0.5867	0.5758	1.86
LDS-Zn((0.5))Fe	0.8243	0.8123	1.46
LDS-Zn(1)Mn	0.5060	0.4969	1.80
LDS-Zn(0.5)Mn	0.5933	0.5879	0.91
LDS-Zn(1)Cu	0.5601	0.5526	1.34
LDS-Zn(0.5)Cu	0.5706	0.5631	1.31
LDS-Zn(1)Mg	0.4819	0.4736	1.72
LDS-Zn(0.5)Mg	0.5873	0.5814	1.01
LDS-Zn(1)Zn	0.6251	0.6133	1.89
LDS-Zn(0.5)Zn	0.7764	0.7630	1.73

Table 7.13 Percentage decrease in weight of LDPE-starch-(EMA-Na)-metal stearate blends after UV exposure for one month followed by biodegradation in culture medium for one month

Sample	Initial weight (g)	Weight after two months (g)	% weight loss
LDS-Na(1)Fe	0.5308	0.5229	1.49
LDS-Na((0.5))Fe	0.4437	0.4380	1.29
LDS-Na(1)Mn	0.4942	0.4895	0.95
LDS-Na(0.5)Mn	0.6044	0.5990	0.89
LDS-Na(1)Cu	0.4659	0.4575	1.80
LDS-Na(0.5)Cu	0.4955	0.4901	1.09
LDS-Na(1)Mg	0.6469	0.6375	1.45
LDS-Na(0.5)Mg	0.7792	0.7685	1.37
LDS-Na(1)Zn	0.5886	0.5814	1.22
LDS-Na(0.5)Zn	0.6660	0.6589	1.07

7.2.6 Water absorption studies

The water absorption characteristics of LDPE-starch-ionomer-metal stearate blends are shown in Tables 7.14 and 7.15. The water absorption tendency decreases with increase in metal stearate concentration. This may be due to the filling up of the free volume of the polymer matrix by the metal stearate particles thus preventing the penetration of water molecules.

Table 7.14 Water absorption of LDPE-starch-(EMA-Zn)-metal stearate blends

Sample	Initial weight (g)	Weight after 24 hours (g)	% water absorption
LDS-Zn(1)Fe	0.2848	0.2888	1.41
LDS-Zn((0.5))Fe	0.3601	0.3652	1.42
LDS-Zn(1)Mn	0.3223	0.3262	1.21
LDS-Zn(0.5)Mn	0.2711	0.2747	1.33
LDS-Zn(1)Cu	0.3759	0.3798	1.04
LDS-Zn(0.5)Cu	0.4548	0.4604	1.23
LDS-Zn(1)Mg	0.3270	0.3304	1.04
LDS-Zn(0.5)Mg	0.3027	0.3062	1.16
LDS-Zn(1)Zn	0.5174	0.5218	0.85
LDS-Zn(0.5)Zn	0.3804	0.3837	0.87

Table 7.15 Water absorption of LDPE-starch-(EMA-Na)-metal stearate blends

Sample	Initial weight (g)	Weight after 24 hours (g)	% water absorption
LDS-Na(1)Fe	0.2868	0.2903	1.22
LDS-Na((0.5))Fe	0.3069	0.3107	1.24
LDS-Na(1)Mn	0.4183	0.4225	1.00
LDS-Na(0.5)Mn	0.3267	0.3304	1.13
LDS-Na(1)Cu	0.2937	0.2965	0.95
LDS-Na(0.5)Cu	0.3913	0.3953	1.02
LDS-Na(1)Mg	0.5254	0.5302	0.91
LDS-Na(0.5)Mg	0.3892	0.3929	0.95
LDS-Na(1)Zn	0.6878	0.6923	0.65
LDS-Na(0.5)Zn	0.4361	0.4397	0.83

7.2.7 FTIR spectroscopy

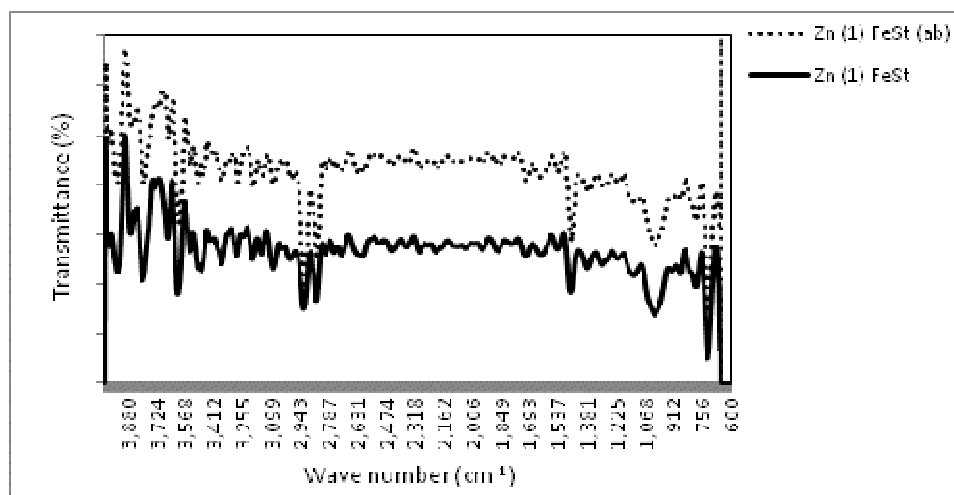


Figure 7.6A FTIR spectra of LDPE-starch-(EMA-Zn)- 1% ferric stearate blend: (—) before biodegradation and (...) after biodegradation (ab)

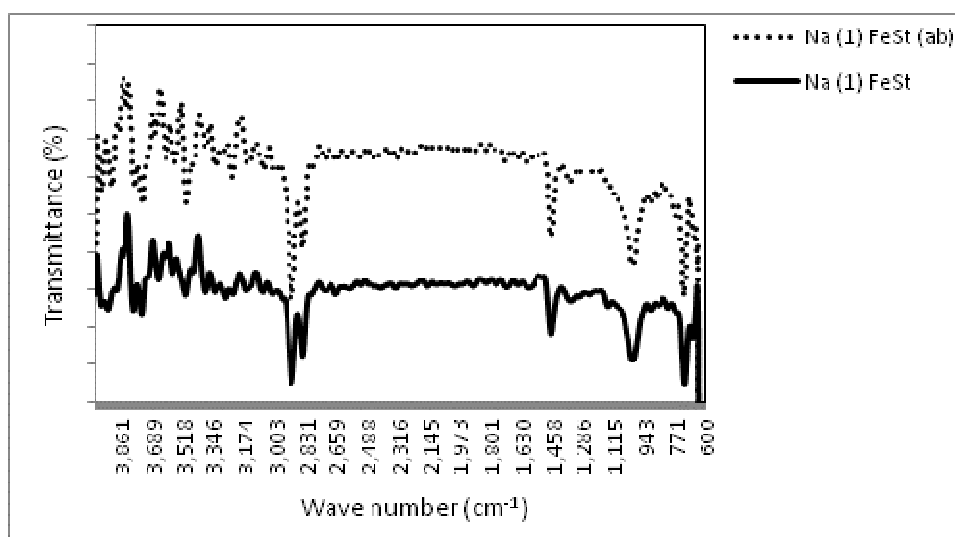


Figure 7.6B FTIR spectra of LDPE-starch-(EMA-Na)-1% ferric stearate blend:
(—) before biodegradation and (...) after biodegradation

Table 7.16 Characteristic FTIR spectral peaks

	Peak position (cm ⁻¹)	Characteristic group
LDPE-starch- (EMA-Zn)-1% ferric stearate	2915, 2847	C-H symmetric stretching
	1535	C=O stretching
	1463	CH ₂ scissor and asymmetric bending
	1373	C-H bending
	1006	O-C stretching
	912	O-H deformation
	717	CH ₂ rocking
LDPE-starch- (EMA-Na)-1% ferric stearate	2911, 2847	C-H symmetric stretching
	1590	C=O stretching
	1463	CH ₂ scissor and asymmetric bending
	1357	C-H bending
	1008	O-C stretching
	916	O-H deformation
	721	CH ₂ rocking

Figures 7.6A and 7.6B present the FTIR spectra of LDPE-starch-(EMA-Zn) and LDPE-starch-(EMA-Na) blends containing 1% ferric stearate. The spectra show characteristic absorption peaks which are reported in Table 7.16. The peaks in the region $3700\text{--}3200\text{ cm}^{-1}$ are attributed to O-H stretching vibrations of the water molecules. The doublet peaks observed in the range $2965\text{--}2800\text{ cm}^{-1}$ are due to C-H stretching [16]. The carboxylate asymmetric stretching vibration bands near 1540 cm^{-1} are typical for stearates. Peak intensities at $2921\text{--}2848\text{ cm}^{-1}$, $1473\text{--}1463\text{ cm}^{-1}$, $1156\text{--}1028\text{ cm}^{-1}$ and $730\text{--}720\text{ cm}^{-1}$ improved a little after biodegradation in culture medium for two months apparently due to the fracture of the polyethylene chain in degradable environments which resulted in an increase in the terminal group numbers. The peaks at $2921\text{--}2848\text{ cm}^{-1}$, $1473\text{--}1463\text{ cm}^{-1}$ and $730\text{--}720\text{ cm}^{-1}$ are due to symmetrical stretching vibration of C-H bonds, bending vibration of middle intensity C-H bonds and the characteristic absorption of the crystalline and amorphous bands. The peaks at 1028 and 1156 cm^{-1} are attributed to C-O-C bond stretching of starch, and the peak near 1019 cm^{-1} is the characteristic peak of the anhydroglucose ring O-C stretch. Presence of notable differences after biodegradation in these regions indicates biodegradation of ferric stearate incorporated blends.

7.2.8 Dynamic mechanical analysis

Figures 7.7A and 7.7B show the variation in storage modulus and loss factor ($\tan \delta$) of LDPE-starch-(EMA-Zn) and LDPE-starch-(EMA-Na) blends containing metal stearates measured over the temperature range from $40\text{ }^{\circ}\text{C}$ to $100\text{ }^{\circ}\text{C}$. The addition of metal stearates increased the storage modulus values, indicating an improvement in the interfacial interaction between the phases of the blends [17].

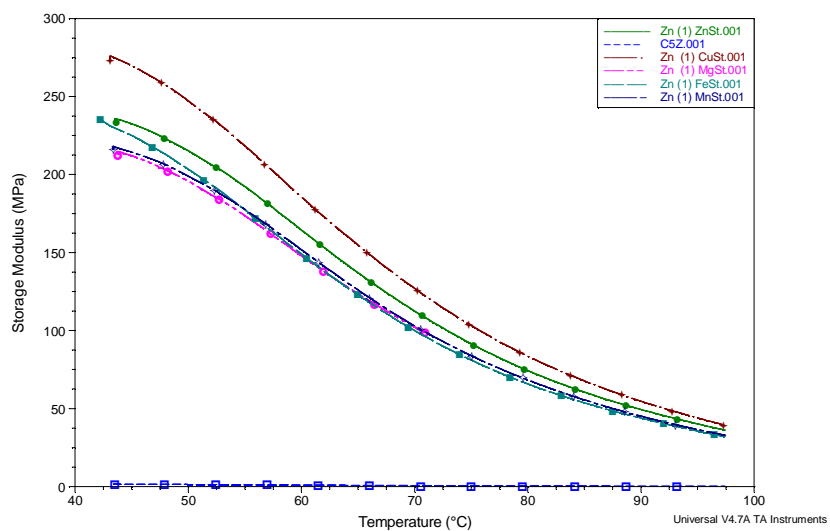


Figure 7.7A DMA curves of LDPE-starch-(EMA- Zn)-1% metal stearate blends

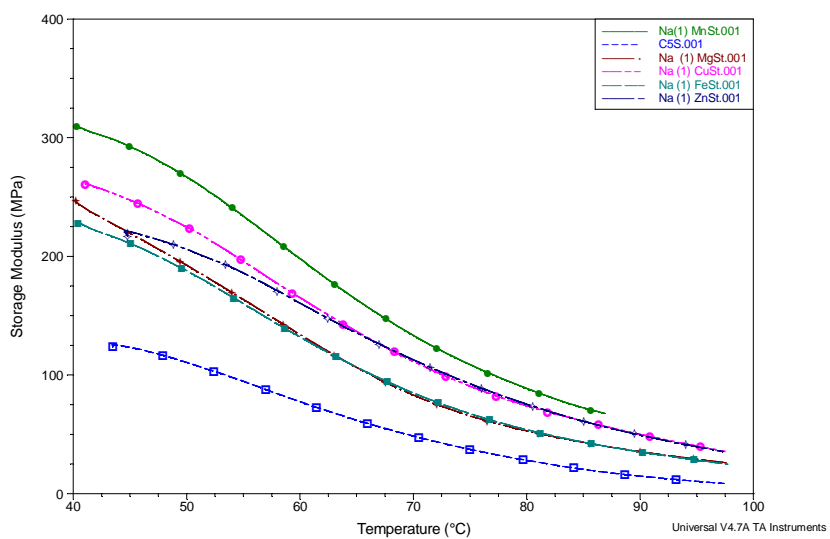


Figure 7.7B DMA curves of LDPE-starch-EMA- Na-1% metal stearate blends

7.2.9 Thermogravimetric analysis (TGA)

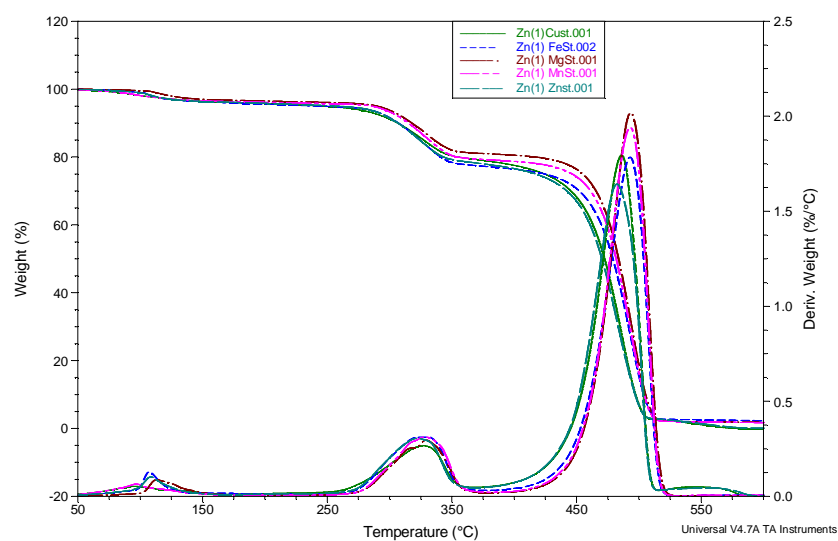


Figure 7.8A TGA thermograms of LDPE-starch-(EMA-Zn)-1% metal stearate blends

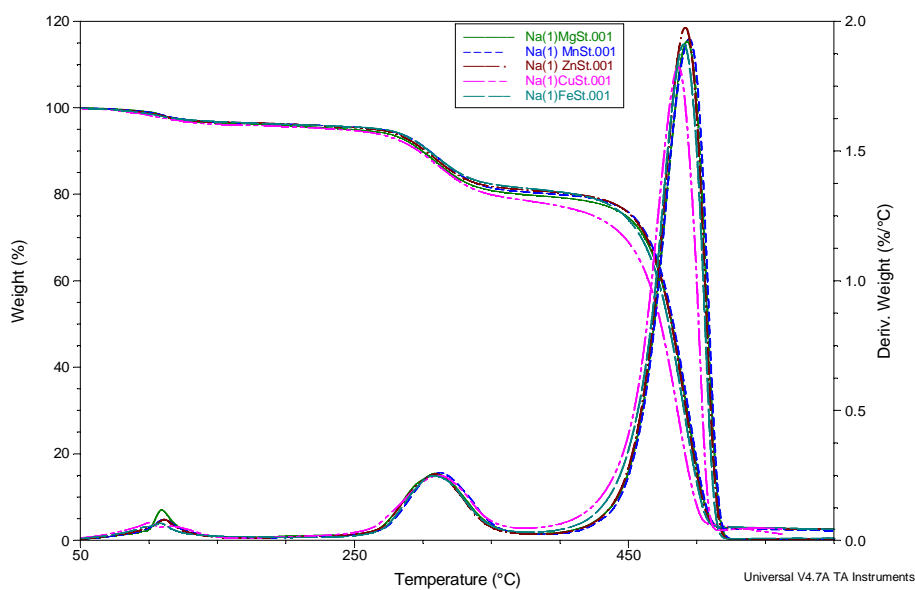


Figure 7.8B TGA thermograms of LDPE-starch-(EMA-Na)-1% metal stearate blends

Table 7.17 TGA results for LDPE-starch-(EMA-Zn)-1% metal stearate blends

Sample	Temperature of	T _{max}	Rate of	Residual
--------	----------------	------------------	---------	----------

	onset of degradation ($^{\circ}\text{C}$)	($^{\circ}\text{C}$)	maximum degradation (%/ $^{\circ}\text{C}$)	weight (%)
LDS-Zn	431.28	490.07	2.082	1.209
LDS-Zn(1)Fe	428.86	492.64	1.784	2.273
LDS-Zn(1)Mn	424.78	492.66	1.941	1.681
LDS-Zn(1)Cu	407.10	485.88	1.795	0.1312
LDS-Zn(1)Mg	434.58	493.18	2.018	1.792
LDS-Zn(1)Zn	413.26	482.06	1.643	0.0784

Figures 7.8A and 7.8B present the thermograms of LDPE-starch-(EMA-Zn)-1% metal stearate and LDPE-starch-(EMA-Na)-1% metal stearate blends that display several decomposition regions. The first weight loss region (around 100 $^{\circ}\text{C}$), can be assigned to the thermal decomposition of the low molecular weight compounds present in the blends. The second weight loss region (250 $^{\circ}\text{C}$ -350 $^{\circ}\text{C}$) attributed to the thermal degradation of the most part of the starch. The third weight loss is located between 420 $^{\circ}\text{C}$ and 525 $^{\circ}\text{C}$ and is the main decomposition region which is assigned to the thermal decomposition of the backbone chains of pure polyethylenes. The temperature of onset of degradation, the maximum decomposition temperature (T_{max}), rate of degradation and weight of residue are shown in Tables 7.17 and 7.18. Results show that addition of metal stearates decreases the temperature of onset of degradation of all the LDPE-starch-(EMA-Zn) blends except for the blend containing magnesium stearate as pro-oxidant, and addition of metal stearates decreases the temperature of onset of degradation of all the LDPE-starch-(EMA-Na) blends except for the blends containing ferric stearate and zinc stearate as pro-oxidants. But the blending process modify the thermogravimetric parameters of pure LDPE ($T_{\text{onset}} = 420$ $^{\circ}\text{C}$, $T_{\text{max}} = 482$ $^{\circ}\text{C}$). Furthermore, the thermal stability of the

starch remains unmodified for all the LDPE-starch-ionomer-metal stearate blends.

Table 7.18 Results of thermogravimetric analysis of LDPE-starch-(EMA-Na)-1% metal stearate blends

Sample	Temperature of onset of degradation ($^{\circ}\text{C}$)	T_{max} ($^{\circ}\text{C}$)	Rate of maximum degradation ($\%/^{\circ}\text{C}$)	Residual weight (%)
LDS-Na	430.41	492.37	2.079	1.87
LDS-Na(1)Fe	431.01	489.94	1.911	2.485
LDS-Na(1)Mn	429.61	493.98	1.931	1.461
LDS-Na(1)Cu	427.02	485.95	1.824	1.426
LDS-Na(1)Mg	430.30	492.65	1.923	2.563
LDS-Na(1)Zn	431.98	491.20	1.976	2.517

7.2.10 Differential scanning calorimetry

Figures 7.9A and Table 7.19 illustrates the thermal behaviour of LDPE-starch-(EMA-Zn)-ferric stearate blend, before and after biodegradation. The results indicate that addition of ferric stearate marginally increases the melting temperature of the blend system, but the crystallinity of the system is negatively influenced by it. This reduction may have enhanced the biodegradation of the samples through the presence of an amorphous phase and thus biodegradation facilitate the crystallization of LDPE by reducing the amorphous phase. The increment of the crystallinity after biodegradation could be attributed to the preferential polymeric chain oxidation that conform the amorphous phase of the LDPE, as well to the formation of new crystallites induced by the chain scission reaction [18].

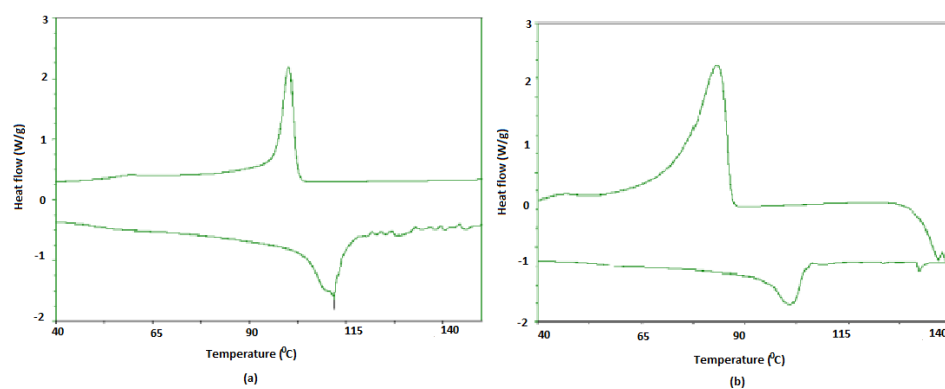


Figure 7.9A DSC curves of LDPE-starch-(EMA- Zn)-1% ferric stearate blend: (a) before biodegradation and (b) after biodegradation

Table 7.19 Results of DSC analysis of LDPE-starch-(EMA-Zn)-1% ferric stearate blend

Sample	T _m (°C)	ΔH _f (J/g)	T _c (°C)	ΔH _c (J/g)	% crystallinity
LDPE	110.00	67.00	96.00	79.00	23.4
LDS-Zn(1)Fe	111.94	59.21	100.16	56.36	20.7
LDS-Zn(1)Fe(ab)	110.99	63.81	93.26	58.92	22.3

Figure 7.9B and Table 7.20 show the thermal behaviour of LDPE-starch-(EMA-Na)-ferric stearate (74/20/5/1) blends before and after biodegradation. Table reveal that the incorporation of ferric stearate enhances the melting temperature (T_m) of pure LDPE. This may be due to the action of ferric stearate as nucleating agent for the formation of crystallites leading to an elevation in T_m [19]. The decline of the crystallinity after biodegradation for two months could be attributed to the initial changes associated with degradation occurring in the amorphous phase of the polymer, with a consequent reduction in the crystalline regions [20-21].

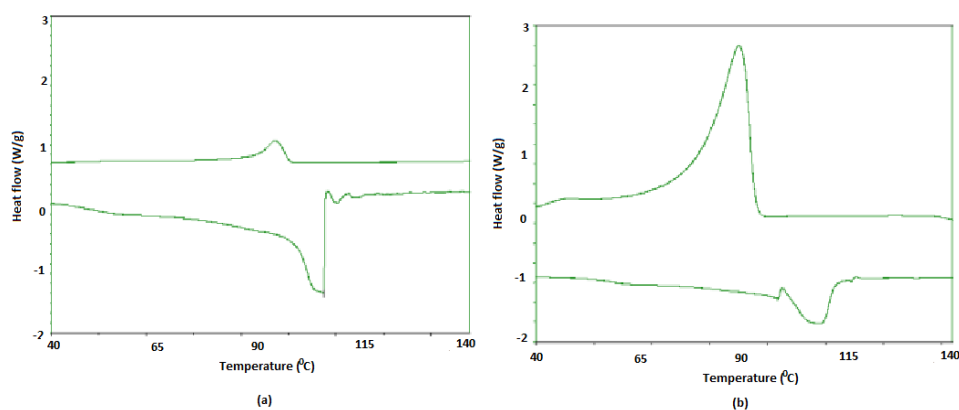


Figure 7.9 B DSC curves of LDPE-starch-(EMA-Na)-1% ferric stearate blend: (a) before biodegradation and (b) after biodegradation

Table 7.20 Results of DSC analysis of LDPE-starch-(EMA-Na)-1% ferric stearate blend

Sample	T _m (°C)	ΔH _f (J/g)	T _c (°C)	ΔH _c (J/g)	% crystallinity
LDPE	110.00	67.00	96.00	79.00	23.4
LDS-Na(1)Fe	111.78	93.58	98.89	13.02	32.6
LDS-Na(1)Fe(ab)	111.52	43.47	93.87	65.71	15.2

7.2.11 Morphological studies

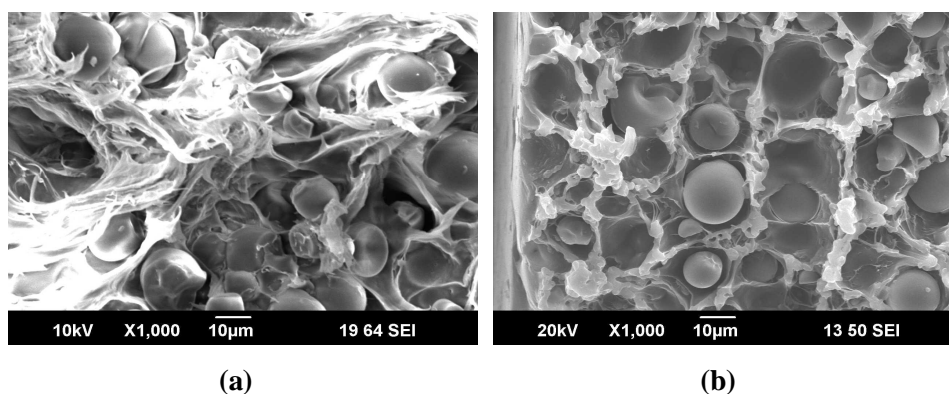


Figure 7.10A Scanning electron micrographs of LDPE-starch-(EMA-Zn) blend containing 1% ferric stearate as prooxidant:
a) before biodegradation and b) after biodegradation for two months

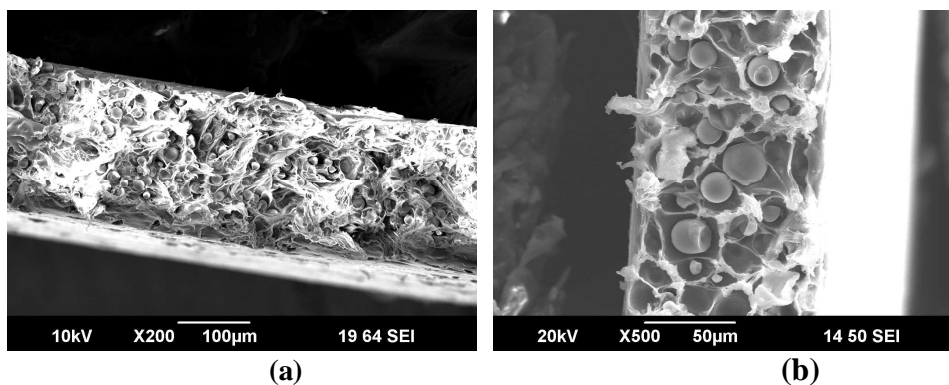


Figure 7.11B Scanning electron micrographs of LDPE-starch-(EMA-Na) (75/20/5) blend containing 1% ferric stearate as prooxidant:
a) before biodegradation and b) after biodegradation for two months

Scanning electron micrographs of fractured surfaces of LDPE-starch-(EMA-Zn)-1% ferric stearate and LDPE-starch-(EMA-Na)-1% ferric stearate (75/20/5) blends before and after they have been subjected to biodegradation in culture medium are presented in figures 7.10A and 7.10B. After two months of biodegradation a number of small cavities are visible in the film due to the removal of starch by microorganisms. But the number of cavities after biodegradation is less in ferric stearate incorporated blend as compared to the LDPE-starch blend (chapter III, Figure 3.20 (b)). This fact indicates that the ferric stearate used as pro-oxidant adversely affect the biodegradation of LDPE.

7.3 Conclusions

Incorporation of metal stearates namely ferric stearate, manganese stearate, cupric stearate, magnesium stearate and zinc stearate in ionomer compatibilized LDPE-starch blends results in an enhancement in tensile strength and elastic modulus, and a reduction in elongation at break. However the incorporation of small quantities of metal stearates results in increase in melt flow index of LDPE. There was a significant reduction in tensile strength of the samples after immersion in culture medium indicating biodegradation of the blends by microorganisms which is also confirmed by FTIR spectroscopy. The water absorption tendency decreases with increase in the concentration of metal stearates. The presence of small quantities of metal stearates induces degradation of LDPE-starch-ionomer blends on exposure to UV radiation. All the samples exhibited a significant reduction in tensile strength and weight after photobiodegradation. Addition of the metal stearates enhances the rate of degradation in the order $\text{FeS} > \text{MnS} > \text{CuS} > \text{MgS}$. The addition of metal stearates increased the storage modulus values. Addition of small quantities of the metal stearates

changes the thermal stability and crystallinity of LDPE. SEM micrographs confirm the biodegradation of the pro-oxidant incorporated blend samples.

References

- [1] Richard, C. F.; San Rafael, C.; US Patent 4197375, 1980.
- [2] Chiellini, E.; Corti, A.; D'Antone, S.; Baciù, R.; Polym Degrad Stab 2006, 91, 2739.
- [3] Khabbaz, F.; Albertson, A. C.; Karlsson, S.; Polym Degrad Stab 1999, 63, 127.
- [4] Albertson, A. C.; Andersson, S. O.; Karlsson, S.; Polym Degrad Stab 1987, 18, 73.
- [5] Puglia, C. D.; Powell, S. R.; Environ Health Perspect 1984, 57, 11.
- [6] Roy, P. K.; Titus, S.; Surekha, P.; Tulsi, E.; Deshmukh, C.; Rajagopal, C.; Polym Degrad Stab 2008, 93, 22.
- [7] Roy, P. K.; Surekha, P.; Raman, R.; Rajagopal, C.; Polym Degrad Stab 2009, 94, 1033.
- [8] Scott, G.; Polym Degrad Stab 1990, 29, 135
- [9] Lim, S.; Jane, J.; Biotechnol Progr 1992, 8, 51.
- [10] Johnson, K. E.; Pometto III, A. L.; Nikolo, Z. L.; Appl Environ Microb 1993, 59, 1155.
- [11] El-Shafei, H. A.; El-Nasser, N. H. A.; Kanosh, A. L.; Ali, M.; Polym Degrad Stab 1998, 62, 361.
- [12] El-Rehim, H. A. A.; Hegazy, E. S. A.; Ali, A. M.; Rabie, A. M.; J Photochem Photobiol A 2004, 163, 547
- [13] Lucas, N.; Bienaime, C.; Belloy, C.; Queneudec, M.; Silvestre, F.; Nava-Saucedo, J. E.; Chemosphere 2008, 73, 429
- [14] Bremner, T.; Rudin, A.; Cook, D. G.; J Appl Polym Sci 1990, 41, 1617.]
- [15] Arkatkar, A.; Arutchelvi, J.; Bhaduri, S.; Uppara, P. V.; Doble, M.; Int Biodeter Biodegr 2009, 63, 106

- [16] Coelho, N. S.; Almeida, Y. M. B.; Vinhas, G. M.; Polimeros Cienc Technol 2008, 18, 270.
- [17] Pedroso, A. G.; Rosa, D. S.; Polym Adv Technol 2005, 16, 310.
- [18] Nhlapo, N.; Motumi, T.; Landman, E.; Verryn, S. M. C.; Focke, W. W.; J Mater Sci 2008, 43, 1033
- [19] Khraishi, N.; Al Robaidi, A.; Polym Degrad Stab 1991, 32, 105.
- [20] Christina, P.; Papadopoulou.; Nikos, K.; Kalfoglou.; Polymer 1999, 40, 905.
- [21] Rosa, D. S.; Grillo, D.; Bardi, M. A. G.; Calil, M. R.; Guedes, C. G. F.; Ramires, E. C.; Frollini, E.; Polym Test 2009, 28, 836.



SUMMARY AND CONCLUSIONS

The present work is an attempt to improve the biodegradability and photodegradability of low density polyethylene (LDPE). Biodegradability of the samples prepared from the blends of low density polyethylene and biopolymers (either starch or dextrin) has been verified using a culture medium containing *Vibrios* - an amylase producing bacteria, and by soil burial. The photodegradability of low density polyethylene and its blends with biopolymers was evaluated by placing the test specimens under a 30 watt shortwave UV lamp and retrieving after one month. The effect of the addition of small quantities of metal oxides (iron oxide, manganese dioxide, titanium dioxide (rutile and anatase grades)) and metal stearates (ferric stearate, manganese stearate, cupric stearate, magnesium stearate and zinc stearate) as pro-oxidants has been studied. The potential of polyethylene-co-methacrylic acid ionomers (zinc salt of polyethylene-co-methacrylic acid (EMA-Zn) and sodium salt of polyethylene-co-methacrylic acid (EMA-Na)) and maleic anhydride (MA) as compatibilizers for low density polyethylene-starch blends too has been evaluated.

The reduction in the mechanical properties of LDPE on incorporation of biopolymers suggests that the filler has no reinforcing effect on LDPE. The blends show lower melt flow rates as compared to neat LDPE due to increased entanglement of the polymer chains of LDPE and biopolymer.

The reduction in the mechanical properties and weight loss of the blends after biodegradability tests in the culture medium and soil suggests that the blends are partially biodegradable. The water absorption values of the blends are higher indicating an enhanced affinity for microbial attack. FTIR peak intensities of LDPE-starch and LDPE-dextrin blends before and after biodegradation studies in shake culture flask reveal the biodegradation of the samples in presence of amylase producing *vibrios*.

Dynamic mechanical analyses results show that pure LDPE has lower storage modulus as compared to the LDPE-biopolymer blend. The thermogravimetric studies indicate that the thermal stability of LDPE is marginally lowered by the incorporation of biopolymers. There is no significant decrease in crystallinity of LDPE in the blends, which shows that LDPE and biopolymer are incompatible. The evidence from scanning electron microscopic studies too suggests that the newly prepared LDPE-biopolymer blends are partially biodegradable.

The addition of the ionomer as a compatibilizer improved the stress-strain properties of the blends. Among the various dosages of ionomers used in this study as compatibilizers, 5 weight % show maximum improvement in mechanical properties in the case of both EMA-Zn and EMA-Na. An increase in the melt flow of the blends was also realized by the addition of the ionomers. Biodegradation studies suggest that the degradation rate of the ionomer compatibilized films was marginally lower than that of the MA compatibilized films. Results of dynamic mechanical analyses indicate that the storage modulus decreases on addition of all the three compatibilizers leading to the flexibilization of the blends. Spectroscopic studies indicate interaction between starch and ionomer. A schematic representation of the polar-polar interactions between the

carboxyl groups of the ionomers and the hydroxyl groups of starch has been proposed. Results of thermogravimetric analyses show improved thermal stability in the case of the ionomer compatibilized blends as compared to the MA compatibilized blends and the uncompatibilized blends. The results of differential scanning calorimetry show decrease in crystallinity on incorporating ionomers as compatibilizers in LDPE-starch blends. Morphological studies show improved dispersion of starch particles in the blends in presence of ionomers as compatibilizers.

Incorporation of small quantities of metal oxides and metal stearates as pro-oxidants causes marginal changes in the mechanical properties of LDPE. The change in the melt flow index of LDPE was insignificant on incorporation of small quantities of metal oxides. However the incorporation of small quantities of metal stearates results in increase in melt flow index of LDPE. The presence of small quantities of both metal oxides and metal stearates induces degradation of LDPE on exposure to UV radiation. The results of the spectroscopic studies reveal the presence of oxidation products after photodegradation. For all the samples, the addition of small quantities of pro-oxidants increased the storage modulus, indicating the stiffening. Addition of small quantities of the pro-oxidants results in an enhancement in crystallinity apparently due to their action as nucleating agents. SEM micrographs of LDPE containing small quantities of ferric oxide and ferric stearate validate photodegradation on exposure to UV radiation for one month.

Incorporation of small quantities of metal oxides and metal stearates in ionomer compatibilized LDPE-starch blends results in marginal changes in the mechanical properties of LDPE. The change in the melt flow index of LDPE was marginal on incorporation of small quantities of metal oxides

and metal stearates. There was significant reduction in the tensile strength of all the samples after immersion in culture medium indicating biodegradation of the blends by microorganisms which is also confirmed from IR spectroscopy. The presence of small quantities of metal oxides and metal stearates induces degradation of LDPE-starch-ionomer blends on exposure to UV radiation. For all the samples, the addition of small quantities of metal oxides and metal stearates increased the storage modulus, indicating stiffening. Addition of small quantities of the metal oxides and metal stearates changes the thermal stability and crystallinity of LDPE. SEM micrographs confirm the biodegradation of the pro-oxidant incorporated blend samples.

Future Outlook

- The development of biodegradable polymeric materials combining high biodegradability with good mechanical properties
- Preparation of biodegradable blends based on various biopolymers other than starch
- Improvement of plasticity of starch for replacing synthetic plastics
- Evaluation of effectiveness of polyethylene-co-methacrylic acid ionomers as compatibilizer for other non polar-polar blend systems
- Evaluation of effectiveness of various ionomers as compatibilizers for immiscible blends

.....❧.....

List of Symbols and Abbreviations

ASTM	- American Society for Testing and Materials
C	- Carbon
Ca	- Calcium
CI	- Carbonyl index
cm	- Centimetre
cm ⁻¹	- Centimetre inverse
cm ³	- Cubic centimetre
CO ₂	- Carbon dioxide
C _p	- Heat flow rate
DCP	- Dicumyl peroxide
DSC	- Differential scanning calorimetry
DTG	- Derivative thermogravimetry
EAA	- Poly(ethylene- <i>co</i> -acrylic acid)
ESC	- Environmental stress cracking
Fe	- Iron
FTIR	- Fourier transform infrared spectroscopy
g/cm ³	- Gram per cubic centimetre
H ₂	- Hydrogen
HDPE	- High density polyethylene
J/g	- Joule per gram
K	- Pottassium
kcal/mol	- Kilocalories per mol
KCl	- Pottasium chloride
Kg	- Kilogram
kN	- Kilo newton
L	- Litre
LCB	- Long chain branching
LDPE	- Low density polyethylene

LLDPE	-	Linear low density polytheylene
MA	-	Maleic anhydride
MFI	-	Melt flow index
Mg	-	Magnesium
Mg	-	Milligram
min	-	Minute
mm	-	Millimetre
MPa	-	Mega pascal
nm	-	Nanometre
Nm	-	Newton metre
PE	-	Polyethylene
PP	-	Polypropylene
SEM	-	Scanning electron microscopy
T _c	-	Crystallization temperature
TGA	-	Thermogravimetric analysis
T _m	-	Melting temperature
UV	-	Ultraviolet
α	-	Alpha
β	-	Beta
γ	-	Gamma
%	-	Percentage
ΔH_c	-	Heat of crystallization
ΔH_f	-	Heat of fusion
°C	-	Degree celcius
°C/min	-	Degree celcius per minute



LIST OF PUBLICATIONS IN INTERNATIONAL JOURNALS

- [1] Studies on biodegradability of linear low density polyethylene-dextrin blends using vibrios from benthic environment, **Zeena P. Hamza**, Anna Dilfi K. F, Thomas Kurian and Saritha G. Bhat, *Progress in Rubber, Plastics and Recycling Technology*, 25 (3),129-139, 2009.
- [2] Biodegradability studies on LDPE-starch blends using amylase-producing vibrios, **Zeena P. Hamza**, Anna Dilfi K. F, Thomas Kurian and Saritha G. Bhat, *International Journal of Polymeric Materials*, 58 (5), 257-266, 2009.
- [3] Effect of amylase producing vibrios from the benthic environment on the biodegradation of low density polyethylene-dextrin blends, Anna Dilfi K. F, **Zeena P. Hamza**, Thomas Kurian and Saritha G. Bhat, *Polymer-Plastics Technology and Engineering*, 48 (6), 602-606, 2009.
- [4] Biodegradability of LLDPE-starch blends using vibrios from benthic environment, Anna Dilfi K. F, **Zeena P. Hamza**, Thomas Kurian and Saritha G. Bhat, *International Journal of Plastics Technology*, 12, 1021-1030, 2008.

LIST OF PAPERS PRESENTED IN CONFERENCES

- [1] Studies on biodegradation of low density polyethylene-dextrin blends, Zeena P. Hamza, Anna Dilfi K. F., Neena George, Raghul Subin S., Thomas Kurian and Saritha G. Bhat, **10th National Seminar on Recent Trends and the Sequels in Chemistry (RTSC-2011)**, Sacred Heart College, Thevara, Kerala, India, December 7-8, 2011.
- [2] Influence of starch on the mechanical properties, morphology and biodegradation of low density polyethylene, Zeena P. Hamza, Anna Dilfi K. F., Raghul Subin S., Thomas Kurian and Saritha G. Bhat, **Polycon-2011, 5th National Conference on Plastics & Rubber Technology (NCPRT)**, Sri Jayachamarajendra College of Engineering, Mysore, April 25-26, 2011.
- [3] Influence of dextrin on the tensile properties, morphology and biodegradation of low density polyethylene, Zeena P. Hamza, Anna Dilfi K. F., Raghul Subin S., Thomas Kurian and Saritha G. Bhat, **International Conference on Advancements in Polymeric Materials (APM 2011)**, CIPET, Chennai, March 25-27, 2011.
- [4] Dextrin filled low density polyethylene films: Mechanical properties, melt flow indices and water absorption, Zeena P. Hamza, Anna Dilfi K. F., Raghul Subin S., Thomas Kurian and Saritha G. Bhat, **International Conference on Materials for the Future**, Govt. Engineering College, Thrissur, Kerala, India, February 23-25, 2011.
- [5] Investigations on tapioca starch filled low density polyethylene films, Zeena P. Hamza, Anna Dilfi K. F., Raghul Subin S., Thomas Kurian and Saritha G. Bhat, **International Conference on Functional Polymers**, NIT Calicut, Kerala, India, January 28-30, 2011.

- [6] Biodegradation of environment-friendly low density polyethylene-dextrin blends, Zeena P. Hamza, Anna Dilfi K. F., Raghul Subin S., Thomas Kurian and Saritha G. Bhat, **International Conference on Polymer Science and Engineering: Emerging Dimensions**, Chandigarh, November 26-27, 2010.
- [7] Thermal properties of partially biodegradable LDPE/Dextrin blends, Zeena P. Hamza, Anna Dilfi K. F., Julie Jose, Raghul Subin S., Thomas Kurian and Saritha G. Bhat, **International Conference on Advances in Polymer Technology**, Kochi, India, February 26-27, 2010.
- [8] Partially biodegradable LLDPE-starch blends, Anna Dilfi K. F., Zeena P. Hamza, Raghul Subin S., Thomas Kurian and Saritha G. Bhat, **International Conference on Advances in Polymer Technology**, Kochi, India, February 26-27, 2010.
- [9] Thermal properties of partially biodegradable LDPE/Starch blends, Zeena P. Hamza, Anna Dilfi K. F., Julie Jose, Thomas Kurian and Saritha G. Bhat, **International Conference on Advancements in Polymeric Materials (APM '10)**, CIPET, Bhubaneswar, February 20-22, 2010.
- [10] Mechanical, thermal and morphological studies on partially biodegradable LLDPE-dextrin blends, Anna Dilfi K. F., Zeena P. Hamza, Julie Jose, Thomas Kurian and Saritha G. Bhat, **97th Indian Science Congress**, Thiruvananthapuram, India, January 3-7, 2010.
- [11] Role of benthic vibrios on the biodegradability of LLDPE, Anna Dilfi K. F., Zeena P. Hamza, Thomas Kurian and Saritha G. Bhat, **CHEMREFERENCE 09**, IIT Chennai, August 23-24, 2009.
- [12] Effect of amylase producing vibrios from the benthic environment on the biodegradation of low density polyethylene-starch blends, Anna Dilfi K. F., Zeena P. Hamza, Raghul Subin S., Thomas Kurian and Saritha G. Bhat, **International Conference on Advances in Polymer Technology**, Kochi, India, September 25-27, 2008.

- [13] Novel bio-plastics based on polyethylenes, Zeena P. Hamza, Anna Dilfi K. F., Thomas Kurian and Saritha G. Bhat, **POLYCHAR 16 World Forum on Advanced Materials**, Lucknow, India, February 17-21, 2008.
- [14] Novel biodegradable plastics based on LDPE and LLDPE, Anna Dilfi K. F., Zeena P. Hamza, Thomas Kurian and Saritha G. Bhat, **POLYCHAR 16 World Forum on Advanced Materials**, Lucknow, India, February 17-21, 2008.
- [15] Biodegradable film grade plastics based on LDPE and LLDPE, Zeena P. Hamza, Anna Dilfi K. F., Thomas Kurian and Saritha G. Bhat, **International Conference on Biodiversity Conservation and Management (BIOCAM 2008)**, Kochi, India, February 3-6, 2008.

.....❧.....

RESUME

ZEENA. P. HAMZA

Nellikathukuzhi House
V. K. C. P. O
Kuzhuvelipady
Ernakulam 682021
Ph: 9446053068
E-mail: zeenaphamza@gmail.com



ACADEMIC QUALIFICATION

- S.S.L.C... (First class with distinction, 1994, Board of Public Examinations, Kerala State)
- Pree Degree... (First class, 1996, Mahatma Gandhi University, Kottayam)
- B.Sc. Chemistry... (First class, 1999, Mahatma Gandhi University, Kottayam)
- M.Sc. Chemistry... (First class, 2001, Mahatma Gandhi University, Kottayam)
- B. Ed... (First class, 2002, Mahatma Gandhi University, Kottayam)

TECHNICAL

- Post graduate diploma in computer application

OTHERS

- NET...(2002)
- SET...(2002)

TEACHING EXPERIENCE

- Asst. Professor in Chemistry....(Govt. Brennen College, Thalassery; since 17-06-08)
- Lecturer in Chemistry...(U.C.College, Aluva; 01-06-05 to 30-03-07)
- Lecturer in Chemistry...(St. Pauls College, Kalamassery, 13-08-04 to 30-03-05)
- HSST in Chemistry...(Govt.H.S.S, Edathala; June 2003 to July 2003)
- HSST in Chemistry...(Al-Manar HSS, Kuzhuvelipady; Sept 2002 to May 2003)

AWARDS

- *RASHTRAPATHI GUIDE AWARD in 1994*

PERSONAL DETAILS

- Father's name : P. E. Hamza
- Mothers name : Laila Hamza
- Date of birth: 02-09-1978
- Sex : Female
- Marital status : Married
- Husband's name : Anise. N. A
- Languages Known : English, Malayalam

REFERENCE

Dr. Thomas Kurian
Professor
Department of Polymer Science and Rubber Technology
Cochin University of Science and Technology
Kochi-22.
Tel: +91-484-2575723
E-mail: drtkurian@gmail.com

.....❧.....